Pathogenesis of Ulcerative Colitis:

The role of Claudin-8 in epithelial barrier function and inflammation

By

Bahman Nedjat-Shokouhi

A thesis submitted to UCL for the degree of

Doctor of Philosophy

Division of Medicine

Declaration

I, Bahman Nedjat-Shokouhi, confirm that the work presented in this thesis is my own. Where information has been derived from other sources, I confirm that this has been indicated in the thesis.

Abstract

Ulcerative colitis is a relapsing and remitting inflammatory bowel disease involving the large bowel. The current hypothesis on the pathogenesis of UC is that an abnormal innate immune response in genetically susceptible individuals, combined with environmental factors, result in excessive activation of the adaptive immune system within lamina propria. The role of abnormal barrier function is widely accepted. Using transcriptomic analysis of punch biopsies of patients with quiescent UC, CLDN8 was identified as grossly downregulated in the intestine. In this thesis, loss of *Cldn8*, a tight junction (TJ) molecule, was shown to result in reduced susceptibility of mice to DSS-induced colitis. *Cldn8* knock out (*Cldn98*-KO) mice, had smaller increase in intestinal permeability to ^{3}H-mannitol, reduced neutrophils and macrophages in inflammatory cell infiltrate in lamina propria during the early phase of inflammation. The inner layer of mucous is sterile in naïve *Cldn8*-KO and WT mice, and remains sterile after the animals have been exposed to DSS-water for 12 hours. Transcriptomic analysis between *Cldn8*-KO and WT mice did not reveal any significant differences between the two groups at different time points. After correction for multiple-testing, no differentially-expressed genes remained. These results suggest that downregulation of CLDN8 in patients with UC is a physiologic response by the intestine to increase local defences against luminal pathogens.

Table of Contents

List of Figures

List of Table

Acknowledgements

This work was supported by the United Kingdom Medical Research Council. I would like to thank and acknowledge the following people who have contributed to this body of work

- Professor Anthony Segal for giving me the opportunity to study in his laboratory and for his guidance, supervision and support.
- Dr Andrew Smith for the guidance, supervision and encouragement
- Dr Joanne Marks for teaching and supervising me for the microsurgery technique for *in vivo* permeability studies in mice
- Dr Philip Smith for sharing his microarray data on humans.
- Dr Joshua Thean Chew for patiently teaching me laboratory techniques
- Dr Nual O'Shea for sharing her tips on performing DSS experiments
- Dr Adam Levine for assistance with bioinformatics, statistics, valuable discussions and critical analysis
- Dr Daniel Marks for his critical feedback
- Professor Gordon Stewart for teaching me how to use a flame photometer
- Sophia Joyce for her support and kindness
- Riccardo, Penelope, Sabrina, Janne and Francesca for advice on various laboratory techniques
- Dr Manuel Rodriguez for assistance with microscopy and histology
- Dr Stuart Bloom for his clinical input and advice into my research

Finally, I thank all the patients and volunteers for kindly participating in this study and my wife and daughter for their uncompromising love, support and patience.

Statement of Collaborative Work

A number of aspects of the work presented in this thesis were conducted as part of a collaboration. These include

- Collection and preparation of samples for microarray studies on human ileo-colonic biopsies were performed jointly with Dr Philip Smith, Dr Farooq Rahman, and Dr Bu-Hayee Hussein.
- *In situ* hybridisation was performed with Dominic Patel at Pathology department, UCLH
- Immunohistochemistry was performed by Ignazio Puccio at the Translational Gastroenterology Group at UCL

List of Abbreviations

α	Alpha
β	Beta
γ	Gamma
κ	Kappa
Á	Amgstrum
5ASA	5-aminosalicylates
A/E	attaching and effacing
AIEC	Adherent–Invasive *Escherichia Coli*
AMP	Anti-Microbial Proteins
APC	Antigen-Presenting Cells
ATP	Adenosine Triphosphate
C. rodentium	*Citrobacter rodentium*
C57BL/6	C57 black 6 mouse strain
CD	Crohn's disease
CDH1	cadherin type 1
cDNA	complementary DNA
Cldn *	Claudin
Cldn *	Claudin
CRC	colorectal cancer
Ct	cycle threshold
CXCL	C-X-C chemokine ligand
DAMP	Damage-Associated Molecular Patterns
DCs	Dendritic Cells
DNA	deoxyribonucleic acid
DNBS	Dinitrobenzene sulfonic acid
DSS	Dextran Sodium Sulphate
EDTA	ethylenediaminetetraacetic acid
EHEC	Enterohemorrhagic *Escherichia coli*
ENaC	epithelial sodium channels
EPEC	Enteropathogenic *Escherichia coli*
FACS	Fluorescence-activated cell sorting
FBS	foetal bovine serum
FCS	Foetal calf serum
FDR	False Discovery Rate
FMT	Faecal Microbiota Transplantation
G	Standard gravity
G	Grams
Gapdh *	glyceraldehyde-3-phosphate dehydrogenase
gDNA	genomic DNA

GEO	Gene Expression Omnibus
GI	Gastrointestinal
GSE	Genomic Spatial Event database
GWAS	Genome-wide association studies
H&E	Hematoxylin & Eosin
HBSS	Hanks balanced salt solution
HC	Healthy Control
HEPES	4-(2-hydroxyethyl)-1-piperazineethanesulfonic acid
Het	Heterozygout
HLA	human leucocyte antigen
HNF4A	hepatocyte nuclear factor-4α
HRP	Horse radish peroxidase
IBD	Inflammatory bowel disease
IEC	Intestinal Epithelial Cells
IFN	Interferon
Ig	Immunoglobulin
IgA	Immunoglobulin A
IL	Interleukin
ILC	Innate Lymphoid Cells
ILF	isolated lymphoid follicles
iMNP	Intestinal mononuclear phagocytes
IPAA	ileal pouch-anal anastomosis
JAM	Junctional Adhesion Molecules
Kb	Kilobases
KO	Knock-Out
L	Litres
LAMB1	laminin-β1
LI	Large intestine
LP	Lamina Propria
MeV	MultiExperiment Viewer Software
Mg	Milligram
$MgCl_2$	Magnesium chloride
Ml	Millilitre
MLN	Mesenteric Lymph Nodes
mM	Millimolar
mRNA	messenger RNA
MUC	Mucin
NACWO	Named Animal Care and Welfare Officer
NF-κβ	nuclear factor- κβ
Ng	Nanograms
NHS	National Health Service
NLR	NOD-like receptor

nM	Nanomolar
NOD2	Nucleotide-binding Oligomerization Domain-containing protein 2
OD	optical density
PAMP	Pathogen-Associated Molecular Patterns
PBS	phosphate buffered saline
PCA	principal component analysis
PCR	Polymerase Chain Reaction
PCR	polymerase chain reaction
PPIA *	peptidylprolyl isomerase A
Ppia *	peptidylprolyl isomerase A/cyclophilin A
PRR	Pattern Recognition Receptors
PSC	primary sclerosing cholangitis
qRT-PCR	quantitative reverse transcription-PCR
qRT-PCR	quantitative real time polymerase chase reaction
RNA	ribonucleic acid
Rpm	revolutions per minute
S	Seconds
SCFA	Short Chain Fatty Acids
SI	Small intestine
SNP	single nucleotide polymorphism
SPF	Specific Pathogen Free
Th	T helper
TI	Terminal Ileum
TI	terminal ileum
TJ	Tight Junction
TLR	Toll-like receptors
TLR	Toll-like receptor
TM	Transmembrane
TNBS	2,4,6- Trinitrobenzene sulfonic acid
TNF	tumour necrosis
Treg	T regulatory cell
U	Units
UC	Ulcerative colitis
UCL	University College London
UCLH	University College London Hospital
UK	United Kingdom
WT	Wild type
ZO	zonula occludens
µl	Microliter
µM	Micromolar

*** Italicised terms refer to genes; non-italicised terms refer to proteins.**

1 Introduction

1.1 NORMAL INTESTINAL HOMEOSTASIS

The gastrointestinal (GI) tract is a unique organ, responsible for ingesting, digesting and absorbing food, followed by excretion of waste as faeces. Along with food mater, significant quantities of exogenous microorganisms, such as bacteria, fungi and viruses also enter. Over the course of evolution, the GI tracts has developed several mechanisms to protect against invasion by pathogens.

1.1.1 MICROBIOME

The healthy GI tract is populated by a commensal microbial community known as the microbiome. Genome sequencing of the human microbiome has identified approximately up to 1,500 species and 3 x 10^6 genes (1), although on average the microbiome of individuals contains only 160 bacterial species, indicating a substantially varied microbiome component among individuals (2,3). Environment factors play a significant role in different microbiome compositions between individuals; even mice with same genetic background, housed in different cages in the same facility have different microbiome composition (4).

The intestine is sterile prior to birth and is colonised afterwards. In adult humans, the bacterial load and diversity increases towards the distal intestine, and reaches its maximum in the colon, with 1011-1013 organisms per gram of faeces, compared to 107-108 in the terminal ileum (TI) or 103-104 in proximal bowel (5).

The host and the microbiota have a mutually beneficial symbiotic relationship that is important for development and maintenance of normal gut homeostasis. The host provides nutrients and breeding environment, whilst the commensal bacteria support host metabolism and the development of the intestinal immune systems. For example, commensal bacteria can produce vitamins B and K (6) as well as providing the host with a source of energy by digesting dietary fibre to Short Chain Fatty Acids (SCFA) such as acetate, propionate and butyrate as end products (7,8). Recent evidence indicated that commensal bacteria may also influence host immunity by directly interacting with intestinal cells or producing several metabolites, including adenosine triphosphate (ATP) (9).

The commensal microbiota play an essential role in protecting the host from pathogenic invaders and limiting the colonisation of the intestine by pathogens

(10,11). Many intestinal bacteria not only produce antimicrobial compounds but also compete for nutrients and attachment sites in the intestine, thus preventing colonisation with pathogenic organisms. There is evidence that commensal bacteria compete for attachment sites on epithelial cells with pathogenic entero-invasive bacteria, thus preventing the attachment and subsequent entry of such bacteria into the host (12). Additionally, because bacteria compete for nutrients in their immediate surroundings, the commensal bacteria can outcompete pathogenic bacteria for resources by sheer force of numbers (13,14). Moreover, resident non-pathogenic bacteria can inhibit the growth of their competitors by producing antimicrobial substances known as bacteriocins, and the ability to synthesize these bacteriocins is widely distributed among gastrointestinal bacteria (14,15).

1.1.2 The Intestinal Mucosal Barrier

The host immune system must tolerate the microbiota, whilst remaining effective against threats posed by the microorganisms. The challenge is complicated by the dynamic nature of the microbiota composition, which is influenced by a wide variety of factors, such as dietary changes (16), antibiotic treatment (17), as well as other pathogens in the GI tracts (18).

To protect the host, the GI tract has developed several mechanisms, which can be broadly classed as anatomical containment and sensing the luminal environment.

1.1.2.1 Anatomical Containment

Physical barrier

The physical barrier consists of the mucous layer and the Intestinal Epithelial Cells (IECs) themselves. Mucous is the first line of defence against pathogens in the intestine. It is a viscous gel-like fluid, secreted by goblet cells, and it is enriched by mucin glycoproteins that form large net-like polymers. There is evidence that mucous secretion is regulated by intestinal microbes or their metabolites (19–22).

The mucous has slightly different properties across the GI tract. In the small intestine, the mucous consists of one layer, but in the colon, it is composed of two layers; a slightly looser outer layer, and an inner layer that is firmly attached to the IECs. The thickness of the mucous increases distally towards the distal colon (*Figure 1-1*) (23). Notably, whilst the outer layer contains large number of intestinal microbes, the inner layer is normally sterile in healthy individuals (24).

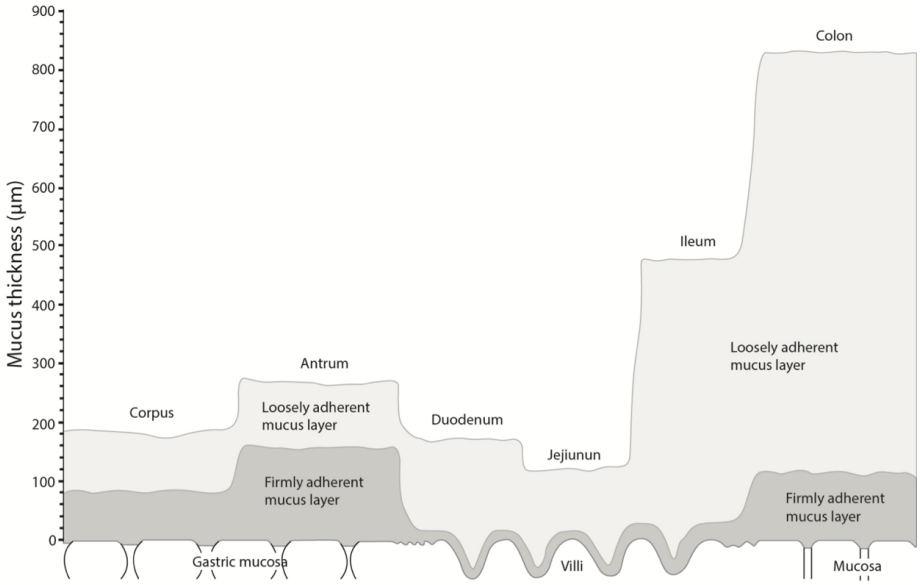

Figure 1-1 – **Mucous thickness measured throughout the gastrointestinal tract of rat** – *Adapted from Atuma et al (25)*

Chemical barrier

In the small intestine, Paneth cells produce Anti-Microbial Proteins (AMP) and defensins and RegIIIγ that are thought to be responsible for protection of mucous from invasion of pathogens (26,27). Secretory IgA is produced by plasma cells, and is released in the lumen after transcytosis (28). However, there are no Paneth cells in the healthy colon, and it is unclear what molecules are responsible for protection of the inner layer of mucous in the large intestine. There is recent evidence that a protein called Lypd8 may play a vital role in the colon. Lypd8 is anchored to the IECs, and constitutively released into the mucous, binding flagellated bacteria, such as *Escherichia*, *Proteus* and *Helicobacter*, inhibiting their invasion of the IECs (29).

1.1.2.2 Mucosal immune system of the large bowel

The mucosal immune system is in direct contact with the external antigenic environment. This section is primarily concerned with the mucosal immune system in the large bowel. The mucosal immune system consists of several parts: the immune effector, and the immune inductive sites. The immune effector site is made up of the intraepithelial lymphocytes (IELs) and immune cells within lamina propria (see below). The immune inductive sites, also known as GALT (Gut associated lymphoid tissue), are organised lymphoid structures consisting of B-cell follicles with germinal centres surrounded by a T-cell zone.

1.1.2.2.1 Gut Associated Lymphoid Tissue

GALT follicles sometimes exist as aggregated forms, such as Peyer's patches in the small intestine, caecal and colonic patches. There are also hundreds of isolated lymphoid follicles scattered throughout the small intestine and colon (30).

Follicle-associated epithelium and M cells

GALT receives its supply of antigens from the mucosal surface across the overlying intestinal epithelium called, 'follicle-associated epithelium' (FAE) (31). FAE has several unique features when compared with other intestinal epithelial cells, to enable its function, enabling close association with luminal bacteria and antigens. FAE is almost devoid of goblet cells and has few Paneth cells in the crypts surrounding FAE. Moreover, the expression of the IgA-transporting polymeric immunoglobulin receptor is low on enterocytes in and around the FAE. A particularly unique feature of FAE is the presence of M cells. M cells are highly active in phagocytosis and transcytosis, and thereby take up luminal bacteria and antigens and deliver them to DCs in the M-cell pocket for initiation of mucosal immune responses. M cells have low lysosomal activity, suggesting they able to transfer intact antigens to DCs in lamina propria, which then process and present the antigens (32).

1.1.2.2.2 Intraepithelial lymphocytes (IELs)

IEL are a subset of T lymphocytes that reside interspersed between epithelial cells. These cells are separated from adjacent enterocytes by a 10 to 20 nm space, and these lymphocyte-epithelial cell contacts have no junctional structure (33).

Hayday and colleagues propose classifying IELs into two cell types: a and b. Type a includes TcRαβ+ cells that primarily recognize antigens presented by conventional MHC class I and II, and are primed within the systemic circulation. Type b cells includes TcRαβ+ CD8αα+ IEls and TcRγδ+ IELs, that respond to antigens not restricted by conventional MHC. Type b cells do not recognise antigens presented by MHC on professional antigen presenting cells, and it is thought that they are primed by epithelial cells in situ (34).

1.1.2.2.3 Lamina Propria (LP) and the draining Mesenteric Lymph Nodes (MLNs)

The LP is the layer of connective tissue between the epithelium and the muscularis mucosa. It is made up of smooth muscle cells, fibroblasts, lymphatics and blood vessels (35). Cells from both innate and adaptive immune system populate the LP. During healthy state, the LP is primarily populated by ILCs, lymphocytes, mononuclear phagocytes, as well as a small neutrophil and mast cell population.

Innate Lymphoid Cells (ILCs) are a group of innate immune cells and belong to the lymphoid lineage. ILCs play an important role in control of intestinal homeostasis by producing cytokines in response to stimuli (36). ILCs produce IL-22 and promote homeostasis and healing during infection in the gut (37,38). IL-22 can kill targeted Gram-positive bacteria by inducing production of RegIIIα by epithelial cells (39). There is also evidence that IL-22 can stimulate production of AMP (40). In addition, IL-6 derived from ILCs enhances IEC proliferation and contributes to healing from mucosal injury (41). When activated, ILCs can produce cytokines such as IFN-γ to protect epithelial cells from injury (42,43).

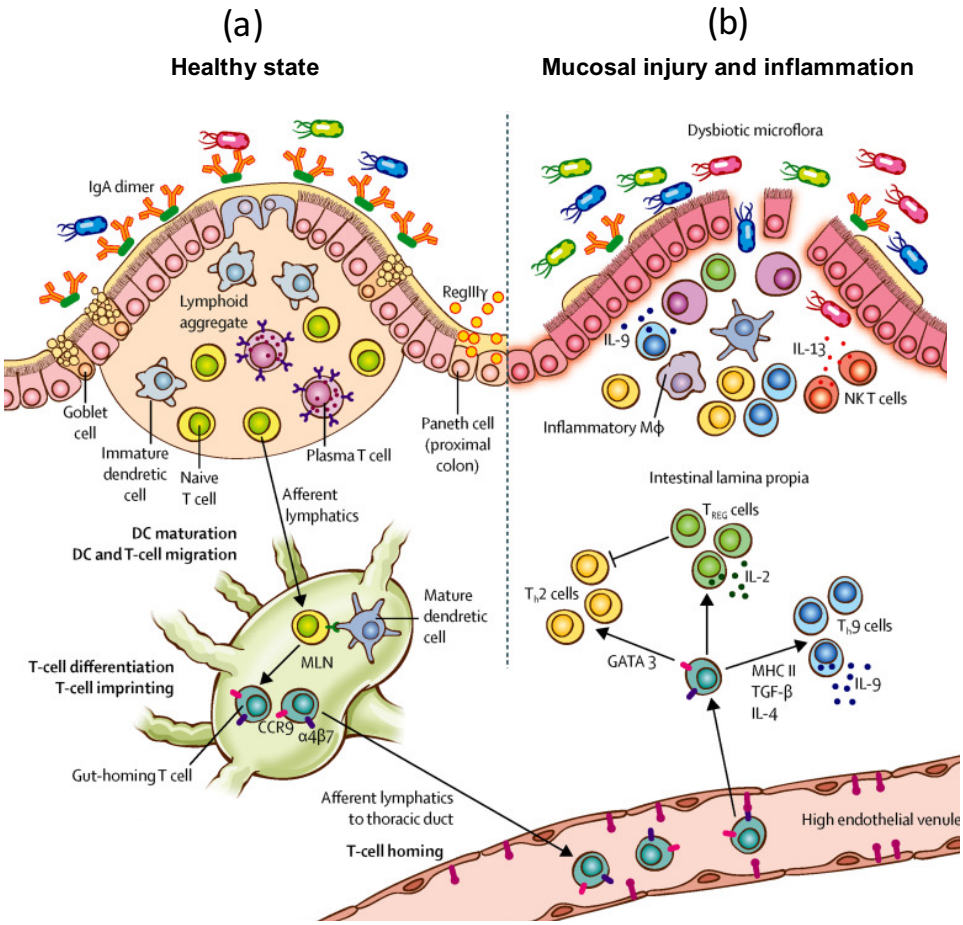

Figure 1-5 – **Overview of intestinal immune system in health and UC.** *(a) During healthy state, the epithelial cells and the mucous produce a physical barrier to entry of luminal pathogens. This is reinforced by chemical barrier that is composed of antimicrobial chemicals such as IgA and RegIIIγ. Dendritic Cells (DCs) migrate to mesenteric lymph nodes (MLNs) where they imprint the resident lymphocytes with gut-homing molecules and trigger naïve T-cells to develop into tolerogenic regulatory T cells (Treg). (b) In UC, damage to the mucosal allows luminal pathogens to enter and initiate an inflammatory response. Adapted from Ungaro et al* (44)

Resident Intestinal Mononuclear Phagocytes

Resident intestinal mononuclear phagocytes (iMNP), as part of the innate immune system, are the first line of defence against invading pathogens. iMNPs have developed efficient mechanisms to clear bacterial encroachment, as well as maintaining epithelial and mucosal homeostasis, whilst orchestrate the host's immune response towards pathogenic organisms.

Historically, iMNPs have been divided into three cell types: monocytes, Dendritic Cells (DCs) and macrophages, with distinct but complementary functions. There is increasing understanding and acceptance that this division of cell-type and roles is too simplistic (45).

Intestinal macrophages orchestrate the innate and adaptive immune responses, via pattern recognition receptions (TLRs and NOD-like receptors) and various signalling pathways (46) . Bone marrow-derived monocytes, which are recruited to the intestine from the blood, are the precursors to intestinal macrophages (47). At the beginning, these monocytes are pro-inflammatory, before signals from the intestinal mucosa modifies them into inflammation anergic resident intestinal macrophages (48). Macrophages have incredible plasticity and can adapt their phenotype and function based on the signals from their environment. Macrophages positioned just beneath the surface epithelium are more tolerogenic than those positioned more deeply in LP, and unlike macrophages in other tissues, intestinal macrophages do not have a pro-inflammation response to microbial stimulation (49,50). Interestingly, despite being phagocytic, intestinal macrophages, lack respiratory burst activity (51) or generation of nitric oxide (52). Intestinal macrophages also promote the proliferation of epithelial progenitor cells through production of produce Prostoglandin E2 (53).

Another class of iMNPs are DCs, which like the intestinal macrophages, are also classed as Antigen-Presenting Cells (APCs). However, unlike intestinal macrophages, intestinal DCs continuously migrate to MLNs, where they modulate the adaptive immune response, though the mechanism regulating this migration to MLN is poorly understood (54). Here, the DCs play two important functions. DCs imprint naïve lymphocytes to express gut-homing molecules, α4β7 and CCR9 (55), and are also able to drive differentiation of naïve CD4 T-cells into regulatory T-cells (Tregs) (56,57). Several mechanisms seem to be responsible in supply of luminal antigens to DCs in healthy state. Goblet cells have been proposed to act as a conduit of that deliver antigens to DCs (58). Another proposed mechanism is that macrophages may acquire antigens by extending transepithelial dendrites, and then

transferring the luminal antigens to DCs via gap junctions (59). Whilst there is some evidence for this in mice (60,61), it is not known whether human intestinal macrophages can also sample luminal antigens in the same way. However, there is also evidence that DCs themselves can extend their dendrites through the epithelial tight junctions to sample the luminal antigens (62). Interestingly given that DCs express tight-junction proteins such as occludin, CLDN1 and ZO-1, the extension of their dendrites through the epithelial cells may not compromise the integrity of the epithelial barrier.

Recent evidence suggests that macrophages also regulate the adaptive immune response in the gut. Macrophages that are directly positioned beneath the epithelial surface are known to be more tolerogenic. This may in part be due to their exposure and take up antigenic material, including food and bacterial particulates, as it emerges from the basolateral epithelial surface (63). Given their high levels of MHCII expression, intestinal macrophages are also considered as APCs (64). Indeed, there is evidence that intestinal macrophages drive differentiation of naïve $CD4^+$ T-cells to Treg (65). However, there is some debate over how macrophages achieve this, as in healthy state, naïve T-cells are absent from the mucosa (66) and intestinal macrophages cannot activate naïve T-cells or migrate to MLNs (67). One possibility is that intestinal macrophages drive maintenance and expansion of Treg cells that have migrated from MLN to mucosa through production of IL-10 (68,69). Interestingly, production of IL-10 by intestinal macrophages is increased after bacterial stimulation (70,71), with evidence that this is dependent on presence of the commensal bacteria in the gut lumen (72). Another possible mechanism, as mentioned above, is that macrophages may transfer antigens to DCs, which in turn migrate to MLNs.

Resident Lymphocytes

In addition to iMNPs, the intestinal LP also contains T-cells and B-cells. Upon reaching the intestinal endothelial venules, the gut-imprinted, α4β7 and CCR9 expressing lymphocytes engage locally expressed MAdCAM, leaving the circulation to enter the intestinal LP.

There are phenotypic and functional differences in lymphoid cells between small intestine (SI) and large intestine (LI), which may be due to differences in nutrient adsorption and luminal bacterial content (73–75). However, these differences have not been fully delineated. For example, there is evidence that in mice, in contrast to the small intestine, B-cells are the predominant lymphocyte present in the LP of the

large intestine (76). Furthermore, there are variations in the functional state of the lymphocytes; for examples, IL-4 producing T-cells have been detected in SI but not in LI, and the percentage of IL-2 producing cells was higher in SI than LI as well (77).

Further differences between SI and LI have been noted in isolated lymphoid follicles (ILFs), develop after birth in the small and large intestines (SI and LI) and represent a dynamic response of the gut immune system to the microbiota. Unlike ILF in the SI, the microbiota inhibits ILF development in the colon (78). The importance of ILFs in the LI is related to their ability to produce IgA, which is one of the most important molecules in the regulation of intestinal homeostasis. Whilst it has been known that B-cells in SI Peyer's patches produce IgA, it is now recognised that B-cells in ILFs carry the same function in the LI. Interestingly, ILF density is inversely proportional to CD25+ Treg population (78).

1.1.2.3 Controlling the permeability and homeostasis

Tight Junctions (TJs)

In addition to the other functions described above, the IECs also play an essential role in intestinal permeability properties and homeostasis, by controlling active transcellular and passive paracellular (intercellular) routes. The coordination between these two pathways serves as the mechanism that creates cell polarization and ensures fluid and solute movement across.

It is well-established that TJ control paracellular permeability (79–81). TJs are complex, charge-selective pores that encircles the apical and lateral surfaces of adjacent cells, controlling the paracellular permeability properties (79), with up to 40 proteins in their structure (82). TJs have four main structural proteins: occludins, junctional adhesion molecules (JAM), tricellulin and claudins (CLDN). These transmembrane proteins in TJs are connected to the cellular cytoskeleton via their PDZ domains, which bind to adaptor proteins such as zonula occludens-1-3, (ZO-1, ZO-2, ZO-3), MAGI-1, or MUPP-1 (83,84). ZO molecules directly bind the actin cytoskeleton (85) (Figure 1-2).

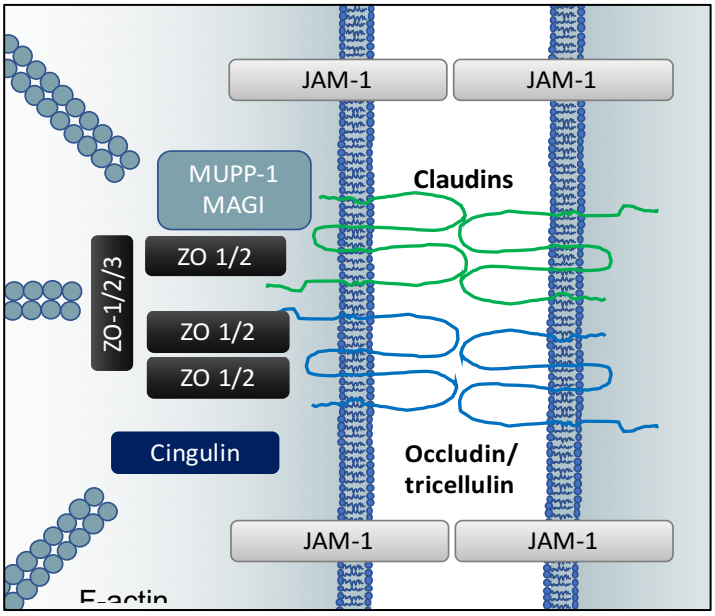

Figure 1-2 – **Schematic diagram of a tight junction (TJ).** *TJs consist of primarily 4 groups of transmembrane proteins (JAM-1, claudins, occludin and tricellulin). Of these, claudins are thought to control the charge-selective properties of TJs. These molecules interact with the cellular cytoplasmic structures, such as actin via adaptor proteins such as ZO-1 to ZO3, MUPP-1, MAGI and cingulin.*

Of the four components of TJs, tricellulin forms a barrier to macromolecules in tricellular tight junctions without affecting ion permeability (86), whilst TJ integrity and characteristics are independent of occludin (87). Occludin knockout mice have normal functioning TJs; however, these mice have significantly reduced chief and parietal cells in the gastric mucosa, suggesting that occludin plays a role in cell differentiation in certain organs (87).

Claudins (CLDNs)

CLDNs are the primary components that control the paracellular permeability characteristics of TJs (88–90). So far, 27 members of the CLDN family have been identified in mammals (91). CLDNs have a molecular weight between 22-27 kDa and are highly conserved across species (90). CLDNs are tetraspan membrane proteins, with two extracellular loops. CLDNs controls the charge selectivity of TJs through their first loop which contains several charges amino acids, which vary across different CLDN molecules (92). The second extracellular loop forms dimers with CLDNs on opposing cell membranes (93). The intracellular carboxy-terminal tail, which contains a PDZ-interacting domain, has the most heterogeneity amongst CLDNs (94).

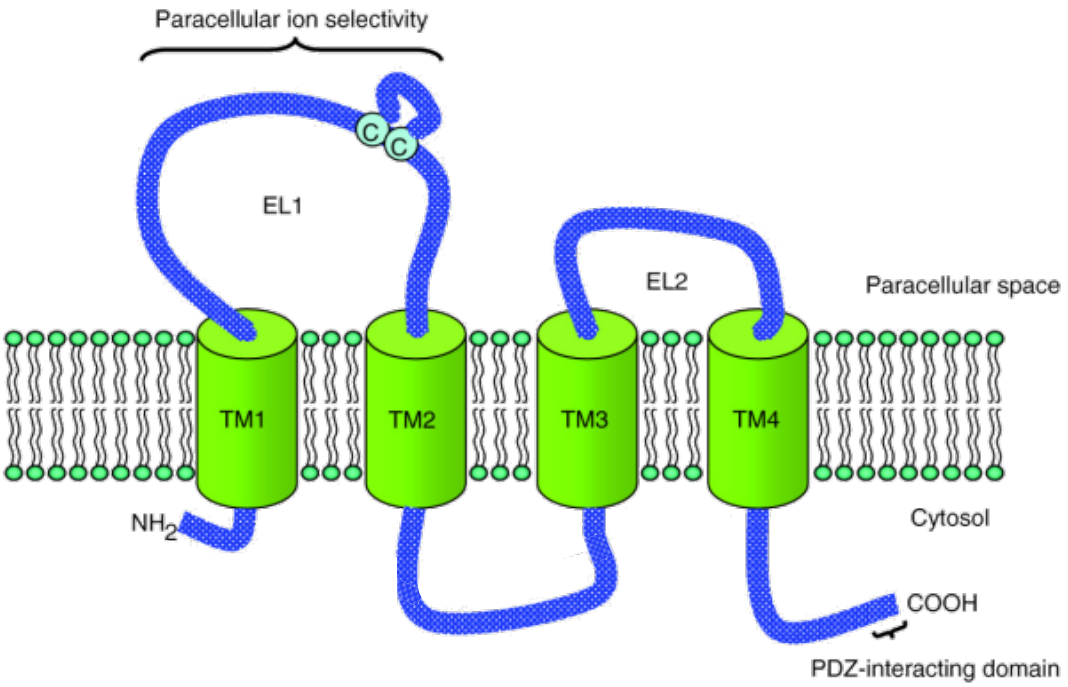

Figure 1-3 – **Schematic representation of a CLDN molecule.** *CLDNs are tetraspan molecules with 4 transmembrane domains (TM1 to TM4), two extracellular (EL1 and EL2) loops, and carboxy-terminal tail which contains a PDZ-interacting domain. Modified from Lal-Nag, et al.* (95)

The coding sequences of most mammalian claudin messenger RNAs (mRNAs) are encoded by only one exon. However, coding sequences of claudins 1, 7, 10, 11, 15, 16, 18, 19, and 25 are composed of several exons. For some of these mRNAs, splice variants have been reported that result in different protein isoforms.

The function and role of CLDNs in the intestine are poorly understood. CLDNs have been divided into two functional groups of “tight” or sealing CLDNs, and “leaky” or pore-forming CLDNs, based on changes to electrical resistance of cultured epithelial monolayers after changes to expression of individual CLDNs (see 56 for detailed review). The overall properties of the TJ, however, are dependent on the complement of other claudins expressed in the TJ. Claudin-1 has barrier-forming properties, and important in the TJ integrity (97). Claudin-2 increases paracellular permeability to sodium and water (98). Claudin-3 has been classified as barrier forming in the intestine, but the converse effect has been reported in lung alveolar epithelia (99). Claudin-5 appears to have barrier forming properties (100), whilst evidence for Claudin-7 functions is conflicting, and reports of Claudin-7 have been made as an anion pore or cation barrier in kidney. In the intestine, Claudin-7 appears to contribute

to barrier function, as loss of Claudin-7 increases paracellular movement of small organic solutes (101). Claudin-8 reduces permeability to monovalent cations (102). Table 1-1 summarises current understanding of the properties of the colonic CLDNs.

Barrier	Cation	1 (103), 3 (104), 4 (105), 5 (106), 8 (102,107,108)
	Anion	7 (109–111)
Pore	Cation	2 (112,98,113), 12 (113)

Table 1-1 – **List of CLDNs expressed in the human large bowel, and their effect on the permeability of the TJs**

In the intestine, the composition of epithelial claudins varies spatially, both along the length of the GI tract as well as in the crypt–luminal axis (114,115), (Figure 1-4). However, the mechanism that control this spatiotemporal expression are not currently understood. So far, CLDNs 1, 2, 3, 4, 5, 7, 8, and 12 have been described in the large intestine (115).

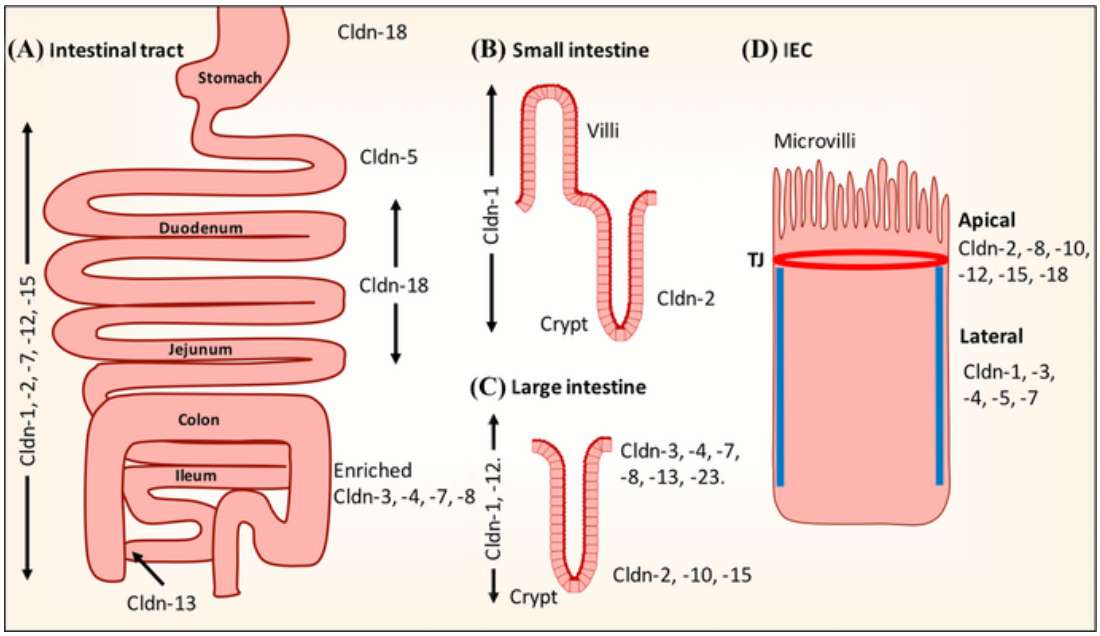

Figure 1-4 – **Schematic representation of reported claudin expression in the GI tracts.** *(A) Along the intestinal tract. (B and C) Crypt–luminal axis of small and large intestine. (D) Membrane distribution in the TJ or in the lateral membrane of intestinal epithelial cells. (Cldn, claudin; IECs, intestinal epithelial cells.) – reproduced from Garcia-Hernandez et al* (115)

In addition to their role in controlling barrier function, CLDNs also appear to regular epithelial homeostasis, proliferation and differentiation (116,117). The mechanisms by which CLDNs influence this homeostasis is poorly understood. It is clear that CLDNs respond to intra-cellular and extra-cellular stimuli. Inflammatory mediators, such as TNF-α and IFN-γ, regulate CLDN expression. During active inflammation there is up-regulation of expression of CLDN2 (118–122), and CLDN12 (118), whilst CLDN7 and CLDN8 are down-regulated (119). Reports on CLDN3 and CLDN4 are conflicting (119,122,123). Changes in expression levels of various CLDNs have bene reported in patients with intestinal inflammation. During an active episode of UC, there is up-regulation of expression of CLDN2 (118–122), and CLDN12(118), whilst CLDN7 and CLDN8 are down-regulated (119). Reports on CLDN3 and CLDN4 are conflicting (119,122,123). Mice models of colitis are more consistent, with reported up-regulation of CLDN-2 (124), and down-regulation of CLDN1 (124,125), 3 (124,125), 5 (124), 7 (124), 8 (124,125). CLDN expression also appears to be influenced by inflammatory cytokines such as TNF-α and IFN-γ that are grossly elevated in colitis patients (120,121,126).

Limited information is available on the transcriptional programs that control CLDN gene expressions. Almost all CLDNs contain a PDZ binding motif, which associates with sub-membrane plaque proteins containing PDZ domains and serve to organise TJ structure. However, the mechanisms that control the association between different claudins with specific plaque proteins are poorly understood.

1.2 ULCERATIVE COLITIS

Inflammatory bowel disease (IBD) encompasses a collection of chronic relapsing-remitting inflammatory diseases predominantly affecting the gastrointestinal tract. Ulcerative colitis (UC) and Crohn's disease (CD) are the two principal sub-types, the aetiologies of which remain poorly understood.

1.2.1 EPIDEMIOLOGY

1.2.1.1 Prevalence and Incidence

The incidence of ulcerative colitis is 1.2 to 20.3 cases per 100,000 persons per year, and its prevalence is 7.6 to 246.0 cases per 100,000 per year, as compared with an incidence of 0.03 to 15.6 cases and a prevalence of 3.6 to 214.0 cases per 100,000 per year for Crohn's disease (127). The highest incidence and prevalence of inflammatory bowel disease are seen in the populations of Northern Europe and North America (128), and lowest in continental Asia (129), and the incidence and prevalence has been raising globally over the last few decades (128).

No sex predominance exists in UC (130–132), and the peak age of onset is in the third decade of life, with a second peak in the sixth decade (132,133). Both the prevalence and incidence of UC has been increasing world-wide over the last century (128), with the highest incidents in northern and western Europe, Canada and Australia (128,130,134). The risk of developing ulcerative colitis in children of migrants from low-incidence to high-incidence countries is similar to non- immigrants (135–137). The trend is also reported in Asia, Middle East and South America (138–141); however, this may be confounded by increasing awareness of UC in these countries.

1.2.2 PATHOGENESIS

Existing literature often describes the pathogenesis of UC and CD together, although important differences exist. The current prevailing hypothesis for pathogenesis of UC is that an abnormal innate immune response in genetically susceptible individuals, combined with environmental factors, result in excessive activation of the adaptive immune system within LP (142,143).

1.2.2.1 Genetic features

There is evidence that differences exist between ethnic populations (144), with higher incidents of UC in Caucasians (145) and the Ashkenazi Jewish Population (146). The concordance rate of UC is 15.4% in monozygotic twins and 3.9% in dizygotic twins

(147). There is a genetic susceptibility, with first-degree relatives of patients with UC at higher risk of developing the disease (148,149).

Genome-wide association studies (GWAS) have so far identified 163 risk susceptibility loci in patients with IBD, of which 110 are shared between UC and CD, and 23 are specific to UC (150). A number of these loci specific to UC are implicated in barrier function and epithelial restitution. These genes include CDH1 (cadherin type 1, a major component of the adherens junction and an important mediator of intercellular adhesion and mucosal repair (151), LAMB1 (laminin-β1 subunit, expressed in the intestinal basement membrane (152), HNF4A (hepatocyte nuclear factor-4α, a transcription factor which regulates expression of key components of the cell-cell junction). Several risk loci linked to other immune system–mediated diseases are associated with ulcerative colitis, particularly HLA-DR and genes involved in helper T-cell types 1 and 17 (Th1 and Th17) differentiation, such as IL-10, IL-7R, IL-23R, and IFN-γ (153).

NOD2

The first genetic variant significantly associated with CD was discovered in the gene encoding nucleotide-binding oligomerization domain 2 *(NOD2),* located on Chromosome 16q12 (154,155). Individuals heterozygote for one of the NOD2 variants have a two- to four-fold risk of developing CD, whilst individuals' homozygote or compound heterozygote have a 20-40 fold risk (156). What is striking is that whilst NOD2 frameshift mutations confer a higher risk of developing CD (Odds Ratio 5.576, p value < 1.62×10^{-10}), it confers protection against developing UC (OR 0.8332, p value = 0.2365) (157). Even though this did not reach statistical significance in UC, it highlights important differences in pathophysiology between CD and UC.

1.2.2.2 Environmental features

In addition to genetic variations between ethnic populations, it is now well established that the incidence increases with a westernised lifestyle and diet (158–160). Smoking confers protection against UC, with patients having milder disease, reduced need for medication and hospital admission (161). Appendisectomy also confers protection if performed early in life (162).

1.2.2.3 Dysbiosis

Dysbiosis, the imbalance of the gut microbiome, may disturb the delicate balance of commensal-host homeostasis, and either result or predispose to inflammation (163).

Dysbiosis is present in patients with IBD as characterised by a higher ratio of pathogenic to commensal bacteria (164), and there is evidence that the density of microbiota is greater in patients with UC or CD than in healthy control subjects (165). While the gut microbiota in healthy subjects show little temporal change, the gut microbiota in IBD patients appear to be unstable (166). The composition of the gut microbiota also differs between active and quiescent stages. A longitudinal study of the gut microbiota in UC patients, conducted for one year, demonstrated that the gut microbiota was unstable in patients with UC even in remission (167). Before relapse of UC, normal anaerobic bacteria such as *Bacteroides*, *Escherichia*, *Eubacterium*, *Lactobacillus* and *Ruminococcus* are decreased and the gut microbiota is also reduced (168).

Moreover, medication also affects the composition of the gut microbiota. Mesalazine, for example, reduces the total bacterial number to almost half (169). A recent study of intense Faecal Microbiota Transplantation (FMT) in patient with UC showed some clinical efficacy (27% steroid-free in FMT group vs 8% in placebo group) (170). In patients with CD there is also ample evidence that modulation of bacteria with antibiotics such as ciprofloxacin is beneficial (171).

Currently, whether dysbiosis is a cause of effect of inflammation and medication in patients with IBD is unclear.

1.2.2.4 Epithelial barrier defect

The epithelial cells in the colon (colonocytes) and the mucous are strongly implicated in the pathogenesis of UC. The colonocytes in patients with UC have reduced expression levels of PPAR-γ, a negative regulator of NF-kB-=dependent inflammation (172,173). These patients also have depleted goblet cells in their colon (174). This is consistent with a reported reduction in trefoil factors, a family of goblet cell derived proteins that are produced in response to mucosal injury and are thought to play a part in mucosal barrier integrity (175,176).

Whilst the inner mucous layer in colon is sterile and impenetrable to bacteria in healthy individuals, in patients with UC, bacteria can penetrate and reach the epithelial cells (174), suggesting a fundamental reduction in barrier function of the epithelial cells and the mucous in patients with UC. This is in keeping with evidence of increased permeability in colon of patients with UC, even during the quiescent state (177,178). The evidence that abnormal permeability may trigger inflammation has been supported by animal studies as well (179).

1.2.2.5 Aberrant immune response

There is increasing evidence that UC and CD develop from different immune abnormalities.

In a series of studies, Professor Segal has demonstrated impaired influx of granulocytes into skin windows and intestine of patients with CD, suggesting that CD may in fact result from an initial weak inflammatory response to clearance of faecal matter in the intestine (180). Impaired recruitment of neutrophils to skin windows injected with heat killed *Escherichia coli* (Hk*Ec*) in patients with quiescent CD (181), provided further evidence that CD is a systemic disease involving the innate immune system and not a gut-specific disease. Notably, impaired bacterial clearance was evident for high, but not low, bacterial doses – an observation that may explain why CD predominantly afflicts the gut. The patients' neutrophils responded normally to in vitro exposure to known chemoattractants. However, following activation with bacterial antigens, macrophages derived from blood monocytes of CD secreted significantly reduced levels of proinflammatory cytokines and chemokines necessary for recruiting neutrophils, most notably TNF-α (181,182). This evidence suggests that CD may be a macrophage primary immunodeficiency disease.

The immune system defects in UC have not been studied as well as in patients with CD. However, current evidence suggests that in contrast to CD, patients with UC have a prolonged acute inflammatory response with concurrent elevation of CXCL10 in circulation. The increased expression levels of CXCL10 have been observed in the colonic mucosa of patients with active UC (183), as well as in response to bacterial stimulation with Hk*Ec* (184). CXCL10 is secreted by a number of cell types, including monocytes and epithelial cells in response to both IFN-γ and IFN-α/β (185), and plays a key role in the integrin activation and migration of cells, including activated T cells (186,187). This abnormal response appears to be due to an aberrant TLR-4 signalling pathway in macrophages of patients with UC, resulting in the over-expression of molecules associated with leukocyte recruitment and activation (PMID: 20360984). Eldelumab is an anti-CXCL10 (also known as IFN-γ-inducible protein 10 [IP-10]) is in clinical trials for patients with IBD (188,189).

1.2.3 PRESENTATION

1.2.3.1 Clinical presentation

Clinical presentation of UC and CD can be very similar with abdominal pain and diarrhoea. However, a hallmark of UC is per rectal bleeding, which is very rare in CD.

On the other hand, patients with CD can suffer from perianal disease (e.g. anal fissures, anorectal abscess), and fistulas, which do not affect patients with UC. UC is a disease of the large bowel and does not affect the rest of the GI tract; CD, on the other hand, can affect any part of GI tract from mouth to anus, though the highest incidence is in the terminal ileum (TI).

Patients with UC usually present with frequent bowel movements, which can be small in volume because of rectal inflammation. Associated symptoms include colicky abdominal pain, urgency, tenesmus, and incontinence (190).

The onset of symptoms is usually gradual and may be preceded by a self-limited episode of rectal bleeding that occurred weeks or months earlier.

Patients may also suffer from systemic symptoms such as fatigue, and weight loss, as well as joint pains, eye problems such as uveitis and episcleritis, and skin issues such as erythema nodusum and pyoderma gangrenosum. Some patients may also develop primary sclerosing cholangitis (PSC), an autoimmune condition affecting the biliary tree.

1.2.3.2 Endoscopic and Histopathological Evaluation

In UC, the inflammatory changes invariably start at the rectum, and then extend in a proximal, continuous and circumferential fashion to involve other parts of the colon. The inflammation in UC is superficial, affecting the mucous. This is different to CD, a condition in which the inflammation is transmural, affecting the full thickness of the bowel. The endoscopic findings in patients with UC include loss of vascular markings due to engorgement of the mucosa, mucosal granularity, petechiae, exudates, erosions, friability, and spontaneous bleeding, depending on the severity of inflammation.

Histological abnormalities in UC include crypt distortion and atrophy (191,192), increased lymphocytes and plasma cells in the LP (basal plasmacytosis), reduction in number of goblet cells or depleted mucin within cells (191), and Paneth cell metaplasia (193,194)

Paneth cells are extremely uncommon in the healthy state of the distal colon (distal to sigmoid). However, in UC, there is significant increase in number of Paneth cells, known as Paneth Cell Metaplasia, which is related to epithelial regeneration and repair (195).

1.2.3.3 Increased risk of colorectal cancer

UC patients, as well as CD patients with colonic disease, are at an increased risk of developing colorectal cancer (CRC) (196,197). Over time, and with treatment, the risk has decreased and may be approaching that of the general population; however, certain populations are still at an increased risk of developing CRC, such as those with increased duration of disease, involvement of longer colon segment, uncontrolled inflammation, and those with PSC (198,199). The reasons for this reduction in risk of developing CRC are not completely clear. However, it may be at least partially related to the bowel cancer screening program (200).

1.2.4 CURRENT TREATMENT OPTIONS IN UC

Currently, there is no cure for either UC or CD, and the primary goal of treatment is to induce and maintain remission, with the long-term aim of preventing complications, which in the case of UC include colectomy and CRC. Despite the differences between CD and UC, currently the current treatment options for both overlap, with the aim of reducing the chronic inflammation.

During acute or severe inflammation, steroid therapy, oral or intravenous depending on severity, is the mainstay. Close monitoring of the inflammatory response (using markers such as C-reactive protein and direct visualisation of the mucosa using endoscopy) is crucial as some patients require step-up treatment to stronger immunosuppressant medication such as cyclosporine or biologic agents, such as infliximab (201).

In patients with mild-moderate disease, first line therapy is the 5-aminosalicylates (5-ASA) drugs, either orally or topically (suppositories or enema). Whilst the mechanism of action of 5-ASAs has not been delineated, there is evidence of reduction of the total luminal bacterial number in patients on 5-ASA drugs (202). Immunomodulators, such as thiopurines (azathioprine or 6-mercaptopurine) may be required in patients who have repeated bouts of flare-up whilst taking 5-ASAs (201).

Anti-TNF-α drugs, such as infliximab and adalimumab, are biologic drugs that are effective at inducing and maintaining remission in moderate to severe disease (203–206). Vedolizumab, is another biologic agent, which blocks the adhesion molecule α4β7 integrin and is approved for moderate to severe ulcerative colitis (207). The α4β7 integrin is expressed on T cells and specifies the recruitment of T cells to the intestinal mucosa by interacting with its ligand MAdCAM-1 (208)

Despite advances in medical therapy, the life time risk of surgery in UC remains at 30-40% (209). Whilst colectomy offers a “cure” for UC, it is not without significant risk. The most commonly performed surgery for ulcerative colitis is restorative proctocolectomy with ileal pouch-anal anastomosis (IPAA). Following IPAA, postoperative complications can occur in up to 33% of patients (210).

Other components of the inflammatory response are being targeted by the newer agents, with up to 27 new drugs for UC in either active clinical trials, or recently completed trials (211). These include agents targeting pan-Janus Kinase Inhibitor, monoclonal antibody blocking the β7 subunit of the heterodimeric integrins α4β7 and αEβ7, and an anti-α4 integrin therapy (AJM300) (212).

1.3 ANIMAL MODELS OF COLITIS

Mice are the most commonly used animal model for experimentation. However, unlike humans, mice do not develop IBD. Hence, several models of colitis have been developed in mice, each causing inflammation through a different pathway, and none perfectly mimics the human disease. Since the aetiology of IBD is still unknown, these varied mouse models of colitis are helpful in studying the varying possible mechanisms, from the effect of epithelial cells, to the role of innate or adaptive immune system. Here, the different models of colitis in mice are summarised and discussed.

1.3.1 MODELS OF COLTIS IN MICE

1.3.1.1 Chemical Induction

1.3.1.1.1 Dextran Sodium Sulphate (DSS)

DSS is a synthetic sulfated polysaccharide composed of dextran and sulfated anhydro-glucose unit that is added to the drinking water of rodents at concentrations of 1-5% (213). The resultant inflammation has many of the features of UC in humans (214), including weight loss, diarrhoea and blood in the stools. Histological changes in DSS-colitis include mucin depletion and epithelial degeneration leading to the formation of cryptitis and crypt abscesses.

The precise mechanism of inflammation in DSS-colitis is not known. There is differential susceptibility to developing colitis by DSS across different mouse strains (215) suggesting a genetic element. DSS is thought to induce colitis in mice partly by forming nano-lipocomplexes with medium-chain-length fatty acids in the large bowel that can fuse with epithelial cell membranes (214). However, even in C57/BL6 mice

which are known to be susceptible to DSS, germ free mice develop significantly less severe colitis than Specific Pathogen Free (SPF) mice. It has also been shown that after exposure to DSS, the inner layer of the mucous in the large bowel that is normally sterile becomes permeable to bacteria (216). Taken together, these results suggest that a major contributor of the inflammation in DSS-colitis are the commensal bacteria in the gut, and that one major contribution of DSS to development of inflammation is the effect it has on the properties of the mucous, and the effect on epithelial layer. DSS-colitis is the most widely used model of colitis in animals.

1.3.1.1.2 2,4,6- Trinitrobenzene sulfonic acid (TNBS)

TNBS is a hapten, which turns into an antigen when bound to tissue proteins, eliciting an immune response (217). Previous studies have shown that it can elicit the number of immunologic responses and represents both forms of IBD, predominantly CD (218). TNBS can be administered through a trocar needle using a rubber catheter inserted via the anus. The recommended dose of TNBS is 0.5–4.0 mg in 45–50 % ethanol intra-rectally, which varies between different mouse strains. For example, such as SJL and BALB/c mice are highly susceptible, whereas C57Bl/6 and 10 mice are resistant (219). Ethanol is required in a high concentration for the TNBS administration. Ethanol acts as a barrier breaker so that TNBS can enter the mucosa to induce colitis, where it covalently binds to the E-amino group of lysine and modify cell surface proteins (220). However, ethanol itself causes severe inflammation in the intestinal mucosa which makes it difficult to distinguish between the ethanol-induced inflammation and hapten-induced inflammation (221).

1.3.1.1.3 Other chemicals used to induce colitis in mice

Dinitrobenzene sulfonic acid (DNBS): DNBS is similar to TNBS in that they both bind to proteins, and act as a hapten, but unlike TNBS, animals treated with DNBS do not develop granulomas (222).

Oxazolone: Oxazolone is another hapten that is administered intra-rectally with ethanol. The effect is a Th2-mediated acute colitis, and is limited to the distal part of the large bowel only (223). However, it has been suggested that oxazolone-induced colitis is dependent on invariant Natural Killer T-cells (NK-T cells) being produced in presence of IL-13 (224).

1.3.1.2 Bacterial induction of colitis

1.3.1.2.1 Citrobacter rodentium induced colitis

Like the human pathogens, Enteropathogenic and Enterohemorrhagic *Escherichia coli* (EPEC and EHEC, respectively), *C. rodentium* is an attaching and effacing (A/E) pathogen, which subverts innate immune system by effectors into infected enterocytes where they reprogram cell signalling (225). *C. rodentium* results in colitis in mice (226), initially colonising the caecum and then the entire large bowel, causing dysbiosis as a result of overgrowth of *C. rodentium* and reduction of intestinal microbiota diversity (227). *C. rodentium* has been used to investigate the innate mucosal responses to infection.

1.3.1.2.2 Salmonella-induced colitis

The gram-negative *Salmonella typhimurium* and *Salmonella dublin* are food-borne enteric bacterial pathogens that can result in intestinal inflammation. The inflammation has similar phenotype to human UC, including epithelial crypt loss, erosion and neutrophilic infiltration (228). However, given the acute nature of bacterial infections, it is likely that *S. typhimurium* infection is not a good model to study the chronic nature of human UC.

1.3.1.2.3 Adherent–invasive E. coli

The commensal Adherent–Invasive *Escherichia Coli* (AIEC) adheres to both small and large intestinal epithelial cells with equal affinity (229). The phenotype of the inflammation resembles UC (230,231). However, induction of inflammation using AIEC in animals requires mild epithelial damage, such as low-dose DSS treatment, during the entire course of the infection.

1.3.1.3 Genetically engineered models of colitis

In genetically engineered models, an existing gene is activated (or “knocked-out”). These can be either complete knock-out, in the whole animal, or conditional knock-outs, in selected organs. Over the years, many genetic models have been developed, highlighting the complex interplay of different cells in pathogenesis of colitis. Whilst a full review is out of the scope of this chapter, a of these mouse models have been summarised below.

1.3.1.3.1 IL-10-Knock out

IL-10$^{-/-}$ deficient mice develop spontaneous colitis (232). IL-10 plays an important physiologic role in intestinal inflammation by maintaining a check on the pro-inflammatory responses to normal antigens and intestinal microbiome (233).

1.3.1.3.2 TGF-β-Knock out

TGF- $\beta^{-/-}$ mice develops multi-organ dysfunction due to macrophage hyper-activation and reduced regulatory T cell activity, including severe colitis. These mice die within 4–5 weeks (234,235). Whilst the exact role of TGF- β in the intestine remains unclear, it appears to be involved in increased production of IL-10 and down-regulation of IL-12 receptor expression (236).

1.3.1.3.3 IL-2-Knock out

IL-$2^{-/-}$ deficient mice develop inflammation in the large intestine that resembles UC by the time they are 8-9 weeks old (237).

1.3.1.3.4 Atg16l1-Knock out

Mice with Atg16l1 deletion in IECs spontaneously develop transmural ileitis in an age-dependent manner (238).

1.3.1.4 Adaptive transfer models of colitis

In these models, intestinal inflammation is induced by selective transfer of certain cell types to immunocompromised host animals. These models have contributed new insights into the predominant role of T cells for mucosal immune regulation.

1.3.1.4.1 CD45RB High Transfer

Adaptive transfer of $CD4^{+}CD45RB^{high}$ T-cells (naïve T cells) from healthy wild-type (WT) mice into recipients that lack T and B cells induces a pan-colitis and small bowel inflammation 8-9 weeks after T-cell transfer (239,240).

1.4 THE THESIS

1.4.1 OUTLINE OF THESIS

The purpose of the investigations in the current study is to elucidate the role CLDN8 plays in the pathogenesis of inflammation in UC.

In this thesis, the transcriptomic data of patients with UC and healthy controls from an earlier dataset performed by Dr Smith in our lab was examined.

I then characterised and studied *Cldn8* deficient mice, investigating a range of parameters including bowel permeability and transcriptomic profiling, in naïve state and in response to DSS-induced colitis. In this set of experiments, DSS was used to induce colitis for several reasons. Firstly, as described above, DSS causes pan-colitis with histologic similarity with human UC. Secondly, the lab has extensive experience

in using DSS, and finally, a preliminary study in early generations of the *Cldn8*$^{-/-}$ had shown promising results. Backcrossing *Cldn8* deficient mice on other transgenic mice (see above) was not feasible given the funding and time limitations of study.

The hypotheses investigated were:

- *Cldn8* plays a protective role against intestinal inflammation
- Loss of *Cldn8* decreases intestinal permeability
- *Cldn8* plays an important role in keeping the inner layer of mucous sterile

2 Materials and Methods

2.1 UC PATIENTS AND HEALTHY CONTROLS

Human studied were performed by Dr Phil Smith. Patients with UC were recruited from the IBD clinic or endoscopy department at University College London Hospital (UCLH). Healthy control (HC) patients were recruited from the endoscopy department at UCLH undergoing routine colonoscopy; all had macroscopically and microscopically normal endoscopy (241). All subjects were between 18 and 75 years of age. Patients were included in the studies if they had a definite clinical and histological diagnosis of quiescent UC. All patients where on either no or minimal treatment; no patient was on steroids or biologic therapy, with some patients on 5-ASA.

Written informed consent was obtained from all participants. Patient details and clinical information were recorded in an encrypted, password protected database, registered and covered by the Data Protection Act, 1998. Access to this database, and the process of obtaining informed consent from the subjects, was restricted to named individuals with up to date certificates in Good Clinical Practice. Clinical details included were name, date of birth, hospital number, duration of disease, treatment, phenotype based on Montreal classification, comorbidities, current and past medication, smoking status, and family history.

Ethical approval was obtained from the Joint UCL/UCLH Committee for the Ethics of Human Research (project number 02/0324) and the NHS National Research Ethics Service, London-Surrey Borders Committee (project number 10/H0806/115).

Paired mucosal pinch biopsies were obtained from macroscopically normal mucosa of the terminal ileum (TI), ascending colon, descending colon, and rectum. Where possible biopsies were taken from all locations. One biopsy was stored in RNAlater stabilization reagent (Qiagen, Germany) at -80°C, and the other placed in 4% formaldehyde (CellPath, Newtown, UK) for histological evaluation by specialist histopathologists. Blood samples were taken from the study participants at the time of endoscopy.

2.2 *Cldn8*-KNOCK OUT AND WILD-TYPE MICE

2.2.1 *CLDN8*-KO MICE

Animal studies were performed in accordance with the United Kingdom Animals (Scientific Procedures) Act 1986 and European Directive 2010/63/EU on the protection of animals used for scientific purposes.

The *Cldn8*-Knock Out (KO) mice were generated by Lexicon Genetics Corporation. The *Cldn8* gene consists of 1 exon and is on Chromosome 21. The target vector, pKOS-53 with LacZ/Neo cassettes, was targeted to the *Cldn8* gene by homologous recombination. A schematic diagram of the targeting strategy, including the expected sizes of the PCR products for the *Cldn8*-KO mice are depicted in Figure *4-4*. The line was reconstituted from frozen embryos from the Mutant Mouse Regional Resouces Centers (MMRRC) (https://www.mmrrc.org). Embryonic stem cells were re-derived from 129/SvEvBrd-derived embryonic stem cells. *Cldn8* heterozygote mice were therefore bred to C57BL/6J albino mice to generate F1 heterozygous animals. These were intercrossed to generate F2 wild type, heterozygous, and homozygous mutant progeny. We took delivery of the F2 progeny.

All earlier experiments in our laboratory, as well as the majority of literature on experimental colitis in mice have been performed on C57BL/6 black mouse strain. Therefore, the *Cldn8*-KO transgenic mice (F2) were backcrossed on to C57BL/6 black WT mice to generate *Cldn8*-KO mice with a C57BL/6 black genetic background. Briefly, the process involved crossing the *Cldn8*-KO mice with non-pedigreed non-sibling C57BL/6 black WT mice (C57BL/6NCrl strain code 027, bought from Charles River laboratories) for several generations. This backcrossing process is essential to generate congenic strains of mice, where they differ genetically in only one locus (*Figure 4-5*).

Due to naturally occurring genetic drift, a mouse strain will diverge into a genetically distinct sub-strain if its breeding colony is separated from the parental breeding colony. To minimise this potential confounding factor, every 10 generations, the *Cldn8*-KO C57BL/6 black mice were crossed on to non-pedigreed non-sibling C57BL/6 black WT mice to prevent genetic drift.

2.2.2 MOUSE GENOTYPING

Mouse genomic deoxyribonucleic acid (gDNA) was extracted from ear clips. The ear clips were incubated over night at 55ºC in 95 µl of gDNA extraction buffer containing 5 µl of 4mg/ml proteinase K (Qiagen). The samples were vortexed at 1400rpm at 55ºC for 10 min in an Eppendorf Thermomixer Comfort (ThermoFisher, MA, USA) then centrifuged (ThermoFisher) at 28,000 g for 10 minutes to pellet the hair. Samples were subsequently transferred to clean new tubes and boiled at 95 ºC for 5 minutes.

Genotyping was performed by polymerase chain reaction (PCR) of the isolated gDNA amplified with *Cldn8* gene specific primers. For WT mice, DNA266-28 and DNA266-24 primers were used for genotyping (expected size 418bp). For *Cldn8*-KO mice, DNA-266-26 and GT-ires primers were used for genotyping (expected size 351bps) (see Appendix 1 – List of Primers).

The PCR reaction volume was made up of 12.5 µl HotStar Taq Mastermix, 1 µl forward primer, 1 µl reverse primer, 1 µl gDNA, made up to 25 µl with RNase-free water. The final concentration in the reaction volume was 2.5U HotStar Taq DNA polymerase, 1xPCR buffer containing 1.5mM $MgCl_2$, 200 µM of each dNTP, 0.4 µM of each primer and a variable amount of gDNA. PCR was carried out on a DNA Engine Tetrad 2® Peltier Thermal Cycler (Bio-Rad, CA, USA) using the conditions in table 2.2 below for 28 cycles. 5 µl Orange J was added to each 25 µl reaction mix and 15 µl was run on a 1% agarose gel and viewed with a ChemiDoc™ Imager (Bio-Rad).

	Temperature	**Time**
Activated	95 ºC	15 minutes
Denatured	95 ºC	45 seconds
Annealed	60ºC	45 seconds
Extended	72ºC	45 seconds (28 cycles)
Extended	72ºC	10 minutes
Cooled	4ºC	*Ad infinitum*

Table 2.2: PCR conditions for genotyping *Cldn8*-KO and WT mice.

2.2.3 OTHER MICE STRAINS

C57BL/6 mice (C57BL/6NCrl strain code 027) were brought from Charles Rivers laboratories. On transfer of mice into the animal unit at UCL, mice were rested for 7 days before experimentation in order to minimise the effect of stress compromising results.

2.2.4 MICE HUSBANDRY

Colonies were generated from WT and *Cldn8*-KO breeding pairs. Mice were bred and maintained under specific-pathogen free (SPF) conditions till 20 months of age, Biological Sciences Unit, UCL and Royal Free Hospital. Animal rooms were temperature controlled (21 ± 1°C) and with a 12 h light/dark cycle (lights on at 07:00h). Mice were housed 3-5 per cage, with free access to food and water. Cages were cleaned once a week as part of the animal room routine. The conditions were monitored by the Named Animal Care and Welfare Officer (NACWO) in animal facility. Mice were fed with Harlan 2018 Teklad Global 18% protein rodent diet. Normal tap water was used. Routine health screens for infection were carried out for parasites and opportunistic infections. Mice between the ages 6 and 12 weeks were used for experimentation. They were matched for age, sex and weight for each study.

2.2.5 METABOLIC CAGE EXPERIMENTS

Metabolic cages were used to analyse the micturition and faeces production in a controlled environment, whilst enabling measurement of animal's food and water consumption in a set period of time. Mice were placed individually in metabolic cages (UNO BV, Netherlands) and allowed to acclimatise for 5 days. Measurements were taken for 24 hours, after which the animals were culled. The metabolic cage consists of a stainless-steel cage with metallic-mesh flooring placed over a funnel to allow collection of urine and faeces. Within the funnel, there is a trap to capture the faeces, whilst allowing the urine to flow in a small container underneath (see Figure 4-13 for detailed description).

2.2.6 MICE FAECAL WATER CONTENT MEASUREMENT

Mice were given free access to water and food. Individual mice were transferred to a cage with no bedding (to prevent any water absorption from the faeces by the bedding material). Spontaneously defecated stools were collected every 15min into pre-weighed eppendorf tubes (Eppendorf, Germany) to minimise atmospheric water-loss. The faeces were then dehydrated in an oven overnight. The eppendorf tubes containing the faeces were weight pre- and post-dehydration to calculate the water content of the faeces.

2.2.7 MICE FAECAL NA^+ AND K^+ CONCENTRATION MEASUREMENTS

Faecal Na^+ and K^+ concentration was measured using a Corning-400 flame photometer (Corning, USA). To do so, dehydrated faeces were reconstituted in 1 ml of distilled water, and mixed with a plunger and then a needle, to ensure all salts in the faeces had dissolved in the distilled water. To sediment the faecal debris, the tubes were centrifuged at 22,000 g (ThermoFisher) and the supernatant was removed. The supernatant was put through the flame photometer at a dilution of 1:800. To measure the Na^+ and K^+ concentration, the flame photometer was set using a "standard" solution with known concentration of sodium (0.2mM) and potassium (0.24 mM).

2.3 DSS-INDUCED MOUSE COLITIS MODEL

Dextran Sodium Sulphate (DSS) was used to induce colitis in mice. DSS is a powder with a molecular weight of 36-50 kDa (MP Biomedicals, UK) that is dissolved in water and the DSS-water is provided to mice instead of normal drinking water.

Acute Colitis: Male and female mice (6-8 weeks old) were provided regular drinking water (control) or DSS water for 7 days, as described previously (U.42). On day 3, the bottles were re-filled with freshly made DSS solution. On day 7, the DSS solution was replaced with normal drinking water.

Chronic Colitis: Mice were provided with DSS water for 7 days as described above. After 14 days on normal drinking water, one group of mice were subjected to a second bout of DSS for 7 days. A separate group of mice were subjected to a second bout of DSS for 7 days, after 36 days on normal drinking water.

Throughout the experiment (acute and chronic phases), the mice were weighed daily, and percentage weight change was calculated using the following formula:

$$\frac{(\text{“Body weight on a given day”} - \text{“Original body weight”})}{\text{“Original body weight}} \times 100$$

Faeces were scored for diarrhoea (0=normal consistency, 3=pasty stools, 5=watery stools) and blood (0=no blood, 1=blood). Presence or absence of blood was checked using a faecal occult blood test kit able to detect small amounts of blood in the faeces using Hema-screen (alpha laboratories, UK). On completion of the study, animals were culled, and large bowels were removed and assessed for length, and histology.

2.4 CYTOKINE ASSAYS

Mouse serum IL-2, INF-γ, IL-4, IL-10, IL-1b, IL-5, KC/GRO (IL-8), IL-6, TNF-α and IL-12p70 levels were determined using the MSD® Mouse Pro-Inflammatory 7-Plex Ultra-Sensitive Kit (Meso Scale Discovery, US) and read on a SECTOR® Imager 6000 (Meso Scale Discovery).

2.5 RNA PREPARATION AND ANALYSIS

2.5.1 RNA EXTRACTION

Human biopsy samples

Studies in humans were carried out by Dr Phil Smith. To harvest total RNA from each biopsy (~25 mg), samples were lysed using RNeasy Fibrous Tissue kit (Qiagen) RLT buffer and 0.14 M β-mercaptoethanol (β-ME) (Sigma-Aldrich, St. Louis, USA), and then homogenised by centrifugation at 10,000 g through a Qiashredder column (Qiagen), according to the manufacturer protocol. To remove protein, samples were incubated for 10 minutes at 55°C with 10 µl Proteinase K (20 mg/ml) (Qiagen). Total RNA was extracted using the RNeasy® Mini Kit (Qiagen) and eluted to 30µl of RNase free water (Qiagen).

RNA concentration was measured using a NanoDrop ND-1000 spectrophotometer (ThermoFisher Scientific) measuring OD_{260}/OD_{280} and OD_{260}/OD_{230} to assess protein and solvent contamination respectively. Samples were included if they had an optical density ratio reading of 1.8-2.0 OD_{260}/OD_{280} and >1.8 OD_{260}/OD_{230}.

Mouse LI tissue samples

To harvest total RNA, tissue samples were measured to ~25 mg. For RNA extraction, a mechanical disruption method was used to break down tissue samples using a bead, in the presence of β-ME-RLT buffer, at 50 Hz for 5 min in the TissueLyser LT (Qiagen). The solution was centrifuged down at 22,000 g for 5min and the supernatant used for RNA extraction, using the RNeasy Mini kit (Qiagen) according to the manufacturer protocol. To remove protein, samples were incubated for 10 minutes at 55°C with 10 µl Proteinase K (20 mg/ml) (Qiagen).

RNA concentration was measured using Qubit™ RNA HS Assay Kit (ThermoFisher), as per manufacturer instructions.

2.5.1.1 Microarray hybridisation

Human samples

Microarray expression studies in humans were carried out by Dr Phil Smith. For each sample, 500 ng of total RNA was amplified using the Illumina TotalPrep-96 RNA Amplification kit (Ambion, UK) and normalised to 150 ng/µl. For each sample, 750 ng was hybridised to Illumina HumanWG-6 v3.0 Expression BeadChips (Illumina, CA, USA) for 16 hours at 58°C. Following hybridisation Beadarrays were washed, stained with streptavidin-Cy3 (GE Healthcare, UK) and scanned using the Beadarray reader. The image was then processed with GenomeStudio® data analysis software (Illumina).

Mouse samples

For each sample, 500 ng of total RNA was amplified using the Illumina TotalPrep-96 RNA Amplification kit (Ambion, UK) and normalised to 150 ng/µl. For each sample, 750 ng was hybridised to Illumina MouseWG-6 v2.0 Expression BeadChips (Illumina) for 16 hours at 58°C. Following hybridisation Beadarrays were washed, stained with streptavidin-Cy3 (GE Healthcare, UK) and scanned using the Beadarray reader. The image was then processed with GenomeStudio® data analysis software (Illumina).

2.5.2 cDNA CONVERSION AND QUALITATIVE PCR

mRNA was converted to cDNA by oligo-d(T) priming and reverse transcription using the Promega reverse transcription kit, as per manufacturer's instructions. qRT-PCR was performed using QuantiFast® SYBR® Green PCR (Qiagen), as per manufacturer's instructions in triplicates on a Mastercycler® ep *realplex* (Eppendorf). Normalized mean gene expression values ± SD were determined from triplicate cycle threshold (Ct) values for each gene and the housekeeping gene peptidylprolyl isomerase A/cyclophilin A (*PPIA*) or glyceraldehyde-3-phosphate dehydrogenase (*GAPDH*). Relative transcript levels were determined by the 2−ΔΔCt method (242) (see Appendix 1 – List of Primers).

2.6 FLUORESCENCE-ACTIVATED CELL SORTING (FACS)

2.6.1 MURINE LI LP CELL ISOLATION

Following dissection, mouse LI were cut longitudinally and washed in ice cold PBS containing 100 U/ml penicillin, 100µg/ml streptomycin to remove faeces. Epithelial cells were removed by incubation of each large bowel in warmed 20 ml of pre-digestion solution [Hanks balanced salt solution, (HBSS) (GIBCO, ThermoFisher Science) containing 10% FBS, 100U/ml penicillin, 100µg/ml streptomycin and 2mM ethylenediaminetetraacetic acid, (EDTA)] at 37°C, agitated at 250 rpm for 30 min. The remaining LP tissue was diced into 1mm pieces and washed with ice cold PBS to remove EDTA. LP tissue was incubated in warm 20 ml digestion solution [HBSS containing 10% FBS, 100 U/ml penicillin, 100 µg/ml streptomycin, 30mg collagenase (Sigma, USA), 1.6 mg DNase I (Sigma) and 15 mg Dispase II (Sigma)] at agitated at 37°C, 250 rpm for 30 minutes, and vortexed for 20s at the start, middle and end of incubation. Finally, LP cells were passed through a 70 µm filter, washed with ice cold PBS.

2.6.2 MURINE LI LP CELL LABELLING WITH ANTIBODIES

Murine bowel LP cells were incubated with the LIVE/DEAD® fixable blue cell stain kit (Invitrogen L23105), blocked in CD16/CD32 Fc block (eBioscience 16-0161; 1:500) prior to staining with CD45 PerCP-Cy™5.5 (BD 550994; 1:200), CD11b V450 (BD 560455; 1:400), CD11c APC (BioLegend 117309; 1:400) and Gr1 PE (BD 553128; 1:400), F4/80 FITC (eBioscience 11-4801; 1:800), CD3 PE-Cy™7 (BD 560591; 1:800), MHCII AF700 (eBioscience 56-5321; 1:400) antibodies. The cells were fixed in 1% formaldehyde after staining. Cells were run on BD LSR II flow cytometer (BD 338301) after optimization with compensation beads (BD 552845).

2.7 IMMUNOBLOT

To optimise the process of western blotting technique, four methods were used to prepare the epithelial whole cell lysates.

Method 1: Mouse large bowel was removed, and washed with ice-cold PBS solution (Life technologies, CA, USA) to remove faecal material, and agitated at 250 rpm for 30min at 37°C in Hank's balance salt solution (Life technologies) with 2mM EDTA (Life technologies), 10% faecal calf-serum (Sigma) and 5% Pencillin-Streptomycin (Sigma) to dislodge the epithelial cells. The bowel tissue was removed, and the cell-suspension was spun at 500 x *g* for 10min at 4°C to pellet the epithelial cells. Up to 1-2 x 10^6 cells were transferred to 100 µl Laemmli sample buffer containing β-ME (Sigma), protease inhibitor (Roche, Switzerland) and phosphatase inhibitors (Sigma).

Method 2: The epithelial cells were harvested as described in Method 1. However, the cells were transferred to RIPA buffer instead of Laemmli buffer.

Method 3: 2cm of tissue was frozen on dry-ice, and powdered using a pestle and mortar. RIPA buffer, containing protease inhibitor (Roche) and phosphatase inhibitors (Sigma) was added to the powdered tissue and the solution was agitated for 1 hour at 4°C, before being spun down at 22,000 g for 10 min at 4°C. The supernatant was transferred to a fresh Eppendorf tube, sample buffer was added, and the solution was boiled at 98°C for 5min.

Method 4: 2cm of tissue was frozen on dry-ice, and slowly thawed on ice. Whole cell lysis buffer, containing protease inhibitor (Roche) and phosphatase inhibitors (Sigma) was added and the tissue was mashed in the Eppendorf tube using a small pestle. The mashed tissue was incubated on ice for 10min before being spun down at 22,000 g for 10 min at 4°C. The supernatant was transferred to a fresh Eppendorf tube, sample buffer was added, and the solution was boiled at 98°C for 5min.

Samples were run on SDS-PAGE gels and transferred onto Hybond-P PVDF membranes (Amersham, GE Healthcare). Membranes were blocked in 5% non-fat milk for 1 hour then probed with primary antibody overnight at 4°C. Membranes were washed in Tris-buffered saline Tween-20 (TBST) then probed with HRP-linked secondary antibody for 1 hour at room temperature. Bound antibody was detected using ECL Plus/Prime (Amersham), exposed to Hyperfilm ECL (Amersham).

2.8 HISTOLOGY AND IMMUNOHISTOCHEMISTRY

2.8.1 HISTOLOGY OF MOUSE LI

Mouse large bowel tissue was fixed in 10% neutral buffered formalin (CellPath) overnight then paraffin-embedded using a Leica TP1050 tissue processor. 5µm sections were cut, underwent automated dewaxing and endogenous peroxidase was blocked using 3-4% (v/v) hydrogen peroxide. The tissue was blocked with 5% Goat Serum (Sigma G67G7) (diluted in distilled water) and stained in VFM Harris' hematoxylin (CellPath), differentiated in 0.2% acid alcohol and stained in Eosin Y (VWR) using a Leica ST4040 linear stainer and mounted in Pertex (Leica).

Immunohistochemical (IHC) analysis for *Cldn8* detection were carried out using the automated Bond-Max system (Leica Biosystems Newcastle, Ltd.) using on board heat-induced antigen retrieval (Bond epitope retrieval solution ER2 for 30 min). Endogenous peroxidase activity was blocked using 0.3% hydrogen peroxide for 5 min. The histological specimens were incubated with the Primary Antibody for 60 min at room temperature. Before the application of the Polymer reagent, the sections were incubated for 30 min at room temperature with 5% Goat Serum (Sigma G67G7). The blocking reagent were diluted with distilled Water. The slides were incubated with Goat Anti-rabbit Poly-HRP-IgG (Polymer reagent) for 60 minutes at room temperature. The reactions were developed using a Bond polymer refine detection kit and followed by colour development with 3,3′-diaminobenzidine tetrahydrochloride as a chromogen for 10 min. During the optimisation process, four different commercially available anti-*Cldn8* antibodies were used (Invitrogen; GeneTex; Santa Cruz; IBL) at different concentrations (1:100, 1:200, 1:400, 1:800). Slides were imaged with a Hamamatsu NanoZoomer 2.0-HT C9600 (Hamamatsu, UK).

2.8.2 *IN SITU HYBRIDIZATION* AND MUCOUS IMMUNOSTAINING

Mouse bowel was stained with DAPI (to stain DNA), anti-MUC2 antibody (to visualise the mucous), and EUB338 (to visualise the luminal bacteria). See Appendix 1 – List of Primers for EUB338.

For *in situ hybridisation* of bacteria and mucous staining, bowel sections were fixed in methacarn, a water-free fixative, to preserve the mucous. Mouse intestine was cut around the most distal faecal pellet. A water-free paraffin embedding process was used to preserve the mucous (Dry methanol 2x 30 min, Absolute ethanol 2x15 min, 1:1 Absolute ethanol/Xylene15 min, Xylene 2x15 min). Paraffin sections were initially dewaxed. The process of dewaxing involved incubating the slides in xylene substitute

twice, 10 min each, followed by 5 min in 100% ethanol, followed by 5 min in 95% ethanol, before air-drying the slides. The process was performed at 60°C. For hybridisation, 500-800 ng of EUB338 probe (Sigma, conjugated with Cy5.5) was added to 100 µl pre-warmed hybridization solution. 50 µl probe-hybridization solution was added to the sections before being covered with glass and incubated over night at 50°C in a humidity chamber. The slides were then washed for 5 min at 50°C using pre-warmed wash solution.

Immunostaining was carried out at 4°C. The slides were rinsed with cold PBS, solutions added as a drop on the sample, and blocked in 5% FCS in PBS for 1h at 4°C, before being incubated with primary antibody (anti-MUC2, Santa Cruz sc-13312) diluted in 5% FCS (1:50) in a humid chamber at 4°C overnight. The slides were then wash 3 times in cold PBS, before being incubated with secondary antibody (conjugated with a fluorophore) diluted in 5% FCS (1:2000), dark at 4°C overnight (ThermoFisher, A-21088, conjugated Alexa Fluor® 680). DAPI (ThermoFisher) was added to the slides for 5 min, to stain for DNA, before being washed with PBS and mounted in a small volume of Prolong Anti-fade (Molecular Probes, P36930), and left to set at room temperature overnight.

2.9 MICE *IN VIVO* COLONIC PERMEABILITY STUDIES

Female *Cldn8*-KO and WT mice were anaesthetized with an intraperitoneal injection of Ketamine 100mg/kg mixed with xylazine 10mg/kg and maintained at 37°C on a thermostatically controlled heating blanket (Harvard Apparatus Ltd, Edenbridge, Kent, UK). The peritoneal content were exposed, ensuring no damage to the intestine during the procedure. A two-centimetre-long self-contained segment of large bowel was created. To create a self-contained segment of the bowel, two cuts were made in the bowel, and both ends tied with a string. The distal cut was made in the most distal part of the large bowel that could be reached in the pelvis without damaging other organs; the distal end of the segment was therefore within 1-cm of the rectum (see Figure 4-1 for graphical representation). Cuts in the bowel were made only to part of the lumen, and not the full width, to avoid damaging the mesentery and its blood supply (Figure 4-1-c). The lumen was cannulated from the proximal end with a fine plastic tube attached to a syringe. The segment was then flushed with warm 0.9% saline to remove any faecal material, followed by air to remove the saline. A uptake buffer containing ^{3}H-mannitol (0.037 MBq) and FITC-Dextran (50mg/ml) was instilled into the lumen and the segment tied off. The volumes instilled into the lumen was 90µl and was chosen in order to fill the intestinal segment whilst avoiding

distension. Care was taken to avoid instilling air into the lumen. Blood (0.5 ml) was collected after 30 min by cardiac puncture and centrifuged at 1500 g for 10 min to obtain plasma. The segment of intestine was removed, and the length and dry weight (after drying over-night in oven) was recorded. The permeability of the intestine was calculated by measuring concentration of ^{3}H-mannitol (PerkinElmer, MA, USA) and FITC-Dextran (Sigma FD40S) in plasma and stock solution, and factoring the dried weight of the segment, and the animal's weight (as a surrogate marker for the blood volume). To measure the radioactivity, 50 ml of the plasma, and 50 ml of stock solution (diluted 1:10 in uptake buffer) were made up to 5 ml in UltimaGold^{TM} (PerkinElmer). The radioactivity was measured in the final solution using Tri-Carb 2900TR Liquid Scintillation Analyzer (Packard BioScience, MA, USA). The final measurement is expressed as a percentage of radioactivity absorbed. To measure fluorescence from FITC-Dextran, FLUOstar Omega (BMG Labtech, Germany) was used to measure fluorescence of FITC; for the measurements, 50 ml of stock solution was used for the standard curve, diluted in naïve serum; and 50 ml of serum from the mouse under experiment.

2.10 REAGENTS

2.10.1 BUFFERS

DNA extraction buffer:

1 ml 1 M Tris pH8 (VWR 103156X), 100 µl 0.5M EDTA (Sigma E6511), 2 ml 1 M NaCl (Sigma S7653) and 50 µl 1% SDS (Sigma L3771) were added to 6.85 ml of distilled water (dH_2O).

3x Laemmli sample buffer

2.4 ml 1 M Tris-HCl pH 6.8 (VWR), 3 ml 10% SDS (Sigma), 3 ml 100% glycerol (BDH 101186M), 1.6 ml 2-mercaptoethanol (Sigma 63689) and 0.006g bromophenol blue (Sigma B0126). Stored at 4°C.

10x RIPA lysis buffer (250ml)

25 ml NP-40 detergent, 12.5 ml 20% SDS, 125 ml of 1M Tris-HCL pH 7.4, 12.5 g Sodium Deoxycholate, 75 ml 5 M NaCl, 12.5 g Sodium Deoxycholate, 5 ml 0.5 M EDTA, 7.5 ml water

10x Transfer buffer

144 g glycine (Sigma G7126), 3.74 g SDS (Sigma L3771) and 30.25 g Tris (VWR 103156X) were dissolved, using a magnetic stirrer, in dH_2O and made up to 1 L with dH_2O.

10x Tris-buffered saline (TBS)

800 g NaCl (Sigma), 20 g KCl (Sigma P4054) and 300 g Tris to dH_2O, made up to 10 litres dH_2O, pH 7.4.

TBS-Tween 0.1%

5 ml of Tween-20 (Sigma P1379) were added to 500 ml of 10x TBS and made up to 5L with dH_2O,

FACS buffer (PBS containing 1% BSA and 0.01% azide)

5 g of bovine albumin (BSA)/albumin faction V (VWR 1120180100) was added to a new bottle of 500 ml PBS pH7.2 (Gibco 20012). 500 µl of 10% sodium azide in dH_2O (Sigma S8032) was added to the 500 ml of PBS and stored at 4°C.

Uptake buffer

12 µl of ^{3}H-mannitol, and 60mg of FITC-Dextran, added to 1188 µl Hepes buffer.

Hepes buffer (pH 7.4)

16 mM Na-Hepes (2.08g), 140 mM NaCl (4.09g), 3.5 mM KCL (0.13g), 1 mM Mannitol (0.091g), in 500 ml distilled water

Carnoy (methanol) fixation (Methacarn)

60% Absolute methanol, 30% Chloroform, 10% Glacial acetic acid

Hybridization solution

20 mM Tris-HCl pH 7.4, 0.9M NaCl, 0.1% SDS (optional: can add 5-20% formamide if high background is a problem)

Washing solution (for in situ hybridisation)

20 mM Tris-HCl, pH 7.4, 0.9 M NaCl

2.10.2 SDS-PAGE GELS

Resolving and stacking gel were made up with 30% w/v Acrylamide/ProtoFLOWGel (SLS H16996), 1.5 M Tris-HCl pH8.8 (resolving gel), 1 M Tris-HCl pH6.8 (stacking gel), dH_2O, 10% SDS (Sigma L3771), freshly made 10% ammonium persulphate (Sigma A7460) and TEMED (Sigma T9281) (added in the order listed with TEMED last, just prior to use). The gels were cast using Mini-PROTEAN® System (Bio-Rad)

2.11 STATISTICAL ANALYSIS

Unless otherwise stated, all statistical calculations were performed using GraphPad Prism 6.00 software on Mac (GraphPad Software Inc, USA). A p-value < 0.05 was considered statistically significant. Unless otherwise stated, statistical significance was calculated using a paired or unpaired two-tailed t-test. For multiple comparison between groups, statistical significance was assessed by one-way ANOVA with Tukey-post-test.

2.11.1 ANALYSIS OF TRANSCRIPTOMIC DATA

Human data

Expression data was normalised after log2 transformation within Genome Studio (Illumina, CA, USA) using a cubic spline normalisation. Data was exported without background subtraction. Detection p-values associated with each probe expression value were also exported. These procedures were all carried at the Wellcome Trust Sanger Institute (Cambridge, UK). Probes that reached a minimum detection p-value of $p<0.01$ in at least two biopsies were included in the subsequent analyses. Data was normalised for chip effects using ComBat normalisation using R statistical programming software, an established algorithm for preventing batch effects in microarray (243). The transcriptomic data from Dr Phil Smith has been deposited in the Gene Expression Omnibus (GEO) with accession no. GSE48634

Mouse data

Expression data was normalised after log2 transformation within Genome Studio (Illumina, CA, USA) using a cubic spline normalisation. Data was exported without background subtraction. Detection p-values associated with each probe expression value were also exported. These procedures were all carried at the UCL Genomics Institute. Probes that reached a minimum detection of uncorrected p-value < 0.01 were included in the subsequent analyses. Correction for multiple testing was performed using the False Discovery Rate (FDR) method. Due to the design of samples on the chips, data could not be normalised using ComBat normalisation.

Differentially expressed genes between groups were computed using MultiExperiment Viewer (MEV) TM4 Microarray Software suite version 4.8 (Dana-Farber Cancer Institute, Boston, USA) (244). Probes were identified that reach a minimum raw fold change of 1 between groups. Principle component analysis (PCA) was performed on the initial microarray dataset to determine if mucosal gene expression profiles could be separated according to mouse genotype and stage of

inflammation. PCA is a mathematical technique to reduce the dimensions of a datasets by calculating the principle components (directions) along which variation in a dataset is maximal. PCA was performed using the PCA tool of MeV TM4 Microarray Software suite, with default settings.

FACS Data

All FACS results analysed using FlowJo X 10.0.7 on Mac (Tree Star Inc, USA).

3 Transcriptomic analysis of human colonic biopsy from patients with UC and healthy controls

3.1 INTRODUCTION

As described in Chapter 1.2, UC is a chronic relapsing-remitting inflammatory disease predominantly affecting the gastrointestinal tract. However, the aetiology of UC is not well understood. Studies of twins have demonstrated am elevated concordance rate of UC is 15.4% in monozygotic twins, compared to 3.9% in dizygotic twins (245). GWAS studies have so far identified 163 risk susceptibility loci in patients with IBD, of which 110 are shared between UC and CD, and 23 are specific to UC (150). However, the identified genetic risk factors only account for 7.5% of disease variance in UC (150). This highlights the role of environmental factors in pathogenesis of UC, and the possibility that epigenetics may partially account for the "hidden heritability" in UC (246).

Epigenetic factors, such as DNA methylation, could mediate gene-environment interactions involved in pathogenesis of diseases (247,248). In addition to the effect of epigenetic factors on the phenotype of the individual, there is evidence of inheritability of epigenetic modifications. Studies in mice have highlighted the effect of dietary intake during pregnancy on the epigenetic reprogramming step in offspring during early development, resulting in an increased susceptibility of the off-springs to DSS-induced colitis (249).

The transcriptomic analysis of the mucosa from patients with UC can therefore potentially identify genes that may be abnormally expressed as a result of germline mutations, environmental factors, or secondary to the pathogenic process itself.

A number of transcriptomic analyses have been conducted in tissue (either via endoscopic biopsy or surgical resections) of patients with UC (250–256). However, in most of these studies, samples were obtained from inflamed tissue (253,255–257). This raises the possibility that the changes in gene expression signatures may be due to tissue damage and repair, as well the inflammatory cell infiltrates.

In an attempt to identify molecules which could be causally related to the development of the disease, Dr Smith, a PhD student with Prof Segal analysed the transcriptomic profile of macroscopically non-inflamed mucosa from patients with UC in clinical remission, as compared to healthy controls (241). All patients where on either no or minimal treatment; no patient was on steroids or biologic therapy, with

some patients on 5-ASA. The focus of analyses in this chapter is the analysis of this data with an emphasis on prominent genes involved in epithelial homeostasis.

3.2 RESULTS

3.2.1 PATIENT COHORT AND SAMPLE COLLECTION

Endoscopic pinch biopsies were obtained from around the bowel (*Figure 3-1*) by Dr Philip Smith from 29 patients with histologically confirmed diagnoses of UC and 31 healthy control (HC) patients undergoing routine colonoscopy, aged 18-75 years old at University College London Hospital (UCLH). HC patients were attending for routine endoscopic investigation of gastrointestinal symptoms and all had macroscopically normal colonoscopies and histologically normal biopsies. Samples were collected in two separate cohorts – an initial cohort and then a verification cohort (5 patients with UC and 4 new HC at a later time point; median, 22 months; range, 21–23 months). Phenotypic and demographic information for the patients are presented in Table 3-1.

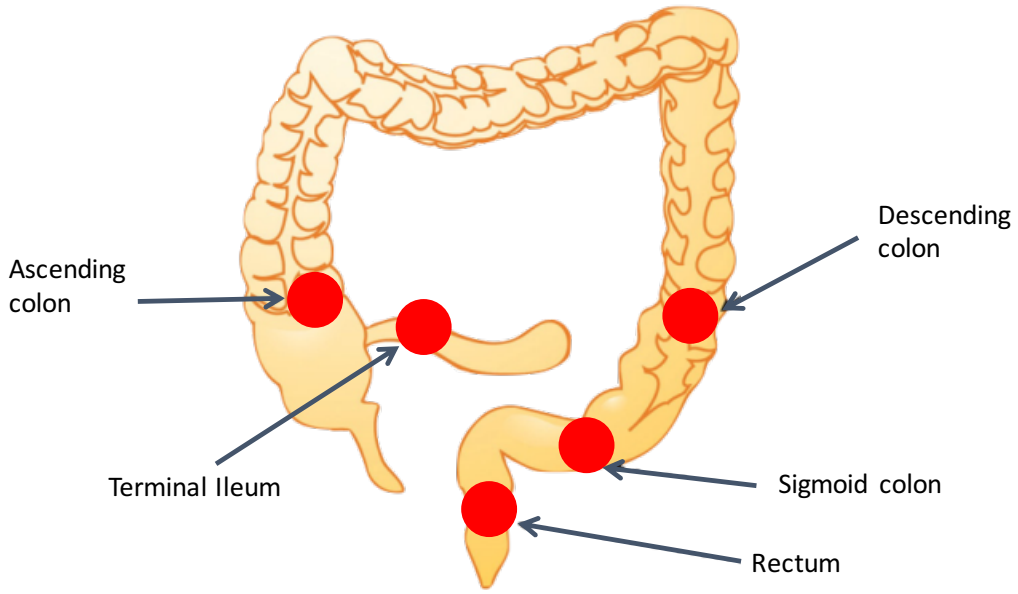

Figure 3-1 – **Location of the biopsies collected during colonoscopy**. *Paired endoscopic pinch biopsies were obtained from macroscopically normal mucosa of the terminal ileum, ascending colon, descending colon, and rectum. Where possible samples were taken from all locations in each subject. One sample was placed in RNA-later stabilization reagent mRNA preparation, and the other was placed in 4% formaldehyde for histological evaluation*.

		UC	HC
Number of patients		24	27
Gender	Male	16	15
	Female	8	11
Age (years) (+/-SEM)		48.3 (+/-3.5)	45.3 (+/-2.9)
Average age at diagnosis (years) (+/-SEM)		30.7 (+/-3.6)	-
Duration of disease (years) (+/-SEM)		17.54 (+/-2.8)	-
Treatment (%)	No treatment	5 (20.8%)	
	5-ASA alone	15 (62.5%)	
	AZA alone	0 (0%)	-
	5-ASA plus AZA	3 (12.5%)	
	5-ASA plus 6-MP	1 (4.2%)	
Phenotype		A1 4	
		A2 16	
		A3 4	
		E1 2	
		E2 11	
		E3 11	
Smoking status (%)	Current smoker	3 (12.5%)	3 (11.1%)
	Ex-smoker	5 (20.8%)	4 (14.8%)
	Never smoked	16 (66.7%)	19 (74.1%)
Family history of IBD (%)		5 (20.8%)	3 (11.1%)
Indications (%)	Establish IBD	0 (0%)	0
	IBD assessment	8 (33.3%)	0
	IBD surveillance	16 (66.7%)	0
	Rectal bleeding		11 (40.7%)
	Exclude IBD		1 (3.7%)
	Diarrhoea		7 (25.9%)
	Surveillance		2 (11.1%)
	COBH		5 (18.5%)
Bowel preparation (%)	Senna and Citramag	21 (87.5%)	19 (74.1%)
	Phosphate enema	3 (12.5%)	7 (25.9%)
	Kleen-prep	0 (0%)	0
	No preparation	0 (0%)	0

Table 3-1 – **Demographics table for initial patient biopsy cohort.** *Phenotypes based on Montreal classification – A = Age at diagnosis (A1 <16 years old, A2 17-40 years old, A3 >40 years old), E = Extent of disease (E1 proctitis, E2 left sided colitis, E3 pan-colitis); SEM, Standard error of the mean; 5-ASA, 5-aminosalicylates; AZA, azathioprine; 6-MP, 6-mercaptopurine; IBD, Inflammatory Bowel Disease; COBH, change in bowel habit; UC, ulcerative colitis; HC, healthy control – Adapted from Dr Phil Smith et al* (241)

3.2.2 CLDN8 HAS ONE OF THE LARGEST FOLD-CHANGE REDUCTIONS OF ANY GENE IN PATIENTS WITH UC

In our cohort of patients with UC, CLDN8 was found to be the second most common under-expressed gene, compared to HC patients (Figure 3-2).

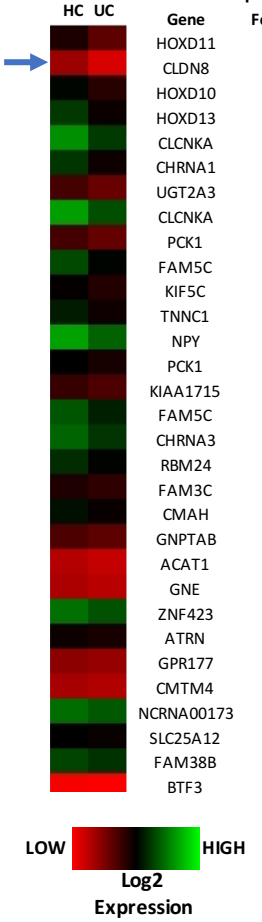

Under-expressed genes in the Rectum

Gene	Fold change	p value	Adj. p value
HOXD11	-2.69	5.24E-7	0.00204
CLDN8	-2.50	0.000105	0.04829
HOXD10	-1.94	3.67E-8	0.00053
HOXD13	-1.75	8.20E-7	0.00269
CLCNKA	-1.73	9.54E-5	0.04555
CHRNA1	-1.72	7.15E-5	0.04095
UGT2A3	-1.71	5.44E-7	0.00204
CLCNKA	-1.67	7.64E-5	0.04095
PCK1	-1.65	0.000108	0.04887
FAM5C	-1.58	1.24E-7	0.00082
KIF5C	-1.55	4.64E-5	0.03481
TNNC1	-1.51	0.00011	0.04898
NPY	-1.50	1.72E-5	0.02454
PCK1	-1.47	3.71E-5	0.03092
KIAA1715	-1.43	4.01E-8	0.00053
FAM5C	-1.41	4.92E-7	0.00204
CHRNA3	-1.36	3.77E-5	0.03092
RBM24	-1.31	6.32E-6	0.01510
FAM3C	-1.30	8.18E-5	0.04214
CMAH	-1.29	7.59E-5	0.04095
GNPTAB	-1.28	2.90E-5	0.03049
ACAT1	-1.27	1.77E-5	0.02454
GNE	-1.27	5.49E-5	0.03793
ZNF423	-1.23	2.07E-5	0.02497
ATRN	-1.19	1.24E-7	0.00082
GPR177	-1.19	7.98E-5	0.04193
CMTM4	-1.18	1.26E-5	0.02232
NCRNA00173	-1.13	1.48E-5	0.02432
SLC25A12	-1.13	7.45E-6	0.01631
FAM38B	-1.13	8.79E-5	0.04440
BTF3	-1.09	3.75E-5	0.03092

Over-expressed genes in the Rectum

Gene	Fold change	p value	Adj. p value
ITLN2	2.74	2.78E-5	0.03047
TNFRSF6B	2.00	3.89E-5	0.03092
PITX1	1.82	1.10E-5	0.02213
MYEOV	1.71	3.27E-6	0.00859
S100P	1.68	6.24E-5	0.04001
CYP2C18	1.58	6.48E-5	0.04053
LOC401115	1.57	2.12E-5	0.02497
PSMB9	1.56	8.98E-5	0.04447
C4BPB	1.54	4.16E-5	0.03216
CASP1	1.53	7.37E-5	0.04095
ACY3	1.44	3.11E-5	0.03092
C2	1.43	3.27E-5	0.03092
AZGP1	1.35	7.12E-5	0.04095
C10orf125	1.34	1.87E-5	0.02454
TMPRSS3	1.34	4.77E-5	0.03481
NFE2L3	1.33	7.13E-5	0.04095
SERPINA1	1.32	1.43E-6	0.00417
LOC100130298	1.30	1.28E-5	0.02232
MB	1.29	7.52E-5	0.04095
TRIM29	1.29	3.76E-5	0.03092
TMEM16A	1.29	2.19E-5	0.02497
IRAK2	1.28	1.86E-5	0.02454
ANO1	1.25	3.36E-5	0.03092
GRIP2	1.25	9.86E-5	0.04624
NPY6R	1.24	5.46E-5	0.03793
CASP4	1.20	5.93E-5	0.03990
LOC729086	1.12	9.37E-5	0.04555
CABP4	1.07	6.25E-5	0.04001

Figure 3-2 – **Heatmap of under- and over-expressed genes in patients with UC, compared to HC patients.** *Results are from transcriptomic analysis of pinch biopsies obtained from the rectum. The table shows genes with fold change of ≤ -1 or ≥ 1. Arrow highlights CLDN8 is downregulated in patients with UC with the second biggest fold change. Data from 24 UC and 27 HC patients. UC, ulcerative colitis; HC; healthy controls – figure adapted from Dr Phil Smith*

3.2.3 EXPRESSION OF CLDN8 AROUND HUMAN COLON IN HC AND PATIENTS WITH UC

As UC is a disease of the large bowel, the expression pattern of CLDN8 was assessed across the large bowel in patients with UC (n=24) and healthy controls (n=26).

Transcription profiles from the bowel of patients with quiescent (macroscopically normal looking mucosa) UC undergoing surveillance colonoscopies were compared with HCs (241).

CLDN8 expression steadily increases distally in the large bowel, with the highest level expressed in rectum, in patients with UC as well as HCs. However, patients with UC has a significant reduction in expression throughout the colon when compared to HCs (*Figure 3-3*). Despite having macroscopically normal mucosa, approximately 30% of the biopsies had evidence of microscopic inflammation. The drop in CLDN8 expression is more marked in patients with histological evidence of UC.

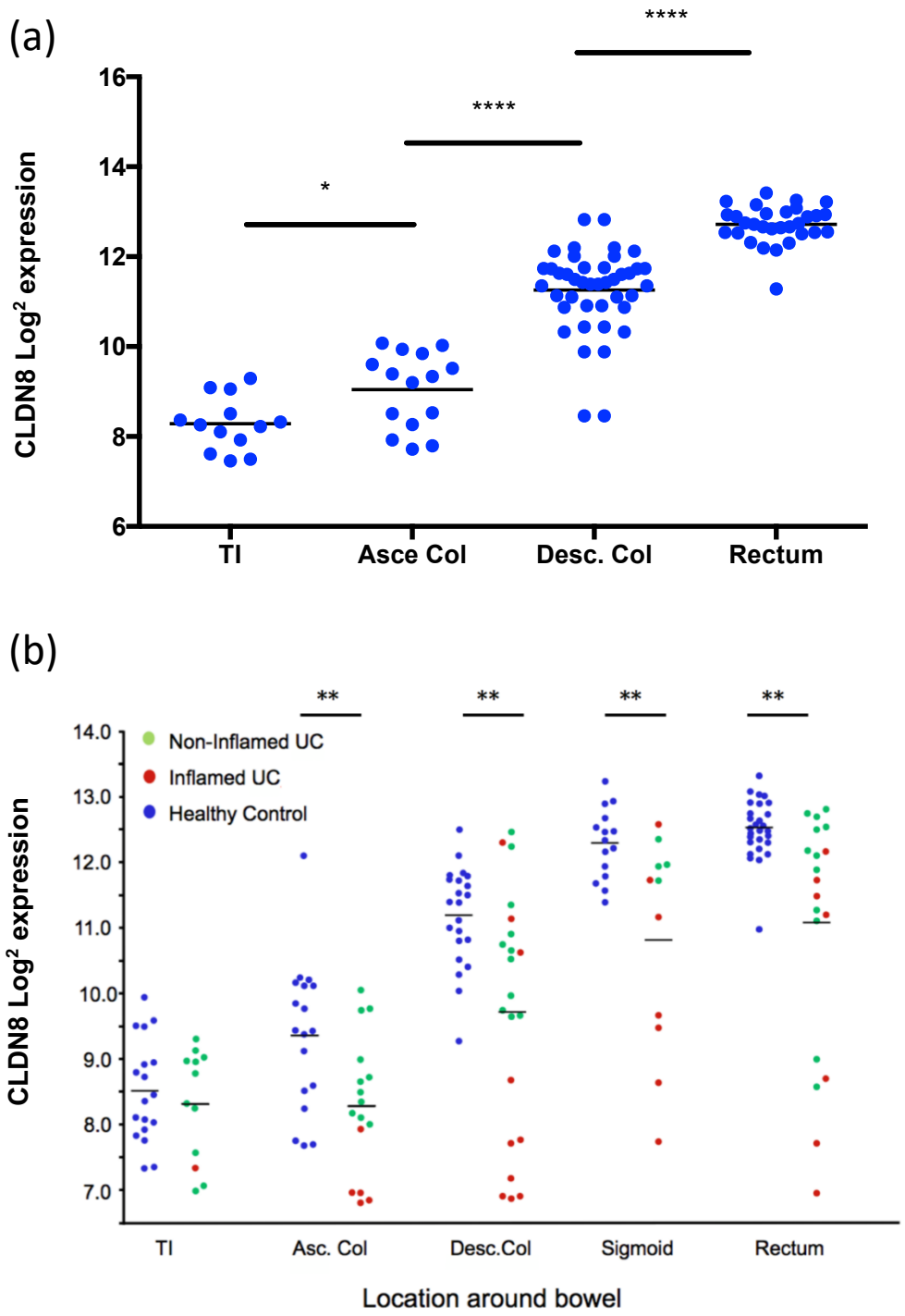

Figure 3-3 – **CLDN8 expression around the large bowel**. *(a) CLDN8 expression levels increase distally in the colon of HCs (b), but patients with UC have significantly lower CLDN8 levels compared to healthy controls (** $p \leq 0.01$ using 1- way Anova test) In these experiments, biopsies were taken throughout the colon, in patients with quiescent UC, and from macroscopically normal mucosa. Green dots represent UC patients with no histologic evidence of inflammation. Red dots represent UC patients with histologic evidence of inflammation. (UC, ulcerative colitis; HC, healthy control, TI, terminal ileum; Asc. col, ascending colon; Desc. col, descending colon) – Adapted from Dr Phil Smith*

3.2.4 EXPRESSION OF CLDN8 IN HUMAN TISSUE

In order to validate the abnormal expression of CLDN8 in patients with UC, TaqMan® real time quantitative PCR was performed. The relative expression of patients with UC were quantified in comparison to HCs. Results were normalised to expression levels of the housekeeping gene *PPIA*, which has been evaluated as a suitable reference gene for normalisation in human samples. The patients with UC had a lower expression levels of CLDN8 as compared to tissue samples from HC patients (*Figure 3-4*).

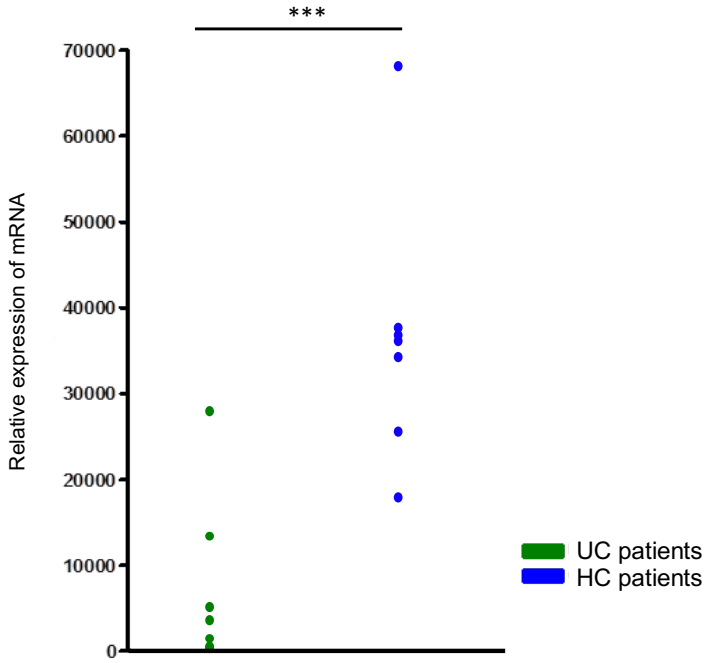

Figure 3-4 – **CLDN8 expression is down-regulated in patients with UC.** *qPCR verification of CLDN8 expression in the rectal biopsy tissue of tissue of patients with UC as compared to HC (*** $p \leq 0.001$ using unpaired t-test) UC, ulcerative colitis; HC, healthy control (PCR performed by Dr Jenny Dunne)*

3.2.5 EXPRESSION LEVELS OF UC-SPECIFIC GENES IDENTIFIED IN GWAS STUDIES

GWAS studies have so far identified 163 risk susceptibility loci in patients with IBD, of which 110 are shared between UC and CD, and 23 are specific to UC (150). Of the 23 UC specific genes identified so far in GWAS studies, in our dataset, only 10 genes showed statistically significant differences in expression between patients with UC and HC (*Figure 3-5*).

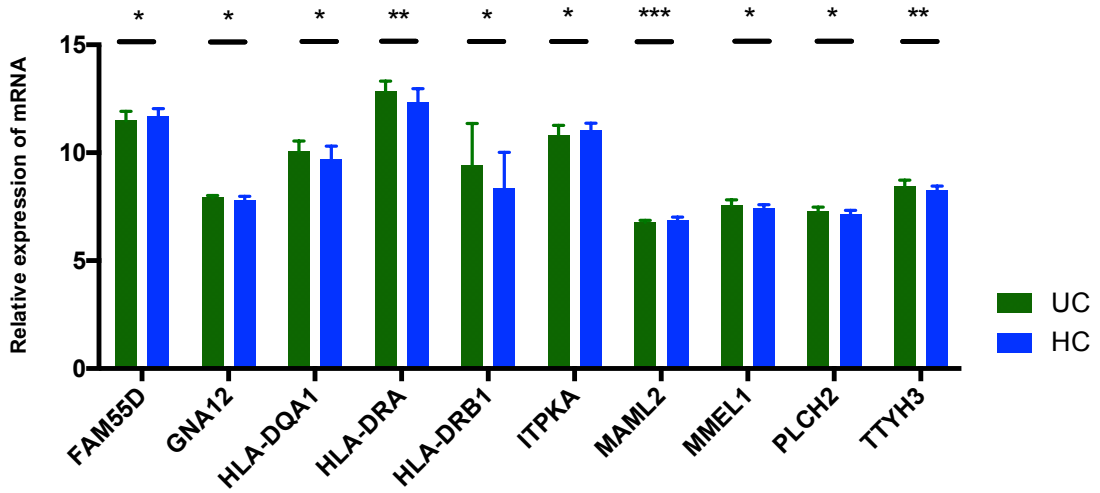

Figure 3-5 – **UC-specific genes identified in GWAS studies.** *Only genes that reached statistical significant between UC vs HC in our dataset have been shown (* $p \leq 0.5$, ** $p \leq 0.01$ using paired t-test). UC, ulcerative colitis; HC, healthy controls*

A number of UC-specific loci are implicated in barrier function and epithelial restitution, including CDH1, LAMB1 and HNF4A. The expression levels of these genes were analysed in our cohort of patients with UC and compared with HCs.

CDH1 (cadherin type 1) is a major component of the adherens junction and an important mediator of intercellular adhesion and mucosal repair (151). Like CLDN8, expression of CDH1 increases distally in humans towards the rectum. However, unlike CLDN8, in patients with UC, the expression levels are slightly elevated. LAMB1 (laminin-β1 subunit) is expressed in the intestinal basement membrane and implicated in a wide variety of biological processes including cell adhesion, differentiation, migration, and signalling (152) and HNF4A (hepatocyte nuclear factor-4α) is a transcription factor that regulates expression of key components of the cell-cell junction. Of these, only the expression level of CDH1 was affected in our cohort of patients with UC (*Figure 3-6*). CDH1 expression levels were increased in our cohort.

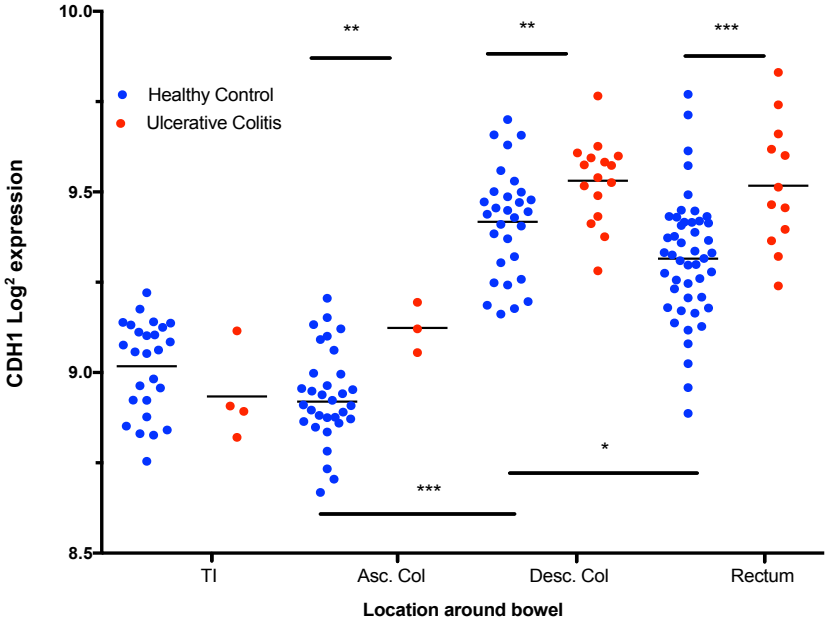

Figure 3-6 – **CDH1 expression around the large bowel.** *CDH1 levels are higher in the distal section of the colon, with slight increase in patients with UC compared to healthy controls (* p ≤ 0.05, ** p ≤ 0.01; *** p ≤ 0.001, using 1-way Anova test); (UC, ulcerative colitis; HC, healthy control; TI, terminal ileum; Asc. col, ascending colon; Desc. col, descending colon)*

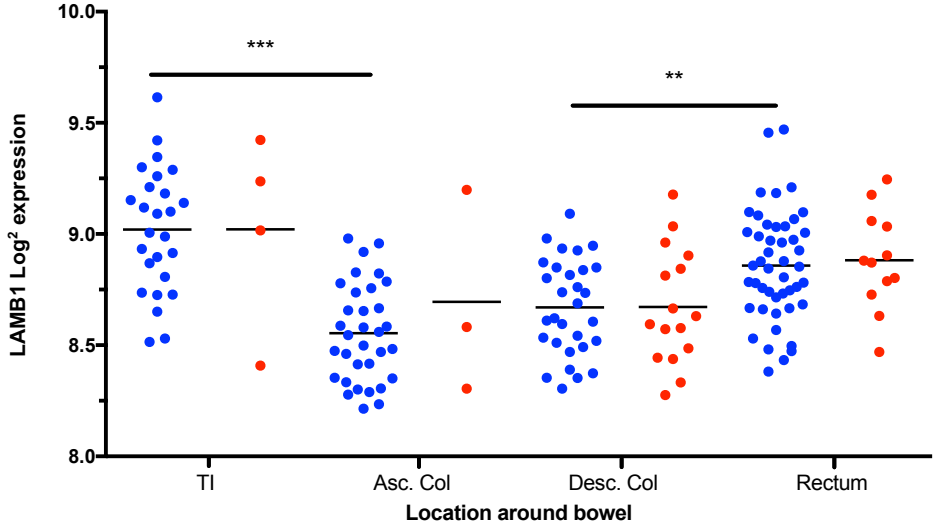

Figure 3-7 – **LAMB1 expression around the large bowel.** *LAMB1 levels are highest in TI, and then drop in colon, with slight increase in rectum. There was no statistically significant difference between patients with UC and HCs. (** p ≤ 0.01; *** p ≤ 0.001, using 1-way Anova test); UC, ulcerative colitis; HC, healthy control, TI, terminal ileum; Asc. col, ascending colon; Desc. col, descending colon*

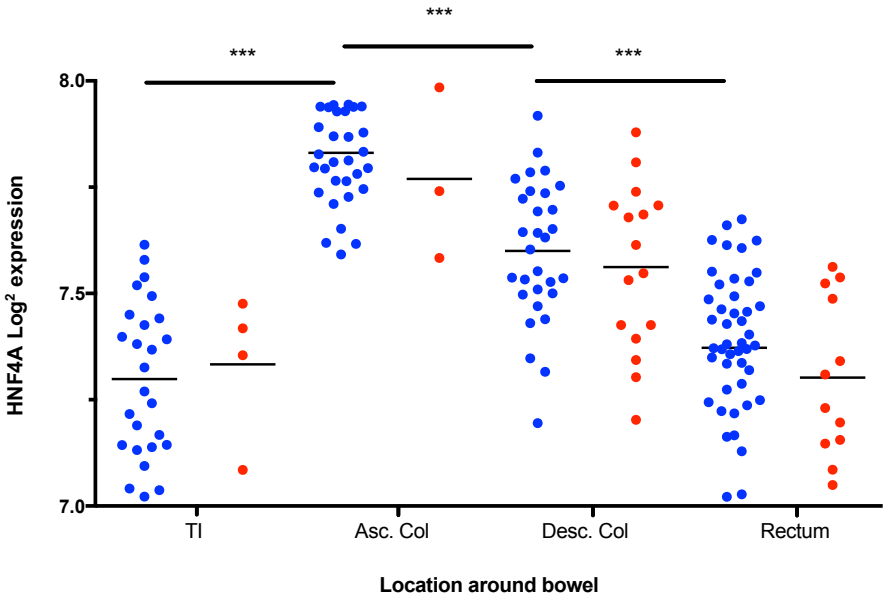

Figure 3-8 – **HNF4A expression around the large bowel.** *HNF4A levels are highest in the proximal section of the colon, with a drop in expression distally towards rectum. There was no statistically significant difference between the patients with UC compared to HCs (*** p ≤ 0.001, using 1-way Anova test); UC, ulcerative colitis; HC, healthy control; TI, terminal ileum; Asc. col, ascending colon; Desc. col, descending colon*

3.2.6 CORRELATION OF CLDN8 EXPRESSION WITH KNOWN MARKERS OF MUCOSAL INFLAMMATION

To examine the relation of CLDN8 with inflammation, CLDN8 expression levels where correlated with expression levels of some of the known inflammatory markers, defensins, ITLN2, IL-8 and S100A8 (*Figure 3-9*). Defensins are small peptides and are active against bacteria, fungi and many enveloped and non-enveloped viruses, and their expression levels are increased in patients with UC (258), and are markers of chronic inflammation. CLDN8 significantly correlates with DEFA1B, DEFA5, DEFA6 and ITLN2 ($p < 0.0001$), but not with IL-8 and S100A8.

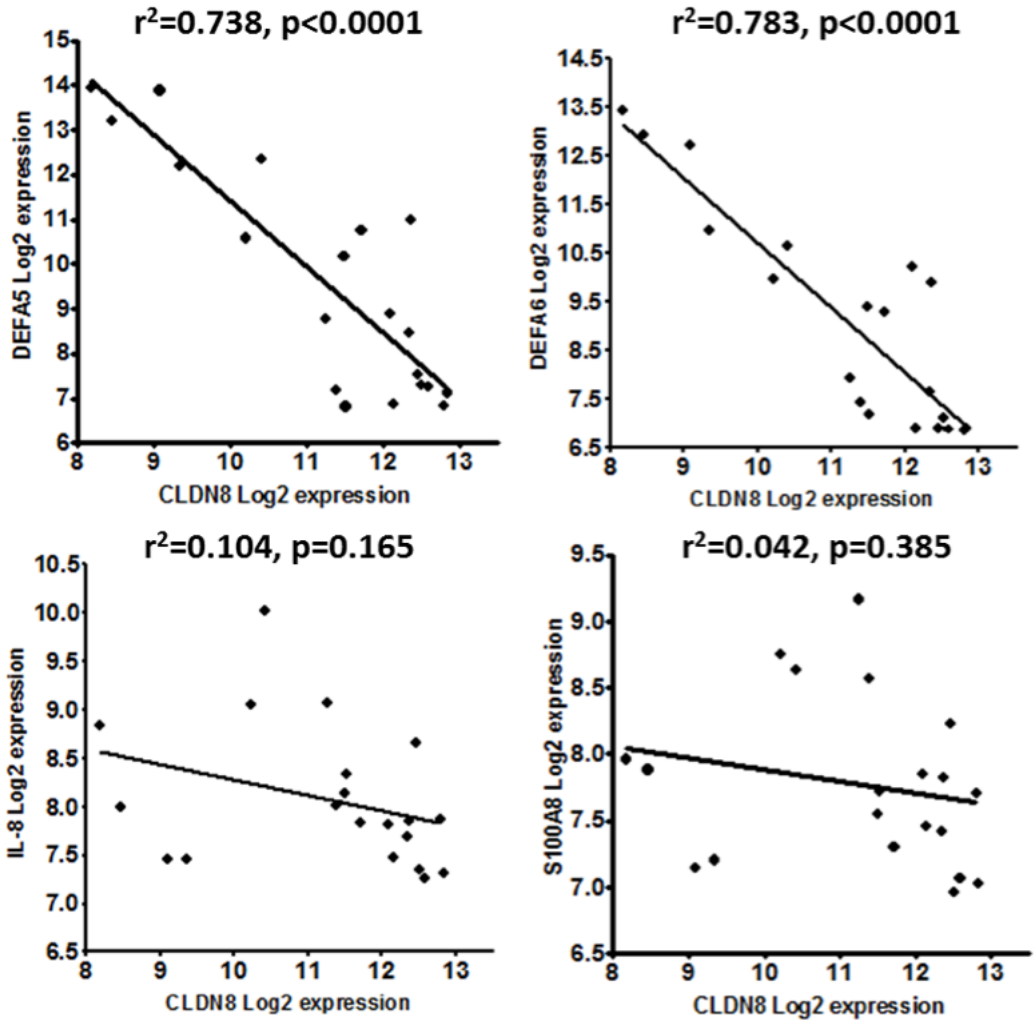

Figure 3-9 - **Correlation of CLDN8 with some known markers of inflammation in the rectum of patients with UC (n=21).** *r^2 correlation coefficient and p-values shown for each analysis – figure from Dr Phil Smith*

3.2.7 CORRELATION OF CLDN8 AND OTHER CLDNS IN THE RECTUM OF PATIENTS WITH UC

Overall, 15 different CLDNs are expressed in the rectal samples of patients with UC, based on the transcriptomic data. These CLDNs are: -1, -2, -3. -4. -5. -7, -8. -11, -12, -14, -15, -16, -18, -19, and -23. Expression levels of these CLDNs were compared with CLDN8 expression (*Figure 3-10*). Of these, the expression levels of 5 CLDNs (-1, -2, -12, -15, -18) were inversely proportional to CLDN8 expression, suggesting that these may either compensate for the loss of CLDN8, or are involved in the same physiologic process that results in loss of CLDN8.

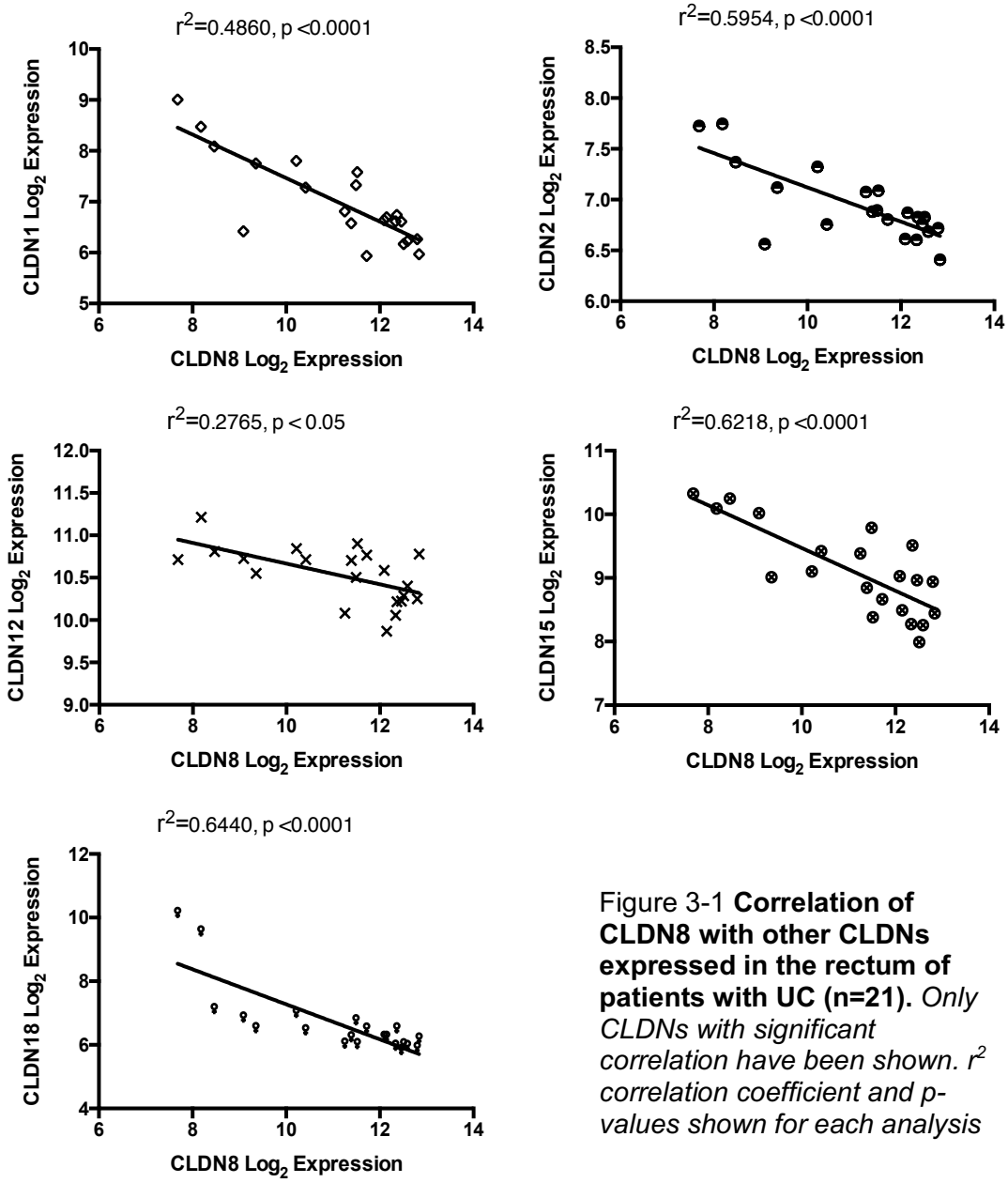

Figure 3-1 **Correlation of CLDN8 with other CLDNs expressed in the rectum of patients with UC (n=21).** *Only CLDNs with significant correlation have been shown. r^2 correlation coefficient and p-values shown for each analysis*

3.3 DISCUSSION

As described above, in an attempt to identify molecules which could be causally related to the development of IBD, Dr Smith, a PhD student with Prof Segal analysed the transcriptomic profile of colonic tissue from patients with UC, as compared to HCs (259).

In this dataset, of the top 4 under expressed genes, 3 belong to the homeobox family of genes (HOXD11, HOXD10, HOXD13), and one (CLDN8) is a TJ molecule, with the second largest fold change of all under expressed genes.

It has previously been noted that CLDN8 is under expressed in patients with UC. In a meta-analysis of a number of transcriptomic studies of colonic tissue of patients with UC, CLDN8 had the largest reduction in expression of all genes (252). However, as described in section 3.1, in most of these studies, samples were obtained from inflamed tissue (253,255–257), raising the likelihood that any observed changes in gene expression may be due to cellular damage and repair processes. The finding that CLDN8 is also under expressed in our dataset is intriguing given that in this unique dataset, the tissue was collected exclusively from macroscopically non-inflamed mucosa and from patients that were either on no treatment or minimal treatment. These findings raise the possibility that CLDN8 may play an important role in the pathogenesis of UC.

It is also interesting to note that in our dataset, CLDN8 appears to be the only TJ molecule with a significant fold change in its expression of ≤ -1 or ≥ 1, after correcting for multiple testing. CLDN8 expression levels are inversely proportional to the expression levels of a number of CLDNs expressed in the large bowel, all of which show an increase in expression levels. Of these, only CLDN1 has similar properties to CLDN8 as a “barrier forming” CLDN and reduce the paracellular permeability; CLDN2 and CLDN12 are known to increase paracellular permeability and the function of CLDN15 and CLDN18 are not yet understood. Taken together, these suggest that the changes in expression levels of CLDNs in the large bowel are unlikely to be simply a response to compensate for the loss of CLDN8.

Interestingly, of all the CLDNs expressed in the large bowel, only CLDN8 expression levels increase significantly from proximal large bowel towards rectum; all other CLDNs are expressed unifor mly throughout the large bowel (data not shown). This is intriguing, especially given the anatomical pattern of disease in UC, where the inflammation extends up for a variable distance from the rectum.

3.4 CONCLUSION

The finding that reduced CLDN8 expression mirrors the disease pattern in quiescent UC may suggest a central role for reduced CLDN8 expression in the pathogenesis of UC. CLDN8 may play an important role in the physical strength of TJs, where the weaker TJs may allow microscopic physical trauma to the mucosa by formed faeces to set off an already abnormal immune response, thus explaining the distal distribution of the disease. The reduction of CLDN8 levels may also play a role in the increased epithelial permeability in UC patients, known to permit elevated levels of inflammatory stimuli to enter the tissue. CLDN8 prevents sodium paracellular back-leakage (260), and may play a role in diarrhoea. This may partly explain the efficacy of corticosteroids in reducing symptoms of diarrhoea in patients with UC. CLDN8 could therefore be an attractive prognostic and therapeutic target in clinical practice.

4 Development and characterisation of the *Cldn8*-Knock Out Mouse

4.1 INTRODUCTION

As discussed in Chapter 1.3, a number of animal models have been developed to investigate bowel inflammation. These include genetically modified animals, chemical and bacterial models to induce colitis. Whilst none of these models can replicate the complex pathology of human IBD, they provide tools to investigate particular molecules involved in the inflammatory process and pathway.

To date, the function of *Cldn8* has only been investigated *in vitro*. These studies have reported that *Cldn8* forms a barrier to cations (including Na^+ and K^+), ammonium and bicarbonate ions (102,108,120). However, these studies are limited and are unable to assess the wider potential role of *Cldn8* in the animal's homeostasis. The use of gene specific knock out animal models enables selective examination of the action of individual molecules *in vivo*.

Mice are the most commonly used animals for *in vivo* experiments, and many of their immunological pathways and processes are shared with humans, despite differences having been reported (261). These factors, in addition to practical reasons that mice are relatively small and have a short gestation period, have resulted in mice becoming an important model for investigation of the inflammatory pathways, and therefore, the mouse immune system is well characterised. Another important physiological similarity between humans and mice is that both have a prenatal sterile gut which is colonised with commensal bacteria during and following birth. We therefore decided to use a mouse model of colitis to investigate the role of *Cldn8* in intestinal inflammation by acquiring a *Cldn8*-Knock Out (*Cldn8*-KO) mouse.

Prior to inducing colitis, it was important to accurately characterise the *Cldn8*-KO mice. The parameters that were measured are detailed in the results section below. These included verification of deletion of *Cldn8* gene, fertility and growth curves, normal physiological functions such as urination and defecation, histological evaluation of the intestine, serum cytokine measurement, as well as LP composition of inflammatory cells. In addition, intestinal permeability to small sugars, and mucous permeability to bacteria were measured in naïve animals.

4.1.1 INTESTINAL PERMEABILITY

The role of various CLDNs in controlling paracellular permeability in the bowel is well established. The CLDNs are traditionally grouped according to their effect on paracellular permeability properties of the epithelial cells, as either having “barrier forming”, “pore forming” or “ambiguous function” (88). CLDN8 has been reported to form a barrier to cations, ammonium and bicarbonate ions (102,108,120).

Changes in permeability have been reported in patients with UC. There is evidence from animal models that changes in permeability may trigger inflammation in the bowel. Mice that are IL-10 deficient, develop spontaneous colitis within 12 weeks, and there is evidence that this is preceded by changes in intestinal permeability from a young age (179,232). Importantly, these mice do not develop inflammation in germ-free conditions. These observations suggest that increased penetration of luminal antigens due to increased permeability is the trigger for inflammation. Similarly, deletion of *Cldn7* in mice enhances paracellular permeability in mice. These mice also spontaneously develop colitis (101).

Various techniques have been used to measure intestinal permeability in mice. The most common technique includes oral or rectal gavage of different sugars, either mannitol, lactulose or dextran (262,263). Different factors, however, influence the uptake of these sugars from the intestinal lumen. These include GI motility, diet, gastric emptying, mucosal blood flow, as well as renal clearance of any tracers used. These factors affect the measurements of permeability, and give rise to false-positive or false-negative results (264,265).

There is evidence that CLDN8 affects the paracellular permeability to acidic and basic ions (H^+, $NH4^+$, $HC3^-$) (108), and also acts as a barrier to monovalent cations including Na^+ and K^+ (102). This raises the possibility that differences in the local concentration may exist between *Cldn8*-KO and WT mice; this may affect the function of the intestinal smooth muscle, which in turn may affect gut motility. Therefore, the basic gavage technique was not appropriate, as it would have been impossible to conclude if any observed variation in experiments between *Cldn8*-KO and WT mice were due to changes in intestinal permeability or motility. Therefore, a different technique was used to measure the intestinal permeability *in vivo* that controlled for any changes in intestinal motility.

***In vivo* permeability studies**

Female *Cldn8*-KO and WT mice were anaesthetized and maintained at 37ºC on a thermostatically controlled heating blanket. The peritoneal content were exposed, ensuring no damage to the intestine during the procedure. A self-contained segment of large bowel was created. The distal cut was made in the most distal part of the large bowel that could be reached in the pelvis without damaging other organs; the distal end of the segment was therefore within 1-cm of the rectum (*Figure 4-1*-a and –b). Cuts in the bowel were made only to part of the lumen, and not the full width, to avoid damaging the mesentery and its blood supply (*Figure 4-1*-c). A transfer buffer containing ^{3}H-mannitol and FITC-Dextran was instilled into the lumen before the segment was tied off. Blood was collected after 30min by cardiac puncture. The concentration of ^{3}H-mannitol and FITC-Dextran were measured in plasma, and factoring the dried weight of the segment, and the animal's weight (as a surrogate marker for the blood volume). There were two reasons for using the dried weight of the segment of intestine, instead of its length. First, as will be discussed in next chapter, large bowel shrinks in mice suffering from DSS colitis, and therefore, using the bowel length can introduce an error in calculation. Second, is that when dissecting the segment away from the mesentery, it is possible to stretch the segment (See Section 2.9 for full details).

This experiment involved delicate micro-surgery on mice. The main challenge involved minimal handling of the intestines to prevent damage to blood vessels, and to the epithelial cells, which could have given rise to false-positive results. Other challenges included occasional spillage of the buffer into the peritoneal cavity, and taking care not to instil air into the lumen after the buffer.

The two sugars, ^{3}H-mannitol and FITC-Dextran were chosen as small and intermediate sized molecules to investigate permeability. ^{3}H-mannitol has a molecular size of 182 kDa and is approximately 4Å is size, which is the same size as the paracellular pore created by CLDNs (79), and FITC-Dextran has a molecular size of 4,000 kDa, is approximately 14Å. ^{3}H-mannitol is neutral and FITC contributes partial negative charge to Dextran at normal pH.

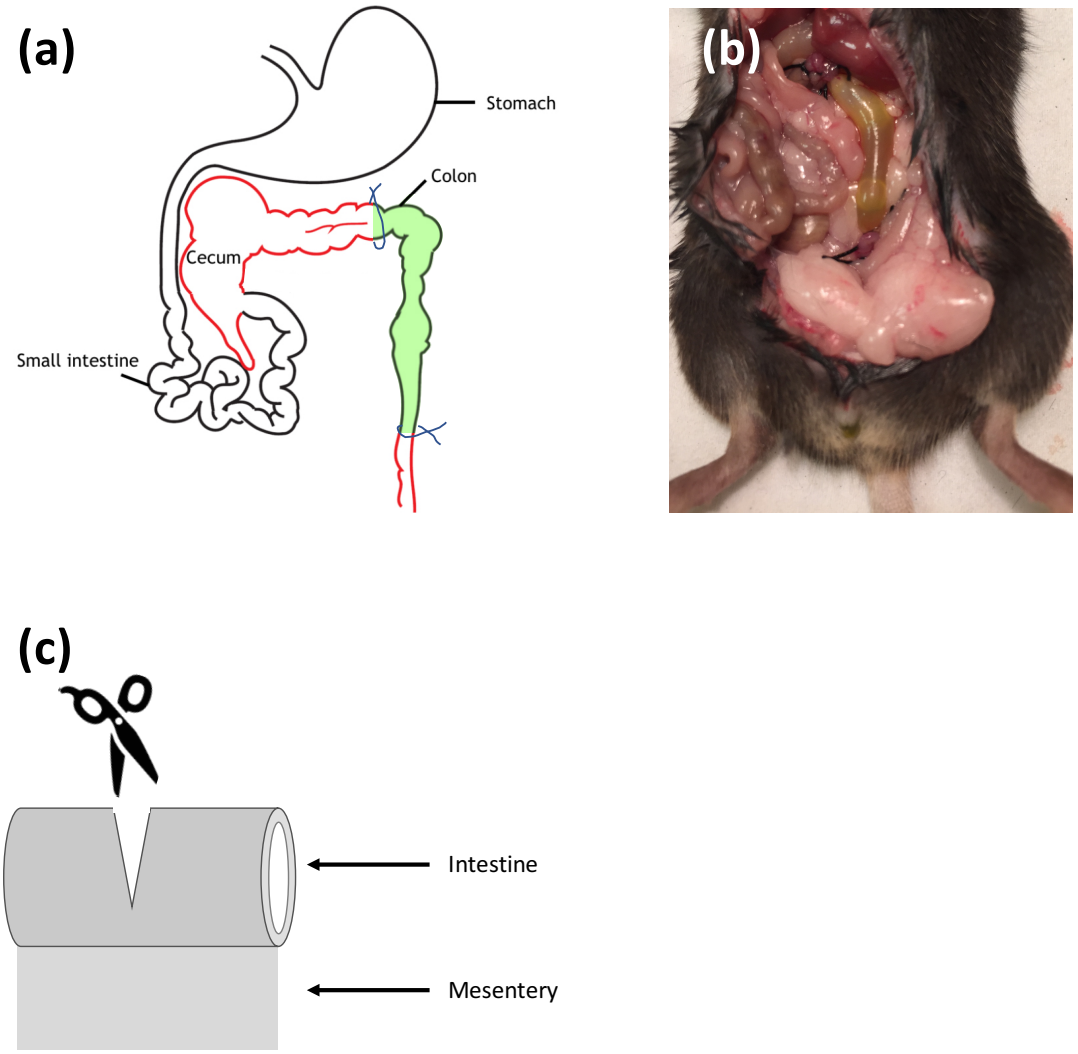

Figure 4-1 – ***In vivo* Permeability Studies in Mice** *(a) Schematic diagram of the mouse GI tract. The highlighted area represents the self-contained segment of the large bowel (b) The segment remains connected to the mesentery and its blood vessels. (c) The bowel is cut only partially to prevent damage to blood vessels in the mesentery.*

4.1.2 MUCOUS PERMEABILITY TO LUMINAL BACTERIA

There is evidence that whilst commensal bacteria penetrate the outer layer of the mucous, the inner layer remains sterile (24,174,266). It has been shown that MUC2 mucin plays an essential role in keeping the inner mucous sterile (24).

However, the effect of CLDNs has not been investigated in relation to the mucous permeability to bacteria. In the large bowel, aldosterone promotes absorption of water, through its effect on absorption of sodium from the luminal side of colonic epithelial cells by simultaneously inducing epithelial sodium channels (ENaC) and CLDN8 expression (107) (*Figure 4-2*). *Cldn8* expression levels may therefore affect the water content and viscosity of the mucous by controlling the luminal concentration of Na^+. This in turn may affect the permeability of the mucous to luminal antigens.

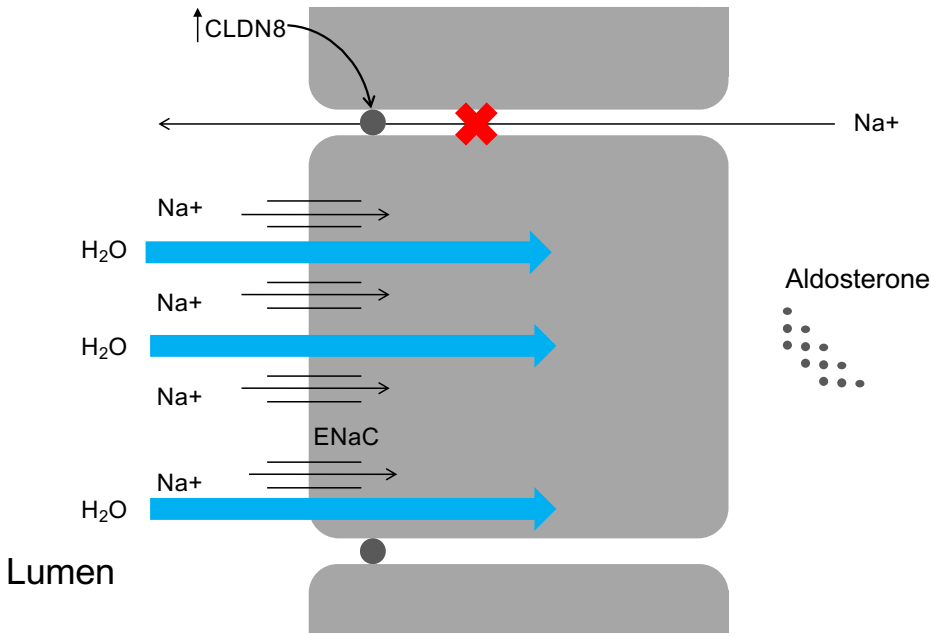

Figure 4-2 – ***Cldn8* expression levels may affect the mucous properties.** *Cldn8 prevents back-leakage of Na^+ through paracellular spaces into the lumen. Aldosterone stimulates expression of Cldn8 and epithelial Na^+ channels (ENaC). Reducing the luminal concentration of Na^+, may result in water content and viscosity of the mucous through osmotic effects of Na^+. (ENaC - epithelial Na^+ channels).*

4.2 RESULTS

4.2.1 COMPARISON OF HUMAN AND MOUSE CLDN8 AMINO ACID SEQUENCES

Amino acid sequences for human and mouse CLDN8 were retrieved from Ensemble. CLDN8 has one transcript in both mice and humans, with one exon. The amino acid sequence for human CLDN8 was aligned to the mouse amino acid sequence for *Cldn8* in SDSC biology work bench. Alignment analysis demonstrated that the amino acid sequence for CLDN8 is highly conserved between human and mouse with 83% homology (*Figure 4-3*).

Human & Mouse CLDN8 Homology

Score	Expect	Method	Identities	Positives	Gaps
404 bits(1037)	3e-148	Compositional matrix adjust.	186/225(83%)	211/225(93%)	0/225(0%)

```
CLDN8_HMN       MATHALEIAGLFLGGVGMVGTVAVTVMPQWRVSAFIENNIVVFENFWEGLWMNCVRQANI
CLDN8_MSE       MATYALQMAALVLGGVGMVGTVAVTIMPQWRVSAFIESNIVVFENRWEGLWMNCMRHANI
                ***:**::*.*.*************:***********.******* ********:*:***

CLDN8_HMN       RMQCKIYDSLLALSPDLQAARGLMCAASVMSFLAFMMAILGMKCTRCTGDNEKVKAHILL
CLDN8_MSE       RMQCKVYDSLLALSPDLQASRGLMCAASVLAFLAFMTAILGMKCTRCTGDDENVKSRILL
                *****:*************:*********::***** *************:*:**::***

CLDN8_HMN       TAGIIFIITGMVVLIPVSWVANAIIRDFYNSIVNVAQKRELGEALYLGWTTALVLIVGGA
CLDN8_MSE       TAGIIFFITGLVVLIPVSWVANSIIRDFYNPLVDVALKRELGEALYIGWTTALVLIAGGA
                ******:***:***********:*******.:*:** *********:*********.***

CLDN8_HMN       LFCCVFCCNEKSSSYRYSIPSHRTTQKSYHTGKKSPSVYSRSQY-
CLDN8_MSE       LFCCVFCCTERSNSYRYSVPSHRTTQRSFHAEKRSPSIYSKSQYV
                ********.*:*.*****:*******:*:*: *:***:**:***
```

Figure 4-3 – **CLDN8 is well conserved throughout species with 83% homology between human and mouse.** *The mouse and human CLDN8 amino acid sequences are aligned. (Ensemble; aligned in SDSC biology work bench).*

4.2.2 GENERATION OF *Cldn8*-KO MICE

Cldn8-KO mice were generated by the Lexicon Genetics Corporation. The entire *Cldn8* gene is encoded in 1 exon. To generate a KO mouse, the target vector, pKOS-53 with LacZ/Neo cassettes, was targeted to the *Cldn8* gene by homologous recombination (*Figure 4-4*). To genotype the mice, genomic DNA was extracted from the ear-punch biopsy, and submitted to PCR. The following primers were used for the PCR reaction: WT (DNA266-28 and DNA266-4), *Cldn8*-KO (DNA266-28, GT ires) - (see Appendix 1 – List of Primers).

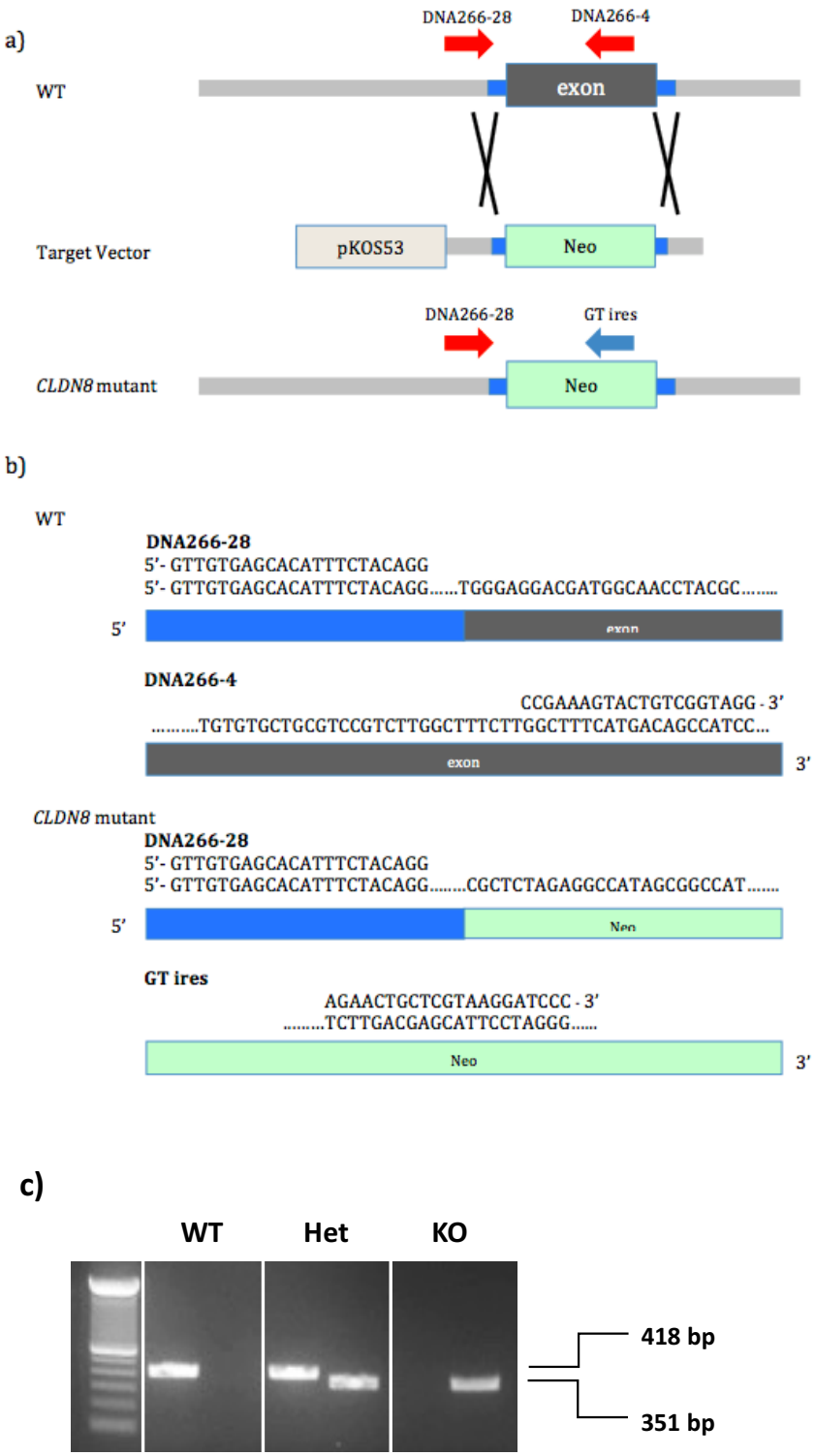

Figure 4-4 – **Generation of *Cldn8*-KO mouse** *(A) Schematic diagram of the targeting strategy for Cldn8-KO mutant mice. WT Cldn8 gene has 1 exon. The target vector, pKOS-53 with a LacZ/Neo cassette, was targeted to Cldn8 gene by homologous recombination. (B), primer DNA266-28, primer DNA266-4, and primer GT ires were used to distinguish WT alleles (418 bps) from mutant alleles (351 bps); (C) PCR verification of Mouse Cldn8 gene deletion, ear punch biopsy DNA was submitted to PCR analysis using primers DNA266-28, DNA266-4, and GT ires*

4.2.3 *Cldn8*-KO MICE

Cldn8 heterozygous mice had been generated using 129/SvEvBrd-derived embryonic stem cells. However, as discussed in section 1.3, genetic factors play an important role in the experimental colitis models in mice, and differences in susceptibility to experimental colitis have been identified among different strains of mice (215). *Cldn8* heterozygote mice were therefore bred to C57BL/6 albino mice to generate F1 heterozygous animals. These were intercrossed to generate F2 wild type, heterozygous, and homozygous mutant progeny. We took delivery of the F2 progeny.

All earlier experiments in our laboratory, as well as the majority of literature on experimental colitis in mice have been performed on C57BL/6 black mouse strain. Therefore, the *Cldn8*-KO transgenic mice (F2) were backcrossed on to C57BL/6 black WT mice to generate *Cldn8*-KO mice with a C57BL/6 black genetic background. Briefly, the process involved crossing the *Cldn8*-KO mice with non-pedigreed non-sibling C57BL/6 black WT mice for several generations. This backcrossing process is essential to generate congenic strains of mice, where they differ genetically in only one locus (*Figure 4-5*).

Female mice reach sexual maturity in 6 weeks, and the time taken from conception to birth can be 3 weeks. It can therefore take up to 9-12 weeks for the next generation of mice to be born (taking into consideration the length of time taken to conceive). The results of experiments in this report are based on mice bred to generation 6 (96.88% homozygosity). All experiments were performed at least once on litter-mate controls. Experiments investigating the acute response to DSS and *in vivo* permeability studies were repeated in generation 10 mice (99.80% homozygosity), to ensure reproducibility.

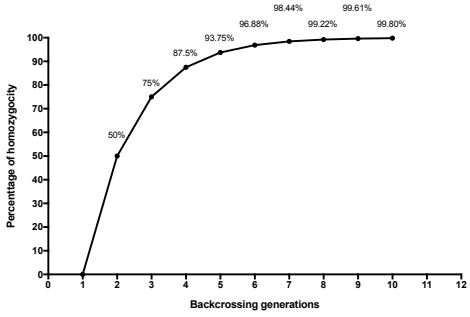

Figure 4-5 – **The effect of backcrossing on homozygosity throughout the process of generating congenic mice.** *The Cldn8-KO were backcrossed onto C57/B6 mice. With each backcross, there is an increase in percentage of C57B/6 DNA that constitutes the genome of the offspring – Adapted from Chapter 1, The Laboratory Mouse* (267)

4.2.4 VERIFICATION OF ABSENCE OF CLDN8 mRNA IN *Cldn8*-KO MICE

In order to confirm that *Cldn8* mRNA was not expressed in *Cldn8*-KO mice, PCR for *Cldn8* was performed on tissue from kidney and bowel of the mice. *Cldn8* mRNA was expressed in tissue obtained WT mice, but not in *Cldn8*-KO mice (*Figure 4-6*). Lack of expression of *Cldn8* in tissue was confirmed using PCR with *Gapdh* as the housekeeping gene.

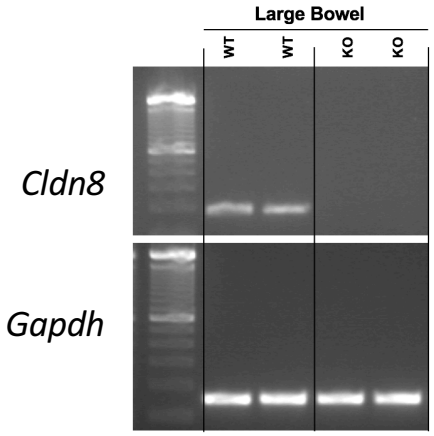

Figure 4-6 – **Genotyping of *Cldn8*-KO and WT mice.** *Confirmation of lack of expression of Cldn8 mRNA in large bowel of Cldn8-KO mice. Using Cldn8 primers, it was confirmed that Cldn8 mRNA is not expressed in Cldn8-KO mice, where as it is expressed in the large bowel tissue of WT mice. Genotyping was performed by PCR of gDNA isolated from mouse ear clips. (WT: wild-type, KO: knock out, Gapdh: Glyceraldehyde 3-phosphate dehydrogenase)*

4.2.5 VERIFICATION OF ABSENCE OF CLDN8 PROTEIN IN *Cldn8*-KO MICE

Several attempts were made to identify CLDN8 protein using Western blot and immunohistochemistry. In total, 4 different available antibodies for CLDN8. For Western blot, different techniques were used for preparing cell lysate. However, none appeared to be specific to CLDN8 as they all stained a protein with the same weight in WT mice (*Figure 4-7*-a). Actin was used as a loading control and confirmed equal amounts of protein were present.

The same was true for immunohistochemistry where the antibody appeared to bind the epithelium in WT mice, but non-specifically bound the tissue in the *Cldn8*-KO mouse. All these antibodies have been used in various publications for identifying CLDN8 (268–271).

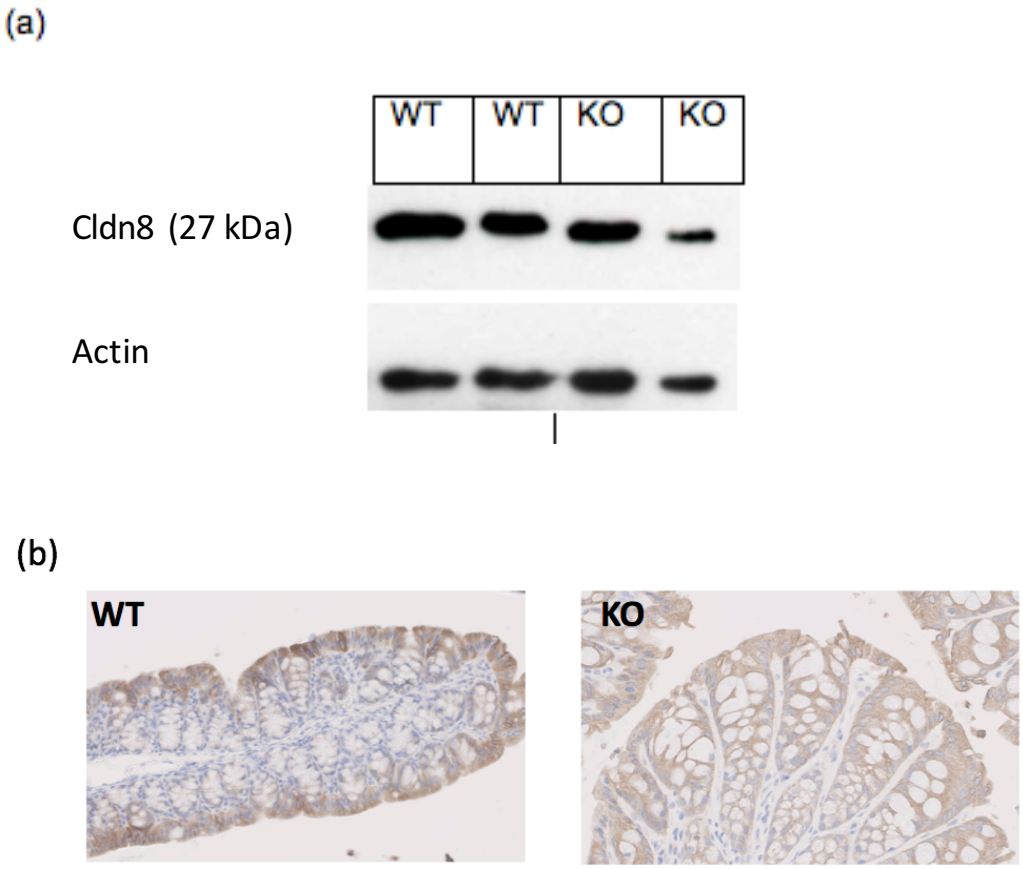

Figure 4-7 – **The antibody to *Cldn8* binds non-*Cldn8* molecules in a non-specific manner.** *(a) Western blot showing band at 25 kDa region in WT and Cldn8-*KO *mice (antibody from Invitrogen; 1:500); (b) Whilst staining with commercially available antibodies against Cldn8 was limited to epithelial layers in the WT mice, in the Cldn8-*KO *mice the antibody binds non-specifically across the bowel tissue (GeneTex antibody; 1:400); WT, wild-type; KO, Cldn8-*KO

4.2.6 OTHER *Cldns* DO NOT COMPENSATE FOR THE LOSS OF *Cldn8* IN *Cldn8*-KO MICE

There was no statistically significant difference in expression of various *Cldns* in the large bowel of *Cldn8*-KO and WT mice on transcriptomic analysis – please see chapter 6 for full details of the transcriptomic analysis.

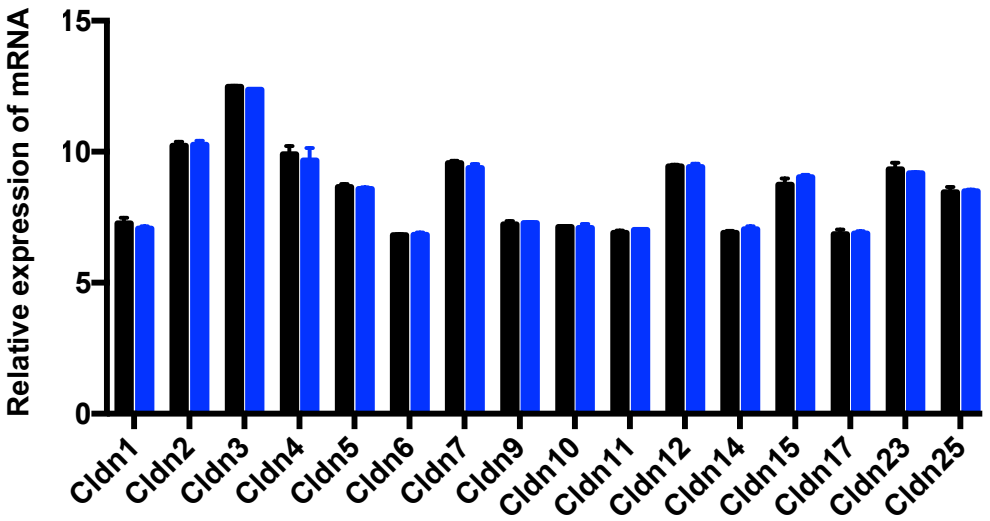

Figure 4-8 –***Transcriptomic analysis of gene expression between Cldn8*-KO and WT mice did not reveal any statistically significant changes in expression of other *Cldns.*** (n=3 per group)

4.2.7 CHARACTERISATION OF THE NAÏVE *Cldn8*-KO MOUSE

In order to assess the feasibility of the *Cldn8*-KO mouse as an appropriate model for investigation of role of CLDN8 in intestinal inflammation, the phenotype of the *Cldn8*-KO was characterised.

No significant differences were detected during breeding or on physical examination and necropsy between naive *Cldn8*-KO and WT mice. Both are black mice with no characteristic markings. Loss of *Cldn8*-KO had no obvious impact on the health of mice maintained in SPF conditions. A handful of mice were kept for one year and did not develop any obvious phenotype, including no colitis phenotype

4.2.7.1 *Cldn8*-KO and WT mice follow similar growth curves

Cldn8-KO (n=78) and WT (n=141) mice were weighed daily for the initial 21 days, and every 5-10 days thereafter for over 80 days. Both groups had the same growth curve for the first three weeks. After this point, the growth curve was separated for males and females, but similar in *Cldn8*-KO and WT groups, and no difference in weight was seen between naive age and sex matched *Cldn8*-KO and WT mice (*Figure 4-9*).

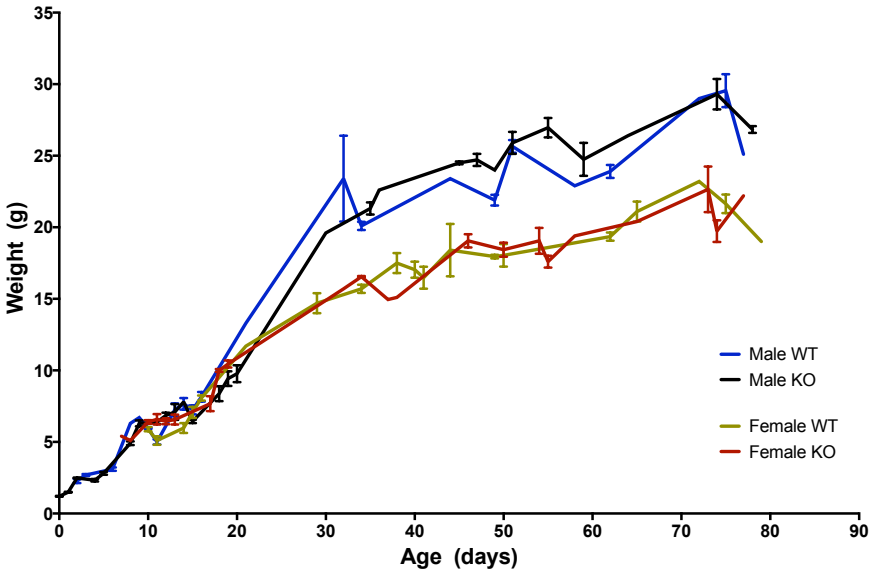

Figure 4-9 – **Cldn8-*KO* and WT mice follow similar growth curves.** *Both groups had the same growth curve for the first three weeks. After this point, the growth curve was separated for males and females, but similar in Cldn8-KO and WT groups, and no difference in weight was seen between naive age and sex matched Cldn8-KO (n=78) and WT mice (n=141)*

4.2.7.2 *Cldn8*-KO and WT mice have similar size and gender ratio of their litter

The breeding pattern of heterozygous parents followed a Mendelian pattern of 2 heterozygous pups to 1 homozygous *Cldn8*-KO and homozygous WT pup. The breeding characteristics were also compared between *Cldn8*-KO mice and WT mice (*Figure 4-10*) from homozygous parents. Overall, 10 litters from each group were compared for litter size and gender ratio. There is no statistical difference between the two groups. The number and size of litters were comparable between knockout and wild type mice and the pups were born in expected Mendelian ratios. The mean percentage of males was 58.83% in *Cldn8*-KO mice and 48.75% in WT mice litter group. The mean litter size was 6.9 in *Cldn8*-KO mice and 7.6 in WT mice litter group.

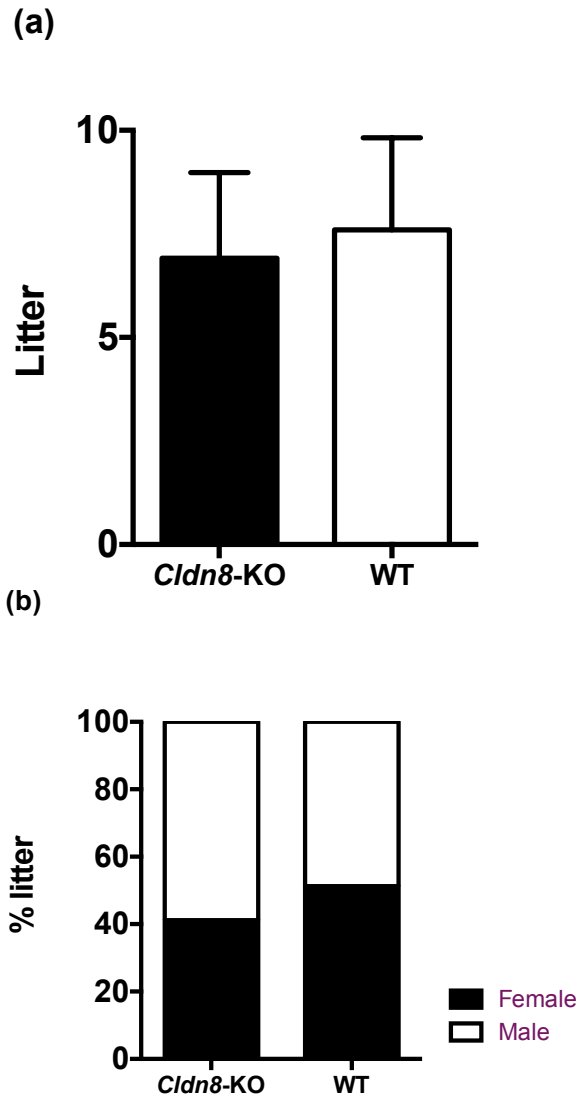

Figure 4-10 – ***Cldn8*-KO mice have similar fertility phenotype to WT.** *There was no statistical difference in the (a) litter size and (b) gender ratio between Cldn8-KO and WT mice.*

4.2.7.3 Faeces from *Cldn8*-KO mice has similar characteristics as that of WT mice

Cldn8-KO mice were maintained in SPF conditions for up to one year. There was no sign of spontaneous colitis or any other adverse phenotype. Stool consistency was the same in *Cldn8*-KO and WT mice with fresh stool samples retrieved from both groups being fully formed with no evidence of PR bleeding. Stool cultures were performed by Deltagen and have been checked subsequently on numerous occasions by the vets at UCL animal services. There was no evidence of opportunistic infection in either strain. In particular, there was no evidence of Helicobacter species which may influence the susceptibility of mice to colitis.

Faeces from *Cldn8*-KO mice (n=10) and WT mice (n=11) was analysed for water content, as well as sodium and potassium concentrations. There was no statistical difference in water content of the faeces between the two groups, expressed as % of the weight of faeces (*Figure 4-11*). There was also no statistical difference in the concentration of sodium and potassium between the two groups (*Figure 4-12*).

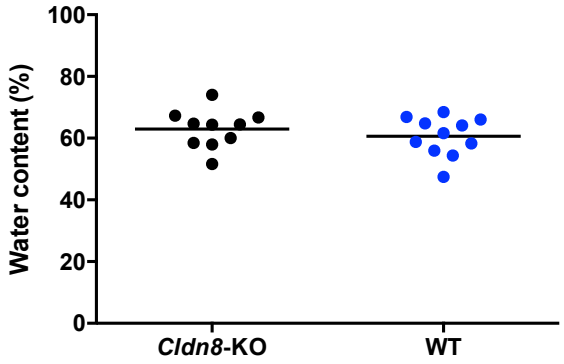

Figure 4-11 – **The faeces from *Cldn8*-KO and WT mice has the same amount of water.** *Faeces of Cldn8-KO (n=10) and WT (n=11) mice was weighed initially when fresh, and then dried overnight in an oven and the dry weight measured again to calculate the weight (and volume) of water as a percentage of the content of faeces.*

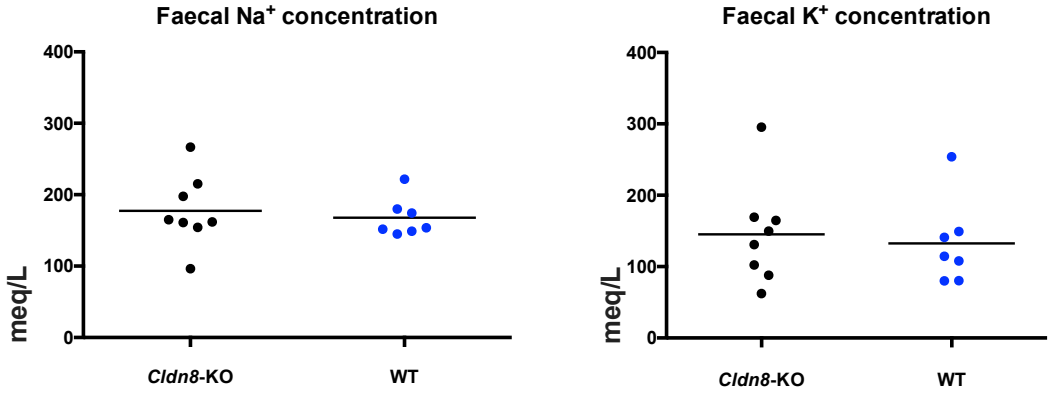

Figure 4-12 – **The faecal Na^+ and K^+ concentration is similar between *Cldn8*-KO and WT mice.** *The faeces of Cldn8-KO (n=10) and WT (n=11) mice was weighed initially when fresh, and then dried overnight in an oven and the dry weight measured again to calculate the weight (and volume) of water as a percentage of the content of faeces (meq/L – milliequivalents of solute per litre of solvent)*

4.2.7.4 Comparison of food and water consumption, and micturition and defecation of *Cldn8*-KO and WT mice

Metabolic cages were used to analyse the micturition and defecation in a controlled environment, whilst enabling measurement of animal's food and water consumption in a set period of time (*Figure 4-13*).

During the acclimatisation period, mice were provided the standard dry chow. However, by the following morning, the hard pellets had been powdered and scattered around, making it impossible to calculate how much of it was eaten by the mice. The powdered chow also fell into the funnel and mixed with urine, creating a thick, viscous material that trapped the faeces. Therefore, the measurements for food, urine and faeces were inaccurate. This was overcome by replacing standard dry chow with water-softened chow. One animal in the WT group appeared to have consumed significantly more water compared to other animals (*Figure 4-14*). This is likely due to insensible losses when the mouse tried to drink water and the water was scattered around. This was not the case for the other 5 mice, suggesting this was an issue with acclimatisation, and repeating the experiment with other mice will provide a more accurate reading. However, the animals appeared distressed on the metal mesh flooring of their cages after a few days, and it was felt that the experiment was unlikely to provide sufficiently accurate data to justify repeating the experiment with larger cohorts. Therefore, the metabolic cage experiments were performed only once, with three animals in each group, and not repeated after this.

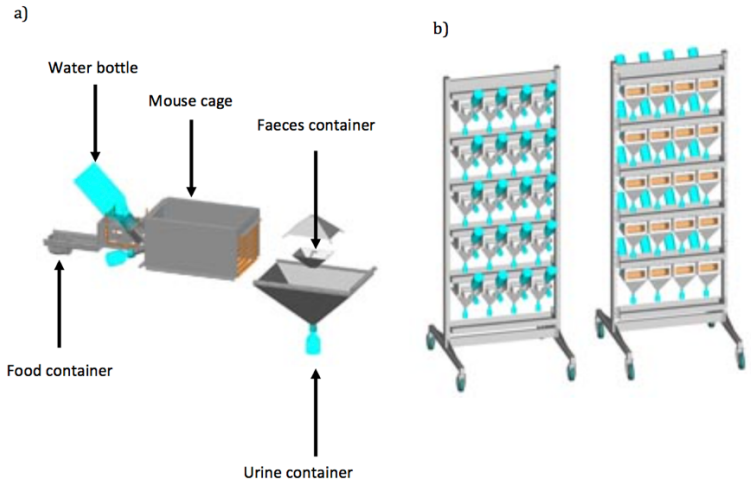

Figure 4-13 – **Schematic drawing of the mouse metabolic cage.** *(a) Different component of an individual metabolic cage, (b) rack system of the metabolic cage. Mice were placed individually in metabolic cages and allowed to acclimate for 5 days. Measurements were taken for 24 hours, after which the animals were culled.*

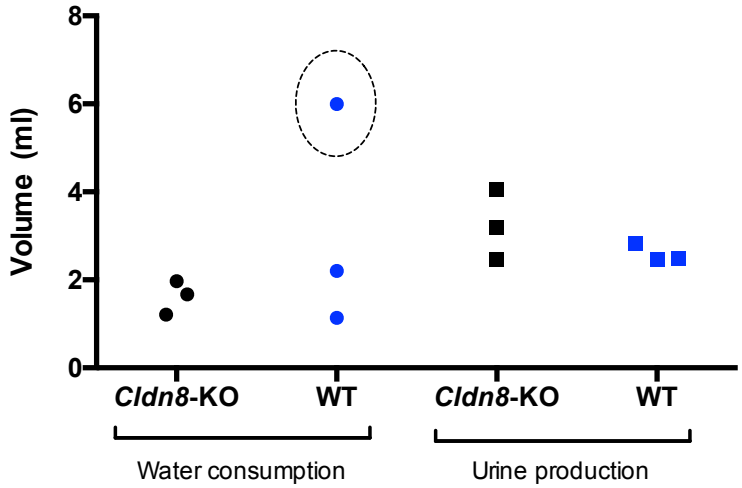

Figure 4-14 – **Comparison of water consumption and urine production of *Cldn8*-KO and WT mice**. *One animal (circled in graph above) in the WT group appeared to have consumed significantly more water compared to other animals. This is likely due to insensible losses when the mouse tried to drink water and the water was scattered around. This was not the case for the other 5 mice. Apart from this outlier, there was no statistical differences between the groups; however, this experiment was only performed once and on a small number of animals.*

4.2.7.5 Macroscopic and Microscopic examination and comparison of colons from *Cldn8*-KO and WT mice

Both macroscopic and microscopic examination of large bowel post mortem revealed no differences between the *Cldn8*-KO and WT mice. Large bowel from both groups was similar in weight and length (Figure 4-15-a). Histological examination of the GI tract (*Figure 4-15*-b) did not demonstrate any differences.

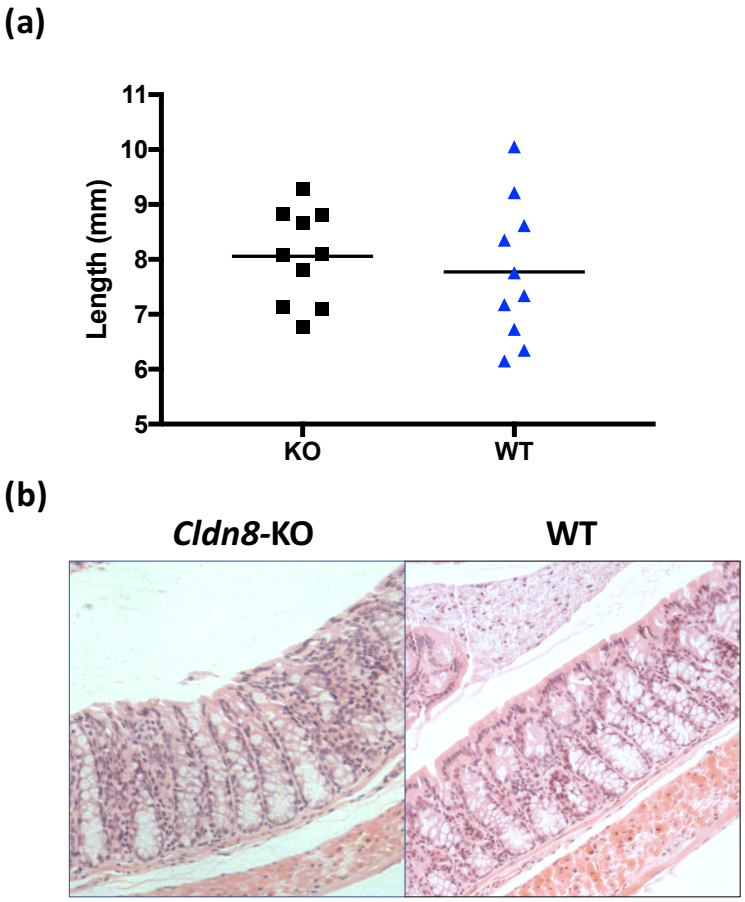

Figure 4-15 – **The macroscopic and microscopic appearances of the LI is similar in *Cldn8*-KO and WT mice** *(a) Length of large bowel is similar in both Cldn8-KO and WT mice. There is no statistical difference in the length of large bowel between Cldn8-KO and WT mice (n=10 per group) (b) Cldn8-KO mice do not exhibit any histological abnormality at baseline state. Histology examination of the naïve large bowel in Cldn8-KO and WT mice reveals no obvious morphological abnormalities or evidence of inflammation on Hematoxylin & Eosin (H&E) staining; LI, large intestine*

4.2.7.6 Baseline Serum Cytokines

Baseline serum cytokine concentrations were measured in naïve state in *Cldn8*-KO or WT mice, using MSD® Mouse Pro-Inflammatory 7-Plex Ultra-Sensitive Kit, which measures IL-2, INF-γ, IL-4, IL-10, IL-1b, IL-5, KC/GRO (IL-8), IL-6, TNF-α (Figure 4-16). Unfortunately probe for IL-12p70 did not provide any readings.

At resting, naïve state, IL-1b and IL-10 are expressed at higher levels in serum of *Cldn8*-KO as compared to WT mice. Expression levels of all other cytokines showed a larger variation in *Cldn8*-KO mice, but this did not reach statistical significant.

The results in Figure 4-16 have been combined from two separate experiments, and therefore are expressed as relative concentrations as opposed to actual concentrations.

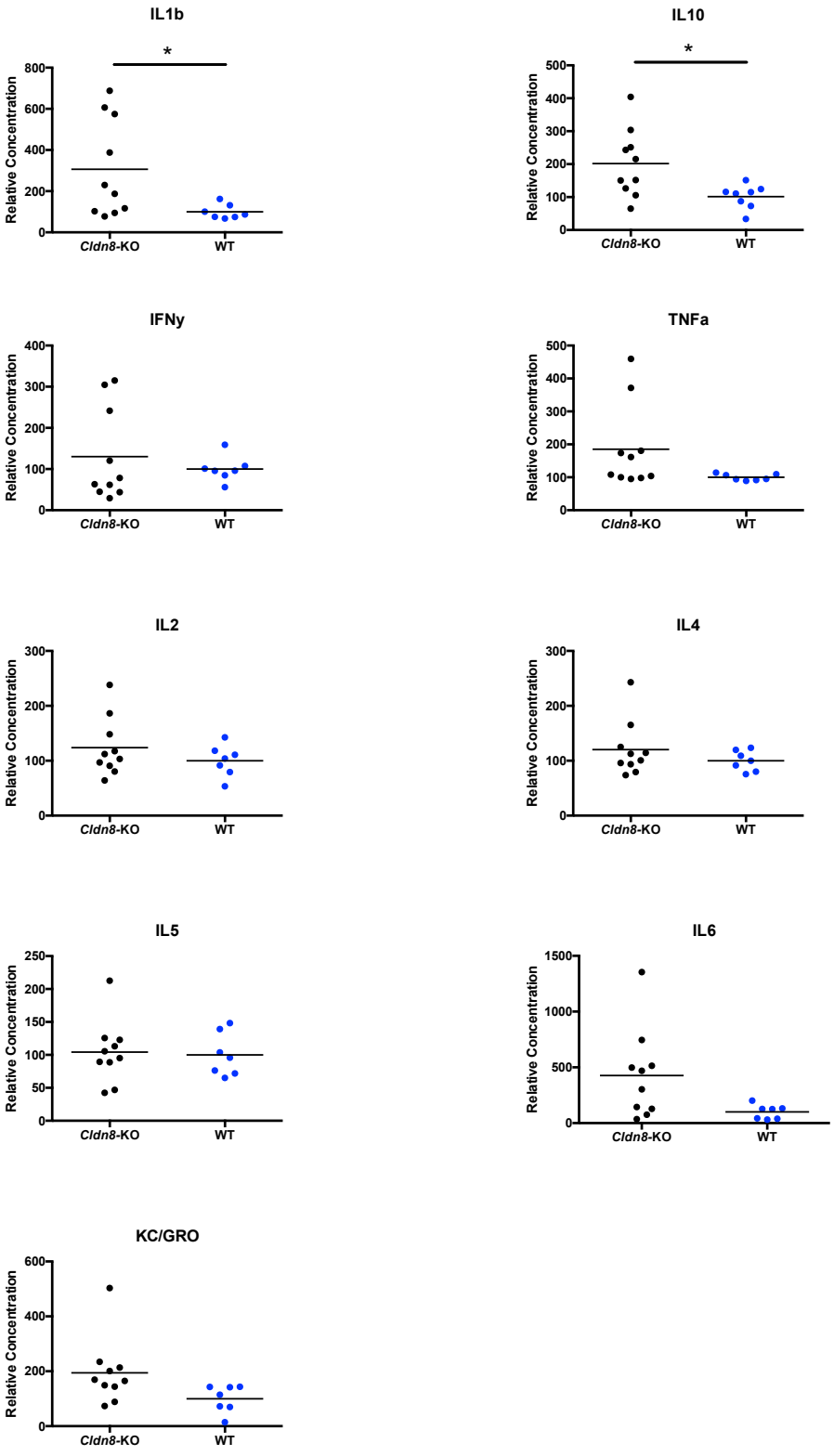

Figure 4-16 – ***Cldn8*-KO have a higher serum concentration of IL-1b and IL-10 at baseline state compared to WT mice.** *Whilst there was no statistical difference in the remaining serum cytokine levels between Cldn8-KO and WT mice, there is higher variability in cytokine concentration levels in Cldn8-KO mice. The results have been combined from two separate experiments and are expressed as relative concentrations as opposed to actual concentrations. (* p ≤ 0.5 using paired t-test)*

4.2.7.7 Baseline cell population in lamina propria (LP) of *Cldn8*-KO and WT mice

Intestinal LP cells, isolated by collagenase digestion of large bowels from naïve *Cldn8*-KO and WT mice were analysed using Fluorescence-activated cell sorting (FACS). No statistically significant differences were identified between the two groups.

Following optimisation of this method the average yield of live LP cells isolated was 26.33%, of which 40.97% were found to be haemopoietic in origin ($CD45^+$). Of these, 2.67% neutrophils ($GR1^{hi}$ $CD11b^+$ $SSC\text{-}A^{hi}$), 3.11% eosinophils ($GR1^{hi}$ $CD11b^+$ $SSC\text{-}A^{int}$), 26.02% were macrophages ($F4/80^+$) and 9.09% were DCs ($F4/80^+$ $CD11c^-$). The gating strategy is presented in Figure 4-17. Comparison of each cells line between Cldn8-KO and WT mice is shown in Figure 4-18.

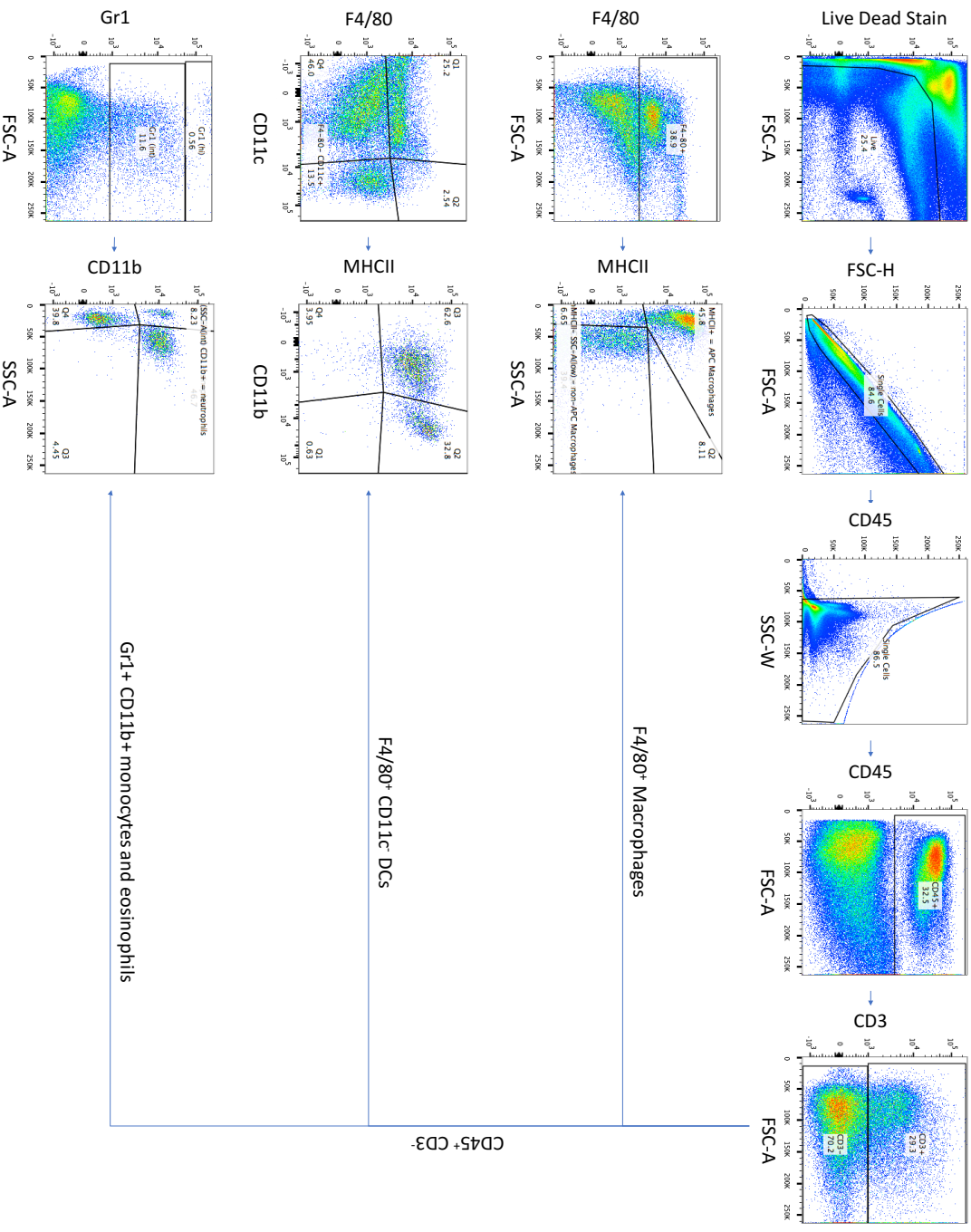

Figure 4-1 – **FACS gating strategy for analysing LP cells from mice**

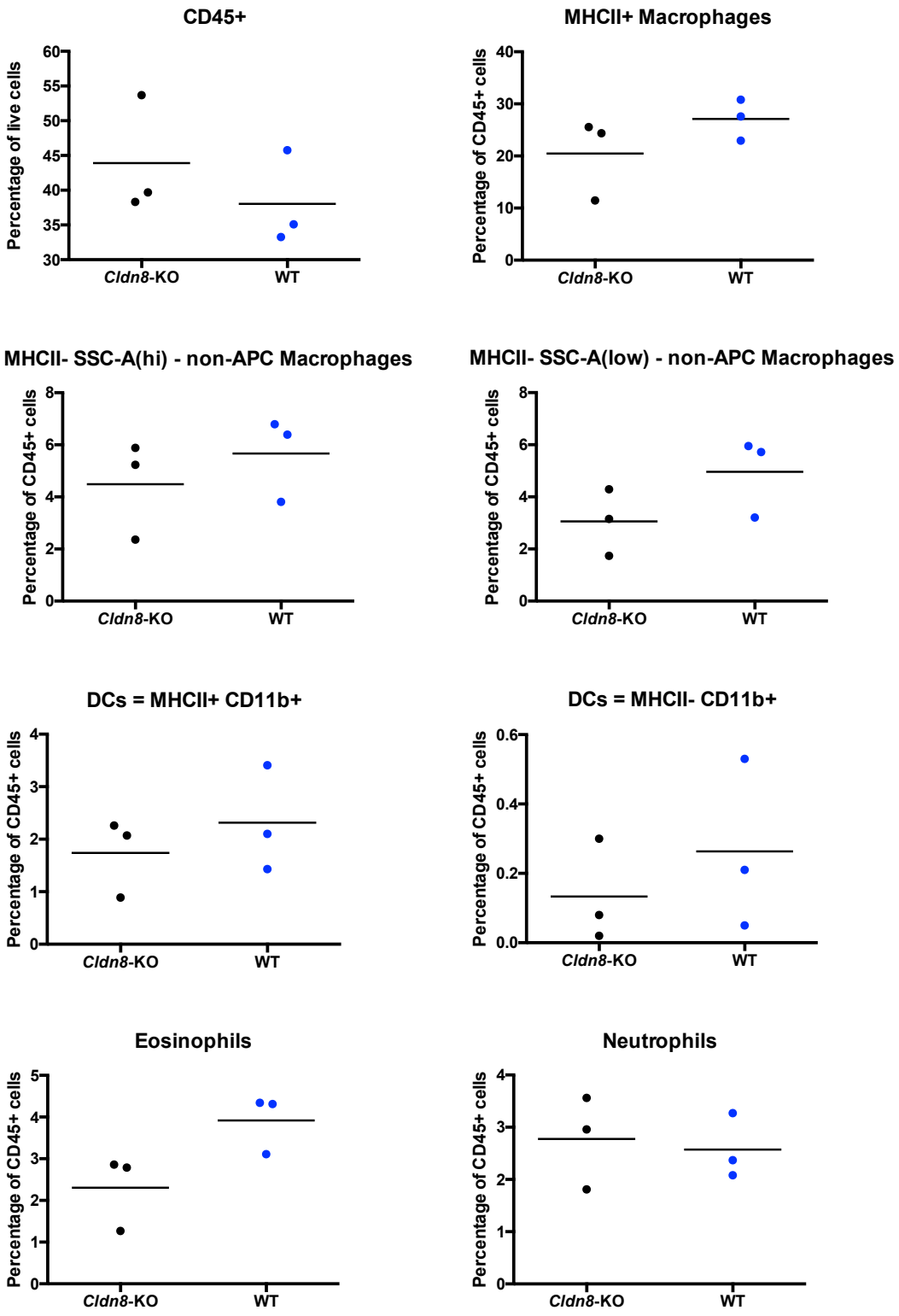

Figure 4-18 – **There is no statistical difference in composition of inflammatory cells in LP of *Cldn8*-KO and WT mice**; *$CD45^+$ is represented as percentage of total live cells; all other cells are represented as percentage of $CD45^+$ cells*

4.2.8 In naïve state, THERE IS NO DIFFERENCE IN INTESTINAL PERMEABILITY OF ^{3}H-MANNITOL AND FITC-DEXTRAN IN *Cldn8*-KO AND WT MICE

Great care was taken to reduce any manual handling of the bowel. However, in some a few of the mice, the 2-cm segment of the large bowel had faeces within the lumen, requiring gentle manual handling to remove the faeces. The two groups were analysed separately, and the results confirm that any manual handling of the bowel results in false-positive results (*Figure 4-19*), due to damage to the delicate epithelial cells. Therefore, in experiments comparing *Cldn8*-KO and WT, only results of animals without any faecal pellets in the bowel segment were used.

In naïve mice there is no difference in permeability of ^{3}H-mannitol or FITC-Dextran between *Cldn8*-KO and WT mice (*Figure 4-20*).

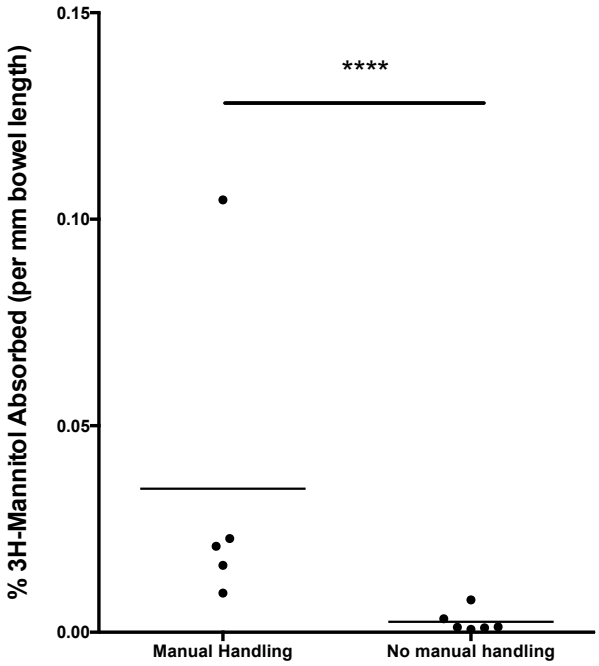

Figure 4-19 – **Manual handling of the intestine results in falsely elevated permeability readings.** *The permeability is higher in animals with faecal pellet in the lumen of bowel segment, which required manual handling to remove. All mice in this experiment were WT (****p ≤ 0.0001 using unpaired t-test)*

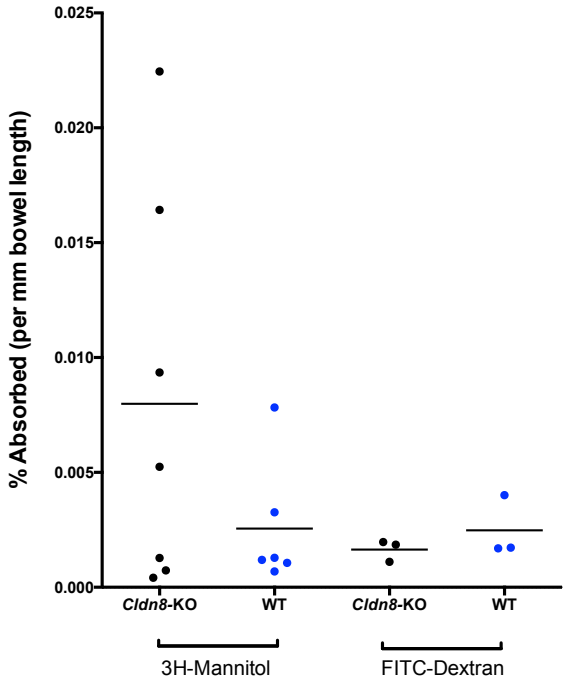

Figure 4-20 – **There is no statistical difference in permeability of ^{3}H-mannitol or FITC-Dextran between *Cldn8*-KO and WT mice in naïve state.**

4.2.9 THE INNER LAYER OF MUCOUS IS STERILE IN *Cldn8*-KO AND WT MICE

To investigate the permeability of inner layer of mucous, sections of the bowel where stained for bacteria luminal bacteria and epithelial DNA (the mucous staining – MUC2 did not work). The inner layer of mucous is sterile in both *Cldn8*-KO and WT mice.

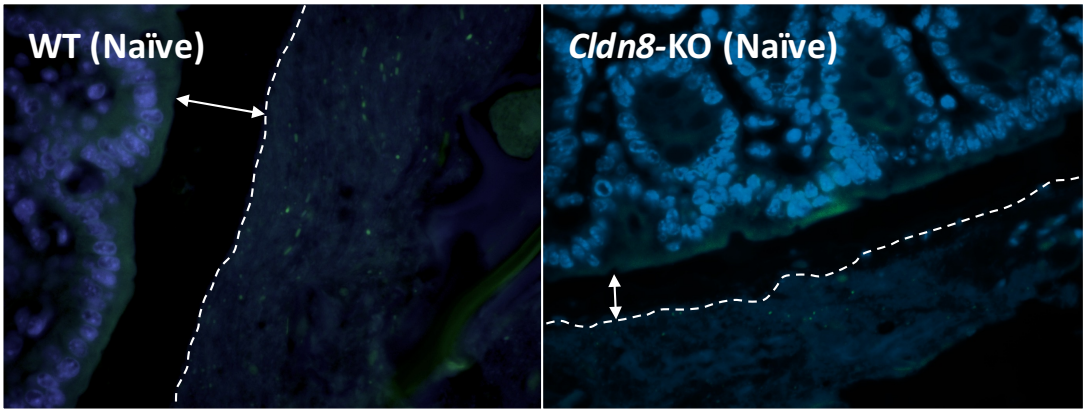

Figure 4-21 – **The inner layer of mucous is sterile in both *Cldn8*-KO and WT mice**. *The epithelial cell nucleus has been stained with DAPI (blue) and luminal bacteria have been stained with EUB338 (green). Sterile mucus layer is marked with a white arrow.*

4.3 DISCUSSION

In Chapter 3, the results of our unique transcriptomic dataset were analysed, and CLDN8 was found to have the second highest fold-change of all under expressed genes in patients with quiescent UC. Additionally, CLDN8 was the only TJ molecule with a significant fold change in its expression of ≤ -1 or ≥ 1, after correcting for multiple testing. Furthermore, CLDN8 expression levels increase significantly from proximal large bowel towards rectum, providing an intriguing possibility of link to the anatomical pattern of UC inflammation, where the inflammation extends up for a variable distance from the rectum. Therefore, the role of CLDN8 in inflammation was chosen for further investigations.

In this chapter, CLDN8 was shown to be highly conserved at amino acid level between humans and mice. It is therefore highly probable that the function of CLDN8 is conserved between humans and mice as well. After establishing deletion of *Cldn8* in the acquired *Cldn8*-KO mice, baseline characteristics of *Cldn8*-KO and WT mice were compared to fully assess the suitability of *Cldn8*-KO mice as an animal model to study the function of *Cldn8* in intestinal inflammation.

It was established that other *Cldns* do not compensate for the loss of *Cldn8* in the *Cldn8*-KO mouse. Also, no difference in fertility, growth or survival were observed between *Cldn8*-KO and WT mice, and *Cldn8*-KO mice did display evidence of spontaneous colitis or systemic inflammation in the naïve state – five animals were housed for one year, but none developed any clinical signs of colitis, including diarrhoea, rectal bleeding or weight loss.

Given the evidence that *Cldn8* acts as a barrier to monovalent cations including Na^+ and K^+ (102), faecal water content faecal Na^+ and K^+ concentration, mucosal permeability to luminal bacteria and intestinal permeability to two differently sized sugars were investigated in the naïve state, and no differences found between *Cldn8*-KO and WT mice. The inner layer of the mucous is also sterile in both *Cldn8*-KO and WT mice.

FACS analysis did not demonstrate any statistical difference in the composition of the inflammatory cells in LP between *Cldn8*-KO and WT mice. However, unfortunately, some of the FACS experiments did not work. In particular, experiments to assess subsets of T-cells, including T_{reg} did not work. This may be relevant given the findings of the cytokine concentrations (see below.)

The *Cldn8*-KO mice, however, had higher serum concentration levels of IL-1b and IL-10 in blood, compared to WT mice. Also, whilst there was no statistically significant difference between the other measured cytokines in the serum (TNF-α, INF-γ, IL-2, IL-4, IL-5, IL-6, KC/GRO between *Cldn8*-KO and WT mice, there was more variation in *Cldn8*-KO mice than WT. These findings were surprising given that *Cldn-8*-KO mice do not develop any abnormal phenotype, have normal intestinal permeability and normal inflammatory cell composition in their LI LP. Furthermore, the two cytokines with elevated concentrations in *Cldn8*-KO mice, IL-1b and IL-10 have opposing effects. IL-1b is a potent proinflammatory cytokine, inducing neutrophil influx and activation, T-cell activation and cytokine production, as well as B-cell activation and antibody production (272,273). IL-10, however, is an immune-inhibitor, and acts as an inhibitor of antigen presentation, inhibiting MHCII and upregulating co-stimulatory molecules CD80 and CD86, on DCs and macrophages (274). Mice lacking IL-10 spontaneously develop intestinal inflammation, preceded by changes in intestinal permeability (232). Recent evidence suggests that IL-10 is responsible for maintaining Foxp3 expression in T_{reg} cells in inflammatory conditions (69). The molecular mechanisms by which IL-10 maintains Foxp3 expression are not yet clear.

4.4 CONCLUSION

The findings in this chapter are intriguing. The *Cldn8*-KO mice do not exhibit any gross phenotypical abnormalities, and no statistically significant difference was observed between any of the measured parameters in the intestine of *Cldn8*-KO and WT mice. Despite these findings, the elevated serum IL-1b and IL-10 serum cytokine concentration levels in *Cldn8*-KO mice raise the possibility of ongoing, low-level inflammation. In the next chapter, effects of chemically induced colitis in mice, using DSS, will be investigated.

5 Characterisation of the *Cldn8*-KO mouse using a chemical induced model of colitis, DSS

5.1 INTRODUCTION

In chapter 4, *Cldn8*-KO mice were characterised in naïve state, and found not to develop spontaneous colitis. Therefore, to investigate the role of *Cldn8* in intestinal inflammation, colitis will be induced in the *Cldn8*-KO mice.

As discussed in Chapter 1.3, given that mice do not develop the equivalent of human IBD, different models of colitis have been developed in mice.

In this chapter, the effect of the chemically-induced colitis using DSS is investigated in *Cldn8*-KO mice. There were several reasons for choosing DSS to investigate the role of *Cldn8* in intestinal inflammation.

Firstly, the chemical toxin DSS is a widely used and published method to induce colitis in mice, and is added to the drinking water at concentrations of 1-5% for 3-7 days (275). In response to DSS, mice develop a predominantly neutrophilic infiltrate with a continuous colitis which resembles UC in humans (214,276). Histological changes in DSS-colitis include mucin depletion and epithelial degeneration leading to the formation of cryptitis and crypt abscesses. A chronic colitis can be induced by recurrent challenges of DSS (276,277).

Secondly, the current evidence suggests that, at least in part, the mechanism of action of DSS may be through its effect on the mucous layer. It has been shown that germ free mice develop significantly less severe colitis than SPF mice, and that in response to DSS exposure, the inner layer of the normally sterile inner mucous in the large bowel becomes permeable to bacteria (216). Taken together, these results suggest that luminal bacteria play a significant role in development of inflammation in DSS-induced colitis, and that one major contribution of DSS to development of inflammation is the effect it has on the properties of the mucous. Therefore, given that as discussed in chapter 4.1.2, loss of *Cldn8* may affect the properties of the mucous, DSS-induced colitis was chosen as the model to investigate the effect of *Cldn8* in intestinal inflammation.

5.2 RESULTS

5.2.1 DSS DOSE RESPONSE

In order to choose an appropriate dose of DSS to induce an experimental colitis, Dr O'Shea had previously performed a dose response study. For this, 25 wild type C57BL/6 male mice, 8-10 weeks old, were divided into 5 cages of equal numbers. Their drinking water was replaced with different concentrations of DSS (1%, 2%, 3%, 5%) dissolved in drinking water for 7 days. One group of mice did not have DSS added to the water and acted as the control group. After 7 days, the DSS was replaced by normal drinking water. Weights were measured and stool samples collected daily. Mice that survived the DSS challenge were culled at D15.

Mice exposed to 3-5% DSS developed severe bloody diarrhoea by day 5, lost >15% of their body weight by day 7 and all had to be culled by day 10 due to severe weight loss. In contrast mice exposed to 1% DSS lost very little weight and had minimal diarrhoea or rectal bleeding. 2% was deemed the ideal concentration of DSS to use for further experiments as mice lost <15% of their original weight which was maximal by day 10, but all had regained their baseline weight and normal stool consistency by the end of the experiment on day 15.

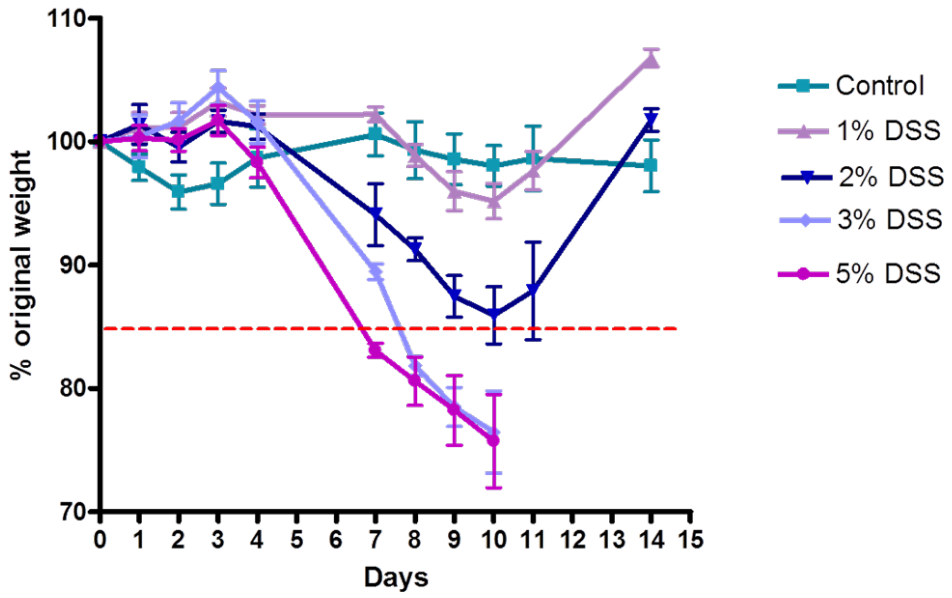

Figure 5-1 – **DSS results in a dose dependent weight loss in C57/B6 mice.** *DSS was dissolved in drinking water for 7 days at different percentages. Mice were weighed daily and plotted as a percentage of their original weight, error bars represent S.E.M. Dotted red line denotes 15% weight loss. Mice were litter mates, age, weight and sex matched, n=5 per group – figure from Dr O'Shea*

5.2.2 CHARACTERISATION OF 2% DSS COLITIS IN WT C57BL/6 MICE

In order to assess the suitability of DSS-induced mouse model of colitis for examination of the role of *Cldn8* in intestinal inflammation, C57BL/6 WT mice were exposed to 2% DSS in their drinking water for 7 days, before being switched back to normal drinking water. The mice's response to colitis was assessed, by measuring body weight and blood in the stool (including occult blood testing). Mice were sacrificed at days 0, 3, 9 and 21 from start of DSS and their large bowels were resected, measured and 5mm snips were taken from distal colon for qPCR measurement of *Cldn8* mRNA levels.

WT mice developed colitis, characterised with weight loss, diarrhoea, blood in their stool, and shortening of their large bowel (*Figure 5-2*). Similar to humans (see Section 3.2.1), and as reported previously in colitis (120,124), *Cldn8* levels dropped early on in the inflammatory process in Day 3. Interestingly, *Cldn8* expression levels showed rebound on Day 9, 2 days after mice were swapped back onto normal drinking water. By Day 21, *Cldn8* mRNA levels were back to baseline levels (*Figure 5-2*-d).

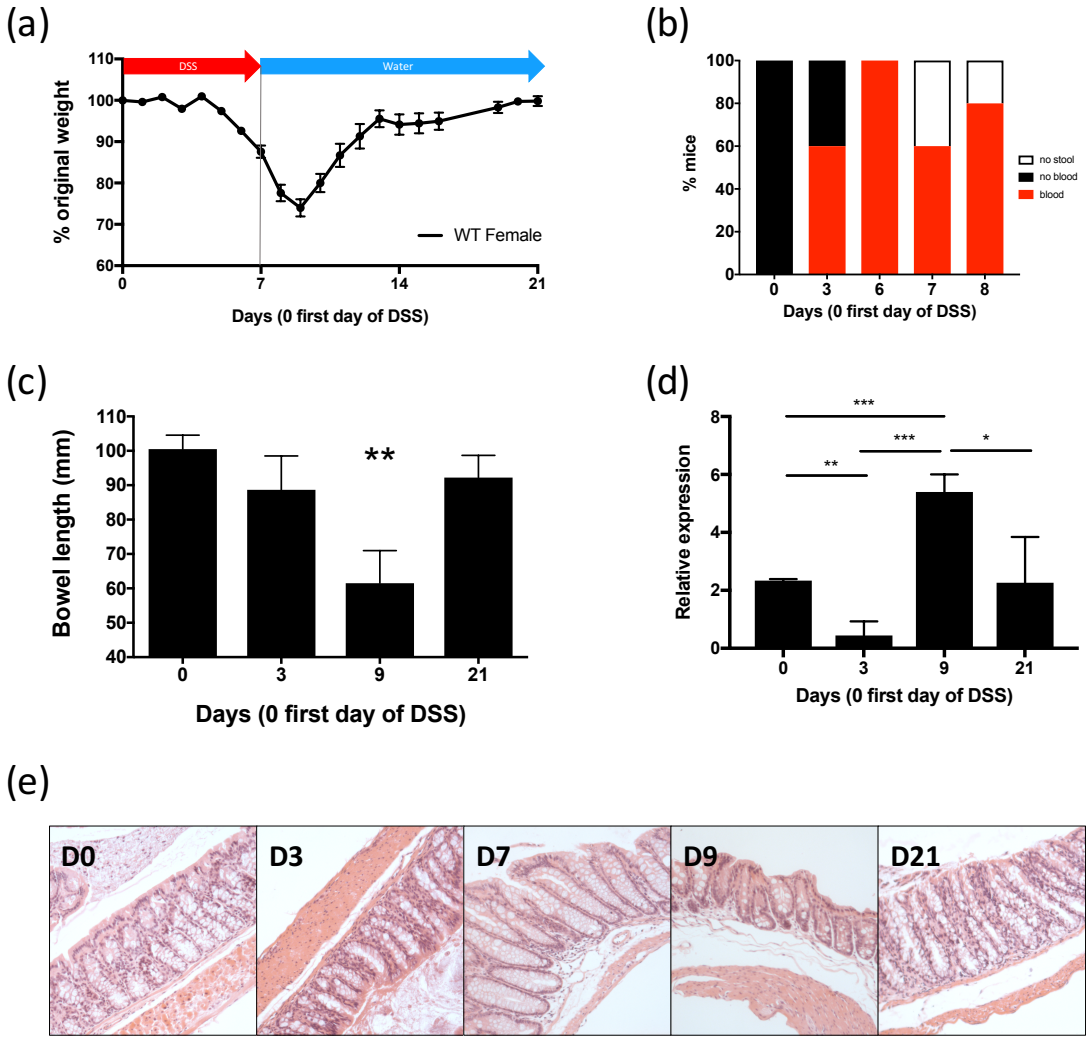

Figure 5-2 – **Mice develop colitis in response to DSS.** *WT mice developed colitis in response to consuming 2% DSS in their drinking water for 7 days, before being switched back to normal drinking water and recovering. Day 0 is traditionally the first day that DSS is started. D21 is 2 weeks after DSS had been stopped. (a) Mice were weighed daily and plotted as a percentage of their original weight, error bars represent S.E.M. (n=12). (b) Mice developed blood in their stools during colitis. As colitis became more severe, some mice did not pass stools within 30min. (c) Length of bowel in mice correlates to the severity of intestinal inflammation. (d) Quantitative PCR of Cldn8 relative to house-keeping gene PPIA in the large bowel was performed. Cldn8 mRNA expression levels drop in response to inflammation; however, there is a rebound in mRNA expression levels of Cldn8 during early recover phase, and return to normal levels by day 21* ***(e)*** *Representative image of H&E stained large bowel tissue (20× magnification, scale bar: 200 μm) on days 0,3, 9 and 21 after the DSS challenge demonstrates effects colitis in WT mice with increased cellular infiltration, crypt distortion, ulceration and goblet cell depletion on day 7. On day 21 there is histologic resolution of inflammation with normal tissue architecture. Error bars represent S.E.M; * $p < 0.5$, ** $p \leq 0.01$, *** $p \leq 0.001$, using unpaired t-test*

5.2.3 ACUTE COLITIS: 2% DSS-INDUCED COLITIS IN *Cldn8*-KO AND WT MICE

Cldn8-KO and WT mice were cohoused in UCL animal facility. Mice were age, weight and sex matched. Diet, ambient temperature, light and living conditions were identical for the two groups. Prior to experimentation mice were rested in the animal facility for at least 7 days to acclimatize. 2% DSS was added to the drinking water on D0 for seven days and then this was replaced with normal drinking water. Mice were assessed for weighed daily, and stool samples were collected daily for assessment of consistency and presence of blood. Mice were sacrificed at days 0, 3, 6, 9, and 14. Post mortem, blood was obtained from cardiac puncture for serum and bowels were resected for qPCR, FACS and histology.

5.2.3.1 Clinical signs

On examination both strains of mice became clinically unwell and developed a colitis during the seven-day exposure to 2% DSS. Clinical signs of diarrhoea, rectal bleeding and weight loss peaked at D9 in both strains.

WT mice were more susceptible to 2% DSS induced colitis than litter mate *Cldn8*-KO mice. This was evident clinically by an increased and more rapid weight loss ($p<0.0001$) (*Figure 5-3*-a) with more severe clinical signs and earlier onset colitis with bloody diarrhoea. Stool from WT mice contains bloods earlier than stool from *Cldn8*-KO mice, in response to DSS (*Figure 5-4*-a). The stool from both groups shows evidence of blood. However, the proportion of WT mice with blood in their stools is higher than *Cldn8*-KO mice within 2 days of DSS. Lack of stools is a feature of severity of colitis, due to reduction in peristalsis of inflamed bowel, and a higher proportion of WT mice did not defecate when compared to *Cldn8*-KO mice (ordinarily mice defecate every 3-5 minutes; in these experiments, “no stool” was defined as lack of defecation for 30 minutes).

Interestingly, *Cldn8*-KO mice develop softer stool in response to DSS more rapidly than WT mice. However, the proportion of *Cldn8*-KO mice that develop severe diarrhoea is smaller than WT mice (*Figure 5-4*-b)

Clinical improvement was seen in both strains from D10 onwards; mice regained their original weights and stool consistency returned to normal (*Figure 5-3*).

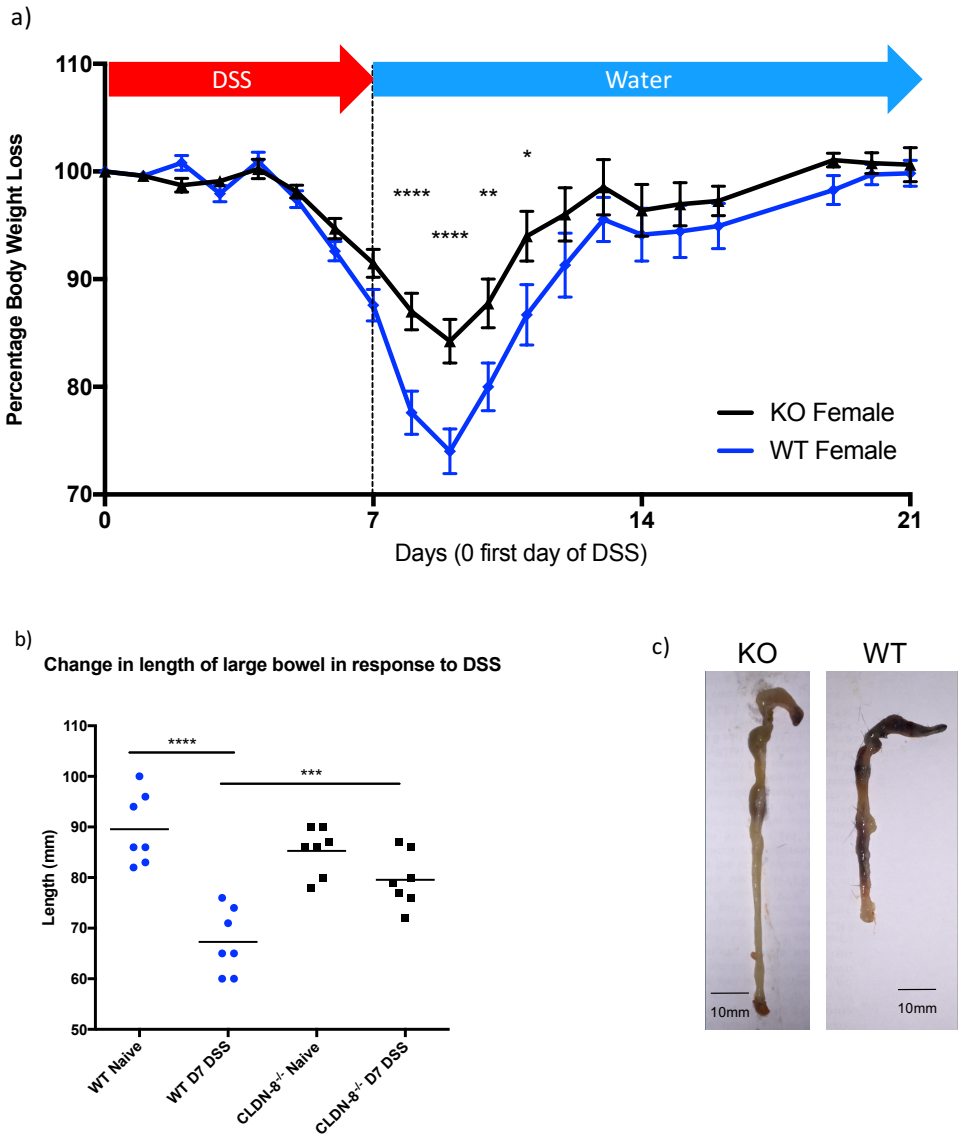

Figure 5-3 – **Loss of *Cldn8* results in reduced susceptibility to DSS induced colitis.** *Cldn8*-KO *and WT litter-mate mice exposed to 7 days of DSS. (a) Cldn8*-KO *mice do not lose as much body weight and are not clinical as unwell as the WT mice, (b) the large bowel in WT mice shrinks significantly more than the large bowel in Cldn8*-KO *(n=7 per genotype (c) Representative photographs of colons resected post mortem from Cldn8*-KO *and WT mice on day 9 post DSS. The colons from WT mice contained bloody stools, seen here in the shrunken caecum, and were significantly shorter than those from Cldn8*-KO *mice. Error bars represent S.E.M; * p < 0.5, ** p ≤ 0. 01, *** p ≤ 0.001, **** p ≤ 0.0001 using unpaired t-test*

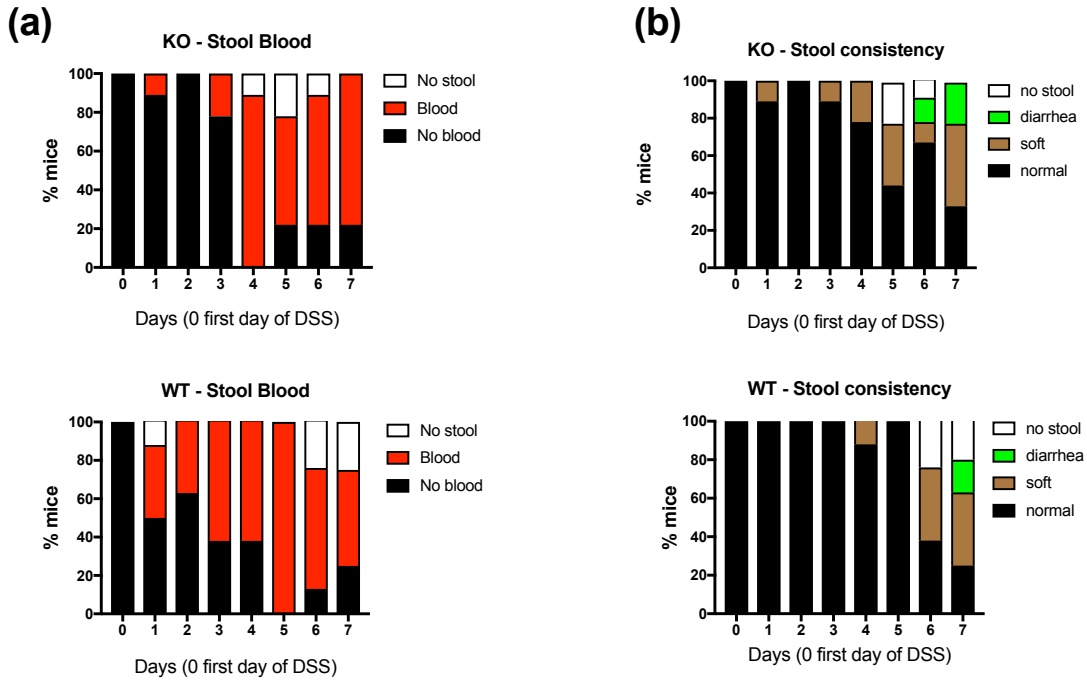

Figure 5-4 – **Rate of onset of colitis is faster in WT mice than in *Cldn8*-KO mice**. *(a) in response to DSS, blood appears in the stools of WT mice in a shorter time than in Cldn8-KO mice. (b) Cldn8-KO mice develop softer stool in response to DSS more rapidly than WT mice. However, the proportion of Cldn8-KO mice that develop severe diarrhoea is smaller than WT mice. Lack of stools is a feature of severity of colitis, due to reduction in peristalsis of inflamed bowel.*

5.2.3.2 Serum Cytokines

During the course of the experiment cardiac puncture was performed on days 0, 3, 6, and 9, in *Cldn8*-KO or WT mice, using MSD® Mouse Pro-Inflammatory 7-Plex Ultra-Sensitive Kit, which measures IL-2, INF-γ, IL-4, IL-10, IL-1b, IL-5, KC/GRO (IL-8), IL-6, TNF-α (Figure 5-5). Unfortunately probe for IL-12p70 did not provide any readings. The results in for D0 have been combined from two separate experiments, and therefore all the results, across multiple dates are expressed as relative concentrations and not actual concentrations.

Table 5-1 summarises the findings.

Days on DSS	Findings
0 (naïve)	Higher IL-1b and IL-10 concentration levels in *Cldn8*-KO mice
3	Higher IL-2 concentration levels in *Cldn8*-KO mice
6	Higher IL-5 concentration levels in *Cldn8*-KO mice
9 (post DSS)	Higher IL-10 concentration levels in WT mice

Table 5-1 – **Summary of differences between cytokine concentration levels between *Cldn8*-KO and WT mice at different stages of DSS inflammation**

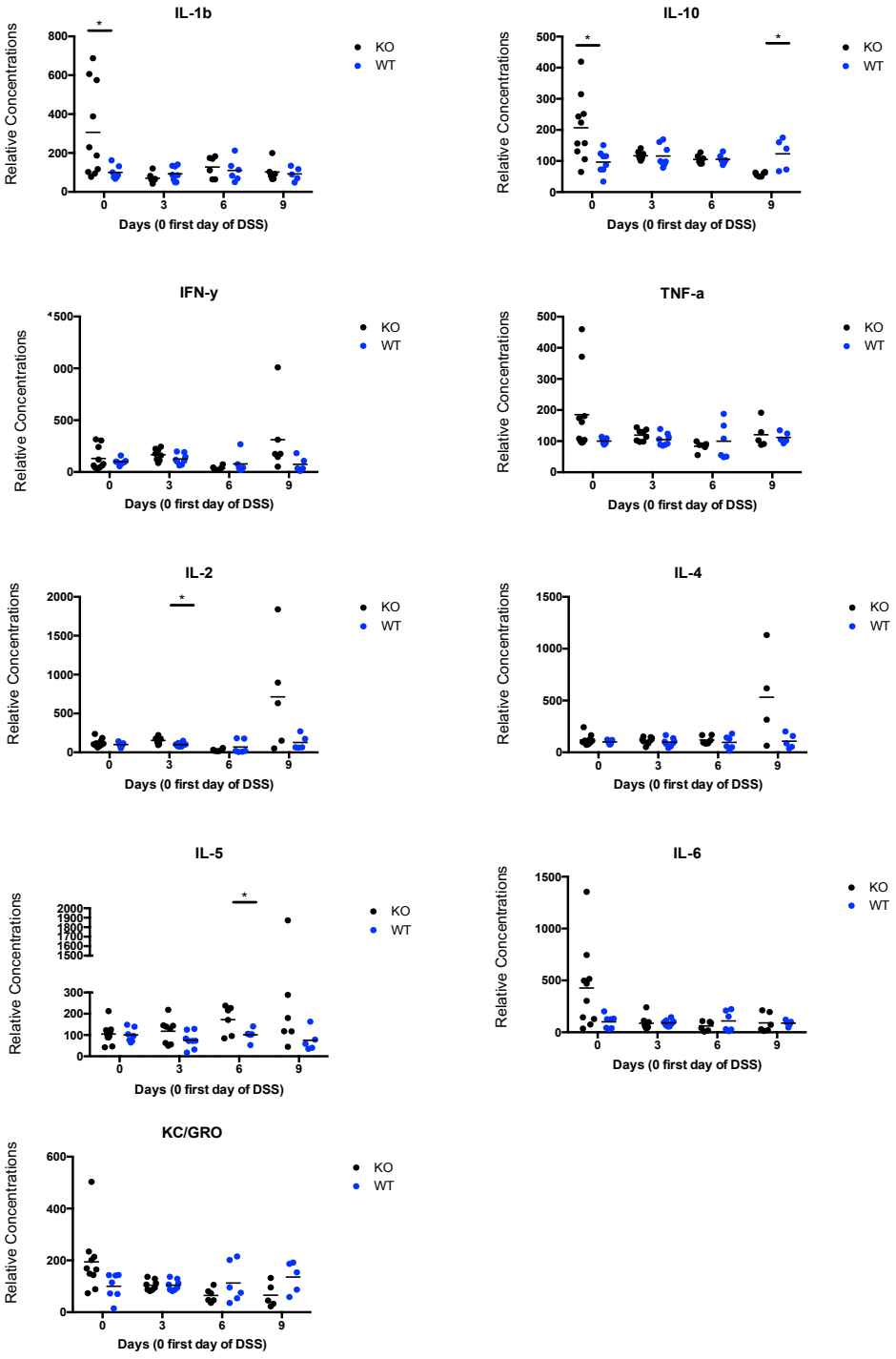

Figure 5-5 – **Serum cytokine concentration levels in *Cldn8*-KO and WT at different stages of DSS inflammation.** *D0 is naïve state, DSS was stopped on D7, and therefore D9 is 2 days post-DSS. In naïve state, Cldn8-KO mice have higher concentration of IL-1b and IL-10. On D3, only IL-2 is expressed at higher concentration in Cld8-KO, on D6 only IL-5 is expressed at higher concentration in Cld8-KO, and on D9, only IL-10 is expressed at higher concentration in WT mice. No other statistically significant difference was observed between the two groups at different stages of DSS-induced inflammation. The results have been combined from two separate experiments and are expressed as relative concentrations as opposed to actual concentrations. (* p < 0.5 using unpaired t-test)*

5.2.4 MICROSCOPIC CHANGES IN RESPONSE TO DSS-INDUCED COLITIS

Mice were culled on Day 0, 3, 7 and 9 to determine histological evidence of colitis. As previously discussed in no macroscopic or microscopic differences were observed in the colon of Cldn8-*KO* naïve mice compared with WT naïve mice.

Consistent with clinical signs, both strains developed evidence of colitis on histology, with increased cell infiltration, crypt elongation, distortion and ulceration. Both groups had histologic signs consistent with severe colitis by day 7. However, there was no statistically significant difference in the histological scores between the *Cldn8*-KO and WT mice at any time point. (*Figure 5-6*).

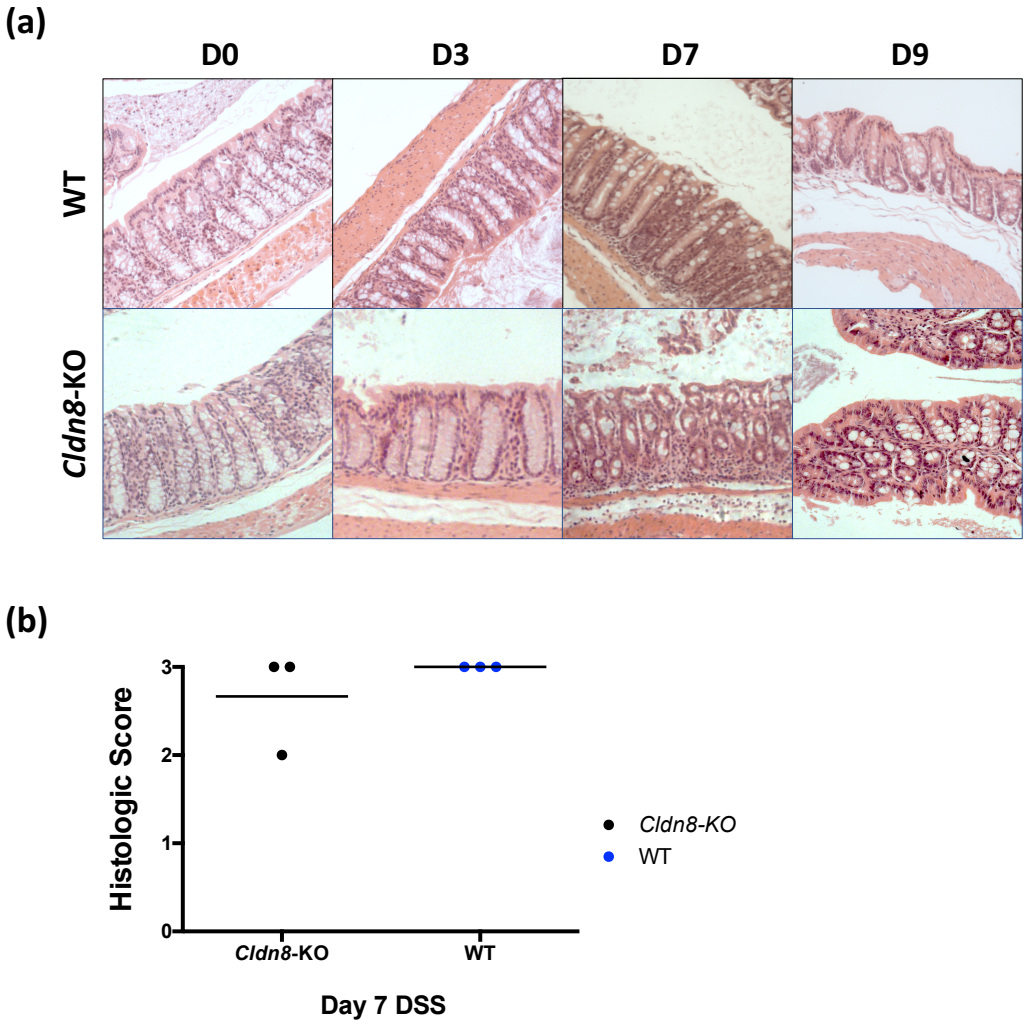

Figure 5-6 – **There is no histological difference between Cldn8-KO and WT mice on DSS.** *(a) Representative image of H&E stained large bowel tissue (20× magnification) on days 0, 3, 7 and 9 after the DSS challenge demonstrates effects colitis in Cldn8-KO and WT mice with increased cellular infiltration, crypt distortion and goblet cell depletion and ulceration on day 7 (b) On days 0, 3, and 9, the histological score was 0 for Cldn8-KO and WT mice. On day 7, both groups had severe inflammation on histology*

5.2.5 THE SEVERITY OF DSS-INDUCED COLITIS IS DIFFERENT BETWEEN MALE AND FEMALE MICE

The severity of DSS-induced colitis is varied between male and female mice in WT mice but not in *Cldn8*-KO mice (*Figure 5-7*). Whilst both male and female WT mice develop colitis and lose weight, this is more pronounced in female WT mice, which lose significantly more weight than their male counterparts. The severity of colitis in male WT mice is similar to that of male *Cldn8*-KO mice. The male WT mice do not recover from colitis as rapidly as their *Cldn8*-KO mice, or even the female WT mice (*Figure 5-7*-a and *Figure 5-7*-c). The rate of recovery is similar in female WT and *Cldn8*-KO mice.

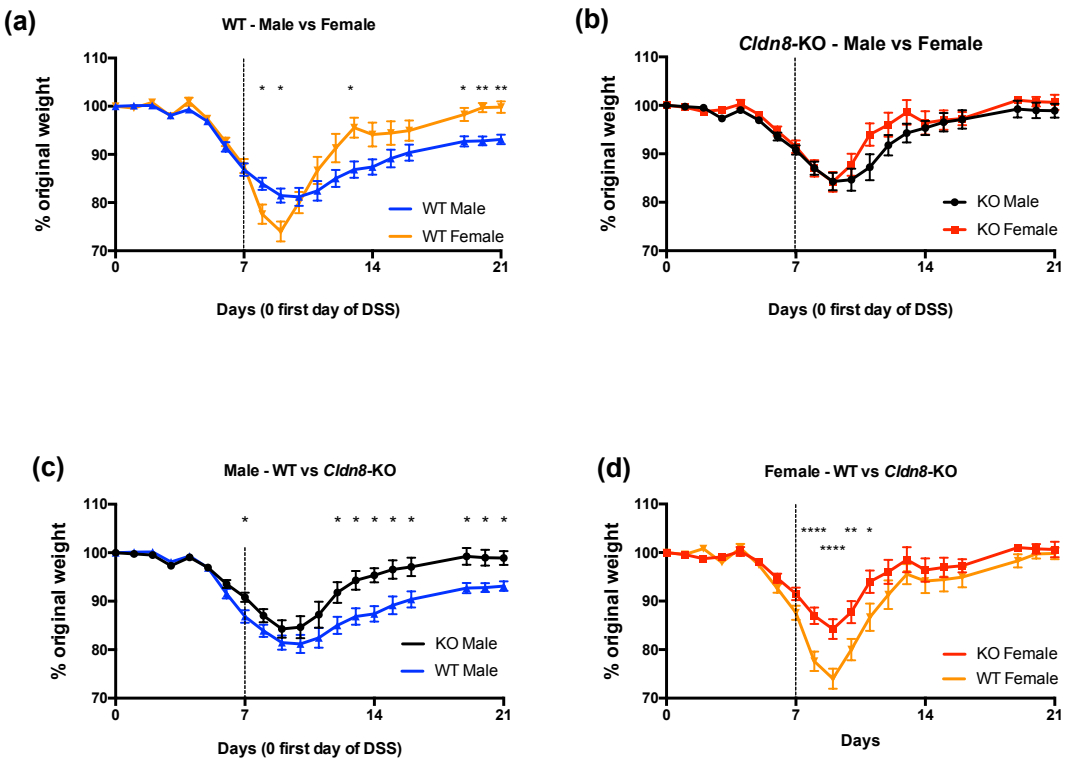

Figure 5-7 – **The severity of DSS-induced colitis is different between male and female mice.** *Female WT mice develop the most severe colitis. The severity of colitis in male WT mice is comparable to that of male and female Cldn8-KO mice. However, male WT mice do not recover as rapidly as the female WT mice, or the male or female Cldn8-KO mice. Error bars represent S.E.M; * p < 0.5, ** p ≤ 0. 01 using unpaired t-test*

5.2.6 CHRONIC COLITIS: REPEAT EXPOSURE OF *Cldn8*-KO AND WT MICE TO 2% DSS

Cldn8-KO and WT mice were exposed to two consecutive 7-day challenges of 2% DSS. After each challenge a period of recovery was permitted; in one experiment, 14 days recovery was permitted between the first and second challenge, and in another experiment, 28 days of recovery was permitted before the final 7 days of DSS.

The period of rest from DSS provided to mice before a repeating the exposure to DSS affected the severity of colitis. Mice develop a relative resistance to developing a second episode of colitis if exposed to DSS within a short period after the first episode of DSS-induced colitis. The colitis in WT mice after 5 weeks of rest was as severe, and mice lost weight at the same rate, as they did during the first bout of DSS induced colitis (*Figure 5-8*-a). However, the WT mice that were exposed to DSS only after 2 weeks of break had significantly milder colitis (*Figure 5-8*-a). This phenomenon was repeated in Cldn8-KO mice as well (*Figure 5-8*-b). This suggests that even though both groups have recovered from their first episode of colitis, and phenotypically mice appear the same at week 2 or week 5 after the first exposure to DSS, important differences exist at molecular level that confer protection from developing another severe episode of colitis. The colitis that mice develop after being exposed to DSS only after 2 weeks of rest is markedly milder than even the colitis developed by Cldn8-KO after their first exposure to DSS (*Figure 5-8*-b).

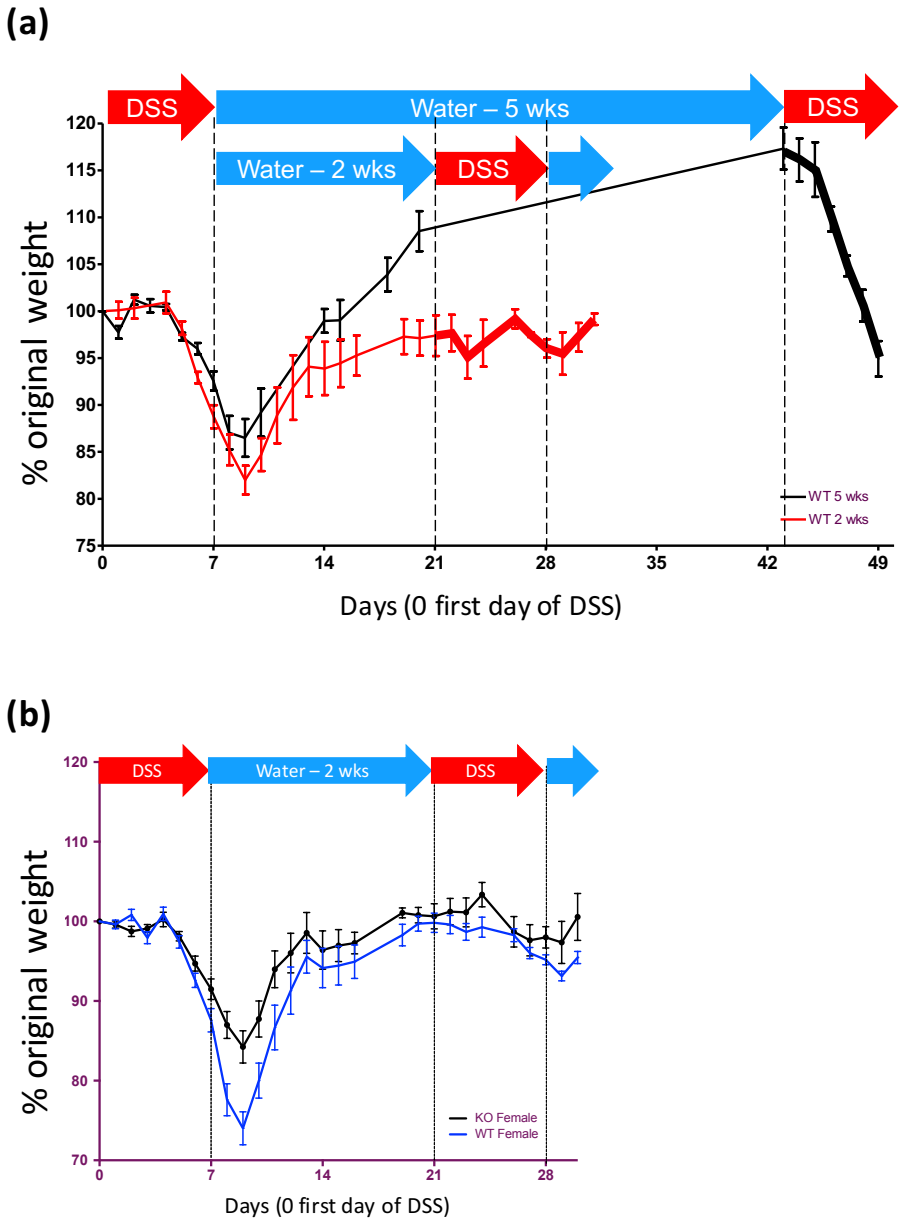

Figure 5-8 – **Mice develop resistance to repeated DSS-induced colitis.** *The period of rest from DSS provided to mice before a repeating the exposure to DSS affected the severity of colitis. Mice develop a relative resistance to developing a second episode of colitis if exposed DSS within 2 weeks of the initial insult (b) but lose this protection after 5 weeks (a) Error bars represent S.E.M – the 5 week DSS experiment in WT mice in (a) was performed by Dr O'Shea*

5.2.7 ASSESSMENT OF CELLULAR INFLAMMATORY RESPONSE IN LP OF *Cldn8*-KO AND WT MICE

As discussed in section 4.2.7.7, no difference was seen in the cellular composition within the colonic LP in naive *Cldn8*-KO mice compared with WT mice. There was no statistical difference in the number of cells in LP of *Cldn8*-KO mice compared with WT mice during DSS inflammation and immediate recovery period (*Figure 5-9*).

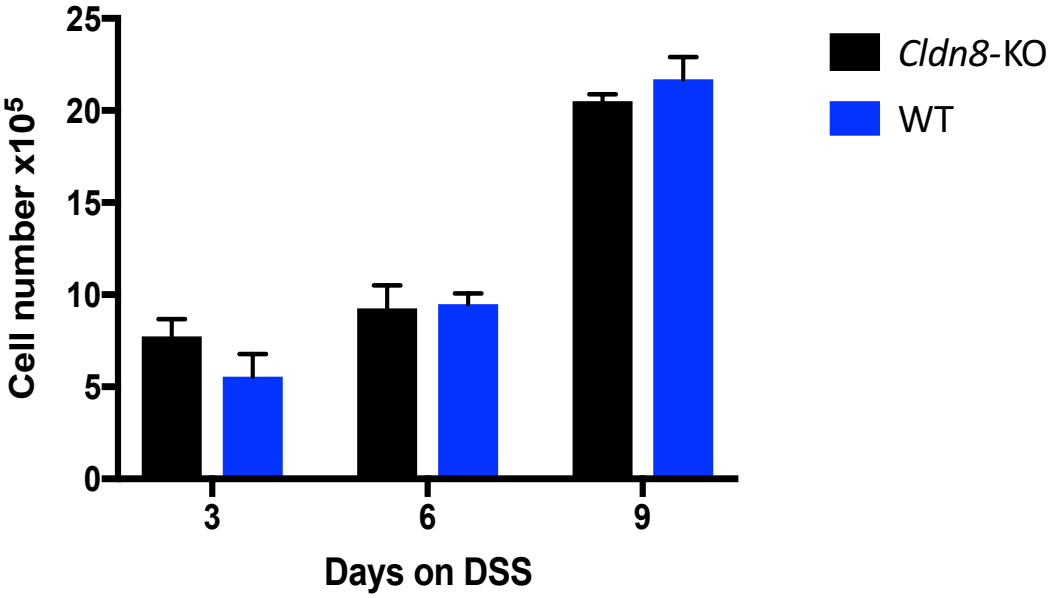

Figure 5-9 – **There is no difference in cellular response to inflammation in LP of *Cldn8*-KO mice compared with WT mice,** *Error bars represent S.E.M; n=3 per group*

FACS analysis of the colonic LP cell populations was performed for each genotype at day 0, 3, 6, 9, 14, following exposure to DSS, as well as second episode of DSS exposure on day 21, 24 and 28. By day 3, a lower proportion of neutrophils ($GR1^{hi}$ $CD11b^{+}$ $SSC\text{-}A^{hi}$) were recruited to the LI in *Cldn8*-KO mice when compared with WT mice. *Cldn8*-KO has lower proportion of recruited neutrophils by day 6 as well, but by day 9, the proportion of neutrophils were comparable between the *Cldn8*-KO and WT mice (*Figure 5-10*-a and -b). On day 3, *Cldn8*-KO also had a lower proportion of macrophages (F4/80+ MHCII+) present in their LP than WT mice (*Figure 5-11*-a and –b). The differences in proportion of other cell types across different time points were not statistically significant.

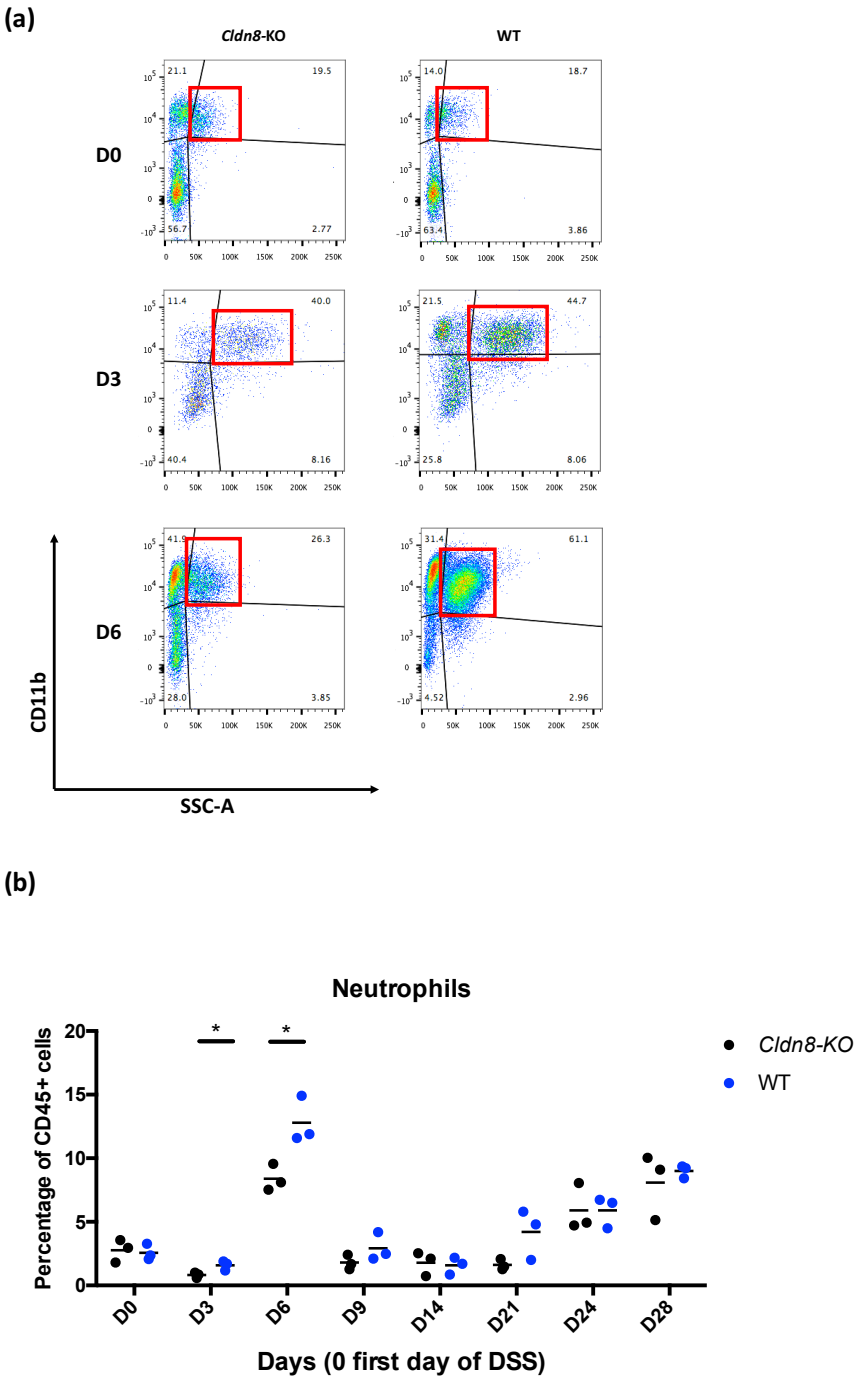

Figure 5-10 – ***Cldn8*-KO mice have an attenuated neutrophilic infiltration into the colon following exposure to DSS.** *Representative FACS plots of isolated colonic LP cells in naïve mice (D0), 3 days (D3) and 6 days (D6) post DSS in Cldn8-KO and* WT*. The proportion of neutrophils (GR1^{hi} CD11b^{+} SSC-A^{hi}) were determined using FACS analysis. The proportion of neutrophils in colonic LP are similar between the naive Cldn8-KO and WT mice (day 0), but the proportion of neutrophils in Cldn8-KO* mice is lowers when compared with WT mice*, on D3 and D6. The proportion of neutrophils did not significantly differ between the groups by Day 9 after initial DSS exposure. The mice were provided another DSS challenge on D21. However, neutrophils made up a significantly smaller proportion of cells on Day 28, than they did on Day 6. Results are expressed as the mean; *p<0.05 using unpaired t-test*

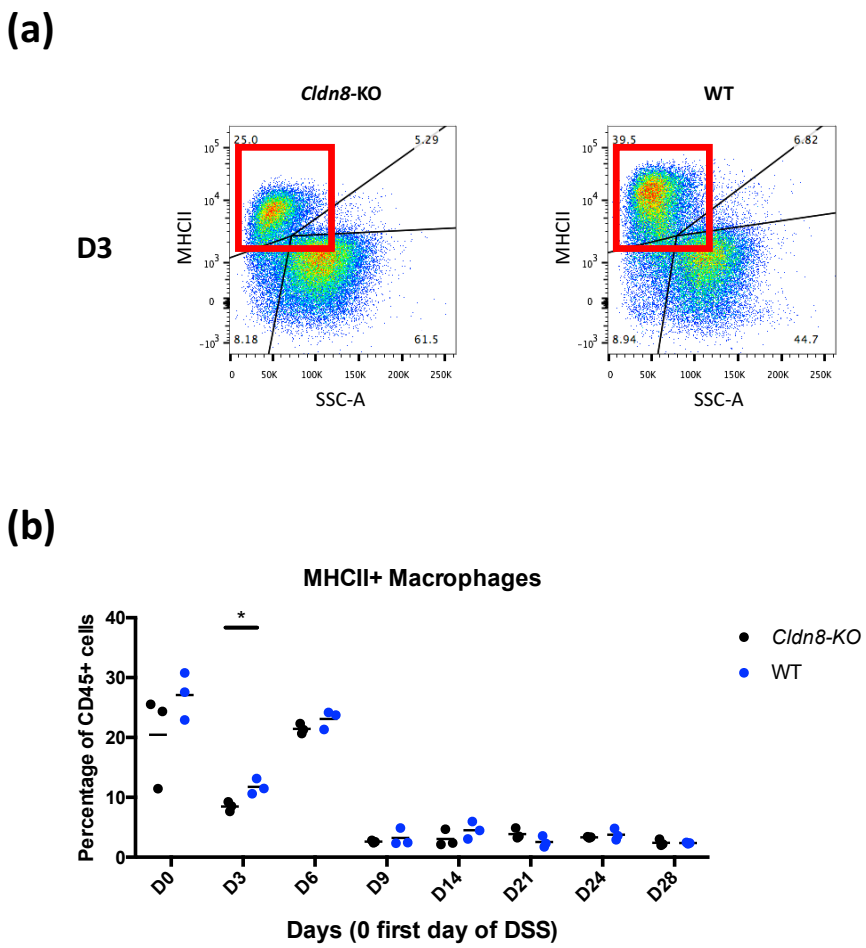

Figure 5-11 – ***Cldn8*-KO mice have a lower proportion of macrophages in the colon LP following exposure to DSS.** *Representative FACS plots of isolated colonic LP cells in naïve mice on day 3 (D3) post DSS in Cldn8-KO and WT. The proportion of antigen-presenting macrophages (F4/80$^+$ MHCII$^+$) were determined using FACS analysis. The proportion of macrophages in colonic LP are similar between the naive Cldn8-KO and WT mice (day 0), but are lower in Cldn8-KO mice on D3 post DSS. The proportion of macrophages did not significantly differ between the groups by Day 6 after initial DSS exposure. The mice were provided another DSS challenge on D21. However, macrophages made up a significantly smaller proportion of cells on Days 21 and 28, than they did on Days 3 and 6. Results are expressed as the mean; *p<0.05 using unpaired t-test*

5.2.8 INCREASED PERMEABILITY TO ^{3}H-MANNITOL IS LESS PRONOUNCED IN *Cldn8*-KO MICE COMPARED TO WT MICE IN EARLY STAGE INFLAMMATION

As discussed in chapter 4.2.8, no differences in permeability were observed in naïve state between *Cldn8*-KO and WT mice. Both groups have increased permeability to ^{3}H-Mannitol and FITC-Dextran by Day 3 of administration of DSS. However, the increased permeability to ^{3}H-mannitol is less marked in *Cldn8*-KO mice as compared to WT mice (*Figure 5-12*-a). This reflects their less severe clinical response to DSS colitis. There is no difference in permeability of ^{3}H-mannitol in both groups by Day 9 on DSS. There is no difference in permeability of FITC-Dextran between *Cldn8*-KO and WT mice. Interestingly, whilst the permeability of ^{3}H-mannitol remained abnormal by Day 9 in both animal groups, the permeability of FITC-Dextran returned to normal by Day 9 post initiation of administration of DSS.

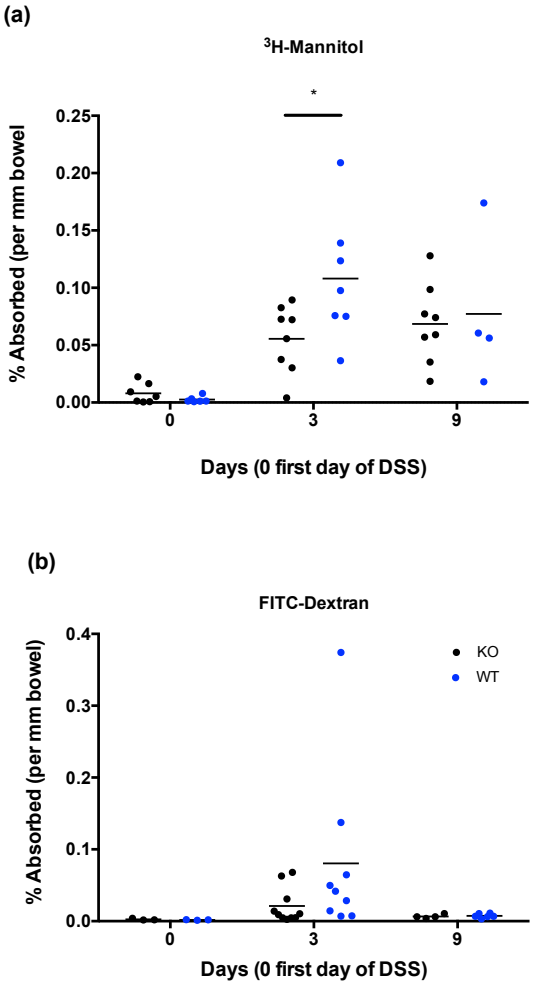

Figure 5-12 – **Permeability of ^{3}H-mannitol and FITC-Dextran is raised in both *Cldn8*-KO and WT mice by D3 of DSS**. However, the increase in permeability of ^{3}H-mannitol is less pronounced in *Cldn8*-KO mice on D3 DSS; ** $p < 0.5$ using unpaired t-test*

5.2.9 THE INNER LAYER OF MUCOUS REMAINS STERILE AFTER 12 HOURS OF EXPOSURE TO DSS IN *Cldn8*-KO AND WT MICE

To investigate the permeability of inner layer of mucous, sections of the bowel where stained for bacteria luminal bacteria and epithelial DNA (the mucous staining – MUC2 did not work), in naïve state and after the animal was exposed to DSS for 12 hours. In both states (naïve as well as post-DSS), the inner layer of mucous was sterile in *Cldn8*-KO and WT mice.

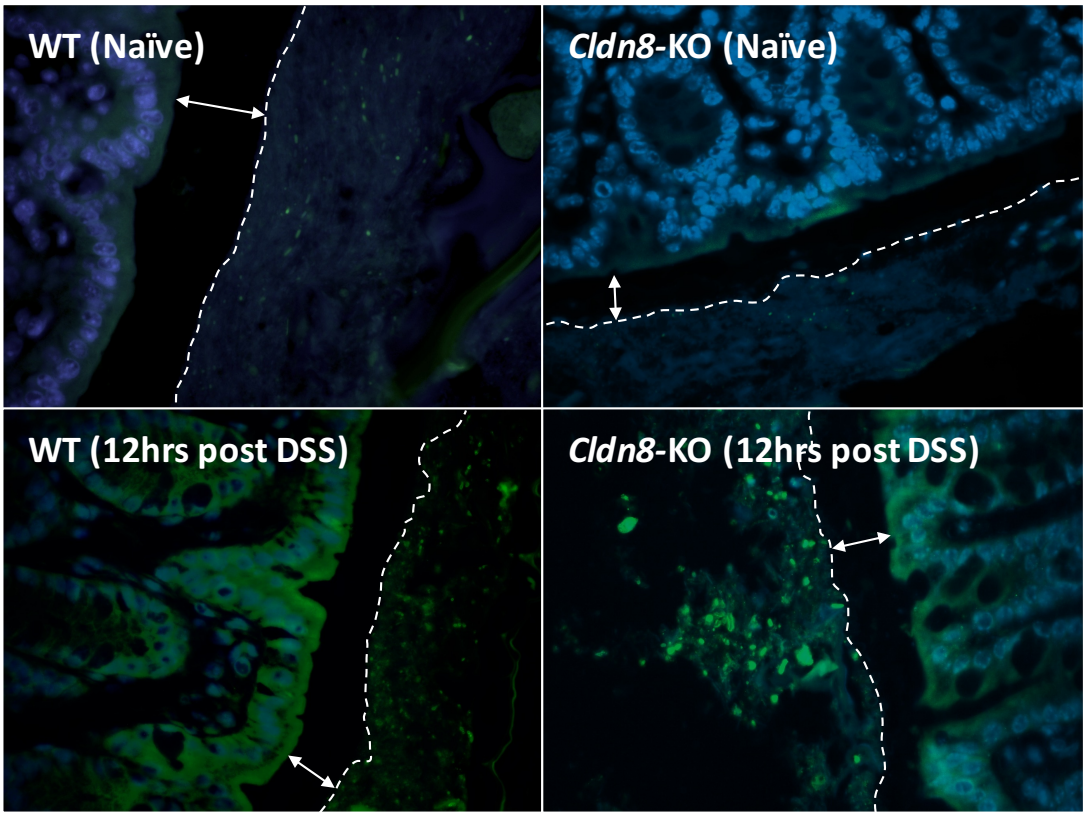

Figure 5-13 – **The inner layer of mucous remains sterile in both *Cldn8*-KO and WT mice after the animals were exposed to DSS for 12 hours.** *The epithelial cell nucleus has been stained with DAPI (blue) and luminal bacteria have been stained with EUB338 (green). Sterile mucus layer is marked with a white arrow*

5.3 DISCUSSION

In Chapter 4, the *Cldn8*-KO mice were characterised in naïve state, and found to have no discernible physiological difference with the C57BL/6 WT mice. In this chapter, effect of DSS-induced colitis on *Cldn8*-KO mice were studied.

DSS was used to induce colitis in mice. In response, *Cldn8* was downregulated in LI in WT mice, returning to baseline as the colitis resolved. This response is similar to observations made by others (120,124).

Interestingly, in WT mice, *Cldn8* is overexpressed during the early phase after DSS insult is removed; this is when the bowel is recovering and epithelial injury is healing. The dynamic response of *Cldn8* locally to intestinal inflammation would suggest that the molecule has a role in the cellular regeneration. This is in keeping with observations that *Cldns* may be involved in cell motility (278).

Most intriguing was the observation that the DSS-induced colitis was significantly milder in *Cldn8*-KO mice than WT mice. This was characterised by reduced weight loss, and significantly healthier appearing LI macroscopically. The finding was mirrored in a smaller increase in the proportion of LI LP neutrophil and macrophage populations as well as smaller raise in intestinal permeability in *Cldn8*-KO, particularly during the early phase of the inflammation.

This was a surprising finding, and contrary to the original hypothesis.

With regards to intestinal permeability, the increase in permeability of ^{3}H-mannitol was lower in *Cldn8*-KO as compared to WT mice. The same was true for FITC-Dextran, though the difference did not reach statistical significance. Interestingly, whilst the permeability of ^{3}H-mannitol remained abnormal by Day 9 in both animal groups, the permeability of FITC-Dextran returned to normal by Day 9 post initiation of administration of DSS. This is an interesting observation, given that the animals were switched back to normal water on Day 7. Taken together, this data suggests that permeability of ^{3}H-mannitol (4Å in size), is likely to be determined by properties of the paracellular spaces between epithelial cells; however, the permeability of FITC-Dextran is likely to be determined by breaks in the epithelial layer, which should start to close as the epithelial cells starts to regenerate after withdrawal of DSS.

The attenuated clinical response of the *Cldn8*-KO mice to DSS was also evidence in the inflammatory cellular infiltrate to the LI LP. By day 3, a lower proportion of neutrophils and macrophages were recruited to the LI in *Cldn8*-KO compared to WT

mice. However, by day 9 the proportion of neutrophils were comparable between the *Cldn8*-KO and WT. Unfortunately, the FACS experiments investigating population of T_{reg} cells did not produce any results.

The precise mechanism of inflammation in DSS-colitis is not known. It is well established that the resultant inflammation has many of the features of UC in humans (214), including weight loss, diarrhoea and blood in the stools, and histological changes including mucin depletion and epithelial degeneration leading to the formation of cryptitis and crypt abscesses. Mice receiving DSS develop evidence of breakdown in the tight junction complex with a loss of tight junction proteins (279), and epithelial apoptosis (280) within the first 24 hours of DSS exposure. The directly toxic effect of DSS on epithelial cells is thought to be secondary to formation of nano-lipocomplexes with medium-chain-length fatty acids in the large bowel that can fuse with epithelial cell membranes (214). The evidence for a directly toxic effect of DSS comes from studies in antibiotic treated (281), and germ free (282,283) mice, which, in response to DSS, developed a significantly less severe colitis than SPF mice with normal intestinal microflora. Further evidence into the pathogenesis of DSS comes from studies of mucous properties. In the LI, the inner layer of the mucous is normally sterile, and impenetrable to luminal bacteria. However, it has also been shown that after exposure to DSS, the inner layer of the mucous in the large bowel that is normally sterile becomes permeable to bacteria (216).

As discussed in chapter 4.1.2, aldosterone promotes absorption of water, through its effect on absorption of sodium from the luminal side of colonic epithelial cells by simultaneously inducing epithelial sodium channels (ENaC) and CLDN8 expression (107) (*Figure 4-2*). This may therefore provide a mechanism for the relative protection against DSS witnessed in *Cldn8*-KO mice, where the mucous may be better hydrated and more resistant to the effects of DSS. To investigate this, investigations were performed to investigate the permeability of mucous in *Cldn8*-KO and WT mice in naïve state and after the animal was exposed to DSS for 12 hours. No differences were observed between *Cldn8*-KO and WT mice at either time point, and the inner layer of the mucous remained sterile after exposure of the animals to DSS for 12 hours. The 12 hour time window was chosen based on previously published reports that the inner layer of mucous becomes permeable after exposure of the animal to DSS for 12 hours (174). It is worth noting that the authors Johansson *et al* had used 3% DSS for their experiments, as opposed to 2% DSS used in experiments in this thesis. This might explain the reason that the inner layer of mucous remained sterile

even in WT mice in these experiments, and that a longer exposure time on 2% DSS may cause the inner layer of mucous to become permeable to bacteria.

The serum concentration of a number of cytokines (IL-1b, IL-2, IL-4, IL-5, IL-6, KC/GRO, TNF-α, INF-y) was measured at different time points during inflammation, and shortly after, during recovery period. The finding that the IL-2, was increased in *Cldn8*-KO mice on day 2 was interesting. IL-2 is the major growth factor for T lymphocytes and plays an important role in stimulating the suppressor function of Tregs (284,285), as well as stimulating generation of effector and memory $CD8^+$ T cells (285). IL-5, which had a higher serum concentration in *Cldn8*-KO mice on day 5 post DSS-induced colitis, induces terminal differentiation of B-cells to immunoglobulin production. IL-5 is mainly produced by activated T helper (Th) 2 cells and mast cells. By day 9, WT mice had higher concentration levels of anti-inflammatory cytokine IL-10 than *Cldn8*-KO mice. This, however, may represent the milder colitis in *Cldn8*-KO mice and faster recovery of their acute inflammatory response. What was particularly intriguing about the concentration of cytokines measured on day 9, was the comparison of concentration levels in *Cldn8*-KO mice on day 0 (naïve) and day 9 (recovery period post DSS). As discussed previously, in naïve state, the mice had a significantly more varied concentration level for most of the cytokines, and IL-10 and IL-1b in particular, appeared to be present at higher concentration in the serum. However, by day 9 (only 2 days after removal of DSS from the mice), IL-10 and IL-1b concentration were very low in *Cldn8*-KO mice, and comparable to the naïve state in WT mice.

Another intriguing finding are the results of the chronic DSS model in mice, where animals were exposed to DSS again, after a variable length of time. When WT mice were exposed to DSS after 5 weeks of rest, they developed colitis as severe as the first bout of exposure. However, when mice were exposed to DSS only after 2 weeks of rest, they had a significantly milder colitis. This protective phenotype was observed in both *Cldn8*-KO and WT mice. In keeping with this finding, the neutrophils and macrophages made up a significantly smaller proportion of cells when the mice were challenged with DSS after 2 weeks, showing a clearly attenuated inflammatory response.

5.4 CONCLUSION

Although DSS colitis resembles microscopic features of IBD, in particular UC, it does not truly reflect the pathophysiology of human IBD. However, in WT mice, *Cldn8* in is downregulated in response to DSS-induced colitis, which is in keeping with the observation in patients with UC where CLDN8 has one of the highest fold changes of any downregulated gene. *Cldn8*-KO mice have an attenuated response to DSS-induced colitis. These results suggest that CLDN8 does have a role in intestinal inflammation, and downregulation of CLDN8 may be a protective mechanism by the intestine. The finding that serum IL-10 levels are slightly elevated in naïve *Cldn8*-KO mice, may provide a possible mechanism for the protective phenotype observed in these mice. As discussed in chapter 4.3, IL-10 is an anti-inflammatory cytokine, and mice lacking IL-10 spontaneously develop intestinal inflammation (232). Recent evidence suggests that the IL-10 is responsible for maintaining Foxp3 expression in T_{reg} cells in inflammatory conditions (69). This may represent a mechanism of action for reduced susceptibility of *Cldn8*-KO mice to developing colitis secondary to DSS. However, as described above, unfortunately, the set of FACS experiments investigating population of T_{reg} cells did not produce any results.

The following chapter uses transcriptomic analysis to investigate the molecular basis for the observed differences to DSS-induced colitis between *Cldn8*-KO and WT mice.

6 Transcriptomic analysis of *Cldn8*-KO and WT mice at naïve state and during DSS inflammation

6.1 INTRODUCTION

As discussed in chapter 1.2, UC is a very heterogeneous disease, and the aetiology is poorly understood. The current prevailing hypothesis for pathogenesis of UC is that an abnormal innate immune response in genetically susceptible individuals, combined with environmental factors, result in excessive activation of the adaptive immune system within LP (142,143). Abnormalities in mucous, epithelial permeability, immune system, as well as the microbiome have all been implicated.

In chapter 3, data from transcriptomic analysis of our unique dataset of patient with quiescent UC was presented, and CLDN8 was identified as the only TJ molecule with a significant fold change in its expression of ≤ -1 or ≥ 1, after correcting for multiple testing. In chapters 4, no physiological differences were identified from the *Cldn8*-KO and the WT mice. Subsequently, in chapter 0, it was demonstrated that *Cldn8*-KO mice's clinical response to DSS is significantly attenuated when compared with WT mic, and that there is a small (but statistically significant) difference in permeability to ^{3}H-mannitol by Day 3.

In this chapter, a 'hypothesis generating' approach is taken to identify a molecular basis for the observed differences to DSS-induced colitis between *Cldn8*-KO and WT mice. Transcriptomic data were analysed using conventional group comparisons.

6.2 RESULTS

6.2.1 QUALITY CONTROL OF MICROARRAY RESULTS

To identify difference in expression between *Cldn8*-KO and WT mice, microarray analysis of genome-wide gene expression was performed, at naïve state (D0), D3 (early-mid-point inflammation), D9 (early recovery phase), and D21 (post recovery). D21 is particularly interesting, because whilst the animals' colitis has clinically recovered by day 21, both *Cldn8*-KO and WT mice display a protective phenotype against developing colitis in response to further bout of DSS, and this protection is only transient as it is lost within a few weeks (see Chapter 5.2.6 for details).

Microarray analysis was performed using Illumina Mouse-WG6 v2.0 Expression BeadChips. Three animals were used per group, per time point (overall 24 animals). Expression data were $\log_2$ transformed with cubic spline normalisation (286) between arrays, by Dr Adam Levine (Figure 6-1). 21,555 out of the total of 45,282 probes (47.6%) were found to be expressed at detectable levels, as determined using the detection p-values associated with each probe (see Materials and Methods section 0 and 2.11.1 for details). Unfortunately, *Cldn8* probes (ILMN_2623145, ILMN_2681236) did not provide any reading for any of the samples (including WT naïve state mice). qRT-PCR was performed to confirm that *Cldn8* was expressed in the original samples (see *Figure 5-2* for qRT-PCR confirmation). This confirmed that *Cldn8* was indeed expressed and that the probe on the BeadChip was faulty.

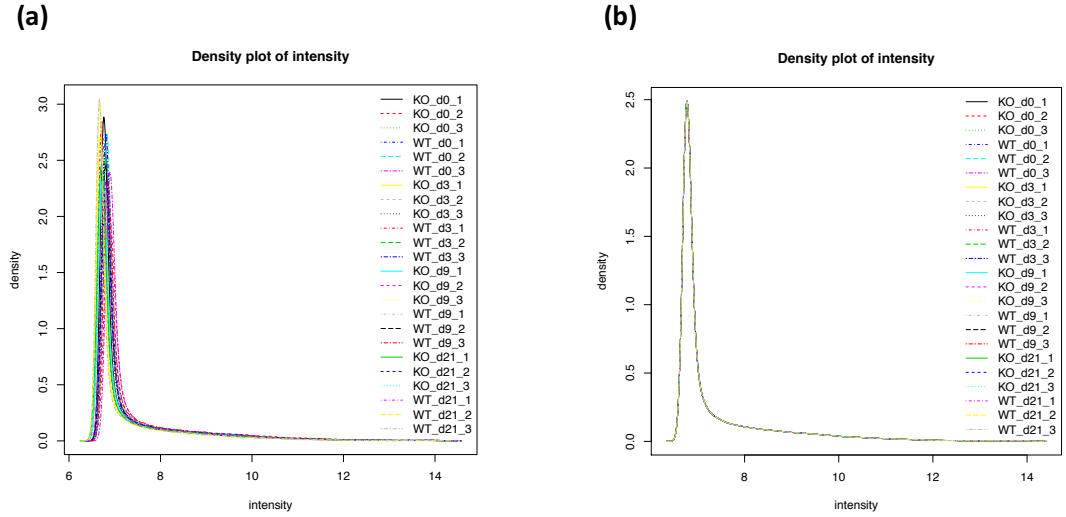

Figure 6-1 – **Cubic spine normalisation.** *Density plots of intensity of each array are superimposed on a single graph for a better comparison between arrays and for an identification of arrays with abnormal distribution. (a) is pre-normalised and (b) is post-Cubic spline normalised data.*

6.2.2 DIFFERENTIALLY EXPRESSED GENES BETWEEN *Cldn8*-KO AND WT MICE

Differentially expressed genes were identified using the Multiple Experiment Viewer (MEV) TM4 software suit (version 10.2), an established software package for statistical analysis of microarray datasets (244). Probes were identified that were significantly different between *Cldn8*-KO and WT mice at the four time-points, using an uncorrected p-value of $p < 0.01$ and a minimum fold change of ≤ -1 or ≥ 1 compared to mean expression in either *Cldn8*-KO mice or the WT mice. See Figure 6-2 for the volcano plots, and Table 6-2 for the list of genes with minimum fold change of ≤ -1 or ≥ 1.

DSS Days	Total no. of differentially expressed genes	Differentially expressed genes with minimum Fc ≤ -1 or ≥ 1
D0 (naïve)	188	10
D3	144	2
D9 (early recovery)	182	2
D21 (protective period)	549	16

Table 6-1 – **Number of differentially expressed genes between *Cldn8*-KO and WT mice at different stages of DSS-induced colitis**. *Whole genome microarray analysis of gene expression was performed using Illumina Mouse WG6.0 v2.0 expression array. Differentially expressed genes were identified using a minimum fold change of ≤ -1 or ≥ 1 and p-value <0.01 (uncorrected for multiple testing). None of the genes remained statistically significant after correction for multiple testing.*

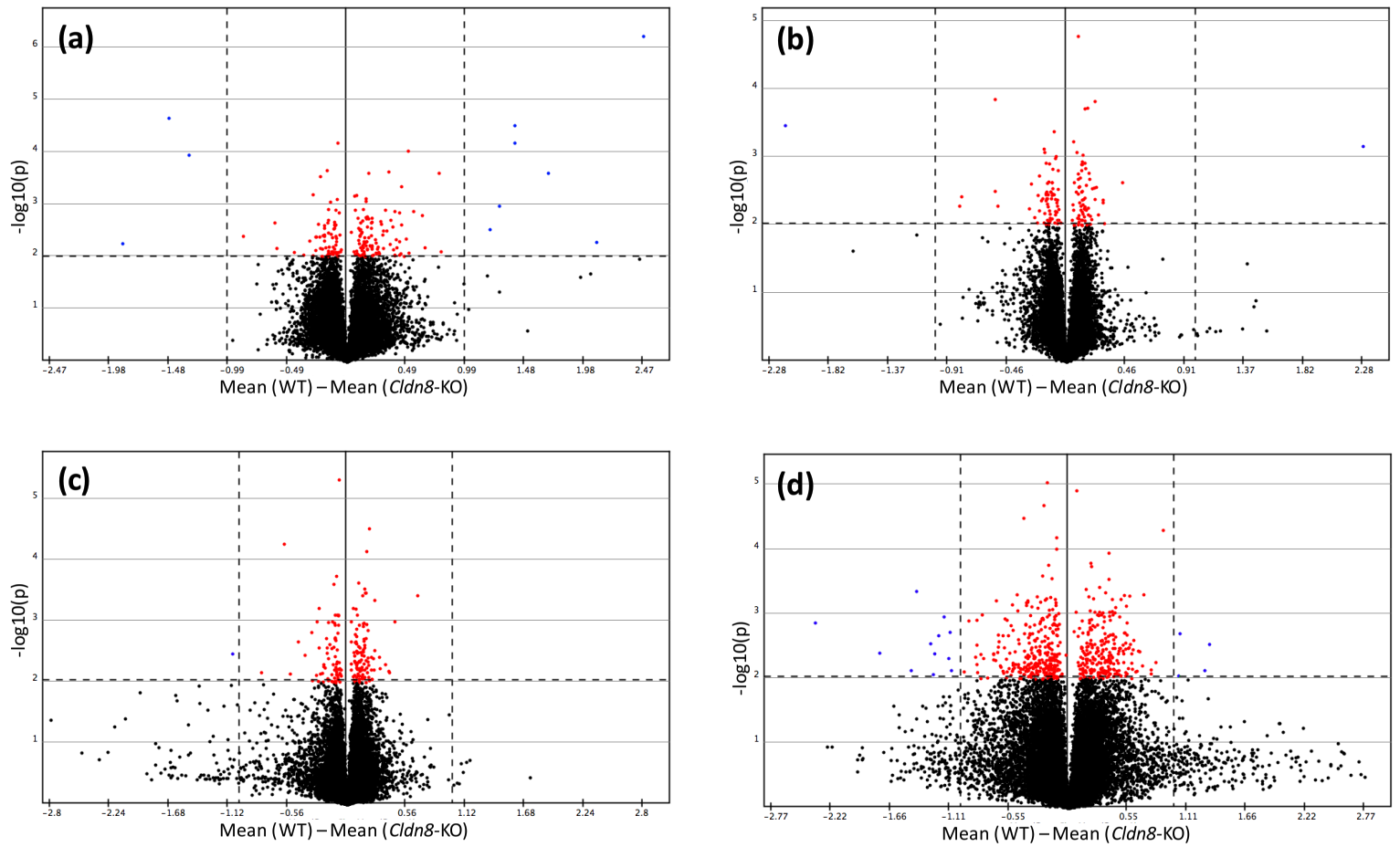

Figure 6-1 – ***Volcano plot of differentially expressed genes in naïve* Cldn8-*KO and WT mice.*** (a) Day 0 – Naïve, (b) Day 3, (c) Day 9, (d) Day 21. Whole genome microarray analysis of gene expression was performed using Illumina Mouse WG6.0 v2.0 expression array. Genes differed in expression at an adjusted p-value < 0.01 are represented as blue and red dots (uncorrected for multiple testing). Genes with a minimum fold change of ≤ -1 or ≥ 1 are represented as blue dots. None of the genes remained statistically significant after correction for multiple testing.

Day 0 (Naïve)			
Probe ID	Gene ID	Fold Change	p-value
Over-expressed genes (p value < 0.01, ≥ 1 fold change)			
ILMN_2935012	Anxa4	1.32	1.11E-04
ILMN_2421925	Wdfy1	1.49	2.15E-05
ILMN_2998658	Erdr1	1.88	5.50E-03
Under-expressed genes (p value < 0.01, ≤ -1 fold change)			
ILMN_2514377	Cxadr	-2.47	5.86E-07
ILMN_1230696	IGL-V1	-2.08	5.17E-03
ILMN_2693858	D14ERTD449E	-1.68	2.45E-04
ILMN_1225825	LOC100039175	-1.40	2.96E-05
ILMN_1232435	Mmrn1	-1.40	6.40E-05
ILMN_2710159	MGC41689	-1.27	1.04E-03
ILMN_2896768	Cbr3	-1.19	2.95E-03

Day 3 DSS			
Probe ID	Gene ID	Fold Change	p-value
Over-expressed genes (p value < 0.01, ≥ 1 fold change)			
ILMN_2684053	Lpo	2.17	3.34E-04
Under-expressed genes (p value < 0.01, ≤ -1 fold change)			
ILMN_2514377	Cxadr	-2.28	6.70E-04

Day 9 DSS			
Probe ID	Gene ID	Fold Change	p-value
Over-expressed genes (p value < 0.01, ≥ 1 fold change)			
ILMN_2738369	Krt6a	1.08	3.32E-03

Day 21 DSS			
Probe ID	Gene ID	Fold Change	p-value
Over-expressed genes (p value < 0.01, ≥ 1 fold change)			
ILMN_2958099	Adssl1	1.32	2.89E-03
ILMN_2759371	Fgfbp1	1.27	7.28E-03
ILMN_1245079	Adssl1	1.04	1.97E-03
ILMN_2602938	Smpdl3b	1.03	8.83E-03
Under-expressed genes (p value < 0.01, ≤ -1 fold change)			
ILMN_2684053	Lpo	-2.37	1.34E-03
ILMN_1222286	LOC666652	-1.77	3.99E-03
ILMN_2909275	Slc46a1	-1.47	7.37E-03
ILMN_1229197	Gm14446	-1.42	4.34E-04
ILMN_2866267	F2rl1	-1.29	2.80E-03
ILMN_2844353	AI747448	-1.27	8.47E-03
ILMN_2592486	Pglyrp1	-1.25	4.03E-03
ILMN_2784078	Mmp15	-1.21	2.12E-03
ILMN_2854943	Gprc5a	-1.16	1.09E-03
ILMN_2828265	SEPT5	-1.12	4.82E-03
ILMN_1246785	Gprc5a	-1.11	1.90E-03
ILMN_2589859	Duoxa2	-1.10	7.45E-03

Table 6-2 – **Differentially expressed genes between *Cldn8*-KO and WT mice at different stages of DSS inflammation.** *Whole genome microarray analysis of gene expression was performed using Illumina Mouse WG6.0 v2.0 expression array. Differentially expressed genes were identified using a minimum fold change of ≥ 1 or ≤ -1 and p-value <0.01 (uncorrected for multiple testing). None of the genes remained statistically significant after correction for multiple testing.*

6.2.2.1 qRT-PCR verification of gene expression

As discussed above in section 6.2.2, after correction for multiple testing, no statistically significant differences were noted between *Cldn8*-KO and WT mice at any time point. However, without correction for multiple testing, some differences were noted at each time point between the *Cldn8*-KO and WT mice. Therefore, the expression of some of these genes was verified using qRT-PCR on the original samples used for microarray analysis, as technical controls.

Cxadr

The Illumina Mouse WG6.0 v2.0 expression array has three probes for *Cxadr* in mice, and one of the probes had shown a consistent difference in expression levels between *Cldn8*-KO and WT mice (Figure 6-3). In humans, CXADR is on chromosome 21. However, in mice *Cxadr* is on chromosome 16, which is the same chromosome as Cldn8, and therefore, it is possible that during the deletion process of *Cldn8*, *Cxadr* may have been affected. The CXADR gene has two splice variants both in humans and mice. PCR primers were developed to cover both variants (see Appendix 1 – List of Primers). After PCR verification, no difference in expression levels were noted between Cldn8-KO and WT (Figure 6-3).

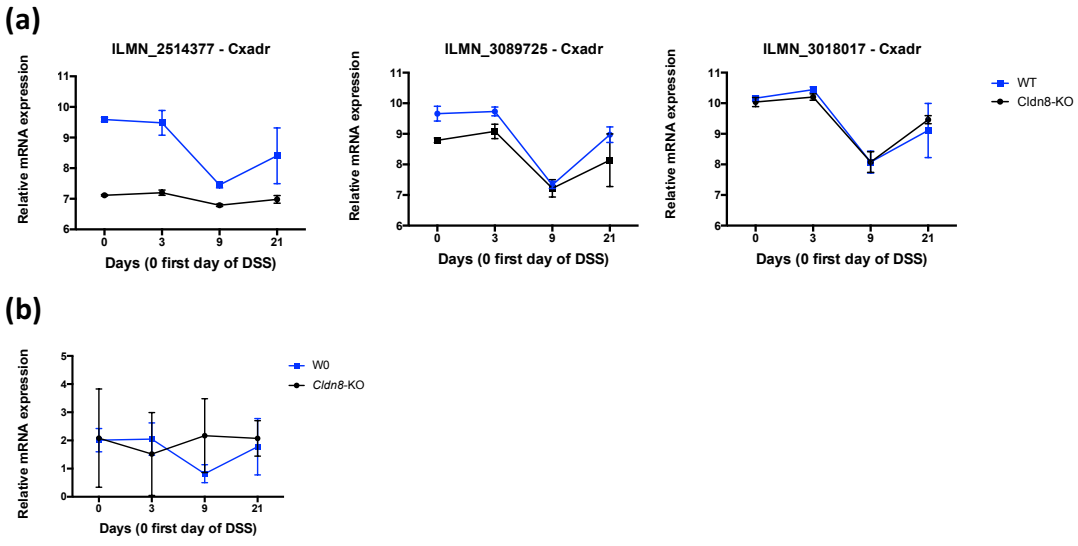

Figure 6-3 – ***Cxadr* expression on Illumina and qRT-PCR** (a) The Illumina Mouse WG6.0 v2.0 expression array has three probes for *Cxadr*. (b) The qRT-PCR verification of *Cxadr* gene did not show any difference between the *Cldn8*-KO and WT mice.

Lpo* and *Duox2

The Illumina Mouse WG6.0 v2.0 expression array has one probe for *Lpo* in mice and one probe for *Duox2*, which showed a difference in expression levels at day 3 and day 21 on DSS, respectively (*Figure 6-4*).

Lactoperoxidase (*Lpo*) activates thiocynate and hydrogen peroxide (produced by *Duox2*) to hypothiocyanite, which has bactericidal properties. The increased activity of *Lpo* seen on the microarray data (Figure 6-4-a) represented a possible mechanism for the relative protection of *Cldn8*-KO to DSS induced colitis when compared to WT mice.

However, qRT-PCR verification of *Lpo* did not show any difference between *Cldn8*-KO and WT mice. Interestingly, *Duox2* had a higher expression in WT on day 9 (2 days after stopping DSS water) than in *Cldn8*-WT mice.

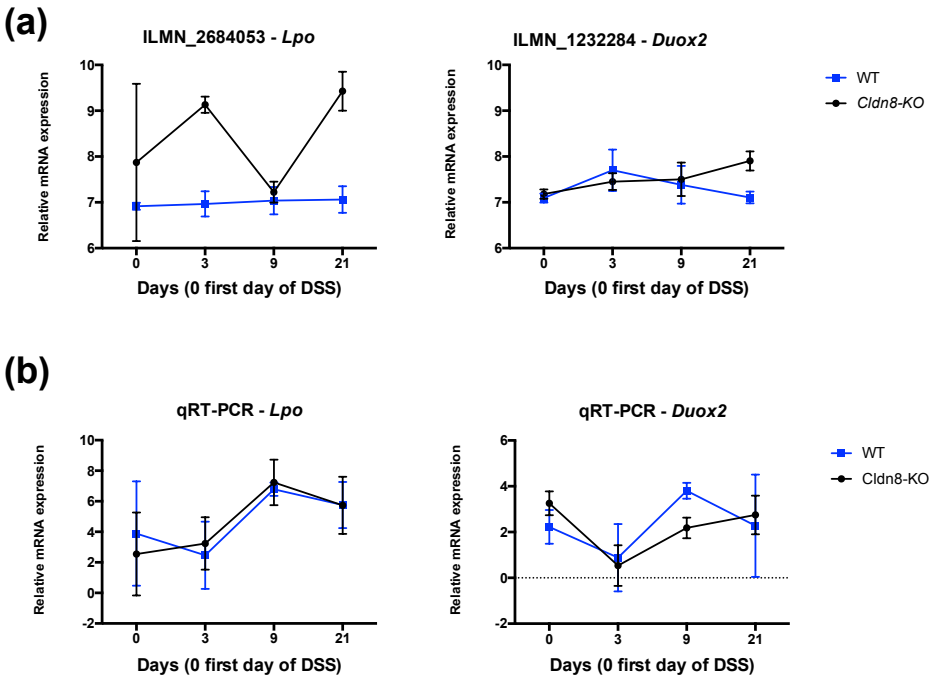

Figure 6-4 – ***Lpo* and *Duox2* expression on Illumina and qRT-PCR** *(a) the Illumina Mouse WG6.0 v2.0 expression array probe expression levels for Lpo and Duox2 suggested a difference in days 3 and 21 of DSS inflammation (b) The qRT-PCR verification of Lpo gene did not show any difference between the Cldn8-KO and WT mice. However, on day 9 of DSS induced colitis experiments, Duox2 had a lower expression in Cldn8-KO mice than in WT.*

6.2.3 PRINCIPLE COMPONENT ANALYSIS

Principle component (PCA) analysis was conducted to determine whether global *Cldn8*-KO and WT mice gene expression profiles could be separated on the basis of disease. PCA is a mathematical algorithm for reducing the dimensionality of datasets, by finding the principal components (directions) along which the variation is minimal. PCA plots of samples, where each data point represents expression values of all the expressed probes in the array, can be used to visually assess similarities and differences between samples and whether they can be grouped (287).

Considering the combined datasets, principal components 1 and 2 accounted for 66.94% and 9.15% of the data variability respectively. A further 4.84% of the variance was explained by principal component 3 (Figure 6-5).

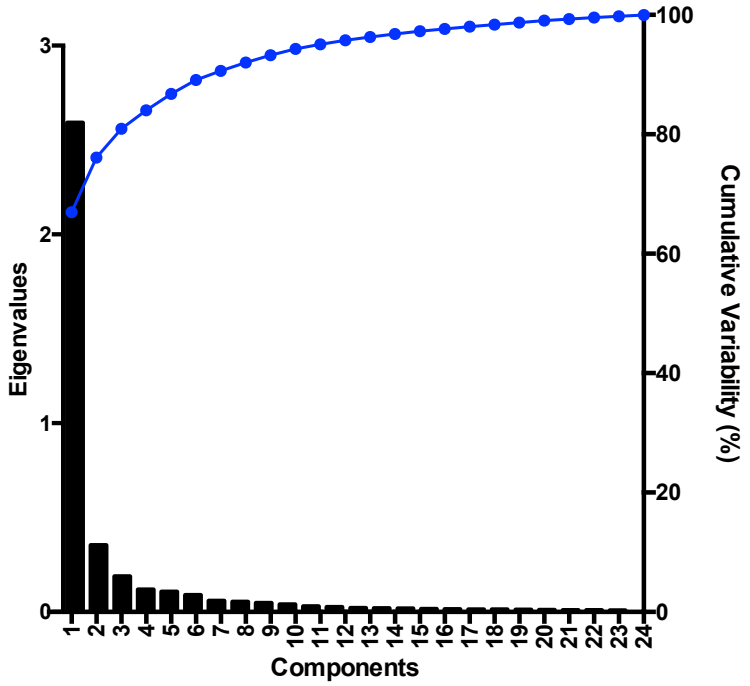

Figure 6-5 – **Scree plot from principal component analysis.** *Eigenvalyes and cumulative variability of the principle components have been superimposed. A total of 24 components were detected in the PCA.*

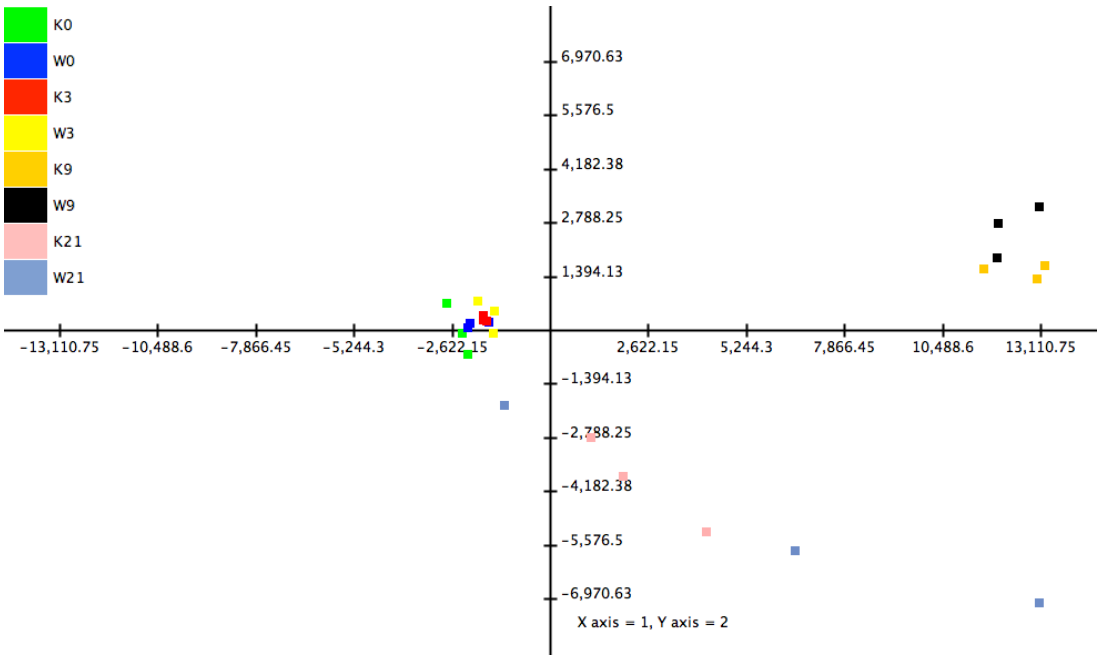

Figure 6-6 – **Principal component analysis of *Cldn8*-KO and WT mice at different time points of DSS-induced colitis.** *Array expression data were log2 transformed and PCA analysis was performed using Multiexperiment Viewer TM4 microarray software suit. Scatter plots for principal components 1 and 2 are shown, with microarray results for each sample represented as a single point. Array samples colour coded by genotype and inflammatory state (K - Cldn8-KO; W - WT)*

6.2.4 DIFFERENTIALLY EXPRESSED GENES AT DIFFERENT DSS TIME POINTS

In this section, changes in gene expression will be analysed across time, in *Cldn8*-KO and WT separately. Differences in changes in gene expression in *Cldn8*-KO and WT mice across time will then be compared.

Differentially expressed genes between naïve animals and different times points during as well as after recovery from DSS-induced colitis were identified using the MEV TM4 software suit (version 10.2). Probes were identified that were significantly different at different time points, using an uncorrected p-value of $p < 0.01$ and a minimum fold change of ≤ -1 or ≥ 1 compared to mean expression in either *Cldn8*-KO mice or the WT mice. Multiple correction testing was performed using false detection rate (FDR) method with a cut off value of < 0.01.

6.2.4.1 WT Mice

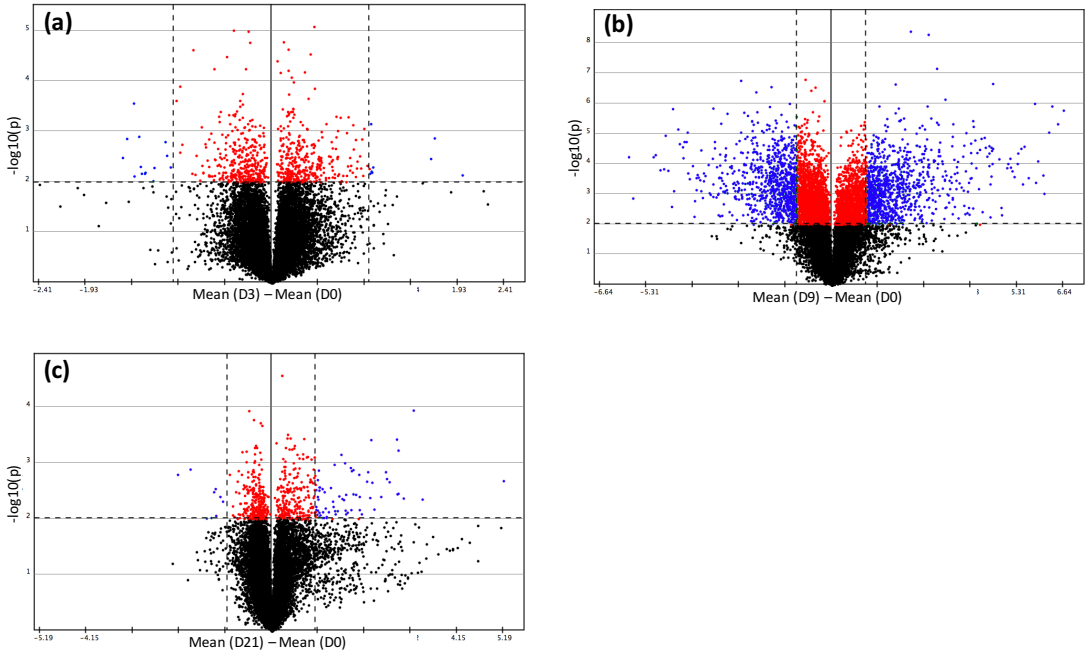

Figure 6-7 - **Volcano plot of differentially expressed genes in WT mice, between D0 (naïve) mice and different stages of DSS-induced inflammation.** *(a) Day 3 (b) Day 9 and (c) Day 21 of DSS-induced inflammation. Whole genome microarray analysis of gene expression was performed using Illumina Mouse WG6.0 v2.0 expression array. Genes differed in expression at an adjusted p-value < 0.01 are represented as blue and red dots (uncorrected for multiple testing). Genes with a minimum fold change of ≤-1 or ≥1 are represented as blue dots. Only genes expressed differently between day 9 and day 0 remained statistically significant after correction for multiple testing, using false detection rate (FDR) cut off value of < 0.01*

WT – D9 vs D0 differentially expressed genes			
Probe ID	Gene ID	Fold Change	p-value
Over-expressed genes (p value < 0.01, ≥ 1 fold change)			
ILMN_2772632	Saa3	6.84	2.24E-07
ILMN_2712075	Lcn2	6.32	1.04E-05
ILMN_2656504	Retnlg	6.09	4.45E-05
ILMN_2803674	S100a9	6.00	2.93E-04
ILMN_1223257	Ccl4	5.98	1.92E-04
ILMN_2710905	S100a8	5.92	9.32E-04
ILMN_2777498	Il1b	5.81	4.96E-04
ILMN_1246800	Serpina3n	5.71	6.50E-06
ILMN_2737685	Mmp13	5.44	2.80E-06
ILMN_2619952	Mmp10	5.30	2.63E-05
Under-expressed genes (p value < 0.01, ≤ -1 fold change)			
ILMN_1232533	Sycn	-6.13	4.86E-05
ILMN_1225061	NA	-5.89	4.91E-07
ILMN_1252131	Klk1b27	-5.01	5.30E-05
ILMN_1238736	NA	-4.95	1.57E-04
ILMN_2980898	Mptx1	-4.89	1.60E-06
ILMN_2731191	Klk1b5	-4.89	1.85E-04
ILMN_2777363	Tgm3	-4.84	3.50E-06
ILMN_1229177	Klk1b26	-4.77	1.41E-04
ILMN_2760199	Klk1	-4.73	4.09E-04
ILMN_1246145	Gsdmc3	-4.57	1.94E-07

Table 6-3 – **Differentially expressed genes in WT mice, between Day 9 on DSS and Day 0 (naïve).** *Overall, 2146 probes (out of 21,554) remained significant after correction for multiple testing using false discovery rate (FDR) cut off value of < 0.01. Only top 10 over-expressed and under-expressed genes are shown here. Whole genome microarray analysis of gene expression was performed using Illumina Mouse WG6.0 v2.0 expression array. Differentially expressed genes were identified using a minimum fold change of ≤ -1 or ≥ 1 and p-value <0.01 (uncorrected for multiple testing).*

6.2.4.2 *Cldn8*-KO Mice

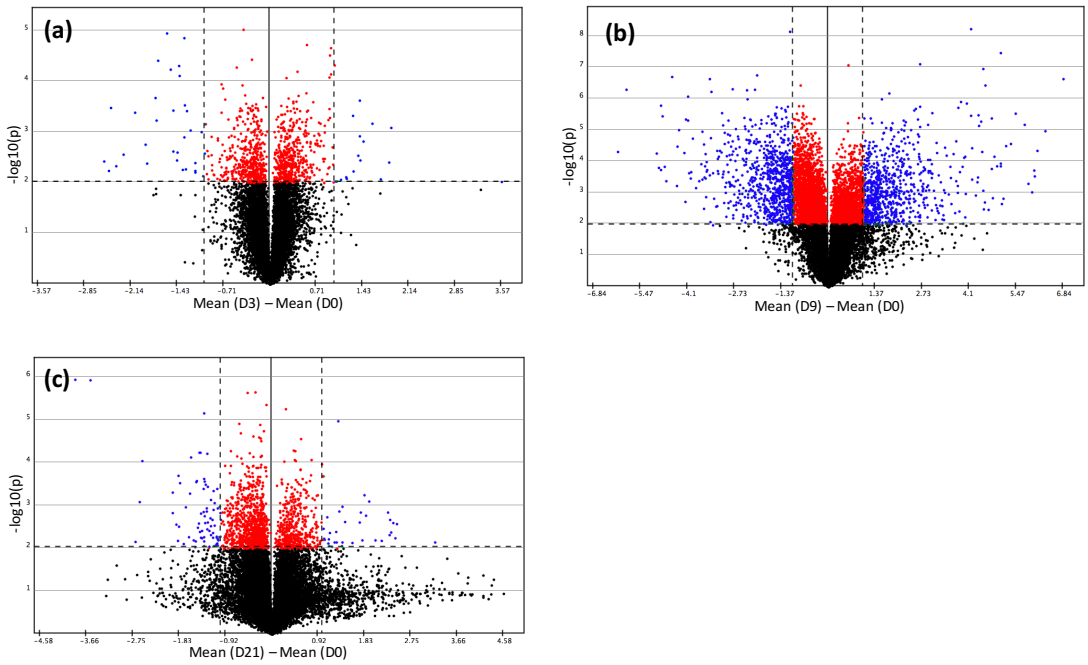

Figure 6-8 - **Volcano plot of differentially expressed genes in *Cldn8*-KO mice, between D0 (naïve) mice and different stages of DSS-induced inflammation.** *(a) Day 3 (b) Day 9 and (c) Day 21 of DSS-induced inflammation. Whole genome microarray analysis of gene expression was performed using Illumina Mouse WG6.0 v2.0 expression array. Genes differed in expression at an adjusted p-value < 0.01 are represented as blue and red dots (uncorrected for multiple testing). Genes with a minimum fold change of ≤-1 or ≥1 are represented as blue dots. Only genes expressed differently between day 9 and day 0 remained statistically significant after correction for multiple testing, using false detection rate (FDR) cut off value of < 0.01*

Cldn8-KO – D9 vs D0 differentially expressed genes			
Probe ID	Gene ID	Fold Change	p-value
Over-expressed genes (p value < 0.01, ≥ 1 fold change)			
ILMN_2772632	Saa3	6.64	1.62E-06
ILMN_2710905	S100a8	6.48	4.67E-06
ILMN_2722616	Krt14	6.31	1.19E-06
ILMN_2803674	S100a9	6.22	8.67E-06
ILMN_1223257	Ccl4	6.08	9.31E-04
ILMN_2777498	Il1b	6.06	2.26E-04
ILMN_2712075	Lcn2	5.90	7.84E-05
ILMN_2656504	Retnlg	5.84	4.03E-04
ILMN_1246800	Serpina3n	5.80	9.62E-07
ILMN_2754364	Ltf	5.63	2.75E-04
Under-expressed genes (p value < 0.01, ≤ -1 fold change)			
ILMN_1225061	NA	-5.82	5.70E-05
ILMN_1252131	Klk1b27	-5.12	5.63E-05
ILMN_1238736	NA	-5.06	4.85E-05
ILMN_2731191	Klk1b5	-4.93	1.51E-04
ILMN_1229177	Klk1b26	-4.82	1.44E-04
ILMN_2980898	1810030J14Rik	-4.78	1.11E-05
ILMN_2760199	Klk1	-4.71	1.61E-04
ILMN_2727309	NA	-4.57	1.47E-06
ILMN_2601519	Abp1	-4.54	7.55E-04
ILMN_2742426	Selenbp1	-4.42	6.97E-06

Table 6-4 – **Differentially expressed genes in WT mice, between Day 9 on DSS and Day 0 (naïve).** *Overall, 2216 probes (out of 21,554) remained significant after correction for multiple testing using false discovery rate (FDR) cut off value of < 0.01. Only top 10 over-expressed and under-expressed genes are shown here. Whole genome microarray analysis of gene expression was performed using Illumina Mouse WG6.0 v2.0 expression array. Differentially expressed genes were identified using a minimum fold change of ≤-1 or ≥1 and p-value <0.01 (uncorrected for multiple testing).*

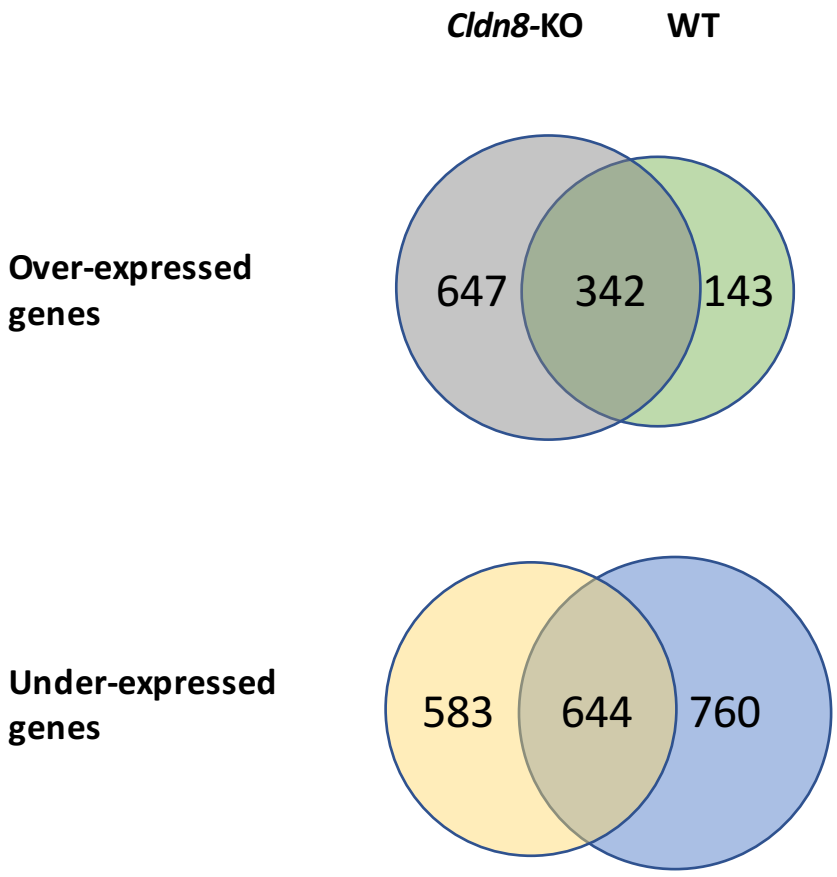

Figure 6-9 – **Venn Diagram of differences in changes in gene expression between D9 and D0 (naïve) on DSS, in *Cldn8*-KO and WT mice.** *Whole genome microarray analysis of gene expression was performed using Illumina Mouse WG6.0 v2.0 expression array. Differentially expressed genes were identified using a minimum fold change of ≤-1 or ≥1 and p-value <0.01, after correction for multiple testing using false discovery rate (FDR) method with cut off value of < 0.01.*

6.2.4.3 Identification of the biological function of the differentially expressed genes at different time points during and after recovery from DSS-induced colitis in WT and *Cldn8*-KO mice

Over and under-expressed differentially expression probes on day 9 of DSS-induced colitis as compared to naïve animals was identified. Probes that remained statistically significant after correction for multiple testing, using false detection rate (FDR) cut off value of < 0.01 were analysed using DAVID Bioinformatics Resources v6.7 to determine gene ontology (GO) processes that were enriched within the probe list. The most significantly enriched GO processes were included antigen processing and presentation of peptide antigen, immune response, inflammatory response, oxidation reduction, and response to wounding (*Table 6-5*).

(a)

GO Term - WT Day 9 DSS vs Day 0 (Naïve)	Gene Count	p-value
oxidation reduction	117	2.07E-14
generation of precursor metabolites and energy	60	1.08E-12
electron transport chain	35	1.53E-11
sulfur metabolic process	27	3.25E-08
cellular respiration	20	1.66E-07
oxidative phosphorylation	19	3.63E-07
coenzyme metabolic process	32	6.91E-07
cofactor metabolic process	37	9.55E-07
fatty acid metabolic process	37	1.25E-06
response to wounding	56	2.99E-06
mitochondrial ATP synthesis coupled electron transport	9	4.55E-06
nitrogen compound biosynthetic process	50	5.32E-06
respiratory electron transport chain	12	7.78E-06
inflammatory response	40	1.01E-05
transmembrane transport	65	3.69E-05
lipid catabolic process	27	4.24E-05
ATP synthesis coupled electron transport	9	4.88E-05
energy derivation by oxidation of organic compounds	22	5.04E-05
coenzyme catabolic process	11	7.56E-05
regulation of phagocytosis	10	1.18E-04

(b)

GO Term - *Cldn8*-KO Day 9 DSS vs Day 0 (Naïve)	Gene Count	p-value
antigen processing and presentation of peptide antigen	21	8.87E-13
antigen processing and presentation of exogenous peptide antigen	17	2.20E-12
antigen processing and presentation of exogenous antigen	18	1.20E-11
immune response	89	1.78E-11
inflammatory response	52	4.01E-10
tube development	56	2.27E-09
oxidation reduction	107	4.61E-09
antigen processing and presentation of peptide antigen via MHC class II	12	8.45E-09
antigen processing and presentation of exogenous peptide antigen via MHC class II	12	8.45E-09
morphogenesis of a branching structure	34	9.73E-09
defense response	78	1.66E-08
response to wounding	65	1.84E-08
antigen processing and presentation	27	2.27E-08
coenzyme metabolic process	36	2.90E-08
cofactor metabolic process	41	7.65E-08
antigen processing and presentation of peptide or polysaccharide antigen via MHC class II	12	1.13E-07
sulfur metabolic process	27	1.29E-07
epithelium development	52	2.70E-07
gland morphogenesis	24	8.27E-07
respiratory system development	30	1.21E-06

Table 6-5 – **Functional analysis of differentially expressed genes for WT and *Cldn8*-KO mice, between days 9 and 0 in DSS-induced intestinal inflammation.** Analysis of functional ontology of the differentially expressed genes between days 9 and 0 on DSS-induced colitis was performed using DAVID Bioinformatics Resources v6.7. Only genes that reached significance after multiple testing correction based on a false discovery rate (FDR) of < 0.01 were included in analysis. The 20 most significantly enriched GO processes within (a) WT and (b) *Cldn8*-KO mice datasets are shown, with associated p-values. The number of genes in each GO process present in the dataset is also included.

6.3 DISCUSSION

In this chapter, the global transcriptomic profile of *Cldn8*-KO and WT mice was interrogated, in naïve state, as well as during and post DSS-induced colitis, in an attempt to identify molecular differences responsible for the attenuated inflammatory response by *Cldn8*-KO observed in chapter 5. Although a number of differentially expressed genes were identified between *Cldn8*-KO and WT mice at each time point, none remained statistically significant after correction for multiple testing.

Also, as discussed in chapter 5, for a short period after recovering from DSS-induced colitis, mice are protected from developing another bout of severe DSS-induced colitis. This protection was seen at 2 weeks after the first challenge, but is lost by week 5 (see chapter 5.2.6 for full details). In an attempt to identify molecular differences responsible for this protective mechanism, differentially expressed genes at different time points were interrogated within each genotype group (e.g. day 3 vs day 0 in WT mice). Although a number of differentially expressed genes were identified between each time point analysis, which could be of functional relevance, only differentially expressed genes between day 9 and day 0 (naïve) remained significant after correction for multiple testing. Many processes were common between *Cldn8*-KO and WT mice, involving inflammatory and recovery processes, suggesting that overall, *Cldn8*-KO and WT mice have similar functional ontologies at on day 9 of DSS-induced intestinal inflammation.

Some of the observed variations in gene expression are likely to be due to limitations of Microarray technology (288). For example, the Illumina Mouse WG6.0 v2.0 expression array has three probes for the *Cxadr* gene, and as discussed above, one of these probes had a significantly different expression profile between *Cldn8*-KO and WT mice (IMN_2514377). However, on qRT-PCR, there was no change in expression of *Cxadr* between *Cldn8*-KO and WT mice. It is likely that this finding is due to a SNP variation in WT mice. The same is true for the *Lpo* gene that was identified and verified with qRT-PCR.

Microarrays have been crucial in science through their ability to simultaneously interrogate tens of thousands of transcripts, and identify differentially expressed genes. However, microarrays have several limitations. There is evidence that a proportion of probes on Illumina chips are unreliable and may fail (288), as was the case for *Cldn8* probe in this study. Background noise and cross-hybridisation of transcripts with probes means that microarrays cannot distinguish between “low”

expression and “no” expression. During analysis, the microarray probe intensity is assumed to be proportional to the concentration of the transcript, but this is dependent on the affinity of the probe and transcript. Polymorophisms within the probe region and differences between mouse strains can influence the microarray. Splice variants present a challenge to microarray data analysis. If the short nucleotide probe on the chip targets a specific splice variant, then other variants of the same gene will be ignored. Another technique for investigating gene expressions is RNA-Seq. RNA-Seq is the direct sequencing of transcripts by high-throughput sequencing technologies. RNA-Seq does not rely on genome annotation for prior probe selection, and has the potential to replace microarrays. RNA-Seq has a number of advantages over microarray, such as ability to detect novel transcripts, and avoiding the problems with splice variants. Unlike microarrays, RNA-Seq also does not suffer from background noise, and cross-hybridisation, and avoids problems with incorrect annotation of the probes (289). However, there are challenges associated with RNA-Seq; in addition to being more expensive, it is also a relatively new technique, and therefore, the data-analytic tools are less developed than they are for microarray.

6.4 CONCLUSION

The finding that after correction for multiple testing, differentially expressed genes between *Cldn8*-KO and WT mice did not remain statistically significant at any time point, may suggest that the main reason for the observed differences between the different mice groups may be the loss of *Cldn8*. In the next, final chapter, a possible role for *Cldn8* and future studies are proposed.

7 General Discussions

7.1 SUMMARY OF FINDINGS

- In transcriptomic analysis performed on colonic pinch biopsies, CLDN8 was found to have one of the largest fold-change reductions of any gene in patients with quiescent UC
- CLDN8 is the only TJ molecule with a differential expression across the large intestine. CLDN8's expression increases distally towards the rectum, mirroring the pattern seen in UC inflammation
- CLDN8 expression levels negatively correlate with markers of chronic inflammation, such as DEFA1B, DEFA5, DEFA6 and ITLN2
- *Cldn8*-KO mice do not develop spontaneous signs of colitis
- *Cldn8*-KO mice have comparable physiology to WT mice in naïve state
- There is a reduction in expression of *Cldn8* mRNA in WT mice in response to inflammation
- The commercially available anti-CLDN8 antibodies in mice are not specific to CLDN8
- There is a rebound expression of *Cldn8* mRNA during the early phase of recovery
- Loss of *Cldn8* in *Cldn8*-KO mice results in reduced susceptibility to DSS induced colitis
- *Cldn8*-KO mice, had smaller increase in intestinal permeability to ^{3}H-mannitol, reduced neutrophils and macrophages in inflammatory cell infiltrate in LP during the early phase of inflammation.
- The increased permeability to ^{3}H-mannitol is less marked in *Cldn8*-KO mice as compared to WT mice, reflecting the less severe clinical response to DSS colitis in *Cldn8*-KO mice.
- Whilst the permeability of ^{3}H-mannitol remained abnormal by Day 9 in both animal groups, the permeability of FITC-Dextran returned to normal by Day 9 post initiation of administration of DSS. Taken together, this data suggests that permeability to larger molecules is determined by gaps in the epithelial cells, but the permeability to small molecules (~4Å in size), it is likely to be determined by properties of the paracellular spaces between epithelial cells.
- There were no gross histologic differences during inflammation between *Cldn8*-KO and WT mice, suggesting that the differences between the two are very subtle

- There is an increase of serum IL-1b and IL-10 in serum of naïve *Cldn8*-KO mice.
- For a shortly period after recovery from DSS-induced colitis, mice are less susceptible to developing another severe DSS-induced colitis. This protection was observed at 2 weeks after stopping DSS-water, and was lost by week 5.
- Female mice are more susceptible to DSS-induced colitis, and lose more weight than their male counterparts. However, female mice also recover much more rapidly, reaching their pre-DSS-induced colitis weight sooner than their male counterparts. This is true in *Cldn8*-KO and WT mice
- The inner layer of mucous is sterile in naïve *Cldn8*-KO and WT mice, and remains sterile after the animals have been exposed to DSS-water for 12 hours
- Transcriptomic analysis between *Cldn8*-KO and WT mice did not reveal any significant differences between the two groups at different time points. After correction for multiple-testing, no differentially-expressed genes remained

7.2 DISCUSSION OF FINDINGS, IMPLICATIONS AND STUDY LIMITATIONS

7.2.1 UC IS ASSOCIATED WITH EPITHELIAL AND MUCOSAL BARRIER ABNORMALITIES

UC is a chronic relapsing IBD. Unlike CD, UC is a disease of the large bowel and does not affect the rest of the GI tract. Patients with UC usually present with frequent bowel movements, which can be small in volume because of rectal inflammation. Patients may also suffer from extra-intestinal manifestations of the disease, such as joint pains, eye problems such as uveitis and episcleritis, and skin issues such as erythema nodusum and pyoderma gangrenosum. Some patients may also develop primary sclerosing cholangitis (PSC), an autoimmune condition affecting the biliary tree. The aetiology of UC is complex, and the current prevailing hypothesis for pathogenesis of UC is that an abnormal innate immune response in genetically susceptible individuals, combined with environmental factors, result in excessive activation of the adaptive immune system within LP (142,143).

The importance of colonic bacteria and abnormalities in mucous barrier are becoming better understood:

- GWAS have identified a number risk loci that are specific to UC and involved in barrier function and epithelial restitution.

- Studies have also found increased permeability in colon of patients with UC, even during the quiescent state (167,168), though as we have found in our studies, even patients may have microscopic inflammation despite macroscopically normal colonic mucosa, and this may influence the results of these studies.

There have been many observations on the response of *Cldns* to inflammation. It is generally accepted that during colitis, CLDN2 is upregulated (119,120,122,124), and CLDN8 is downregulated (120,124,290). However, evidence for other CLDNs is mixed. For example, some studies have found CLDN1 to be upregulated (290,291), downregulated (124,292), or not changed in expression (119,120,293). One significant problems so far, has been that given the large number of CLDNs expressed in the large bowel, investigators have been selective in the ones they have studied using qRT-PCR. As a result, the data has been patchy across different studies.

However, there is now strong evidence from human transcriptomic analysis studies, both in inflamed tissue (252), and also from our own data set from patients with quiescent disease (241) that CLDN8 is likely to be the main TJ involved during inflammation. In these studies, not only has CLDN8 had one of the largest fold changes in expression of any identified gene, but CLDN8 has also been the only TJ gene with a significant fold change in expression levels.

Despite the observations described above, there is very little evidence on the role of TJ molecules in intestinal inflammation. It has been shown that loss of *Cldn7*, one of the most prominent *Cldns* in intestine, in mice, will result in spontaneous intestinal inflammation (101), and that *Cldn2* deficient mice are more susceptible to DSS-induced colitis (294).

CLDN8 has been reported to form a barrier to cations, ammonium and bicarbonate ions (102,108). Therefore, it had been proposed that the combined increased expression of “pore-forming” CLDN2 (98) and reduction in “barrier forming” CLDN8 (102,108) may predispose to inflammation by increasing intestinal permeability to luminal antigens. The *a priori* hypothesis for this study was that reduced CLDN8 expression would worsen the inflammatory response; instead it appears to be protective.

7.2.2 LOSS OF *CLDN8* IS PROTECTS AGAINST DSS-INDUCED COLITIS

The evidence presented in this thesis is that loss of *Cldn8* confers relative protection against DSS-induced colitis in *Cldn8*-KO mice, compared with WT mice, as evidenced by clinical features such as reduced weight loss in *Cldn8*-KO mice. However, the differences were very subtle, and minimal, including minor differences in LP inflammatory cell infiltrates (neutrophils and macrophages) and differences in permeability to ^{3}H-mannitol (and not larger FITC-Dextran) on Day 3 of DSS-induced inflammation only.

7.2.3 POTENTIAL ROLE OF THE MUCOUS BARRIER

Bacterial load increases towards the distal intestine, reaching a maximum in the colon, with 10^{13} organisms per gram of faeces. The first line of defense against these pathogens is the mucus layer, produced by the epithelial goblets cells. The thickness of the mucus layer steadily increases from the proximal to the distal large bowel (295,296), and is composed of an outer loosely adherent layer, and an inner more adherent layer (25), which is normally sterile (174,266,297).

There is evidence that bacteria are able to penetrate the normally impenetrable impermeable inner mucus layer in the colon of patients with UC (216). Similarly, in mice, it has been shown that the inner mucus layer is impermeable to fluorescent beads with a diameter in the same size range as bacteria (2 μm), and that DSS changes the properties of the inner mucus layer such that it was thinner and permeable to bacteria (216).

The main component of the mucus layer is MUC2 (297), which has an important protective mechanism; MUC2 knockout mice are susceptible to developing spontaneous colitis similar to UC, and have an increased susceptibility to DSS-induced colitis (298–301). Whilst mucous thickness is normal in patients with quiescent UC (302), mucin 2 (MUC2) synthesis and secretion are decreased in active UC due to alterations in sulphation (303).

In addition to MUC2, the mucous layer also contains positively-changed Anti-Microbial Peptides (AMPs). The cationic character of AMPs result in electrostatic attraction to the negatively-charged phospholipids of microbial membranes, and their hydrophobicity subsequently aids integration into the microbial cell membrane, leading to disruption (304). Two main classes of AMPs are produced by the colonic

epithelium: defensins and cathelicidins. There is evidence of abnormality in β-defensins may play a role in development of inflammation in CD and UC (305).

As discussed above, *Cldn2*-KO develop a more severe colitis in response to DSS than WT mice (294), and increased expression of *Cldn2* confers protection against DSS colitis (306). Also as described above, there is also evidence that during inflammation, *Cldn8* expression is down-regulated whilst *Cldn*2 expression is up-regulated (119,124).

Cldn2 and *Cldn8* have opposing characteristics (307). Whilst *Cldn8* acts as a barrier to cations (102,108), *Cldn2* induces cation-selective channels in tight junctions of epithelial cells (98). *Cldn8* is also involved in sodium and water homeostasis in the colon (107), by preventing back-leakage of the former into the lumen. The changes in *Cldn* expression during inflammation may therefore be an attempt to strengthen the mucous barrier by increasing its water content and the defensins contained within it, thereby reducing exposure of the immune system to bowel microbiota. The additional protection could provide some relief towards the minor insults, but not sustained challenges such as continuous DSS-water for 7 days. Therefore, the results of experiments in this study, such as lower increases intestinal permeability in *Cldn8*-KO mice on day 3 post DSS, may represent a slight delay in the inflammatory process in *Cldn8*-KO mice as a result of slightly “stronger” mucous barrier.

To investigate this possibility, permeability of the inner layer of mucous to bacteria was investigated, in naïve state as well as at 12 hours after exposure of the animals to DSS. However, in both points, the inner layer of mucous remained sterile in *Cldn8*-KO and WT mice. DSS-induced colitis is significantly less severe in mice treated with antibiotics (281) or germ free mice (282,283). This, combined with evidence that DSS results in permeability of the inner layer of mucous to bacteria, is clear evidence of the invasion of luminal bacteria is an important, albeit not the sole, trigger for DSS-induced colitis. Therefore, the findings that the inner layer of mucous remained sterile even in WT mice suggest that the duration of exposure of the mice to DSS was too short to show any discernible difference in mucous properties of the *Cldn8*-KO and WT mice.

7.2.4 POTENTIAL ROLE OF CYTOKINES

Evidence from these experiments suggest that there is an increase in serum concentration of IL-1b and IL-10 in serum of *Cldn8*-KO naïve mice. IL-10 has been

well established as an anti-inflammatory cytokine, and *IL-10*-KO mice have been known to spontaneously develop colitis (179,232). Treating *IL-10*-KO mice with normally sub-lethal doses of LPS can be fatal (308). Recent evidence suggests that the protective mechanism of IL-10 may be through its effect on maintaining Foxp3 expression in T_{reg} cells in inflammatory conditions (69). This may represent a mechanism of action for reduced susceptibility of *Cldn8*-KO mice to developing colitis secondary to DSS However, as described above, unfortunately, the set of FACS experiments investigating population of T_{reg} cells did not produce any results.

7.2.5 RECOVERY PERIOD

Two further observations in this study are interesting, and would warrant further exploration.

First, is the observation that there is rebound in expression levels of *Cldn8* mRNA in the first few days after DSS-water has been stopped and the bowel is recovering. This is potentially important given the increasing evidence in the role of *Cldns* in cell motility, and their effect on intestinal morphology. For example, *Cldn15* deficient mice are born and grow normally, but have an enlarged upper small intestinal phenotype, megaintestine (309). These *Cldn15*-KO mice showed enhanced proliferation of normal cryptic cells after weaning without diseased states such as polyps or cancer, resulting in megaintestine, in which the upper small intestine was approximately 2 times larger than normal in length and diameter.

Relatively little information in known about the role of *Cldn8* in intestinal development. As shown in these studies, *Cldn8*-KO mice have normal intestinal appearances, both macroscopically and microscopically.

However, *Cldn8* has been associated with various malignancies, including prostate cancer (310), osteosarcomas (311,312), colorectal cancer (290,313,314). Apart from prostate cancer, where the expression of CLDN8 was found to be increased, in all other cancers, CLDN8 expression has been found to be downregulated.

The findings that CLDN8 is downregulated in response to inflammation may, therefore, have a direct implication for human disease. As discussed in chapter 1.2.3.3, patients with UC are at an increased risk of developing colorectal cancer (196,197). Over time, and with treatment, the risk has decreased and may be approaching that of the general population; however, certain populations are still at an increased risk of developing CRC, such as those with increased duration of

disease, involvement of longer colon segment, uncontrolled inflammation, and those with PSC (198,199). The reasons for this reduction in risk of developing CRC are not completely clear, and whist there is evidence that the bowel cancer screening program may be impacting cancer risk (200), the optimal surveillance period remains unclear. CLDN8 may, therefore, present an important opportunity for a marker for risk-stratification of patients with increased risk of developing colorectal cancer.

Second, is the observation that for a short period after recovering from DSS-induced colitis, mice develop a relative resistance, and further challenges with DSS result in a significantly attenuated inflammatory response. This protection is lost after a short period. This is a potentially significant finding, which warrants further investigation. UC is a relapsing-remitting disease, with unpredictable flare-ups. A greater understanding of the potential protective mechanisms post-inflammation can potentially aid with better decisions on timing of initiation or escalation of therapy. In addition, clearer understanding of the intestine's protective mechanisms may aid with development of novel therapies that can enhance the protective mechanisms and have a lower systemic side-effect profile compared to the strong immune-suppressant agents currently used in treatment of UC.

7.2.6 Limitations of Extrapolating the findings from mice to humans

CLDN8 mRNA expression is downregulated in response to inflammation in humans and mice. CLDN8 amino acid is also highly conserved between humans and mice. However, any conclusions drawn from mouse studies regarding human physiology and disease must be made cautiously due to limitations of animal models.

The first cause for caution is that WT mice do not spontaneously develop colitis, and none of the models of colitis that have been developed in mice would be fully representative of human disease. Whilst the inflammatory pathways and processes overlap between the different models of mouse colitis, each model has a slightly different emphasis on different aspects of mouse physiology. Since the aetiology of IBD is still unknown, these varied mouse models of colitis are helpful in studying the varying possible mechanisms, from the effect of epithelial cells, to the role of innate or adaptive immune system. However, none perfectly mimics the human disease. In this study, DSS-induced colitis was chosen as the initial inflammatory model because of the evidence that DSS affects the permeability of the inner layer of mucous. DSS is also the only model that, similar to the pattern of disease in UC, results in a continuous colitis, whereas bacterial infection models produce a patchy colitis, which is more in keeping with CD. However, given the importance of bacterial invasion into

the inner layer of the mucous during UC, it would be worth performing experiments with *C. rhodentium*, which is an attaching and effacing (A/E) pathogen, and may also provide further insights into the mucous layer properties of *Cldn8*-KO mice, as it penetrates the mucous layer before reaching the epithelial cells.

The second cause for caution in interpreting the results of investigations performed on mice is that whilst there are significant similarities between the mouse and human immunology, differences do exist, both systemically as well as in the intestine. For example, balance of lymphocytes and neutrophils in mice is quite different to humans; whereas human blood is neutrophil rich (50–70% neutrophils, 30 –50% lymphocytes), mouse blood is lymphocytes rich (75–90% lymphocytes, 10–25% neutrophils) (315). In addition, in humans, neutrophils are a rich source of leukocyte defensins, but defensins are not expressed by neutrophils in mice (316).

7.3 CONCLUSION

CLDN8 was identified as one of the genes with the most significant downregulation in expression on a transcriptomic analysis of patients with quiescent UC, raising the possibility that CLDN8 plays a fundamental role in intestinal inflammation. Loss of *Cldn8* in *Cldn8*-KO mice results in a relative resistance to DSS-induced colitis. It is therefore plausible that downregulation of CLDN8 in patients with UC is a physiologic response by the intestine to increase local defences against luminal pathogens.

7.4 FUTURE WORK

Further work is now required to further ascertain the mechanism(s) by which *Cldn8* protects the intestine against inflammation. Also, additional work is necessary to better understand the protective mechanisms that exist for a short period of time after recovery from intestinal inflammation.

7.4.1 PROPOSED STUDIES

1- Study the effect of DSS on permeability of inner layer of mucous to luminal bacteria over a longer time course, allowing enough time for DSS to affect the permeability of mucous layer
2- Study the T_{reg} population in detail in *Cldn8*-KO mice, and its relation to IL-10
3- Assess effect of loss of *Cldn8* on cellular proliferation in the intestine using bromodeoxyuridine (BrdU)
4- Detailed investigation of the effect of loss of *Cldn8* on the renal physiology (whilst this is not directly related to intestinal inflammation, the *Cldn8*-KO

mouse would be an appropriate model to investigate the role of *Cldn8* in renal homeostasis and pathophysiology)

5- Using bacterial models of inflammation to assess the effect of loss of *Cldn8* on intestinal inflammation; in particular using *C. rodentium* to assess mucous layer properties in *Cldn8*-KO mice.
6- Using cell lines, investigate the pathways controlling expression of CLDN8
7- Produce an antibody to CLDN8 protein that is specific to more accurately assess the expression levels of CLDN8 than currently feasible with mRNA detection (this may not be feasible as CLDNs share significant portions of their amino acid sequence, and the main variations is in the EC1 and EC2 and the intracellular C-terminus)
8- Study effect of lack of *Cldn8* on susceptibility of mice in developing CRC
9- Investigate the transient protective mechanisms that result in an attenuated inflammatory response to repeat challenges of DSS shortly after recovery.

7.4.2 HUMAN STUDIES

Perform longitudinal studies in humans to measure variations in CLDN8 expression. This would help determine if patients can be stratified into more accurate risk groups for developing CRC.

8 References

1. Qin J, Li R, Raes J, Arumugam M, Burgdorf KS, Manichanh C, et al. A human gut microbial gene catalogue established by metagenomic sequencing. Nature [Internet]. 2010 Mar 4 [cited 2017 Jul 9];464(7285):59–65. Available from: http://www.ncbi.nlm.nih.gov/pubmed/20203603

2. Harmsen HJM., de Goffau MC. The human gut microbiota. Adv Exp Med Biol [Internet]. 2016;902:95–108. Available from: https://www.scopus.com/inward/record.uri?eid=2-s2.0-84979057738&partnerID=40&md5=cf4aebcff1863b45b3ee2f9406f42b6d

3. Lee YK, Mazmanian SK. Has the Microbiota Played a Critical Role in the Evolution of the Adaptive Immune System? Science (80-) [Internet]. 2010;330(6012):1768–73. Available from: http://www.sciencemag.org/cgi/doi/10.1126/science.1195568

4. Hasegawa M, Inohara N, E. WS, G N, C. LE, H MK, et al. Regulation of the gut microbiota by the mucosal immune system in mice. Int Immunol [Internet]. 2014 Sep 1 [cited 2017 Jul 10];26(9):481–7. Available from: https://academic.oup.com/intimm/article-lookup/doi/10.1093/intimm/dxu049

5. Hao W-L, Lee Y-K. Microflora of the Gastrointestinal Tract. In: Public Health Microbiology [Internet]. 2004. p. 491–502. Available from: http://dx.doi.org/10.1385/1-59259-766-1:491

6. Kau AL, Ahern PP, Griffin NW, Goodman AL, Jeffrey I. Human nutrition, the gut microbiome, and immune system: envisioning the future. Nature. 2012;474(7351):327–36.

7. Topping DL, Clifton PM. Short-chain fatty acids and human colonic function: roles of resistant starch and nonstarch polysaccharides. Physiol Rev. 2001;81(3):1031–64.

8. Mcdermott AJ, Huffnagle GB. The microbiome and regulation of mucosal immunity. Immunology. 2014;142(1):24–31.

9. Atarashi K, Nishimura J, Shima T, Umesaki Y, Yamamoto M, Onoue M, et al. ATP drives lamina propria TH17 cell differentiation. Nature [Internet]. 2008;455(7214):808–12. Available from: http://www.nature.com/doifinder/10.1038/nature07240

10. Hooper L V., Macpherson AJ. Immune adaptations that maintain homeostasis with the intestinal microbiota. Nat Rev Immunol [Internet]. 2010 Mar;10(3):159–69. Available from: http://www.nature.com/doifinder/10.1038/nri2710

11. Macpherson AJ, Uhr T. Compartmentalization of the mucosal immune responses to commensal intestinal bacteria. Ann N Y Acad Sci. 2004 Dec;1029:36–43.

12. Guarner F, Malagelada J-R. Gut flora in health and disease. Lancet (London, England) [Internet]. 2003;361(9356):512–9. Available from: http://www.ncbi.nlm.nih.gov/pubmed/12583961

13. Bull MJ, Plummer NT. Part 1: The Human Gut Microbiome in Health and Disease. Integr Med (Encinitas) [Internet]. 2014 Dec [cited 2017 Jul 10];13(6):17–22. Available from: http://www.ncbi.nlm.nih.gov/pubmed/26770121

14. Guarner F, Malagelada J-R. Gut flora in health and disease. Lancet (London, England). 2003;361(9356):512–9.

15. Bull MJ, Plummer NT. Part 1: The Human Gut Microbiome in Health and Disease. Integr Med (Encinitas). 2014 Dec;13(6):17–22.

16. Maslowski KM, Mackay CR. Diet, gut microbiota and immune responses. Nat Immunol [Internet]. 2011 Jan [cited 2017 Jul 10];12(1):5–9. Available from: http://www.ncbi.nlm.nih.gov/pubmed/21169997

17. Willing BP, Russell SL, Finlay BB. Shifting the balance: antibiotic effects on host–microbiota mutualism. Nat Rev Microbiol [Internet]. 2011 Apr 28 [cited 2017 Jul 10];9(4):233–43. Available from: http://www.ncbi.nlm.nih.gov/pubmed/21358670

18. Gill N, Wlodarska M, Finlay BB. Roadblocks in the gut: barriers to enteric infection. Cell Microbiol [Internet]. 2011 May [cited 2017 Jul 10];13(5):660–9. Available from: http://www.ncbi.nlm.nih.gov/pubmed/21392202

19. Kim YS, Ho SB. Intestinal Goblet Cells and Mucins in Health and Disease: Recent Insights and Progress. Curr Gastroenterol Rep [Internet]. 2010 Oct 13 [cited 2017 Jul 10];12(5):319–30. Available from: http://www.ncbi.nlm.nih.gov/pubmed/20703838

20. Moro K, Yamada T, Tanabe M, Takeuchi T, Ikawa T, Kawamoto H, et al. Innate production of TH2 cytokines by adipose tissue-associated c-Kit+Sca-1+ lymphoid cells. Nature [Internet]. 2010 Jan 28 [cited 2017 Jul 10];463(7280):540–4. Available from: http://www.ncbi.nlm.nih.gov/pubmed/20023630

21. Price AE, Liang H-E, Sullivan BM, Reinhardt RL, Eisley CJ, Erle DJ, et al. Systemically dispersed innate IL-13-expressing cells in type 2 immunity. Proc Natl Acad Sci [Internet]. 2010 Jun 22 [cited 2017 Jul 10];107(25):11489–94. Available from: http://www.ncbi.nlm.nih.gov/pubmed/20534524

22. Shimotoyodome A, Meguro S, Hase T, Tokimitsu I, Sakata T. Short chain fatty acids but not lactate or succinate stimulate mucus release in the rat colon. Comp Biochem Physiol A Mol Integr Physiol [Internet]. 2000 Apr [cited 2017 Jul 10];125(4):525–31. Available from: http://www.ncbi.nlm.nih.gov/pubmed/10840229

23. Johansson ME V., Phillipson M, Petersson J, Velcich A, Holm L, Hansson GC. The inner of the two Muc2 mucin-dependent mucus layers in colon is devoid of bacteria. Proc Natl Acad Sci [Internet]. 2008 Sep 30 [cited 2017 Jul 10];105(39):15064–9. Available from: http://www.pnas.org/cgi/doi/10.1073/pnas.0803124105

24. Johansson ME V., Phillipson M, Petersson J, Velcich A, Holm L, Hansson GC. The inner of the two Muc2 mucin-dependent mucus layers in colon is devoid of bacteria. Proc Natl Acad Sci. 2008 Sep;105(39):15064–9.

25. Atuma C, Strugala V, Allen A, Holm L. The adherent gastrointestinal mucus gel layer: thickness and physical state in vivo. Am J Physiol Gastrointest Liver Physiol [Internet]. 2001 May [cited 2014 Dec 30];280(5):G922-9. Available from: http://www.ncbi.nlm.nih.gov/pubmed/11292601

26. Cash HL, Whitham C V, Behrendt CL, Hooper L V. Symbiotic bacteria direct expression of an intestinal bactericidal lectin. Science [Internet]. 2006 Aug 25 [cited 2017 Jul 10];313(5790):1126–30. Available from: http://www.sciencemag.org/cgi/doi/10.1126/science.1127119

27. Vaishnava S, Behrendt CL, Ismail AS, Eckmann L, Hooper L V. Paneth cells directly sense gut commensals and maintain homeostasis at the intestinal host-microbial interface. Proc Natl Acad Sci U S A [Internet]. 2008 Dec 30 [cited 2017 Jul 10];105(52):20858–63. Available from: http://www.pnas.org/cgi/doi/10.1073/pnas.0808723105

28. Mantis NJ, Rol N, Corthésy B. Secretory IgA's complex roles in immunity and mucosal homeostasis in the gut. Vol. 4, Mucosal Immunology. 2011. p. 603–11.

29. Okumura R, Kurakawa T, Nakano T, Kayama H, Kinoshita M, Motooka D, et al. Lypd8 promotes the segregation of flagellated microbiota and colonic epithelia. Nature [Internet]. 2016 Mar 30 [cited 2017 Jul 10];532(7597):117–21. Available from: http://www.ncbi.nlm.nih.gov/pubmed/27027293

30. Brandtzaeg P, Kiyono H, Pabst R, Russell MW. Terminology: Nomenclature of mucosa-associated lymphoid tissue. Mucosal Immunol. 2008;1(1):31–7.

31. Neutra MR, Pringault E, Kraehenbuhl J-P. Antigen Sampling Across Epithelial Barriers and Induction of Mucosal Immune Responses. Annu Rev Immunol [Internet]. 1996;14(1):275–300. Available from: http://arjournals.annualreviews.org/doi/abs/10.1146/annurev.immunol.14.1.275

32. Kanaya T, Ohno H. The Mechanisms of M-cell Differentiation. 2014;33(3):91–7.

33. Cebra, JJ; Shroff K. Peyer's patches as inductive sites for IgA commitment. Ogra P L, Mestecky J, Lamm M E, Strober W, McGhee JR, Bienenstock J, Ed Handb Mucosal Immunol London. 1994;151.

34. Hayday A, Theodoridis E, Ramsburg E, Shires J. Intraepithelial lymphocytes: Exploring the Third Way in immunology. Vol. 2, Nature Immunology. 2001. p. 997–1003.

35. Mowat AM. Anatomical basis of tolerance and immunity to intestinal antigens. Nat Rev Immunol [Internet]. 2003;3(4):331–41. Available from: http://www.nature.com/doifinder/10.1038/nri1057

36. Ferguson A. Intraepithelial lymphocytes of the small intestine. Gut. 1977;18(11):921–37.

37. Sonnenberg GF, Monticelli LA, Elloso MM, Fouser LA, Artis D. CD4+ Lymphoid Tissue-Inducer Cells Promote Innate Immunity in the Gut. Immunity [Internet]. 2011 Jan 28 [cited 2017 Jul 10];34(1):122–34. Available from:

http://www.ncbi.nlm.nih.gov/pubmed/21194981

38. Zenewicz LA, Yancopoulos GD, Valenzuela DM, Murphy AJ, Stevens S, Flavell RA. Innate and Adaptive Interleukin-22 Protects Mice from Inflammatory Bowel Disease. Immunity [Internet]. 2008 Dec 19 [cited 2017 Jul 10];29(6):947–57. Available from: http://www.ncbi.nlm.nih.gov/pubmed/19100701

39. Mukherjee S, Zheng H, Derebe MG, Callenberg KM, Partch CL, Rollins D, et al. Antibacterial membrane attack by a pore-forming intestinal C-type lectin. Nature [Internet]. 2013 Nov 20 [cited 2017 Jul 10];505(7481):103–7. Available from: http://www.ncbi.nlm.nih.gov/pubmed/24256734

40. Mizoguchi A. Healing of intestinal inflammation by IL-22. Inflamm Bowel Dis [Internet]. 2012 Sep 1 [cited 2017 Jul 10];18(9):1777–84. Available from: http://content.wkhealth.com/linkback/openurl?sid=WKPTLP:landingpage&an=00054725-201209000-00022

41. Kuhn KA, Manieri NA, Liu T-C, Stappenbeck TS. IL-6 stimulates intestinal epithelial proliferation and repair after injury. Karhausen J, editor. PLoS One [Internet]. 2014 Dec 5 [cited 2017 Jul 12];9(12):e114195. Available from: http://dx.plos.org/10.1371/journal.pone.0114195

42. Wang H-C, Zhou Q, Dragoo J, Klein JR. Most murine CD8+ intestinal intraepithelial lymphocytes are partially but not fully activated T cells. J Immunol [Internet]. 2002 Nov 1 [cited 2017 Jul 13];169(9):4717–22. Available from: http://www.ncbi.nlm.nih.gov/pubmed/12391179

43. Boismenu R, Havran WL. Modulation of epithelial cell growth by intraepithelial gamma delta T cells. Science [Internet]. 1994 Nov 18 [cited 2017 Jul 13];266(5188):1253–5. Available from: http://www.ncbi.nlm.nih.gov/pubmed/7973709

44. Ungaro R, Mehandru S, Allen PB, Peyrin-Biroulet L, Colombel J-F. Ulcerative colitis. Lancet [Internet]. 2017 Apr 29 [cited 2017 Jul 13];389(10080):1756–70. Available from: http://www.ncbi.nlm.nih.gov/pubmed/27914657

45. Guilliams M, Ginhoux F, Jakubzick C, Naik SH, Onai N, Schraml BU, et al. Dendritic cells, monocytes and macrophages: a unified nomenclature based on ontogeny. Nat Rev Immunol [Internet]. 2014 Jul 18 [cited 2017 Jul 13];14(8):571–8. Available from: http://www.ncbi.nlm.nih.gov/pubmed/25033907

46. O'Neill LAJ. The interleukin-1 receptor/Toll-like receptor superfamily: 10 years of progress. Immunol Rev [Internet]. 2008 Dec [cited 2017 Jul 13];226(1):10–8. Available from: http://doi.wiley.com/10.1111/j.1600-065X.2008.00701.x

47. Smythies LE, Maheshwari A, Clements R, Eckhoff D, Novak L, Vu HL, et al. Mucosal IL-8 and TGF-ß recruit blood monocytes: evidence for cross-talk between the lamina propria stroma and myeloid cells. J Leukoc Biol [Internet]. 2006;80(3):492–9. Available from: http://www.jleukbio.org/content/80/3/492.abstract

48. Smythies LE, Shen R, Bimczok D, Novak L, Clements RH, Eckhoff DE, et al. Inflammation anergy in human intestinal macrophages is due to Smad-

induced IkappaBalpha expression and NF-kappaB inactivation. J Biol Chem. 2010;285(25):19593–604.

49. Bain CC, Scott CL, Uronen-Hansson H, Gudjonsson S, Jansson O, Grip O, et al. Resident and pro-inflammatory macrophages in the colon represent alternative context-dependent fates of the same Ly6Chi monocyte precursors. Mucosal Immunol [Internet]. 2013 May 19 [cited 2017 Jul 13];6(3):498–510. Available from: http://www.nature.com/doifinder/10.1038/mi.2012.89

50. Smythies LE, Sellers M, Clements RH, Mosteller-Barnum M, Meng G, Benjamin WH, et al. Human intestinal macrophages display profound inflammatory anergy despite avid phagocytic and bacteriocidal activity. J Clin Invest [Internet]. 2005 Jan 3 [cited 2017 Jul 13];115(1):66–75. Available from: http://www.jci.org/articles/view/19229

51. Rugtveit J, Haraldsen G, Høgåsen AK, Bakka A, Brandtzaeg P, Scott H. Respiratory burst of intestinal macrophages in inflammatory bowel disease is mainly caused by CD14+L1+ monocyte derived cells. Gut [Internet]. 1995 Sep [cited 2017 Jul 13];37(3):367–73. Available from: http://www.ncbi.nlm.nih.gov/pubmed/7590432

52. Roberts PJ, Riley GP, Morgan K, Miller R, Hunter JO, Middleton SJ. The physiological expression of inducible nitric oxide synthase (iNOS) in the human colon. J Clin Pathol [Internet]. 2001 Apr [cited 2017 Jul 13];54(4):293–7. Available from: http://www.ncbi.nlm.nih.gov/pubmed/11304846

53. Pull SL, Doherty JM, Mills JC, Gordon JI, Stappenbeck TS. Activated macrophages are an adaptive element of the colonic epithelial progenitor niche necessary for regenerative responses to injury. Proc Natl Acad Sci U S A [Internet]. 2005 Jan 4 [cited 2017 Jul 13];102(1):99–104. Available from: http://www.pnas.org/cgi/doi/10.1073/pnas.0405979102

54. Cerovic V, Bain CC, Mowat AM, Milling SWF. Intestinal macrophages and dendritic cells: what's the difference? Trends Immunol [Internet]. 2014 Jun [cited 2017 Jul 13];35(6):270–7. Available from: http://linkinghub.elsevier.com/retrieve/pii/S147149061400060X

55. Weiner HL, da Cunha AP, Quintana F, Wu H. Oral tolerance. Immunol Rev [Internet]. 2011 May [cited 2017 Jul 11];241(1):241–59. Available from: http://doi.wiley.com/10.1111/j.1600-065X.2011.01017.x

56. Coombes JL, Siddiqui KRR, Arancibia-Cárcamo C V, Hall J, Sun C-M, Belkaid Y, et al. A functionally specialized population of mucosal CD103+ DCs induces Foxp3+ regulatory T cells via a TGF-beta and retinoic acid-dependent mechanism. J Exp Med [Internet]. 2007 Aug 6 [cited 2017 Jul 13];204(8):1757–64. Available from: http://www.jem.org/lookup/doi/10.1084/jem.20070590

57. Sun C-M, Hall JA, Blank RB, Bouladoux N, Oukka M, Mora JR, et al. Small intestine lamina propria dendritic cells promote de novo generation of Foxp3 T reg cells via retinoic acid. J Exp Med [Internet]. 2007 Aug 6 [cited 2017 Jul 13];204(8):1775–85. Available from: http://www.jem.org/lookup/doi/10.1084/jem.20070602

58. McDole JR, Wheeler LW, McDonald KG, Wang B, Konjufca V, Knoop KA, et al. Goblet cells deliver luminal antigen to CD103+ dendritic cells in the small

intestine. Nature [Internet]. 2012 Mar 14 [cited 2017 Jul 13];483(7389):345–9. Available from: http://www.ncbi.nlm.nih.gov/pubmed/22422267

59. Mazzini E, Massimiliano L, Penna G, Rescigno M. Oral tolerance can be established via gap junction transfer of fed antigens from CX3CR1^{+} macrophages to CD103^{+} dendritic cells. Immunity [Internet]. 2014 Feb 20 [cited 2017 Jul 13];40(2):248–61. Available from: http://linkinghub.elsevier.com/retrieve/pii/S107476131400003X

60. Mann ER, Li X. Intestinal antigen-presenting cells in mucosal immune homeostasis: Crosstalk between dendritic cells, macrophages and B-cells. World Journal of Gastroenterology. 2014. p. 9653–64.

61. Schulz O, Jaensson E, Persson EK, Liu X, Worbs T, Agace WW, et al. Intestinal CD103+, but not CX3CR1+, antigen sampling cells migrate in lymph and serve classical dendritic cell functions. J Exp Med. 2009 Dec;206(13):3101–14.

62. Rescigno M, Urbano M, Valzasina B, Francolini M, Rotta G, Bonasio R, et al. Dendritic cells express tight junction proteins and penetrate gut epithelial monolayers to sample bacteria. Nat Immunol. 2001;2(4):361–7.

63. Müller AJ, Kaiser P, Dittmar KEJ, Weber TC, Haueter S, Endt K, et al. Salmonella gut invasion involves TTSS-2-dependent epithelial traversal, basolateral exit, and uptake by epithelium-sampling lamina propria phagocytes. Cell Host Microbe [Internet]. 2012 Jan 19 [cited 2017 Jul 13];11(1):19–32. Available from: http://linkinghub.elsevier.com/retrieve/pii/S1931312811004069

64. Bogunovic M, Ginhoux F, Helft J, Shang L, Hashimoto D, Greter M, et al. Origin of the Lamina Propria Dendritic Cell Network. Immunity [Internet]. 2009 Sep 18 [cited 2017 Jul 13];31(3):513–25. Available from: http://www.ncbi.nlm.nih.gov/pubmed/19733489

65. Denning TL, Wang Y, Patel SR, Williams IR, Pulendran B. Lamina propria macrophages and dendritic cells differentially induce regulatory and interleukin 17-producing T cell responses. Nat Immunol [Internet]. 2007 Oct 16 [cited 2017 Jul 13];8(10):1086–94. Available from: http://www.nature.com/doifinder/10.1038/ni1511

66. MacDonald TT, Pender SL. Lamina propria T cells. Chem Immunol [Internet]. 1998 [cited 2017 Jul 13];71:103–17. Available from: http://www.ncbi.nlm.nih.gov/pubmed/9761950

67. Schulz O, Jaensson E, Persson EK, Liu X, Worbs T, Agace WW, et al. Intestinal CD103+, but not CX3CR1+, antigen sampling cells migrate in lymph and serve classical dendritic cell functions. J Exp Med [Internet]. 2009 Dec 21 [cited 2017 Jul 13];206(13):3101–14. Available from: http://www.jem.org/lookup/doi/10.1084/jem.20091925

68. Hadis U, Wahl B, Schulz O, Hardtke-Wolenski M, Schippers A, Wagner N, et al. Intestinal tolerance requires gut homing and expansion of FoxP3+ regulatory T cells in the lamina propria. Immunity [Internet]. 2011 Feb 25 [cited 2017 Jul 17];34(2):237–46. Available from: http://linkinghub.elsevier.com/retrieve/pii/S1074761311000379

69. Murai M, Turovskaya O, Kim G, Madan R, Karp CL, Cheroutre H, et al. Interleukin 10 acts on regulatory T cells to maintain expression of the transcription factor Foxp3 and suppressive function in mice with colitis. Nat Immunol [Internet]. 2009 Nov 27 [cited 2017 Jul 17];10(11):1178–84. Available from: http://www.nature.com/doifinder/10.1038/ni.1791

70. Rivollier A, He J, Kole A, Valatas V, Kelsall BL. Inflammation switches the differentiation program of Ly6Chi monocytes from antiinflammatory macrophages to inflammatory dendritic cells in the colon. J Exp Med [Internet]. 2012 Jan 16 [cited 2017 Jul 17];209(1):139–55. Available from: http://www.jem.org/lookup/doi/10.1084/jem.20101387

71. Bain CC, Scott CL, Uronen-Hansson H, Gudjonsson S, Jansson O, Grip O, et al. Resident and pro-inflammatory macrophages in the colon represent alternative context-dependent fates of the same Ly6Chi monocyte precursors. Mucosal Immunol. 2013 May;6(3):498–510.

72. Ueda Y, Kayama H, Jeon SG, Kusu T, Isaka Y, Rakugi H, et al. Commensal microbiota induce LPS hyporesponsiveness in colonic macrophages via the production of IL-10. Int Immunol [Internet]. 2010 Dec [cited 2017 Jul 17];22(12):953–62. Available from: https://academic.oup.com/intimm/article-lookup/doi/10.1093/intimm/dxq449

73. Donaldson DS, Bradford BM, Artis D, Mabbott NA. Reciprocal regulation of lymphoid tissue development in the large intestine by IL-25 and IL-23. Mucosal Immunol [Internet]. 2015 May [cited 2017 Jul 17];8(3):582–95. Available from: http://www.ncbi.nlm.nih.gov/pubmed/25249168

74. Brandtzaeg P, Farstad IN, Haraldsen G. Regional specialization in the mucosal immune system: Primed cells do not always home along the same track. Vol. 20, Immunology Today. 1999. p. 267–77.

75. Guy-Grand D, Vassalli P. Gut intraepithelial lymphocyte development. Vol. 14, Current Opinion in Immunology. 2002. p. 255–9.

76. Reséndiz-Albor AA, Esquivel R, López-Revilla R, Verdín L, Moreno-Fierros L. Striking phenotypic and functional differences in lamina propria lymphocytes from the large and small intestine of mice. Life Sci [Internet]. 2005 Apr 29 [cited 2017 Jul 17];76(24):2783–803. Available from: http://www.ncbi.nlm.nih.gov/pubmed/15808880

77. Reséndiz-Albor AA, Esquivel R, López-Revilla R, Verdín L, Moreno-Fierros L. Striking phenotypic and functional differences in lamina propria lymphocytes from the large and small intestine of mice. Life Sci. 2005 Apr;76(24):2783–803.

78. Donaldson DS, Bradford BM, Artis D, Mabbott NA. Reciprocal regulation of lymphoid tissue development in the large intestine by IL-25 and IL-23. Mucosal Immunol. 2015 May;8(3):582–95.

79. Anderson JM, Van Itallie CM. Physiology and function of the tight junction. Cold Spring Harb Perspect Biol [Internet]. 2009 Aug;1(2):a002584. Available from: http://www.pubmedcentral.nih.gov/articlerender.fcgi?artid=2742087&tool=pmcentrez&rendertype=abstract

80. Shen L. Tight junctions on the move: molecular mechanisms for epithelial barrier regulation. Ann N Y Acad Sci [Internet]. 2012 Jul [cited 2013 Oct 8];1258:9–18. Available from: http://www.pubmedcentral.nih.gov/articlerender.fcgi?artid=3690943&tool=pmcentrez&rendertype=abstract

81. Schulzke J-D, Günzel D, John LJ, Fromm M. Perspectives on tight junction research. Ann N Y Acad Sci [Internet]. 2012 Jun [cited 2013 Oct 11];1257:1–19. Available from: http://www.ncbi.nlm.nih.gov/pubmed/22671584

82. Schneeberger EE, Lynch RD. The tight junction: a multifunctional complex. AJP Cell Physiol. 2004 Jun;286(6):C1213–28.

83. Guillemot L, Paschoud S, Pulimeno P, Foglia A, Citi S. The cytoplasmic plaque of tight junctions: A scaffolding and signalling center. Biochim Biophys Acta - Biomembr [Internet]. 2008 Mar [cited 2017 Jul 28];1778(3):601–13. Available from: http://www.ncbi.nlm.nih.gov/pubmed/18339298

84. Aijaz S, Balda MS, Matter K. Tight Junctions: Molecular Architecture and Function. In: International review of cytology [Internet]. 2006 [cited 2017 Jul 28]. p. 261–98. Available from: http://www.ncbi.nlm.nih.gov/pubmed/16487793

85. Howarth AG, Stevenson BR. Molecular environment of ZO-1 in epithelial and non-epithelial cells. Cell Motil Cytoskeleton [Internet]. 1995 [cited 2017 Jul 28];31(4):323–32. Available from: http://www.ncbi.nlm.nih.gov/pubmed/7553918

86. Krug SM, Amasheh S, Richter JF, Milatz S, Günzel D, Westphal JK, et al. Tricellulin forms a barrier to macromolecules in tricellular tight junctions without affecting ion permeability. Mol Biol Cell [Internet]. 2009 Aug [cited 2015 Feb 14];20(16):3713–24. Available from: http://www.pubmedcentral.nih.gov/articlerender.fcgi?artid=2777931&tool=pmcentrez&rendertype=abstract

87. Schulzke JD, Gitter AH, Mankertz J, Spiegel S, Seidler U, Amasheh S, et al. Epithelial transport and barrier function in occludin-deficient mice. Biochim Biophys Acta - Biomembr. 2005;1669:34–42.

88. Amasheh S, Fromm M, Günzel D. Claudins of intestine and nephron - a correlation of molecular tight junction structure and barrier function. Acta Physiol (Oxf) [Internet]. 2011 Jan [cited 2013 Oct 8];201(1):133–40. Available from: http://www.ncbi.nlm.nih.gov/pubmed/20518752

89. Krug SM, Günzel D, Conrad MP, Lee I-FM, Amasheh S, Fromm M, et al. Charge-selective claudin channels. Ann N Y Acad Sci [Internet]. 2012 Jun [cited 2013 Oct 8];1257:20–8. Available from: http://www.ncbi.nlm.nih.gov/pubmed/22671585

90. Krause G, Winkler L, Mueller SL, Haseloff RF, Piontek J, Blasig IE. Structure and function of claudins. Biochim Biophys Acta [Internet]. 2008 Mar [cited 2013 Oct 8];1778(3):631–45. Available from: http://www.ncbi.nlm.nih.gov/pubmed/18036336

91. Mineta K, Yamamoto Y, Yamazaki Y, Tanaka H, Tada Y, Saito K, et al.

Predicted expansion of the claudin multigene family. FEBS Lett [Internet]. 2011 Feb 18 [cited 2017 Jul 28];585(4):606–12. Available from: http://www.ncbi.nlm.nih.gov/pubmed/21276448

92. Colegio OR, Van Itallie CM, McCrea HJ, Rahner C, Anderson JM. Claudins create charge-selective channels in the paracellular pathway between epithelial cells. AJP Cell Physiol. 2002 Jul;283(1):C142–7.

93. Piontek J, Winkler L, Wolburg H, Muller SL, Zuleger N, Piehl C, et al. Formation of tight junction: determinants of homophilic interaction between classic claudins. FASEB J. 2007 Aug;22(1):146–58.

94. Lal-nag M, Morin PJ. Protein family review The claudins. Genome Biol. 2009;10(8).

95. Lal-Nag M, Morin PJ. The claudins. Genome Biol. 2009;10(8):235.

96. Van Itallie CM, Anderson JM. Claudins and epithelial paracellular transport. Annu Rev Physiol [Internet]. 2006 Jan [cited 2013 Sep 27];68:403–29. Available from: http://www.ncbi.nlm.nih.gov/pubmed/16460278

97. Saeedi BJ, Kao DJ, Kitzenberg DA, Dobrinskikh E, Schwisow KD, Masterson JC, et al. HIF-dependent regulation of claudin-1 is central to intestinal epithelial tight junction integrity. Mol Biol Cell [Internet]. 2015;26(12):2252–62. Available from: http://www.molbiolcell.org/cgi/doi/10.1091/mbc.E14-07-1194

98. Amasheh S, Meiri N, Gitter AH. Claudin-2 expression induces cation-selective channels in tight junctions of epithelial cells. J Cell Sci. 2002;115:4969–4976.

99. Mitchell L a, Overgaard CE, Ward C, Margulies SS, Koval M. Differential effects of claudin-3 and claudin-4 on alveolar epithelial barrier function. Am J Physiol Lung Cell Mol Physiol [Internet]. 2011;301(1):L40–9. Available from: http://www.pubmedcentral.nih.gov/articlerender.fcgi?artid=3129905&tool=pmcentrez&rendertype=abstract

100. Ohtsuki S, Sato S, Yamaguchi H, Kamoi M, Asashima T, Terasaki T. Exogenous expression of claudin-5 induces barrier properties in cultured rat brain capillary endothelial cells. J Cell Physiol. 2007;210(1):81–6.

101. Tanaka H, Takechi M, Kiyonari H, Shioi G, Tamura A, Tsukita S. Intestinal deletion of *Claudin-7* enhances paracellular organic solute flux and initiates colonic inflammation in mice. Gut [Internet]. 2015 Oct [cited 2017 Jul 28];64(10):1529–38. Available from: http://www.ncbi.nlm.nih.gov/pubmed/25691495

102. Yu ASL, Enck AH, Lencer WI, Schneeberger EE. Claudin-8 expression in Madin-Darby canine kidney cells augments the paracellular barrier to cation permeation. J Biol Chem [Internet]. 2003 May 9 [cited 2013 Oct 8];278(19):17350–9. Available from: http://www.ncbi.nlm.nih.gov/pubmed/12615928

103. Furuse M, Hata M, Furuse K, Yoshida Y, Haratake A, Sugitani Y, et al. Claudin-based tight junctions are crucial for the mammalian epidermal barrier. J Cell Biol. 2002 Mar;156(6):1099–111.

104. Günzel D, Fromm M. Claudins and Other Tight Junction Proteins. In: Comprehensive Physiology [Internet]. Hoboken, NJ, USA: John Wiley & Sons, Inc.; 2012 [cited 2017 Jul 28]. p. 1819–52. Available from: http://www.ncbi.nlm.nih.gov/pubmed/23723025

105. Hou J, Renigunta A, Yang J, Waldegger S. Claudin-4 forms paracellular chloride channel in the kidney and requires claudin-8 for tight junction localization. PNAS. 2010;107(42):18010–5.

106. Amasheh S, Schmidt T, Mahn M, Florian P, Mankertz J, Tavalali S, et al. Contribution of claudin-5 to barrier properties in tight junctions of epithelial cells. Cell Tissue Res [Internet]. 2005 Apr 28 [cited 2013 Oct 8];321(1):89–96. Available from: http://link.springer.com/10.1007/s00441-005-1101-0

107. Amasheh S, Milatz S, Krug SM, Bergs M, Amasheh M, Schulzke J-D, et al. Na+ absorption defends from paracellular back-leakage by claudin-8 upregulation. Biochem Biophys Res Commun [Internet]. 2009 Jan 2 [cited 2013 Oct 8];378(1):45–50. Available from: http://www.ncbi.nlm.nih.gov/pubmed/19000657

108. Angelow S, Kim K-J, Yu ASL. Claudin-8 modulates paracellular permeability to acidic and basic ions in MDCK II cells. J Physiol [Internet]. 2006 Feb 15 [cited 2013 Sep 21];571(Pt 1):15–26. Available from: http://www.pubmedcentral.nih.gov/articlerender.fcgi?artid=1805644&tool=pmcentrez&rendertype=abstract

109. Alexandre MD, Lu Q, Chen Y-H. Overexpression of claudin-7 decreases the paracellular Cl- conductance and increases the paracellular Na+ conductance in LLC-PK1 cells. J Cell Sci. 2005;118(Pt 12):2683–93.

110. Alexandre MD, Jeansonne BG, Renegar RH, Tatum R, Chen YH. The first extracellular domain of claudin-7 affects paracellular Cl- permeability. Biochem Biophys Res Commun. 2007;357(1):87–91.

111. Tanaka H, Takechi M, Kiyonari H, Shioi G, Tamura a., Tsukita S. Intestinal deletion of Claudin-7 enhances paracellular organic solute flux and initiates colonic inflammation in mice. Gut [Internet]. 2015;1–10. Available from: http://gut.bmj.com/cgi/doi/10.1136/gutjnl-2014-308419

112. Rosenthal R, Milatz S, Krug SM, Oelrich B, Schulzke J-D, Amasheh S, et al. Claudin-2, a component of the tight junction, forms a paracellular water channel. J Cell Sci. 2010;123(Pt 11):1913–21.

113. Fujita H, Sugimoto K, Inatomi S, Maeda T, Osanai M, Uchiyama Y, et al. Tight Junction Proteins Claudin-2 and -12 Are Critical for Vitamin D-dependent Ca2+ Absorption between Enterocytes. Mol Biol Cell [Internet]. 2008 May 1 [cited 2017 Jul 16];19(5):1912–21. Available from: http://www.ncbi.nlm.nih.gov/pubmed/18287530

114. Fujita H, Chiba H, Yokozaki H, Sakai N, Sugimoto K, Wada T, et al. Differential expression and subcellular localization of claudin-7, -8, -12, -13, and -15 along the mouse intestine. J Histochem Cytochem [Internet]. 2006 Aug [cited 2013 Oct 29];54(8):933–44. Available from: http://www.ncbi.nlm.nih.gov/pubmed/16651389

115. Garcia-Hernandez V, Quiros M, Nusrat A. Intestinal epithelial claudins: expression and regulation in homeostasis and inflammation. Ann N Y Acad Sci [Internet]. 2017 Jun [cited 2017 Jul 28];1397(1):66–79. Available from: http://www.ncbi.nlm.nih.gov/pubmed/28493289

116. Ding L, Lu Z, Foreman O, Tatum R, Lu Q, Renegar R, et al. Inflammation and disruption of the mucosal architecture in claudin-7-deficient mice. Gastroenterology [Internet]. 2012 Feb [cited 2013 Sep 24];142(2):305–15. Available from: http://www.pubmedcentral.nih.gov/articlerender.fcgi?artid=3267838&tool=pmcentrez&rendertype=abstract

117. Pope JL, Bhat AA, Sharma A, Ahmad R, Krishnan M, Washington MK, et al. Claudin-1 regulates intestinal epithelial homeostasis through the modulation of Notch-signalling. Gut [Internet]. 2014 Jun 13 [cited 2013 Oct 8];63(4):1–13. Available from: http://www.ncbi.nlm.nih.gov/pubmed/23766441

118. Lameris AL, Huybers S, Kaukinen K, Mäkelä TH, Bindels RJ, Hoenderop JG, et al. Expression profiling of claudins in the human gastrointestinal tract in health and during inflammatory bowel disease. Scand J Gastroenterol [Internet]. 2013 Jan 3 [cited 2013 Oct 8];48(1):58–69. Available from: http://www.ncbi.nlm.nih.gov/pubmed/23205909

119. Oshima T, Miwa H, Joh T. Changes in the expression of claudins in active ulcerative colitis. J Gastroenterol Hepatol [Internet]. 2008 Dec [cited 2013 Oct 8];23 Suppl 2:S146-50. Available from: http://www.ncbi.nlm.nih.gov/pubmed/19120888

120. Zeissig S, Bürgel N, Günzel D, Richter J, Mankertz J, Wahnschaffe U, et al. Changes in expression and distribution of claudin 2, 5 and 8 lead to discontinuous tight junctions and barrier dysfunction in active Crohn's disease. Gut [Internet]. 2007 Jan 1 [cited 2013 Oct 8];56(1):61–72. Available from: http://www.pubmedcentral.nih.gov/articlerender.fcgi?artid=1856677&tool=pmcentrez&rendertype=abstract

121. Fries W, Muja C, Crisafulli C, Cuzzocrea S, Mazzon E, Interna M, et al. Dynamics of enterocyte tight junctions : effect of experimental colitis and two different anti-TNF strategies. Am J Physiol Gastrointest Liver Physiol. 2008;294:G938–47.

122. Prasad S, Mingrino R, Kaukinen K, Hayes KL, Powell RM, MacDonald TT, et al. Inflammatory processes have differential effects on claudins 2, 3 and 4 in colonic epithelial cells. Lab Invest [Internet]. 2005 Sep [cited 2013 Oct 16];85(9):1139–62. Available from: http://www.ncbi.nlm.nih.gov/pubmed/16007110

123. Anderson C a, Boucher G, Lees CW, Franke A, D'Amato M, Taylor KD, et al. Meta-analysis identifies 29 additional ulcerative colitis risk loci, increasing the number of confirmed associations to 47. Nat Genet [Internet]. 2011 Feb 6 [cited 2013 Sep 30];43(3):246–52. Available from: http://www.nature.com/doifinder/10.1038/ng.764

124. Xia X-M, Wang F-Y, Zhou J, Hu K-F, Li S-W, Zou B-B. CXCR4 antagonist AMD3100 modulates claudin expression and intestinal barrier function in experimental colitis. Bereswill S, editor. PLoS One [Internet]. 2011 Jan 3 [cited

2013 Oct 8];6(11):e27282. Available from: http://www.pubmedcentral.nih.gov/articlerender.fcgi?artid=3207859&tool=pmcentrez&rendertype=abstract

125. Li Q, Zhang Q, Zhang M, Wang C, Zhu Z, Li N, et al. Effect of n-3 polyunsaturated fatty acids on membrane microdomain localization of tight junction proteins in experimental colitis. FEBS J [Internet]. 2008 Feb [cited 2013 Oct 8];275(3):411–20. Available from: http://www.ncbi.nlm.nih.gov/pubmed/18167140

126. Capaldo CT, Nusrat A. Cytokine regulation of tight junctions. Biochim Biophys Acta [Internet]. 2009 Apr [cited 2013 Oct 3];1788(4):864–71. Available from: http://www.ncbi.nlm.nih.gov/pubmed/18952050

127. Loftus E V. Clinical epidemiology of inflammatory bowel disease: Incidence, prevalence, and environmental influences. Gastroenterology [Internet]. 2004 May [cited 2017 Jul 17];126(6):1504–17. Available from: http://www.ncbi.nlm.nih.gov/pubmed/15168363

128. Molodecky N a., Soon IS, Rabi DM, Ghali W a., Ferris M, Chernoff G, et al. Increasing incidence and prevalence of the inflammatory bowel diseases with time, based on systematic review. Gastroenterology [Internet]. 2012 Jan [cited 2017 Jul 17];142(1):46–54.e42. Available from: http://dx.doi.org/10.1053/j.gastro.2011.10.001

129. Ahuja V, Tandon RK. Inflammatory bowel disease in the Asia-Pacific area: a comparison with developed countries and regional differences. J Dig Dis [Internet]. 2010 Jun [cited 2017 Jul 17];11(3):134–47. Available from: http://doi.wiley.com/10.1111/j.1751-2980.2010.00429.x

130. Bernstein CN, Wajda A, Svenson LW, MacKenzie A, Koehoorn M, Jackson M, et al. The Epidemiology of Inflammatory Bowel Disease in Canada: A Population-Based Study. Am J Gastroenterol [Internet]. 2006 Jul [cited 2017 Jul 17];101(7):1559–68. Available from: http://www.ncbi.nlm.nih.gov/pubmed/16863561

131. Cosnes J, Gower–Rousseau C, Seksik P, Cortot A. Epidemiology and Natural History of Inflammatory Bowel Diseases. Gastroenterology [Internet]. 2011 May [cited 2017 Jul 17];140(6):1785–1794.e4. Available from: http://www.ncbi.nlm.nih.gov/pubmed/21530745

132. Loftus E V. Clinical epidemiology of inflammatory bowel disease: Incidence, prevalence, and environmental influences. Gastroenterology. 2004 May;126(6):1504–17.

133. Cosnes J, Gower–Rousseau C, Seksik P, Cortot A. Epidemiology and Natural History of Inflammatory Bowel Diseases. Gastroenterology. 2011 May;140(6):1785–1794.e4.

134. Shivananda S, Lennard-Jones J, Logan R, Fear N, Price A, Carpenter L, et al. Incidence of inflammatory bowel disease across Europe: is there a difference between north and south? Results of the European Collaborative Study on Inflammatory Bowel Disease (EC-IBD). Gut [Internet]. 1996 Nov [cited 2017 Jul 17];39(5):690–7. Available from: http://www.ncbi.nlm.nih.gov/pubmed/9014768

135. Benchimol EI, Mack DR, Guttmann A, Nguyen GC, To T, Mojaverian N, et al. Inflammatory Bowel Disease in Immigrants to Canada And Their Children: A Population-Based Cohort Study. Am J Gastroenterol. 2015 Apr;110(4):553–63.

136. Benchimol EI, Manuel DG, To T, Mack DR, Nguyen GC, Gommerman JL, et al. Asthma, Type 1 and Type 2 Diabetes Mellitus, and Inflammatory Bowel Disease amongst South Asian Immigrants to Canada and Their Children: A Population-Based Cohort Study. Zhang H, editor. PLoS One [Internet]. 2015 Apr 7 [cited 2017 Jul 17];10(4):e0123599. Available from: http://www.ncbi.nlm.nih.gov/pubmed/25849480

137. Carr I, Mayberry JF. The effects of migration on ulcerative colitis: a three-year prospective study among Europeans and first- and second- generation South Asians in Leicester (1991-1994). Am J Gastroenterol. 1999 Oct;94(10):2918–22.

138. Ng SC, Tang W, Ching JY, Wong M, Chow CM, Hui AJ, et al. Incidence and phenotype of inflammatory bowel disease based on results from the Asia-pacific Crohn's and colitis epidemiology study. Gastroenterology [Internet]. 2013 Jul [cited 2017 Jul 17];145(1):158–165.e2. Available from: http://linkinghub.elsevier.com/retrieve/pii/S0016508513005003

139. Sood A, Midha V, Sood N, Bhatia AS, Avasthi G. Incidence and prevalence of ulcerative colitis in Punjab, North India. Gut. 2003 Nov;52(11):1587–90.

140. Tozun N, Atug O, Imeryuz N, Hamzaoglu HO, Tiftikci A, Parlak E, et al. Clinical characteristics of inflammatory bowel disease in Turkey: a multicenter epidemiologic survey. J Clin Gastroenterol [Internet]. 2009 Jan [cited 2017 Jul 17];43(1):51–7. Available from: http://content.wkhealth.com/linkback/openurl?sid=WKPTLP:landingpage&an=00004836-200901000-00009

141. Victoria CR, Sassak LY, Nunes HR de C. Incidence and prevalence rates of inflammatory bowel diseases, in midwestern of São Paulo State, Brazil. Arq Gastroenterol. 2009;46(1):20–5.

142. Xavier RJ, Podolsky DK. Unravelling the pathogenesis of inflammatory bowel disease. Nature [Internet]. 2007 Jul 26 [cited 2017 Jul 17];448(July):427–34. Available from: http://www.ncbi.nlm.nih.gov/pubmed/17653185

143. Ungaro R, Mehandru S, Allen PB, Peyrin-Biroulet L, Colombel J-F. Ulcerative colitis. Lancet. 2017 Apr;389(10080):1756–70.

144. Ahuja V, Tandon RK. Inflammatory bowel disease in the Asia-Pacific area: a comparison with developed countries and regional differences. J Dig Dis. 2010 Jun;11(3):134–47.

145. Gearry RB, Richardson AK, Frampton CM, Dodgshun AJ, Barclay ML. Population-based cases control study of inflammatory bowel disease risk factors. J Gastroenterol Hepatol [Internet]. 2010 Feb [cited 2017 Jul 17];25(2):325–33. Available from: http://www.ncbi.nlm.nih.gov/pubmed/20074146

146. Lynch HT, Brand RE, Locker GY. Inflammatory bowel disease in Ashkenazi

Jews: implications for familial colorectal cancer. Fam Cancer [Internet]. 2004 [cited 2017 Jul 17];3(3–4):229–32. Available from: http://link.springer.com/10.1007/s10689-004-9548-9

147. Brant SR. Update on the heritability of inflammatory bowel disease: The importance of twin studies. Inflamm Bowel Dis [Internet]. 2011 Jan [cited 2017 Jul 17];17(1):1–5. Available from: http://www.ncbi.nlm.nih.gov/pubmed/20629102

148. Monsén U, Broström O, Nordenvall B, Sörstad J, Hellers G. Prevalence of inflammatory bowel disease among relatives of patients with ulcerative colitis. Scand J Gastroenterol [Internet]. 1987 Mar [cited 2015 Jan 30];22(2):214–8. Available from: http://www.ncbi.nlm.nih.gov/pubmed/3576128

149. Tysk C, Lindberg E, Järnerot G, Flodérus-Myrhed B. Ulcerative colitis and Crohn's disease in an unselected population of monozygotic and dizygotic twins. A study of heritability and the influence of smoking. Gut. 1988;29:990–6.

150. Jostins L, Ripke S, Weersma RK, Duerr RH, McGovern DP, Hui KY, et al. Host-microbe interactions have shaped the genetic architecture of inflammatory bowel disease. Nature [Internet]. 2012 Nov 1 [cited 2013 Sep 16];491(7422):119–24. Available from: http://www.pubmedcentral.nih.gov/articlerender.fcgi?artid=3491803&tool=pmcentrez&rendertype=abstract

151. Herszterg S, Pinheiro D, Bellaiche Y. A multicellular view of cytokinesis in epithelial tissue. Trends Cell Biol. 2013;24(5):285–93.

152. Aumailley M. The laminin family. Cell Adhes Migr. 2013;7(January 2015):48–55.

153. Thompson AI, Lees CW. Genetics of ulcerative colitis. Inflamm Bowel Dis [Internet]. 2011 Mar [cited 2017 Jul 17];17(3):831–48. Available from: http://content.wkhealth.com/linkback/openurl?sid=WKPTLP:landingpage&an=00054725-201103000-00017

154. Hugot JP, Chamaillard M, Zouali H, Lesage S, Cézard JP, Belaiche J, et al. Association of NOD2 leucine-rich repeat variants with susceptibility to Crohn's disease. Nature. 2001;411(6837):599–603.

155. Ogura Y, Bonen DK, Inohara N, Nicolae DL, Chen FF, Ramos R, et al. A frameshift mutation in NOD2 associated with susceptibility to Crohn's disease. Nature. 2001;411(6837):603–6.

156. Economou M, Trikalinos TA, Loizou KT, Tsianos E V., Ioannidis JPA. Differential effects of NOD2 variants on Crohn's disease risk and phenotype in diverse populations: A metaanalysis. Am J Gastroenterol. 2004;99(12):2393–404.

157. NOD2 [Internet]. IBD Exome Browser. Available from: https://ibd.broadinstitute.org/variant/16-50763778-G-GC

158. Danese S, Sans M, Fiocchi C. Inflammatory bowel disease: the role of environmental factors. Autoimmun Rev [Internet]. 2004 Jul [cited 2017 Jul

17];3(5):394–400. Available from: http://www.ncbi.nlm.nih.gov/pubmed/15288007

159. Loftus E V, Silverstein MD, Sandborn WJ, Tremaine WJ, Harmsen WS, Zinsmeister AR. Ulcerative colitis in Olmsted County, Minnesota, 1940-1993: incidence, prevalence, and survival. Gut [Internet]. 2000 Mar [cited 2017 Jul 17];46(3):336–43. Available from: http://www.ncbi.nlm.nih.gov/pubmed/10673294

160. Chapman-Kiddell CA, Davies PSW, Gillen L, Radford-Smith GL. Role of diet in the development of inflammatory bowel disease. Inflamm Bowel Dis [Internet]. 2010 Jan [cited 2017 Jul 17];16(1):137–51. Available from: http://content.wkhealth.com/linkback/openurl?sid=WKPTLP:landingpage&an=00054725-201001000-00023

161. Birrenbach T, Böcker U. Inflammatory bowel disease and smoking: a review of epidemiology, pathophysiology, and therapeutic implications. Inflamm Bowel Dis [Internet]. 2004 Nov [cited 2017 Jul 17];10(6):848–59. Available from: http://www.ncbi.nlm.nih.gov/pubmed/15626903

162. Birrenbach T, Böcker U. Inflammatory bowel disease and smoking: a review of epidemiology, pathophysiology, and therapeutic implications. Inflamm Bowel Dis. 2004 Nov;10(6):848–59.

163. Holzapfel WH, Haberer P, Snel J, Schillinger U, Huis in't Veld JH. Overview of gut flora and probiotics. Int J Food Microbiol [Internet]. 1998 May 26 [cited 2017 Jul 17];41(2):85–101. Available from: http://www.ncbi.nlm.nih.gov/pubmed/9704859

164. Lopez J, Grinspan A. Fecal Microbiota Transplantation for Inflammatory Bowel Disease. Gastroenterol Hepatol (N Y) [Internet]. 2016 Jun [cited 2017 Jul 17];12(6):374–9. Available from: http://www.ncbi.nlm.nih.gov/pubmed/27493597

165. Sartor RB. Microbial Influences in Inflammatory Bowel Diseases. Gastroenterology [Internet]. 2008 Feb [cited 2017 Jul 17];134(2):577–94. Available from: http://www.ncbi.nlm.nih.gov/pubmed/18242222

166. Matsuoka K, Kanai T. The gut microbiota and inflammatory bowel disease. Semin Immunopathol [Internet]. 2015 Jan 25 [cited 2017 Jul 17];37(1):47–55. Available from: http://www.ncbi.nlm.nih.gov/pubmed/25420450

167. Martinez C, Antolin M, Santos J, Torrejon A, Casellas F, Borruel N, et al. Unstable composition of the fecal microbiota in ulcerative colitis during clinical remission. Am J Gastroenterol [Internet]. 2008 Mar [cited 2017 Jul 17];103(3):643–8. Available from: http://www.nature.com/doifinder/10.1111/j.1572-0241.2007.01592.x

168. Ott SJ, Plamondon S, Hart A, Begun A, Rehman A, Kamm MA, et al. Dynamics of the mucosa-associated flora in ulcerative colitis patients during remission and clinical relapse. J Clin Microbiol. 2008;46(10):3510–3.

169. Andrews CN, Griffiths TA, Kaufman J, Vergnolle N, Surette MG, Rioux KP. Mesalazine (5-aminosalicylic acid) alters faecal bacterial profiles, but not mucosal proteolytic activity in diarrhoea-predominant irritable bowel

syndrome. Aliment Pharmacol Ther [Internet]. 2011 Aug [cited 2017 Jul 17];34(3):374–83. Available from: http://doi.wiley.com/10.1111/j.1365-2036.2011.04732.x

170. Paramsothy S, Kamm MA, Kaakoush NO, Walsh AJ, van den Bogaerde J, Samuel D, et al. Multidonor intensive faecal microbiota transplantation for active ulcerative colitis: a randomised placebo-controlled trial. Lancet [Internet]. 2017 Mar 25 [cited 2017 Jul 17];389(10075):1218–28. Available from: http://www.ncbi.nlm.nih.gov/pubmed/28214091

171. Prantera C. What role do antibiotics have in the treatment of IBD? Nat Clin Pract Gastroenterol Hepatol [Internet]. 2008 Dec 30 [cited 2017 Jul 17];5(12):670–1. Available from: http://www.nature.com/doifinder/10.1038/ncpgasthep1273

172. Seed B, Jiang C, Ting AT. PPAR-gamma agonists inhibit production of monocyte inflammatory cytokines. Nature [Internet]. 1998 Jan 1 [cited 2017 Jul 17];391(6662):82–6. Available from: http://www.ncbi.nlm.nih.gov/pubmed/9422509

173. Dubuquoy L, Jansson EA, Deeb S, Rakotobe S, Karoui M, Colombel J-F, et al. Impaired expression of peroxisome proliferator-activated receptor gamma in ulcerative colitis. Gastroenterology [Internet]. 2003 May [cited 2017 Jul 17];124(5):1265–76. Available from: http://www.ncbi.nlm.nih.gov/pubmed/12730867

174. Johansson M, Gustafsson J, Holmén-Larsson J, Jabbar K, Xia L, Xu H, et al. Bacteria penetrate the normally impenetrable inner colon mucus layer in both murine colitis models and patients with ulcerative colitis. Gut [Internet]. 2014 Feb [cited 2017 Jul 17];63(2):281–91. Available from: http://gut.bmj.com/lookup/doi/10.1136/gutjnl-2012-303207

175. Mashimo H, Wu DC, Podolsky DK, Fishman MC. Impaired defense of intestinal mucosa in mice lacking intestinal trefoil factor. Science [Internet]. 1996 Oct 11 [cited 2017 Jul 17];274(5285):262–5. Available from: http://www.ncbi.nlm.nih.gov/pubmed/8824194

176. Podolsky DK, Isselbacher KJ. Glycoprotein composition of colonic mucosa. Specific alterations in ulcerative colitis. Gastroenterology [Internet]. 1984 Nov [cited 2017 Jul 17];87(5):991–8. Available from: http://www.ncbi.nlm.nih.gov/pubmed/6090262

177. Gecse K, Róka R, Séra T, Rosztóczy A, Annaházi A, Izbéki F, et al. Leaky gut in patients with diarrhea-predominant irritable bowel syndrome and inactive ulcerative colitis. Digestion [Internet]. 2012 Jan [cited 2013 Oct 8];85(1):40–6. Available from: http://www.ncbi.nlm.nih.gov/pubmed/22179430

178. Welcker K, Martin A, Kölle P, Siebeck M, Gross M. Increased intestinal permeability in patients with inflammatory bowel disease. Eur J Med Res [Internet]. 2004 Oct 29 [cited 2015 Jan 30];9(10):456–60. Available from: http://www.ncbi.nlm.nih.gov/pubmed/15546811

179. Arrieta MC, Madsen K, Doyle J, Meddings J. Reducing small intestinal permeability attenuates colitis in the IL10 gene-deficient mouse. Gut [Internet]. 2009 Jan 1 [cited 2013 Oct 16];58(1):41–8. Available from:

http://www.ncbi.nlm.nih.gov/pubmed/18829978

180. Segal AW, Loewi G. Neutrophil dysfunction in Crohn's disease. Lancet. 1976;308(7979):219–21.

181. Smith AM, Rahman FZ, Hayee B, Graham SJ, Marks DJB, Sewell GW, et al. Disordered macrophage cytokine secretion underlies impaired acute inflammation and bacterial clearance in Crohn's disease. J Exp Med. 2009 Aug;206(9):1883–97.

182. Sewell GW, Rahman FZ, Levine AP, Jostins L, Smith PJ, Walker AP, et al. Defective tumor necrosis factor release from Crohn's disease macrophages in response to toll-like receptor activation: Relationship to phenotype and genome-wide association susceptibility loci. Inflamm Bowel Dis. 2012;18(11):2120–7.

183. Østvik AE, Granlund A vB, Bugge M, Nilsen NJ, Torp SH, Waldum HL, et al. Enhanced Expression of CXCL10 in Inflammatory Bowel Disease. Inflamm Bowel Dis [Internet]. 2013 Feb [cited 2017 Jul 29];19(2):265–74. Available from: http://www.ncbi.nlm.nih.gov/pubmed/22685032

184. Rahman FZ, Smith AM, Hayee B, Marks DJB, Bloom SL, Segal AW. Delayed resolution of acute inflammation in ulcerative colitis is associated with elevated cytokine release downstream of TLR4. Bereswill S, editor. PLoS One [Internet]. 2010 Jan 26 [cited 2013 Oct 8];5(3):e9891. Available from: http://www.pubmedcentral.nih.gov/articlerender.fcgi?artid=2847519&tool=pmcentrez&rendertype=abstract

185. Luster AD, Unkeless JC, Ravetch J V. Gamma-interferon transcriptionally regulates an early-response gene containing homology to platelet proteins. Nature [Internet]. [cited 2017 Jul 29];315(6021):672–6. Available from: http://www.ncbi.nlm.nih.gov/pubmed/3925348

186. Bonecchi R, Bianchi G, Bordignon PP, D'Ambrosio D, Lang R, Borsatti A, et al. Differential expression of chemokine receptors and chemotactic responsiveness of type 1 T helper cells (Th1s) and Th2s. J Exp Med [Internet]. 1998 Jan 5 [cited 2017 Jul 29];187(1):129–34. Available from: http://www.ncbi.nlm.nih.gov/pubmed/9419219

187. Taub DD, Lloyd AR, Conlon K, Wang JM, Ortaldo JR, Harada A, et al. Recombinant human interferon-inducible protein 10 is a chemoattractant for human monocytes and T lymphocytes and promotes T cell adhesion to endothelial cells. J Exp Med [Internet]. 1993 Jun 1 [cited 2017 Jul 29];177(6):1809–14. Available from: http://www.ncbi.nlm.nih.gov/pubmed/8496693

188. Sandborn WJ, Rutgeerts P, Colombel J-F, Ghosh S, Petryka R, Sands BE, et al. Eldelumab [anti-interferon-γ-inducible protein-10 antibody] Induction Therapy for Active Crohn's Disease: a Randomised, Double-blind, Placebo-controlled Phase IIa Study. J Crohn's Colitis [Internet]. 2017 Jul 22 [cited 2017 Jul 29];11(7):811–9. Available from: http://www.ncbi.nlm.nih.gov/pubmed/28333187

189. Sandborn WJ, Colombel J-F, Ghosh S, Sands BE, Dryden G, Hébuterne X, et al. Eldelumab [Anti-IP-10] Induction Therapy for Ulcerative Colitis: A

Randomised, Placebo-Controlled, Phase 2b Study. J Crohn's Colitis [Internet]. 2016 Apr [cited 2017 Jul 29];10(4):418–28. Available from: http://www.ncbi.nlm.nih.gov/pubmed/26721935

190. Silverberg MS, Satsangi J, Ahmad T, Arnott IDR, Bernstein CN, Brant SR, et al. Toward an integrated clinical, molecular and serological classification of inflammatory bowel disease: report of a Working Party of the 2005 Montreal World Congress of Gastroenterology. Can J Gastroenterol [Internet]. 2005 Sep [cited 2017 Jul 17];19 Suppl A:5A–36A. Available from: http://www.ncbi.nlm.nih.gov/pubmed/16151544

191. Jenkins D, Balsitis M, Gallivan S, Dixon MF, Gilmour HM, Shepherd NA, et al. Guidelines for the initial biopsy diagnosis of suspected chronic idiopathic inflammatory bowel disease. The British Society of Gastroenterology Initiative. J Clin Pathol [Internet]. 1997 Feb [cited 2017 Jul 29];50(2):93–105. Available from: http://www.ncbi.nlm.nih.gov/pubmed/9155688

192. Washington K, Greenson JK, Montgomery E, Shyr Y, Crissinger KD, Polk DB, et al. Histopathology of ulcerative colitis in initial rectal biopsy in children. Am J Surg Pathol [Internet]. 2002;26(11):1441–9. Available from: http://www.ncbi.nlm.nih.gov/pubmed/12409720

193. Kornbluth A, Sachar DB, Practice Parameters Committee of the American College of Gastroenterology. Ulcerative Colitis Practice Guidelines in Adults: American College of Gastroenterology, Practice Parameters Committee. Am J Gastroenterol [Internet]. 2010 Mar 12 [cited 2017 Jul 17];105(3):501–23. Available from: http://www.ncbi.nlm.nih.gov/pubmed/20068560

194. Magro F, Langner C, Driessen A, Ensari A, Geboes K, Mantzaris GJ, et al. European consensus on the histopathology of inflammatory bowel disease. J Crohn's Colitis [Internet]. 2013 Nov [cited 2017 Jul 17];7(10):827–51. Available from: http://www.ncbi.nlm.nih.gov/pubmed/23870728

195. Tanaka M, Saito H, Kusumi T, Fukuda S, Shimoyama T, Sasaki Y, et al. Spatial distribution and histogenesis of colorectal Paneth cell metaplasia in idiopathic inflammatory bowel disease. J Gastroenterol Hepatol. 2001;16(August):1353–9.

196. Ekbom A, Helmick C, Zack M, Adami H-O. Ulcerative Colitis and Colorectal Cancer. N Engl J Med [Internet]. 1990 Nov 1 [cited 2017 Jul 17];323(18):1228–33. Available from: http://www.ncbi.nlm.nih.gov/pubmed/2215606

197. Ekbom A, Helmick C, Zack M, Adami HO. Increased risk of large-bowel cancer in Crohn's disease with colonic involvement. Lancet (London, England) [Internet]. 1990 Aug 11 [cited 2017 Jul 17];336(8711):357–9. Available from: http://www.ncbi.nlm.nih.gov/pubmed/1975343

198. Choi C-HR, Rutter MD, Askari A, Lee GH, Warusavitarne J, Moorghen M, et al. Forty-Year Analysis of Colonoscopic Surveillance Program for Neoplasia in Ulcerative Colitis: An Updated Overview. Am J Gastroenterol [Internet]. 2015 Jul 31 [cited 2017 Jul 17];110(7):1022–34. Available from: http://www.nature.com/doifinder/10.1038/ajg.2015.65

199. Beaugerie L, Itzkowitz SH. Cancers Complicating Inflammatory Bowel Disease. Longo DL, editor. N Engl J Med [Internet]. 2015 Apr 9 [cited 2017 Jul

17];372(15):1441–52. Available from: http://www.ncbi.nlm.nih.gov/pubmed/25853748

200. Desai D, Desai N. Colorectal cancer surveillance in inflammatory bowel disease: A critical analysis. World J Gastrointest Endosc [Internet]. 2014;6(11):541–8. Available from: http://www.pubmedcentral.nih.gov/articlerender.fcgi?artid=4231493&tool=pmcentrez&rendertype=abstract

201. Dignass A, Lindsay JO, Sturm A, Windsor A, Colombel J-F, Allez M, et al. Second European evidence-based consensus on the diagnosis and management of ulcerative colitis Part 2: Current management. J Crohn's Colitis [Internet]. 2012 Dec [cited 2017 Jul 29];6(10):991–1030. Available from: http://www.ncbi.nlm.nih.gov/pubmed/23040451

202. Andrews CN, Griffiths TA, Kaufman J, Vergnolle N, Surette MG, Rioux KP. Mesalazine (5-aminosalicylic acid) alters faecal bacterial profiles, but not mucosal proteolytic activity in diarrhoea-predominant irritable bowel syndrome. Aliment Pharmacol Ther. 2011 Aug;34(3):374–83.

203. Järnerot G, Hertervig E, Friis-Liby I, Blomquist L, Karlén P, Grännö C, et al. Infliximab as rescue therapy in severe to moderately severe ulcerative colitis: a randomized, placebo-controlled study. Gastroenterology [Internet]. 2005 Jun [cited 2017 Jul 18];128(7):1805–11. Available from: http://www.ncbi.nlm.nih.gov/pubmed/15940615

204. Rutgeerts P, Sandborn WJ, Feagan BG, Reinisch W, Olson A, Johanns J, et al. Infliximab for Induction and Maintenance Therapy for Ulcerative Colitis. N Engl J Med [Internet]. 2005 Dec 8 [cited 2017 Jul 18];353(23):2462–76. Available from: http://www.ncbi.nlm.nih.gov/pubmed/16339095

205. Reinisch W, Sandborn WJ, Hommes DW, D'Haens G, Hanauer S, Schreiber S, et al. Adalimumab for induction of clinical remission in moderately to severely active ulcerative colitis: results of a randomised controlled trial. Gut [Internet]. 2011 Jun 1 [cited 2017 Jul 18];60(6):780–7. Available from: http://gut.bmj.com/cgi/doi/10.1136/gut.2010.221127

206. Sandborn WJ, Feagan BG, Marano C, Zhang H, Strauss R, Johanns J, et al. Subcutaneous golimumab induces clinical response and remission in patients with moderate-to-severe ulcerative colitis. Gastroenterology [Internet]. 2014 Jan [cited 2017 Jul 18];146(1):85-95-5. Available from: http://linkinghub.elsevier.com/retrieve/pii/S0016508513008469

207. Colombel J-F, Sands BE, Rutgeerts P, Sandborn W, Danese S, D'Haens G, et al. The safety of vedolizumab for ulcerative colitis and Crohn's disease. Gut [Internet]. 2017 May [cited 2017 Jul 18];66(5):839–51. Available from: http://www.ncbi.nlm.nih.gov/pubmed/26893500

208. Mora JR, Von Andrian UH. Specificity and plasticity of memory lymphocyte migration. Curr Top Microbiol Immunol [Internet]. 2006 [cited 2017 Jul 29];308:83–116. Available from: http://www.ncbi.nlm.nih.gov/pubmed/16922087

209. Hancock L, Windsor AC, Mortensen NJ. Inflammatory bowel disease: the view of the surgeon. Colorectal Dis [Internet]. 2006 May [cited 2017 Jul 18];8 Suppl

1(s1):10–4. Available from: http://doi.wiley.com/10.1111/j.1463-1318.2006.00986.x

210. Fazio VW, Kiran RP, Remzi FH, Coffey JC, Heneghan HM, Kirat HT, et al. Ileal pouch anal anastomosis: analysis of outcome and quality of life in 3707 patients. Ann Surg [Internet]. 2013 Apr [cited 2017 Jul 18];257(4):679–85. Available from: http://content.wkhealth.com/linkback/openurl?sid=WKPTLP:landingpage&an=00000658-201304000-00015

211. Khanna R, Jairath V, Vande Casteele N, Mosli MH, Zou G, Parker CE, et al. Efficient Early Drug Development for Ulcerative Colitis. Gastroenterology [Internet]. 2016 May [cited 2017 Jul 18];150(5):1056–60. Available from: http://www.ncbi.nlm.nih.gov/pubmed/27018491

212. Khanna R, Jairath V, Vande Casteele N, Mosli MH, Zou G, Parker CE, et al. Efficient Early Drug Development for Ulcerative Colitis. Gastroenterology. 2016 May;150(5):1056–60.

213. Low D, Nguyen DD, Mizoguchi E. Animal models of ulcerative colitis and their application in drug research. Drug Des Devel Ther [Internet]. 2013 Nov [cited 2017 Jul 18];7:1341–57. Available from: http://www.dovepress.com/animal-models-of-ulcerative-colitis-and-their-application-in-drug-rese-peer-reviewed-article-DDDT

214. Laroui H, Ingersoll SA, Liu HC, Baker MT, Ayyadurai S, Charania MA, et al. Dextran sodium sulfate (DSS) induces colitis in mice by forming nano-lipocomplexes with medium-chain-length fatty acids in the colon. Niess J-H, editor. PLoS One [Internet]. 2012 Jan 9 [cited 2013 Sep 25];7(3):e32084. Available from: http://www.pubmedcentral.nih.gov/articlerender.fcgi?artid=3302894&tool=pmcentrez&rendertype=abstract

215. Mähler M, Bristol IJ, Leiter EH, Workman a E, Birkenmeier EH, Elson CO, et al. Differential susceptibility of inbred mouse strains to dextran sulfate sodium-induced colitis. Am J Physiol [Internet]. 1998 Mar [cited 2017 Jul 18];274(3 Pt 1):G544–51. Available from: http://www.ncbi.nlm.nih.gov/pubmed/9530156

216. Johansson ME V., Gustafsson JK, Sjöberg KE, Petersson J, Holm L, Sjövall H, et al. Bacteria penetrate the inner mucus layer before inflammation in the dextran sulfate colitis model. Ernberg IT, editor. PLoS One [Internet]. 2010 Jan 18 [cited 2013 Sep 30];5(8):e12238. Available from: http://www.pubmedcentral.nih.gov/articlerender.fcgi?artid=2923597&tool=pmcentrez&rendertype=abstract

217. Zheng L, Gao Z-Q, Wang S-X. A chronic ulcerative colitis model in rats. World J Gastroenterol [Internet]. 2000 Feb [cited 2017 Jul 18];6(1):150–2. Available from: http://www.ncbi.nlm.nih.gov/pubmed/11819549

218. Motavallian-Naeini A, Andalib S, Rabbani M, Mahzouni P, Afsharipour M, Minaiyan M. Validation and optimization of experimental colitis induction in rats using 2, 4, 6-trinitrobenzene sulfonic acid. Res Pharm Sci [Internet]. 2012 Jul [cited 2017 Jul 18];7(3):159–69. Available from: http://www.ncbi.nlm.nih.gov/pubmed/23181094

219. Kawada M, Arihiro A, Mizoguchi E. Insights from advances in research of chemically induced experimental models of human inflammatory bowel disease. World J Gastroenterol [Internet]. 2007 Nov 14 [cited 2017 Jul 18];13(42):5581–93. Available from: http://www.ncbi.nlm.nih.gov/pubmed/17948932

220. Yamada Y, Marshall S, Specian RD, Grisham MB. A comparative analysis of two models of colitis in rats. Gastroenterology [Internet]. 1992;102(5):1524–34. Available from: http://www.ncbi.nlm.nih.gov/pubmed/1314749

221. Ekström GM. Oxazolone-induced colitis in rats: effects of budesonide, cyclosporin A, and 5-aminosalicylic acid. Scand J Gastroenterol [Internet]. 1998;33(2):174–9. Available from: http://www.ncbi.nlm.nih.gov/pubmed/9517529

222. Morris G, Beck P, Herridge M, Depew W, Szewczuk M, Wallace J. Hapten-induced model of chronic inflammation and ulceration in the rat colon. Gastroenterology. 1989;96(3):795–803.

223. Kawada M, Arihiro A, Mizoguchi E. Insights from advances in research of chemically induced experimental models of human inflammatory bowel disease. World J Gastroenterol. 2007 Nov;13(42):5581–93.

224. Wirtz S, Neurath MF. Mouse models of inflammatory bowel disease. Adv Drug Deliv Rev [Internet]. 2007 Sep 30 [cited 2017 Jul 18];59(11):1073–83. Available from: http://www.ncbi.nlm.nih.gov/pubmed/23448795

225. Wong ARC, Pearson JS, Bright MD, Munera D, Robinson KS, Lee SF, et al. Enteropathogenic and enterohaemorrhagic Escherichia coli: Even more subversive elements. Vol. 80, Molecular Microbiology. 2011. p. 1420–38.

226. Mundy R, MacDonald TT, Dougan G, Frankel G, Wiles S. Citrobacter rodentium of mice and man. Cell Microbiol [Internet]. 2005 Dec [cited 2013 Oct 8];7(12):1697–706. Available from: http://www.ncbi.nlm.nih.gov/pubmed/16309456

227. Lupp C, Robertson ML, Wickham ME, Sekirov I, Champion OL, Gaynor EC, et al. Host-Mediated Inflammation Disrupts the Intestinal Microbiota and Promotes the Overgrowth of Enterobacteriaceae. Cell Host Microbe. 2007;2(2):119–29.

228. Mizoguchi E. Chitinase 3–Like-1 Exacerbates Intestinal Inflammation by Enhancing Bacterial Adhesion and Invasion in Colonic Epithelial Cells. Gastroenterology [Internet]. 2006 Feb [cited 2017 Jul 18];130(2):398–411. Available from: http://www.ncbi.nlm.nih.gov/pubmed/16472595

229. Jensen SR, Fink LN, Nielsen OH, Brynskov J, Brix S. Ex vivo intestinal adhesion of Escherichia coli LF82 in Crohn's disease. Microb Pathog [Internet]. 2011 Dec [cited 2017 Jul 18];51(6):426–31. Available from: http://www.ncbi.nlm.nih.gov/pubmed/21911052

230. Low D, Tran HT, Lee I-A, Dreux N, Kamba A, Reinecker H-C, et al. Chitin-binding domains of Escherichia coli ChiA mediate interactions with intestinal epithelial cells in mice with colitis. Gastroenterology [Internet]. 2013 Sep [cited 2017 Jul 25];145(3):602–12.e9. Available from:

http://linkinghub.elsevier.com/retrieve/pii/S001650851300749X

231. Mizoguchi E. Chitinase 3–Like-1 Exacerbates Intestinal Inflammation by Enhancing Bacterial Adhesion and Invasion in Colonic Epithelial Cells. Gastroenterology. 2006 Feb;130(2):398–411.

232. Kühn R, Löhler J, Rennick D, Rajewsky K, Müller W. Interleukin-10-deficient mice develop chronic enterocolitis. Cell. 1993;75(2):263–74.

233. Unutmaz D, Pulendran B. The gut feeling of Treg cells: IL-10 is the silver lining during colitis. Nat Immunol [Internet]. 2009 Nov [cited 2018 Feb 4];10(11):1141–3. Available from: http://www.nature.com/doifinder/10.1038/ni1109-1141

234. Kulkarni AB, Huh CG, Becker D, Geiser A, Lyght M, Flanders KC, et al. Transforming growth factor beta 1 null mutation in mice causes excessive inflammatory response and early death. Proc Natl Acad Sci U S A [Internet]. 1993;90(2):770–4. Available from: http://www.pubmedcentral.nih.gov/articlerender.fcgi?artid=45747&tool=pmcentrez&rendertype=abstract

235. Shull MM, Ormsby I, Kier AB, Pawlowski S, Diebold RJ, Yin M, et al. Targeted disruption of the mouse transforming growth factor-b1 gene results in multifocal inflammatory disease. Nature [Internet]. 1992;359(6397):693–9. Available from: http://www.ncbi.nlm.nih.gov/entrez/query.fcgi?cmd=Retrieve&db=PubMed&dopt=Citation&list_uids=1436033

236. Boismenu R, Chen Y. Insights from mouse models of colitis. J Leukoc Biol [Internet]. 2000 Mar;67(3):267–78. Available from: http://www.ncbi.nlm.nih.gov/pubmed/10733087

237. Baumgart DC, Olivier WA, Reya T, Peritt D, Rombeau JL, Carding SR. Mechanisms of intestinal epithelial cell injury and colitis in interleukin 2 (IL2)-deficient mice. Cell Immunol [Internet]. 1998 Jul 10 [cited 2018 Feb 4];187(1):52–66. Available from: http://linkinghub.elsevier.com/retrieve/pii/S0008874998913077

238. Tschurtschenthaler M, Adolph TE, Ashcroft JW, Niederreiter L, Bharti R, Saveljeva S, et al. Defective ATG16L1-mediated removal of IRE1α drives Crohn's disease-like ileitis. J Exp Med [Internet]. 2017;1–22. Available from: http://www.ncbi.nlm.nih.gov/pubmed/28082357

239. Powrie F. T cells in inflammatory bowel disease: protective and pathogenic roles. Vol. 3, Immunity. 1995. p. 171–4.

240. Powrie F, Leach MW, Mauze S, Menon S, Caddle LB, Coffman RL. Inhibition of Th1 responses prevents inflammatory bowel disease in scid mice reconstituted with CD45RBhi CD4+ T cells. Immunity [Internet]. 1994 Oct [cited 2018 Feb 4];1(7):553–62. Available from: http://www.ncbi.nlm.nih.gov/pubmed/7600284

241. Smith PJ, Levine AP, Dunne J, Guilhamon P, Turmaine M, Sewell GW, et al. Mucosal Transcriptomics Implicates Under Expression of BRINP3 in the Pathogenesis of Ulcerative Colitis. Inflamm Bowel Dis [Internet]. 2014 Oct

[cited 2017 Jul 25];20(10):1802–12. Available from: http://www.ncbi.nlm.nih.gov/pubmed/25171508

242. Livak KJ, Schmittgen TD. Analysis of relative gene expression data using real-time quantitative PCR and the 2(-Delta Delta C(T)) Method. Methods. 2001;25:402–8.

243. Johnson WE, Li C, Rabinovic A. Adjusting batch effects in microarray expression data using empirical Bayes methods. Biostatistics. 2007;8(1):118–27.

244. Saeed AI, Sharov V, White J, Li J, Liang W, Bhagabati N, et al. TM4: a free, open-source system for microarray data management and analysis. Biotechniques [Internet]. 2003 Feb [cited 2017 Aug 12];34(2):374–8. Available from: http://www.ncbi.nlm.nih.gov/pubmed/12613259

245. Brant SR. Update on the heritability of inflammatory bowel disease: The importance of twin studies. Inflamm Bowel Dis. 2011 Jan;17(1):1–5.

246. Ventham NT, Kennedy NA, Nimmo ER, Satsangi J. Beyond gene discovery in inflammatory bowel disease: the emerging role of epigenetics. Gastroenterology [Internet]. 2013;145(2):293–308. Available from: http://www.ncbi.nlm.nih.gov/pubmed/23751777

247. Waterland RA, Jirtle RL. Transposable elements: targets for early nutritional effects on epigenetic gene regulation. Mol Cell Biol [Internet]. 2003;23(15):5293–300. Available from: http://www.pubmedcentral.nih.gov/articlerender.fcgi?artid=165709&tool=pmcentrez&rendertype=abstract

248. Tobi EW, Lumey LH, Talens RP, Kremer D, Putter H, Stein AD, et al. DNA methylation differences after exposure to prenatal famine are common and timing- and sex-specific. Hum Mol Genet. 2009;18(21):4046–53.

249. Schaible TD, Harris RA, Dowd SE, Smith CW, Kellermayer R. Maternal methyl-donor supplementation induces prolonged murine offspring colitis susceptibility in association with mucosal epigenetic and microbiomic changes. Hum Mol Genet. 2011;20(9):1687–96.

250. Arijs I, Li K, Toedter G, Quintens R, Van Lommel L, Van Steen K, et al. Mucosal gene signatures to predict response to infliximab in patients with ulcerative colitis. Gut. 2009 Dec;58(12):1612–9.

251. Olsen J, Gerds TA, Seidelin JB, Csillag C, Bjerrum JT, Troelsen JT, et al. Diagnosis of ulcerative colitis before onset of inflammation by multivariate modeling of genome-wide gene expression data. Inflamm Bowel Dis. 2009 Jul;15(7):1032–8.

252. Clark PM, Dawany N, Dampier W, Byers SW, Pestell RG, Tozeren A. Bioinformatics analysis reveals transcriptome and microRNA signatures and drug repositioning targets for IBD and other autoimmune diseases. Inflamm Bowel Dis [Internet]. 2012 Dec [cited 2013 Sep 27];18(12):2315–33. Available from: http://www.ncbi.nlm.nih.gov/pubmed/22488912

253. Dieckgraefe BK, Stenson WF, Korzenik JR, Swanson PE, Harrington CA.

Analysis of mucosal gene expression in inflammatory bowel disease by parallel oligonucleotide arrays. Physiol Genomics [Internet]. 2000 Nov 9 [cited 2017 Jul 25];4(1):1–11. Available from: http://www.ncbi.nlm.nih.gov/pubmed/11074008

254. Kim M, Lee S, Yang S-K, Song K, Lee I. Differential expression in histologically normal crypts of ulcerative colitis suggests primary crypt disorder. Oncol Rep. 2006 Oct;16(4):663–70.

255. Noble CL, Abbas AR, Cornelius J, Lees CW, Ho G-T, Toy K, et al. Regional variation in gene expression in the healthy colon is dysregulated in ulcerative colitis. Gut [Internet]. 2008 Oct 29 [cited 2013 Oct 8];57(10):1398–405. Available from: http://gut.bmj.com/cgi/doi/10.1136/gut.2008.148395

256. Toedter G, Li K, Marano C, Ma K, Sague S, Huang CC, et al. Gene expression profiling and response signatures associated with differential responses to infliximab treatment in ulcerative colitis. Am J Gastroenterol. 2011 Jul;106(7):1272–80.

257. Neurath MF, Travis SPL. Mucosal healing in inflammatory bowel diseases: a systematic review. Gut [Internet]. 2012 Nov [cited 2014 Sep 6];61(11):1619–35. Available from: http://www.ncbi.nlm.nih.gov/pubmed/22842618

258. Wehkamp J, Harder J, Weichenthal M, Mueller O, Herrlinger KR, Fellermann K, et al. Inducible and constitutive beta-defensins are differentially expressed in Crohn's disease and ulcerative colitis. Inflamm Bowel Dis [Internet]. 2003;9(4):215–23. Available from: http://www.ncbi.nlm.nih.gov/pubmed/12902844

259. Smith PJ, Levine AP, Dunne J, Guilhamon P, Turmaine M, Sewell GW, et al. Mucosal Transcriptomics Implicates Under Expression of BRINP3 in the Pathogenesis of Ulcerative Colitis. Inflamm Bowel Dis. 2014 Oct;20(10):1802–12.

260. Amasheh S, Milatz S, Krug SM, Bergs M, Amasheh M, Schulzke J-D, et al. Na+ absorption defends from paracellular back-leakage by claudin-8 upregulation. Biochem Biophys Res Commun [Internet]. 2009 Jan 2 [cited 2017 Jul 28];378(1):45–50. Available from: http://www.ncbi.nlm.nih.gov/pubmed/19000657

261. Mestas J, Hughes CCW. Of mice and not men: differences between mouse and human immunology. J Immunol [Internet]. 2004 Mar 1 [cited 2017 Jul 26];172(5):2731–8. Available from: http://www.ncbi.nlm.nih.gov/pubmed/14978070

262. Katouzian F, Sblattero D, Not T, Tommasini A, Giusto E, Meiacco D, et al. Dual sugar gut-permeability testing on blood drop in animal models. Clin Chim Acta. 2005;352(1–2):191–7.

263. Maxton DG, Bjarnason I, Reynolds AP, Catt SD, Peters TJ, Menzies IS. Lactulose, 51Cr-labelled ethylenediaminetetra-acetate, L-rhamnose and polyethyleneglycol 400 as probe markers for assessment in vivo of human intestinal permeability. Clin Sci. 1986;71(1):71–80.

264. Peeters M, Hiele M, Ghoos Y, Huysmans V, Geboes K, Vantrappen G, et al.

Test conditions greatly influence permeation of water soluble molecules through the intestinal mucosa: need for standardisation. Gut [Internet]. 1994;35(10):1404–8. Available from: http://www.pubmedcentral.nih.gov/articlerender.fcgi?artid=1375014&tool=pmcentrez&rendertype=abstract

265. Menzies IS, Zuckerman MJ, Nukajam WS, Somasundaram SG, Murphy B, Jenkins AP, et al. Geography of intestinal permeability and absorption. Gut [Internet]. 1999 Apr [cited 2017 Aug 12];44(4):483–9. Available from: http://www.ncbi.nlm.nih.gov/pubmed/10075954

266. van der Waaij L a, Harmsen HJM, Madjipour M, Kroese FGM, Zwiers M, van Dullemen HM, et al. Bacterial population analysis of human colon and terminal ileum biopsies with 16S rRNA-based fluorescent probes: commensal bacteria live in suspension and have no direct contact with epithelial cells. Inflamm Bowel Dis [Internet]. 2005 Oct [cited 2015 Feb 2];11(10):865–71. Available from: http://www.ncbi.nlm.nih.gov/pubmed/16189415

267. Hedrich H. The Laboratory Mouse (HANDBOOK OF EXPERIMENTAL ANIMALS). Academic Press; 2012.

268. Kiuchi-Saishin Y, Gotoh S, Furuse M, Takasuga A, Tano Y, Tsukita S. Differential expression patterns of claudins, tight junction membrane proteins, in mouse nephron segments. J Am Soc Nephrol [Internet]. 2002 Apr [cited 2017 Aug 12];13(4):875–86. Available from: http://www.ncbi.nlm.nih.gov/pubmed/11912246

269. Lechpammer M, Resnick MB, Sabo E, Yakirevich E, Greaves WO, Sciandra KT, et al. The diagnostic and prognostic utility of claudin expression in renal cell neoplasms. Mod Pathol. 2008;21:1320–9.

270. Jeansonne B, Lu Q, Goodenough DA, Chen YH. Claudin-8 interacts with multi-PDZ domain protein 1 (MUPP1) and reduces paracellular conductance in epithelial cells. Cell Mol Biol (Noisy-le-grand). 2003;49(1):13–21.

271. Chiba H, Osanai M, Murata M, Kojima T, Sawada N. Transmembrane proteins of tight junctions. Biochim Biophys Acta [Internet]. 2008;1778(3):588–600. Available from: http://www.sciencedirect.com/science/article/pii/S0005273607003045

272. Van Damme J, De Ley M, Opdenakker G, Billiau A, De Sommer P. Homogeneous interferon-inducing 22K factor is related to endogenous pyrogen and interleukin-1. Nature. 1985;314:266–8.

273. Dinarello CA. Biologic Basis for Interleukin-I in Disease. J Am Soc Hematol. 1996;87(15):2095–147.

274. Mosser DM, Zhang X. Interleukin-10: New perspectives on an old cytokine. Vol. 226, Immunological Reviews. 2008. p. 205–18.

275. Low D, Nguyen DD, Mizoguchi E. Animal models of ulcerative colitis and their application in drug research. Drug Des Devel Ther. 2013 Nov;7:1341–57.

276. Okayasu I, Hatakeyama S, Yamada M, Ohkusa T, Inagaki Y, Nakaya R. A novel method in the induction of reliable experimental acute and chronic

ulcerative colitis in mice. Gastroenterology. 1990 Mar;98(3):694–702.

277. Cooper HS, Murthy SN, Shah RS, Sedergran DJ. Clinicopathologic study of dextran sulfate sodium experimental murine colitis. Lab Invest [Internet]. 1993 Aug [cited 2017 Jul 26];69(2):238–49. Available from: http://www.ncbi.nlm.nih.gov/pubmed/8350599

278. Escudero-Esparza A, Jiang WG, Martin TA. Claudin-5 is involved in breast cancer cell motility through the N-WASP and ROCK signalling pathways. J Exp Clin Cancer Res [Internet]. 2012 May 4 [cited 2017 Aug 5];31(1):43. Available from: http://www.ncbi.nlm.nih.gov/pubmed/22559840

279. Poritz LS, Garver KI, Green C, Fitzpatrick L, Ruggiero F, Koltun W a. Loss of the tight junction protein ZO-1 in dextran sulfate sodium induced colitis. J Surg Res [Internet]. 2007;140(1):12–9. Available from: http://www.ncbi.nlm.nih.gov/pubmed/17418867

280. Araki Y, Mukaisyo K, Sugihara H, Fujiyama Y, Hattori T. Increased apoptosis and decreased proliferation of colonic epithelium in dextran sulfate sodium-induced colitis in mice. Oncol Rep [Internet]. 2010;24(4):869–74. Available from: http://www.ncbi.nlm.nih.gov/pubmed/20811666

281. Hans W, Schölmerich J, Gross V, Falk W. The role of the resident intestinal flora in acute and chronic dextran sulfate sodium-induced colitis in mice. Vol. 12, European journal of gastroenterology & hepatology. 2000. p. 267–73.

282. Hudcovic T, Štěpánková R, Cebra J, Tlaskalová-Hogenová H. The role of microflora in the development of intestinal inflammation: acute and chronic colitis induced by dextran sulfate in germ-free and conventionally reared immunocompetent and immunodeficient mice. Folia Microbiol (Praha) [Internet]. 2001;46(6):565–72. Available from: http://eutils.ncbi.nlm.nih.gov/entrez/eutils/elink.fcgi?dbfrom=pubmed&id=11898350&retmode=ref&cmd=prlinks%5Cnpapers3://publication/doi/10.1007/BF02818004

283. Kitajima S, Morimoto M, Sagara E, Shimizu C, Ikeda Y. Dextran Sodium Sulfate-Induced Colitis in Germ-Free IQI / Jic Mice. Exp Anim. 2001;50(5):387–95.

284. Chinen T, Kannan AK, Levine AG, Fan X, Klein U, Zheng Y, et al. An essential role for the IL-2 receptor in Treg cell function. Nat Immunol [Internet]. 2016;(December 2015):1–14. Available from: http://www.nature.com/doifinder/10.1038/ni.3540%5Cnhttp://www.ncbi.nlm.nih.gov/pubmed/27595233

285. Boyman O, Sprent J. The role of interleukin-2 during homeostasis and activation of the immune system. Nat Rev Immunol [Internet]. 2012;12(3):180–90. Available from: http://dx.doi.org/10.1038/nri3156

286. Johnstone D, Riveros C, Heidari M, Graham R, Trinder D, Berretta R, et al. Evaluation of Different Normalization and Analysis Procedures for Illumina Gene Expression Microarray Data Involving Small Changes. Microarrays [Internet]. 2013;2(2):131–52. Available from: http://www.mdpi.com/2076-3905/2/2/131/

287. Ringnér M. What is principal component analysis? Nat Biotechnol [Internet]. 2008;26(3):303–4. Available from: http://dx.doi.org/10.1038/nbt0308-303

288. Barbosa-Morais NL, Dunning MJ, Samarajiwa SA, Darot JFJ, Ritchie ME, Lynch AG, et al. A re-annotation pipeline for Illumina BeadArrays: Improving the interpretation of gene expression data. Nucleic Acids Res. 2009;38(3).

289. Mutz K-O, Heilkenbrinker A, Lönne M, Walter J-G, Stahl F. Transcriptome analysis using next-generation sequencing. Curr Opin Biotechnol [Internet]. 2013;24:22–30. Available from: http://www.ncbi.nlm.nih.gov/pubmed/23020966

290. Gröne J, Weber B, Staub E, Heinze M, Klaman I, Pilarsky C, et al. Differential expression of genes encoding tight junction proteins in colorectal cancer: frequent dysregulation of claudin-1, -8 and -12. Int J Colorectal Dis [Internet]. 2007 Jun [cited 2013 Oct 8];22(6):651–9. Available from: http://www.ncbi.nlm.nih.gov/pubmed/17047970

291. Barmeyer C, Harren M, Schmitz H, Heinzel-Pleines U, Mankertz J, Seidler U, et al. Mechanisms of diarrhea in the interleukin-2-deficient mouse model of colonic inflammation. Am J Physiol Gastrointest Liver Physiol [Internet]. 2004 Feb;286(2):G244-52. Available from: http://www.ncbi.nlm.nih.gov/pubmed/14715519

292. Alex P, Zachos NC, Nguyen T, Gonzales L, Chen T-E, Conklin LS, et al. Distinct cytokine patterns identified from multiplex profiles of murine DSS and TNBS-induced colitis. Inflamm Bowel Dis [Internet]. 2009 Mar [cited 2013 Oct 8];15(3):341–52. Available from: http://www.pubmedcentral.nih.gov/articlerender.fcgi?artid=2643312&tool=pmcentrez&rendertype=abstract

293. Bürgel N, Bojarski C, Mankertz J, Zeitz M, Fromm M, Schulzke J. Mechanisms of diarrhea in collagenous colitis. Gastroenterology [Internet]. 2002 Aug [cited 2013 Oct 16];123(2):433–43. Available from: http://linkinghub.elsevier.com/retrieve/pii/S001650850200121X

294. Nishida M, Yoshida M, Nishiumi S, Furuse M, Azuma T. Claudin-2 regulates colorectal inflammation via myosin light chain kinase-dependent signaling. Dig Dis Sci. 2013;58:1546–59.

295. Swidsinski A, Loening-Baucke V, Lochs H, Hale L-P. Spatial organization of bacterial flora in normal and inflamed intestine: a fluorescence in situ hybridization study in mice. World J Gastroenterol. 2005;11(8):1131–40.

296. Pullan RD. Colonic mucus, smoking and ulcerative colitis. Ann R Coll Surg Eng. 1996;78(2):85–91.

297. Johansson ME V, Philipson M, Petersson J, Velcich A, Holm L, Hansson GC. The inner of the two Muc2 mucin-dependent mucus layers in colon is devoid of bacteria. Proc Natl Acad Sci U S A. 2008;105(39):15064–9.

298. Heazlewood CK, Cook MC, Eri R, Price GR, Tauro SB, Taupin D, et al. Aberrant mucin assembly in mice causes endoplasmic reticulum stress and spontaneous inflammation resembling ulcerative colitis. PLoS Med. 2008;5:0440–60.

299. Lu P, Burger-van Paassen N, van der Sluis M, Witte-Bouma J, Kerckaert J-P, van Goudoever JB, et al. Colonic gene expression patterns of mucin Muc2 knockout mice reveal various phases in colitis development. Inflamm Bowel Dis [Internet]. 2011 Oct [cited 2013 Oct 16];17(10):2047–57. Available from: http://www.ncbi.nlm.nih.gov/pubmed/21910166

300. Van der Sluis M, De Koning BAE, De Bruijn ACJM, Velcich A, Meijerink JPP, Van Goudoever JB, et al. Muc2-deficient mice spontaneously develop colitis, indicating that MUC2 is critical for colonic protection. Gastroenterology [Internet]. 2006 Jul [cited 2015 Jan 31];131(1):117–29. Available from: http://www.ncbi.nlm.nih.gov/pubmed/16831596

301. Petersson J, Schreiber O, Hansson GC, Gendler SJ, Velcich A, Lundberg JO, et al. Importance and regulation of the colonic mucus barrier in a mouse model of colitis. Am J Physiol Gastrointest Liver Physiol [Internet]. 2011 Feb [cited 2015 Feb 14];300(2):G327-33. Available from: http://www.pubmedcentral.nih.gov/articlerender.fcgi?artid=3302190&tool=pmcentrez&rendertype=abstract

302. Strugala V, Dettmar PW, Pearson JP. Thickness and continuity of the adherent colonic mucus barrier in active and quiescent ulcerative colitis and Crohn's disease. Int J Clin Pract. 2008;62(May):762–9.

303. Van Klinken BJ, Van der Wal JW, Einerhand AW, Büller HA, Dekker J. Sulphation and secretion of the predominant secretory human colonic mucin MUC2 in ulcerative colitis. Gut. 1999;44:387–93.

304. Yeaman MR, Yount NY. Mechanisms of antimicrobial peptide action and resistance. Pharmacol Rev [Internet]. 2003 Mar [cited 2014 Nov 14];55(1):27–55. Available from: http://www.ncbi.nlm.nih.gov/pubmed/12615953

305. Wehkamp J, Fellermann K, Herrlinger KR, Baxmann S, Schmidt K, Schwind B, et al. Human beta-defensin 2 but not beta-defensin 1 is expressed preferentially in colonic mucosa of inflammatory bowel disease. Eur J Gastroenterol Hepatol [Internet]. 2002 Jul [cited 2015 Feb 2];14(7):745–52. Available from: http://www.ncbi.nlm.nih.gov/pubmed/12169983

306. Ahmad R, Chaturvedi R, Olivares-Villagómez D, Habib T, Asim M, Shivesh P, et al. Targeted colonic claudin-2 expression renders resistance to epithelial injury, induces immune suppression, and protects from colitis. Mucosal Immunol [Internet]. 2014 Mar 26 [cited 2014 May 16];(February):1–14. Available from: http://www.ncbi.nlm.nih.gov/pubmed/24670427

307. Amasheh S, Milatz S, Krug SM, Markov AG, Günzel D, Amasheh M, et al. Tight junction proteins as channel formers and barrier builders. Ann N Y Acad Sci [Internet]. 2009 May [cited 2013 Oct 16];1165:211–9. Available from: http://www.ncbi.nlm.nih.gov/pubmed/19538309

308. Berg DJ, Kühn R, Rajewsky K, Müller W, Menon S, Davidson N, et al. Interleukin-10 is a central regulator of the response to LPS in murine models of endotoxic shock and the Shwartzman reaction but not endotoxin tolerance. J Clin Invest. 1995;96(5):2339–47.

309. Tamura A, Kitano Y, Hata M, Katsuno T, Moriwaki K, Sasaki H, et al. Megaintestine in claudin-15-deficient mice. Gastroenterology [Internet]. 2008

Feb [cited 2013 Dec 12];134(2):523–34. Available from: http://www.ncbi.nlm.nih.gov/pubmed/18242218

310. Ashikari D, Takayama K, Obinata D, Takahashi S, Inoue S. CLDN8, an androgen-regulated gene, promotes prostate cancer cell proliferation and migration. Cancer Sci [Internet]. 2017 Jul [cited 2017 Aug 6];108(7):1386–93. Available from: http://www.ncbi.nlm.nih.gov/pubmed/28474805

311. Musa M, Kannan TP, Mustafa S. Cell Proliferation Study of Human Osteosarcoma Cell Line (U2OS) using Alamar Blue Assayand Live Cell Imaging. IOSR J Dent Med Sci [Internet]. 2013;8(2):2279–861. Available from: www.iosrjournals.org

312. Qi J, Yang Y, Hao P, Xu J. Transcription Factor SOX9 Promotes Osteosarcoma Cell Growth by Repressing Claudin-8 Expression. Tohoku J Exp Med [Internet]. 2017 [cited 2017 Aug 24];241(1):55–63. Available from: http://www.ncbi.nlm.nih.gov/pubmed/28123165

313. Shangkuan W-C, Lin H-C, Chang Y-T, Jian C-E, Fan H-C, Chen K-H, et al. Risk analysis of colorectal cancer incidence by gene expression analysis. PeerJ [Internet]. 2017 Feb 15 [cited 2017 Aug 24];5:e3003. Available from: http://www.ncbi.nlm.nih.gov/pubmed/28229027

314. Bujko M, Kober P, Mikula M, Ligaj M, Ostrowski J, Siedlecki J. Expression changes of cell-cell adhesion-related genes in colorectal tumors. Oncol Lett [Internet]. 2015;9(6):2463–70. Available from: http://www.pubmedcentral.nih.gov/articlerender.fcgi?artid=4473523&tool=pmcentrez&rendertype=abstract

315. Doeing DC, Borowicz JL, Crockett ET. Gender dimorphism in differential peripheral blood leukocyte counts in mice using cardiac, tail, foot, and saphenous vein puncture methods. BMC Clin Pathol [Internet]. 2003;3(1):3. Available from: http://www.biomedcentral.com/1472-6890/3/3

316. Risso A. Leukocyte antimicrobial peptides: multifunctional effector molecules of innate immunity. J Leukoc Biol [Internet]. 2000;68(6):785–92. Available from: http://www.ncbi.nlm.nih.gov/pubmed/11129645

9 Appendices

APPENDIX 1 – LIST OF PRIMERS

Primers used for Genotyping

DNA266-28	5'-GTTGTGAGCACATTTCTACAGG
DNA266-24	5'-GGATGGCTGTCATGAAAGCC
GT ires	5'-CCCTAGGAATGCTCGTCAAGA

Primers used for qRT-PCR

Name	Forward Primer	Reverse Primer
Cldn8	GACAGCCATCCTCGGAATGA	GCGGCTCTTCACGTTCTCA
Lpo	CCTCTGGTTCGAGGTCTGTT	CCACAGAAAGCTCTCCAGGA
Duox2	TCTGAACCTGCTCTCCTTGG	CCTTGTCTACCTGCCCAGAA
Cxadr	CTGTCACAGGAAACGCAGAG	CCAAGTCCCCAGTGAAGACT
Ppia	GGGCCGCGTCTCCTTT	ATCCTTTCTCTCCAGTGCTCAGA
Gapdh	AAGGTCATCCCAGAGCTGAA	CTGCTTCACCACCTTCTTGA

EUB338

Probe sequence (5′ to 3′) – GCTGCCTCCCGTAGGAGT - Cy5.5 conjugated

APPENDIX 2 – PUBLICATIONS

PAPERS

Provision of out-of-hours services for acute upper gastrointestinal bleeding in England: results of the 2014–2015 BSG/NHS England national survey, *Frontline Gastroenterology* Jan 2017, 8 (1) 8-12, **Nedjat-Shokouhi B**, Glynn M, Denton ERE, Greenfield SM (PMID: 28839878)

Critical Role of the Disintegrin Metalloprotease ADAM-like Decysin-1 [ADAMDEC1] for Intestinal Immunity and Inflammation, O'Shea NR, Chew TS, Dunne J, Marnane R, **Nedjat-Shokouhi B**, Smith PJ, Bloom SL, Smith AM, Segal AW, *J Crohns Colitis*. 2016 Dec;10(12):1417-1427. Epub 2016 May 25 (PMID: 27226416)

The setting up and running of a cross-county out-of-hours gastrointestinal bleed service: a possible blueprint for the future, **Shokouhi BN**, Khan M, Carter M, et al, *Frontline Gastroenterol.* 2013 Jul;4(3):227-231 ("Editors Choice"), (PMID: 28839729)

BOOK CHAPTERS

Gastroenterology and Hepatology, associate editor, Oxford Handbook of Acute Medicine, 4th edition, *in print*

Lower GI and IBD associate editor, Oxford Handbook of Gastroenterology and Hepatology, 3rd edition, *in progress*

APPENDIX 3 – ORAL PRESENTATIONS

2014 UCL PhD Seminars: Pathogenesis of Ulcerative Colitis: The role of Claudin-8 in epithelial barrier function and inflammation

2014 UCLH lunch-time Gastroenterology seminar: Pathogenesis of Ulcerative Colitis: The role of Claudin-8 in epithelial barrier function and inflammation

APPENDIX 4 – COMMITTEE MEMBERSHIPS

2013-2016	British Society of Gastroenterology: Trainee representative to IBD Committee
2016	UCL Genetic Institute's bioinformatics talk: Patient involvement in providing phenotype data – rewards and challenges
2015	UCL Bright Ideas: judge for UCL Bright Ideas award
2015	UCL Infection, Immunology and Inflammation Symposium: Poster judge
2015	Digestive Disease Federation (DDF): Poster judge (IBD Section)